JULY-SEPTEMBER 2017 VOL. 9 № 3 (34)

ISSN 2075-8251

ActaNaturae

Death Receptors: New Opportunities in Cancer Therapy

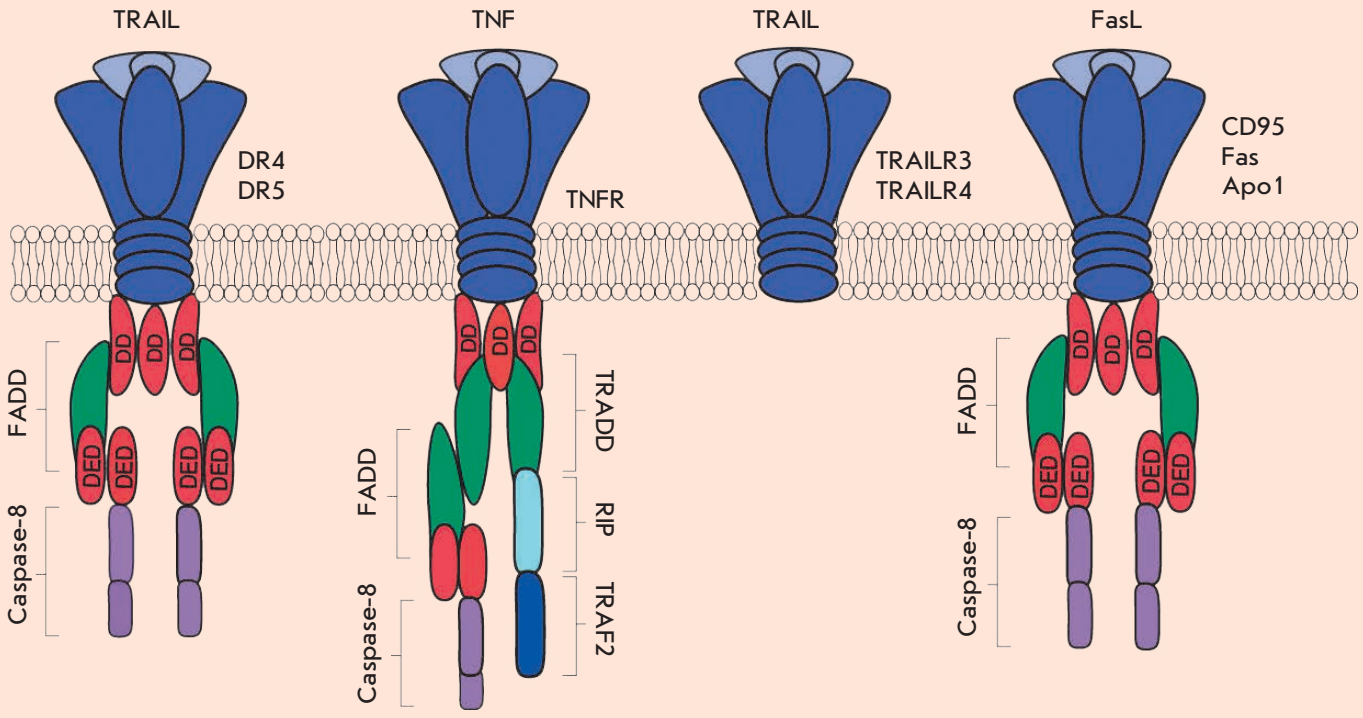

Non-bulky Lesions in Human DNA: The Ways of Formation, Repair, and Replication

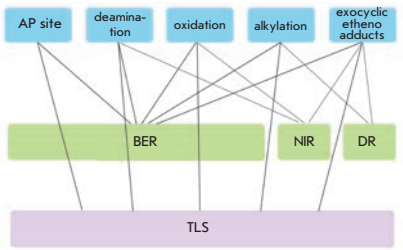

Basic pathways of non-bulky DNA lesions repair in humans

A.V. Ignatov, K.A. Bondarenko, A.V. Makarova

DNA damage is a major cause of replication interruption, mutations, and cell death. In this review, authors summarize the types and mechanisms of formation and repair of non-bulky DNA lesions, and authors provide an overview of the role of specialized DNA polymerases in translesion DNA synthesis.

Proteasomes in Protein Homeostasis of Pluripotent Stem Cells

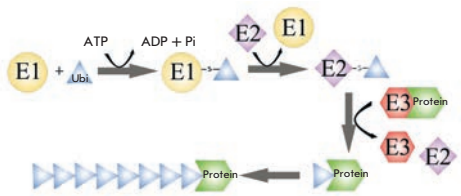

The ubiquitin-proteasome system

A.V. Selenina, A.S. Tsimokha, A.N. Tomilin

Embryonic stem cells and induced pluripotent stem cells are subjects of high interest not only in basic research, but also in various applied fields, particularly, in regenerative medicine. The molecular mechanisms that control protein homeostasis in these cells remain largely unknown. The ubiquitin-proteasome system (UPS) acts via post-translational protein modifications and protein degradation and, therefore, is involved in the control of virtually all cellular processes. Therefore, studying the biological role and action mechanisms of the UPS in pluripotent cells will help us to both better understand the biology of cells and to develop novel approaches in regenerative medicine.

Change in the Content of Immunoproteasomes and Macrophages in Rat Liver At the Induction of Donor-Specific Tolerance

Ya.D. Karpova, V.D. Ustichenko, N.M. Alabedal'karim, A.A. Stepanova, Yu.V. Lyupina, K.I. Boguslavski, G.A. Bozhok, N.P. Sharova

Induction of donor specific tolerance (DST) by the introduction of donor cells into a recipient's portal vein is one of the approaches used to solve the problem of transplant engraftment. However, the mechanism of DST development remains unclear to this moment. In the present work, authors first studied the change in the content of immunoproteasomes and macrophages of the liver at early stages of the development of allospecific portal tolerance in rats by Western blotting and flow cytofluorimetry.

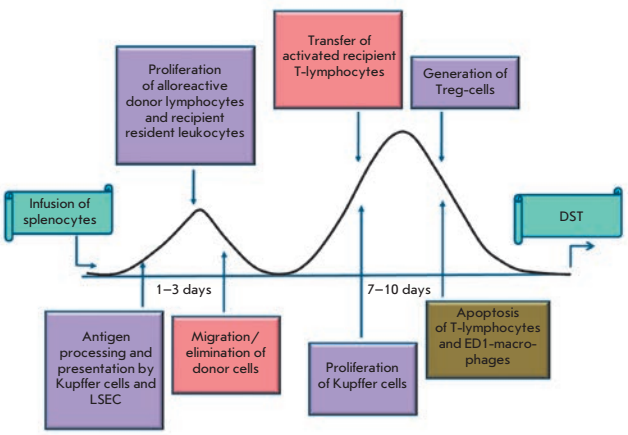

Scheme of DST induction and development

ActaNaturae
JULY–SEPTEMBER 2017 VOL. 9 № 3 (34)

Founders
Ministry of Education and
Science of the Russian Federation,
Lomonosov Moscow State University,
Park Media Ltd

Phone/Fax: +7 (495) 727 38 60
E-mail: vera.knorre@gmail.com, actanaturae@gmail.com

Номер подписан в печать 27 сентября 2017 г.
Тираж 200 экз. Цена свободная.
Отпечатано в типографии «МИГ ПРИНТ»

Indexed in Pubmed, Web of Science, Scopus, and RISC

CONTENTS

REVIEWS

RESEARCH ARTICLES

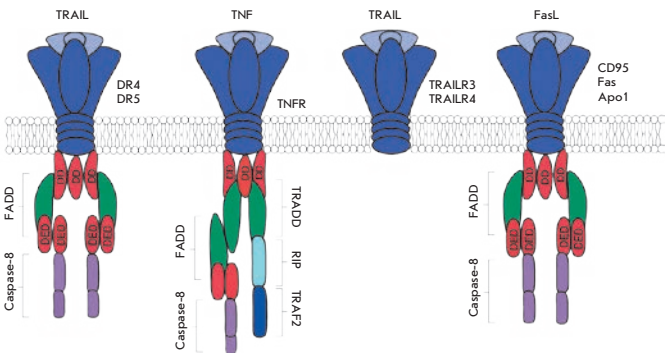

IMAGE ON THE COVER PAGE
(see the article by Ukrainskaya *et al.*)

Virus-Vectored Ebola Vaccines

I.V. Dolzhikova[1]*, E.A. Tokarskaya[1], A. S. Dzharullaeva[1], A. I. Tukhvatulin[1], D. V. Shcheblyakov[1], O.L. Voronina[1], S. I. Syromyatnikova[2], S. V. Borisevich[2], V. B. Pantyukhov[2], V. F. Babira[3], L. V. Kolobukhina[4], B. S. Naroditsky[1], D. Y. Logunov[1], A. L. Gintsburg[1]

[1]Federal Research Centre of Epidemiology and Microbiology named after Honorary Academician N. F. Gamaleya, Ministry of Health, Gamaleya Str. 18, Moscow, 123098, Russia

[2]48 Central Research Institute, Ministry of Defense, Oktjabr'skaja Str. 11, Sergiev Posad-6, Moscow oblast, 141306, Russia

[3]No. 7 Main Military Clinical Hospital named after academician N. N. Burdenko, Ministry of Defense, Novaja Str. 4, Sergiev Posad-6, Moscow oblast, 141306, Russia

[4]Infectious Clinical Hospital № 1, Moscow Healthcare Department, Volokolamskoe shosse, 63, Moscow, 125367, Russia

*E-mail: i.dolzhikova@gmail.com

Received: March 02, 2017; in final form June 05, 2017

ABSTRACT **The Ebola virus disease (EVD) is one of the most dangerous infections affecting humans and animals. The first EVD outbreaks occurred in 1976 in Sudan and Zaire. Since then, more than 20 outbreaks have occurred; the largest of which (2014–2016) evolved into an epidemic in West Africa and claimed the lives of more than 11,000 people. Although vaccination is the most effective way to prevent epidemics, there was no licensed vaccine for EVD at the beginning of the latest outbreak. The development of the first vaccines for EVD started in 1980 and has come a long technological way, from inactivated to genetically engineered vaccines based on recombinant viral vectors. This review focuses on virus-vectored Ebola vaccines that have demonstrated the greatest efficacy in preclinical trials and are currently under different phases of clinical trial. Particular attention is paid to the mechanisms of immune response development, which are important for protection from EVD, and the key vaccine parameters necessary for inducing long-term protective immunity against EVD.**

KEYWORDS **Ebola vaccines, virus-vectored vaccines, recombinant viral vectors, Ebola virus.**

ABBREVIATIONS **Ad3, ChAd3 – recombinant replication-defective chimpanzee adenovirus type 3; Ad5 – recombinant replication-defective human adenovirus type 5; Ad26 – recombinant replication-defective human adenovirus type 26; BDBV – Bundibugyo Ebolavirus; GMT – geometric mean titer; GMC –geometric mean concentration; GP – glycoprotein; MARV – Marburg virus; MVA – recombinant Modified Vaccinia Virus Ankara; NP – nucleoprotein; RESTV – Reston Ebolavirus; SUDV – Sudan Ebolavirus; TAFV – Tai Forest Ebolavirus; VSV – live-attenuated recombinant vesicular stomatitis virus; ZEBOV – Zaire Ebolavirus; EVD – Ebola virus disease; PFU – plaque-forming unit; NtAb – virus-neutralizing antibody; VP – viral particle; IFN-gamma – interferon gamma; AE – adverse event.**

EBOLA VIRUS DISEASE

The Ebola virus causes one of the most dangerous diseases affecting humans and primates. The Ebola virus disease (EVD) is characterized by a severe course, general intoxication, and a high mortality rate reaching 90% [1–3]. The genus Ebola virus (*Ebolavirus*) is a member of the Filoviridae family. Viral particles of all viruses from the Filoviridae family (order Mononegavirales) have a characteristic filament-like shape, and their genome is represented by a single-stranded RNA with negative polarity. There are three filovirus genera: *Ebolavirus*, *Marburgvirus*, and *Cuevavirus*. Of these, *Ebolaviruses* and *Marburgviruses* have marked pathogenicity to humans, and the Ebola virus (EBOV) is the most dangerous pathogen. To date, five Ebola virus species have been identified: *Bundibugyo ebolavirus* (BDBV), *Zaire ebolavirus* (ZEBOV), *Reston ebolavirus* (RESTV), *Sudan ebolavirus* (SUDV), and *Tai Forest ebolavirus* (TAFV); of these, ZEBOV, SUDV, and BDBV are the most dangerous for humans [4, 5].

EVD was first detected in Yambuku (Democratic Republic of the Congo, the northern part of Zaire) and in Nzara (Sudan) in 1976. In the same year, the EVD agent, Ebola virus (*Ebolavirus*), was first isolated from a patient who lived near the Ebola River [6, 7].

Since the time of pathogen isolation and to this day, more than 20 EVD outbreaks have occurred, the largest of which (2014–2016) turned into an epidemic (28,616

cases) and claimed the lives of more than 11,000 people [8]. By the time of this epidemic, neither preventive nor therapeutic agents for EVD were licensed in the world. At the same time, a specific heterologous (horse) immunoglobulin against Ebola fever was developed at the Virology Center of the Research Institute of the Russian Defense Ministry for urgent prophylaxis and treatment of high-risk groups; the immunoglobulin had 100% protective activity in experiments with monkeys [9]. Due to the high mortality rate in the last EVD epidemic and spread of the virus outside Africa, a WHO Committee was convened in early August 2014. The Committee concluded that the EVD outbreak was an extraordinary event of international importance, which significantly accelerated the development of preventive and therapeutic agents for EVD. After 2 years, several vaccines had been developed. They are currently under different phases of clinical trial, and two vaccines developed in Russia have been registered for medical use.

EVD VACCINES: HISTORY AND DEVELOPMENT STRATEGIES

The most effective and economical way to protect against infectious diseases is vaccine prevention. However, there was no vaccine approved for use by the beginning of the last Ebola outbreak (2014–2016).

The development of the first vaccines for Ebola fever began after the identification of the virus and was mainly focused on attempts to create an effective vaccine based on an inactivated Ebola virus (*Figure*). In 1980, the first candidate vaccine on the basis of a heat- or formalin-inactivated Ebola virus was tested on guinea pigs and exhibited 100% protection [10]. But despite the high efficacy in guinea pigs, the vaccine did not provide the proper level of protection to primates from lethal infection [11]. Another disadvantage of this vaccine was the extremely dangerous production condition. All these facts prevented the introduction of the vaccine into clinical practice (*Figure*).

It took more than 15 years to develop an effective and safe vaccine. This was associated with the fact that the expression features of the main protective antigen, Ebola virus GP, remained unclear for a long time. The breakthrough came in 1995, when an article by V.E. Volchkov et al. [12] was published. It was shown that RNA editing by viral polymerase resulted in several GP forms, of which only 20% were the full-length envelope antigen GP [12] (*Figure*). The same study found that GP expressed in eukaryotic cells undergoes extensive glycosylation, which subsequently happens to be critical for the preservation of immunogenicity and antigen protection [12, 13].

Understanding the biosynthesis peculiarities of various GP forms led, first of all, to the generation of candidate DNA vaccines. The plasmid vectors that were used for constructing the vaccines contained the full-length glycoprotein GP gene or the nucleoprotein gene of Ebola virus. These vaccines showed a sufficiently high protection level in animal studies, with the efficacy of the DNA vaccine carrying the Ebola virus glycoprotein GP gene being higher than that of the vaccine carrying the Ebola virus nucleoprotein NP gene [14]. However, the use of these vaccines required multiple (5 times) administration of the drug to achieve a high level of protection [15], which was a critical limiting factor for their effective use during epidemic development.

The problem of multiple vaccination was resolved as the recombinant viral vector technology was developed (*Figure*). In contrast to DNA vaccines, these vectors provide a high and long-lasting level of target transgene expression, which enables the induction of protective immunity after one or two immunizations [16–18]. Experiments with direct comparison demonstrated much faster formation of the immune response to a recombinant viral vector- based candidate vaccine compared to a plasmid DNA-based vaccine [16]. It should be noted that immunization was associated not only with the humoral immune response, but also with a more pronounced cellular (CD8+ and CD4+) immune response, which later occurred to be the key aspect of protection against Ebola fever. Various studies have demonstrated that it is cellular immunity that plays a key role in the formation of protective immunity to the Ebola virus [19, 20]. Directed depletion of CD3+ (CD8+ and CD4+) cells in monkeys immunized against EVD caused a decrease in vaccinated protective immunity, which resulted in the death of all the animals from Ebola virus infection. If only CD8+ cells were depleted, the protective response also decreased in immunized monkeys: 80% of the animals died. At the same time, passive transfer of high-titer polyclonal antibodies to the Ebola virus from vaccinated monkeys to naive ones provided incomplete protection against lethal infection: 75% of the animals died despite the high titers of common IgGs and NtAbs in peripheral blood serum [20]. The importance of cellular immunity was indirectly confirmed by the fact that the peripheral blood of people who survived EVD contained an increased number of specific CD8+ cells compared to the blood of healthy people. At the same time, the number of specific CD4+ cells did not actually increase [21].

Summarizing the more than thirty-year history of studies aimed at developing an effective EVD vaccine, it may be concluded that the "ideal" vaccine for Ebola fever should induce cellular and humoral immune responses, be administered a minimum number of times, and induce prolonged protective immunity.

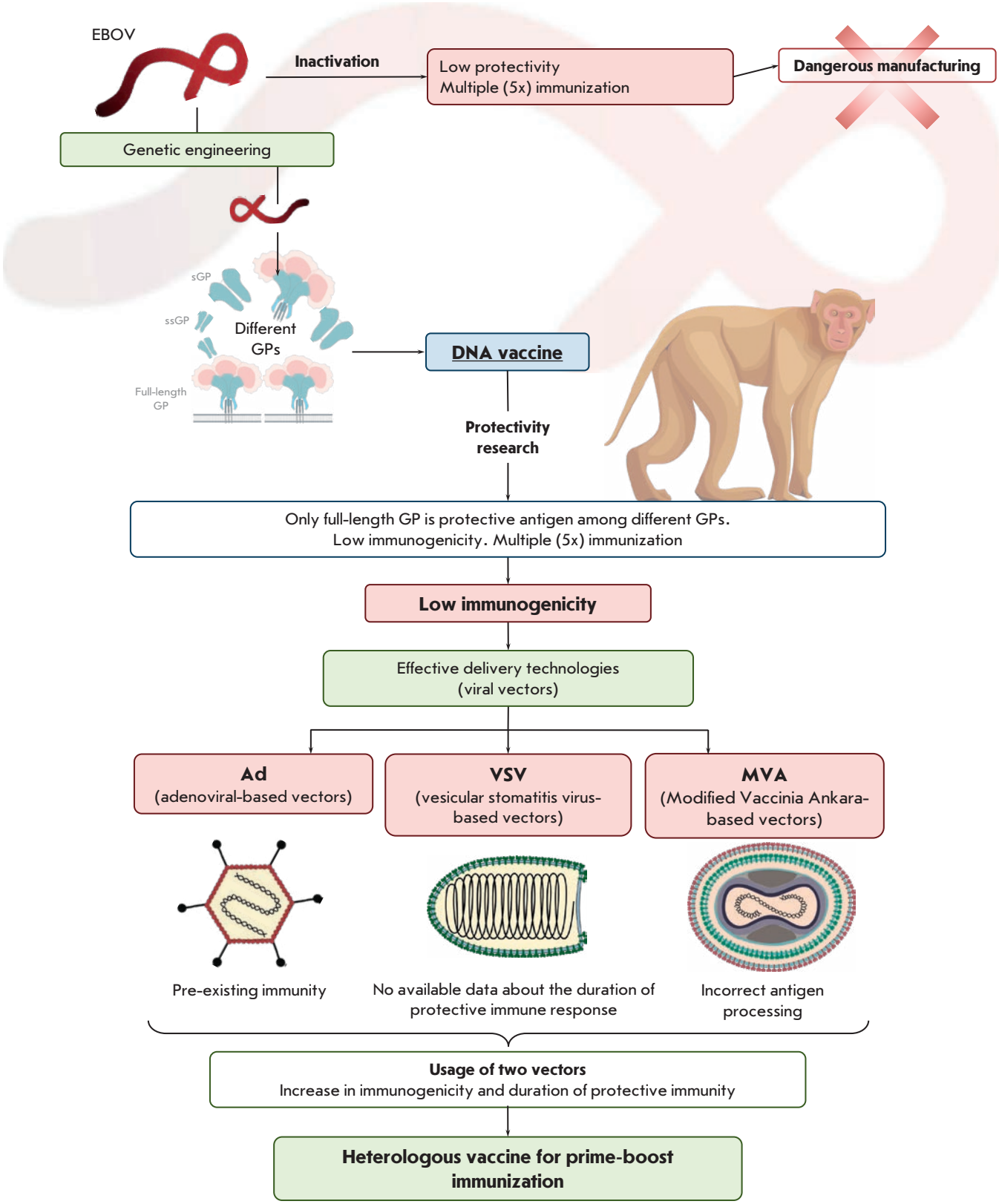

Ebola vaccine development strategies

The use of recombinant viral vectors provides all the indicated conditions; in this regard, the vaccines developed on the basis of these conditions were supported by the WHO as a promising direction for the development of Ebola vaccines during the last EVD epidemic.

VECTORED VACCINES AGAINST EVD UNDER CLINICAL TRIALS

The bulk of the developed vaccines for Ebola fever are based on the use of recombinant viral vectors expressing the protective antigen GP, a full-length Ebola virus surface glycoprotein.

Phase 3 clinical trials of a recombinant vesicular stomatitis virus (VSV)-based vaccine have now been completed. VSV-based vaccines encoding GP of the Zaire (1995 Kikwit) and Sudan Ebola virus have demonstrated efficacy in a series of preclinical trials in primates [22, 23]. The high immunogenicity of a VSV-based vaccine has been demonstrated in a series of clinical trials [24, 25]: The vaccine induced a high level of GP-specific antibodies (*Table*) associated with protection in primate studies. Clinical trials conducted in Europe and Africa have demonstrated that the use of a VSV-based vaccine at various doses leads to the induction of the humoral immune response, with the levels of GP-specific antibodies being similar. Phase 3 clinical trials in Guinea (using ring vaccination) demonstrated 100% efficacy of the vaccine [26, 27].

A recombinant human adenovirus serotype 5 (Ad5)-based vaccine encoding full-length 2014 ZEBOV GP passed phase 1 clinical trials in China [28, 29]. Administration of a high vaccine dose (1.6×10^{11} vp) induced a high level of GP-specific antibodies at a titer of 1 : 1,306 in 100% of volunteers 1 month after vaccination, and the T-cell response had a maximum on day 14 but decreased by day 28 of the study. Six months after vaccination, the GP antibody titer significantly decreased and amounted to 1 : 198 (*Table*). The volunteers were re-vaccinated 6 months after the primary vaccination. Four weeks after the re-vaccination, the vaccine induced a high level of GP-specific antibodies (titer of 1 : 11,825) in the blood serum of the volunteers. One year after the revaccination, the titer of GP-specific antibodies in the blood serum of the volunteers was 1 : 857. One of the main problems limiting the use of Ad5-based vectors is a wide prevalence of pre-existing immunity to Ad5 (the presence of Ad5 neutralizing antibodies) in the population. The presence of Ad5 antibodies before vaccination was shown to lead to the induction of a lower GP-specific humoral and T-cell response after vaccination [29, 30]. However, clinical trials in China demonstrated that the use of a high dose of an Ad5-based vaccine may reduce the negative effect of pre-existing immunity on the formation of a GP-specific immune response [29].

Another way to solve the problem of pre-existing immunity to a vaccine vector is to use recombinant vector serotypes with rare pre-existing immunity in the human population [31]; e.g., human adenovirus serotype 26 or adenovirus chimpanzee serotype 3 (Ad3).

The Ad3-based vaccine passed phase 1 clinical trials and progressed to phases 2 and 3. Ad3-based vaccine vectors carry the *GP* gene of the Mayinga-Zaire 1976 Ebola virus or the *GP* gene of the Gulu-Sudan Ebola virus. The results of phase 1 clinical trials conducted in the United States [32] demonstrated that the vaccine induced a high level of GP-specific antibodies (titer of 1 : 2,037) and a T-cell response, which were associated with protectivity in a NHP model. However, clinical trials in England [33] reported a low titer (1 : 469) of GP-specific antibodies (mean values did not reach levels protective for primates); the T-cell response had a maximum at day 14 of the study and decreased by day 28.

One of the problems of the developed vaccines for EVD is the reduction in the protective immune response a few months after immunization. This problem can be solved by using heterologous prime-boost vaccination (*Figure*). This vaccination strategy against Ebola was recommended by the WHO as the most promising one [34]. It should also be noted that recombinant viral vectors have certain disadvantages (pre-existing immunity to an Ad5-based vaccine vector [35], incorrect processing of target antigens when using a MVA-based vaccine vector [36], and lack of data on the duration of the protective immune response for VSV-based vaccine vectors [37]) that can be eliminated by using heterologous vaccination (*Figure*).

A series of preclinical trials in primates [38] demonstrated that homologous vaccination with an Ad3 (Ad3 + Ad3)-based vector results in 100% short-term protection (5 weeks); but with this vaccination regimen, protection decreased to 33% in 8 months. For heterologous (Ad3 + MVA) vaccination, protection was 100% 8 months after boosting.

A heterologous vaccine based on Ad3 and recombinant Modified Vaccinia Ankara (MVA) virus passed phase 1 clinical trials. Ad3-based vaccine vectors carry the *GP* gene of the Mayinga-Zaire 1976 Ebola virus or the Gulu-Sudan Ebola virus; MVA vectors (multivalent MVA-BN-filo) carry the *GP* genes of EBOV, SUDV, and MARV and the *NP* gene of TAFV. The use of heterologous vaccination enabled a many-fold amplification of both the humoral and cellular immune responses [39]. Furthermore, the use of a vaccine based on an Ad3 and MVA combination preserved high titers (1 : 1,750) of GP-specific antibodies 6 months after boosting.

Vaccines under different phases of clinical trials

Vaccine	Dose	Antigen origin	Immune response (titer of EBOV GP-specific IgGs)	Most common AE	Reference
Ad5	Low (2×10^9 vp) High (2×10^{10} vp)	EBOV SUDV	GMT: Low: 85 (Day 28) High: 155 (Day 28)	Headache	[30]
Ad5	Low (4×10^{10} vp) High (1.6×10^{11} vp)	EBOV	GMT: Low: 682.7 (Day 28) High: 1,305.7 (Day 28)	Pain at the injection site	[28]
Ad5	Prime-boost (6 months) Low (4×10^{10} vp) High (1.6×10^{11} vp)	EBOV	GMT: Low: 682.7 (Day 28) 575.5 (6 months) 6,110 (Day 28 after boosting) 674.1 (12 months after boosting) High: 1,305.7 (Day 28) 197.9 (6 months) 11,825 (Day 28 after boosting) 856.8 (12 months after boosting)	Pain at the injection site	[29]
Ad26+MVA	Group 1 Priming: Ad26 (5×10^{10} vp) Boosting: MVA (10^8 $TCID_{50}$) Group 2: Priming: MVA (10^8 $TCID_{50}$) Boosting: Ad26 (5×10^{10} vp)	EBOV; SUDV; MARV; TAFV	GMC: Group 1: 7,553 (Day 21) Group 2: 18,474 (Day 21)	Pain at the injection site	[41]
ChAd3	Low (2×10^{10} vp) High (2×10^{11} vp)	EBOV; SUDV	GMT: Low: 331 (Day 28) High : 2,037 (Day 28)	Fever	[32]
ChAd3+MVA	Priming: ChAd3 Group 1 (1×10^{10} vp) Group 2 (2.5×10^{10} vp) Group 3 (5×10^{10} vp) Boosting: MVA 1.5×10^8 PFU 3×10^8 PFU	EBOV; SUDV; MARV; TAFV	GMT: Priming: 758 (6 months) Boosting: 1,750 (6 months)	Pain at the injection site	[33, 42]
ChAd3	Group 1 (2.5×10^{10} vp) Group 2 (5×10^{10} vp)	EBOV; SUDV	GMC: Group 1: 51 μg/ml (Day 28) Group 2: 44.9 μg/ml (Day 28)	Fatigue	[43]
ChAd3+MVA	Priming: ChAd3 Group 1 (1×10^{10} vp) Group 2 (2.5×10^{10} vp) Group 3 (5×10^{10} vp) Group 4 (1×10^{11} vp) Boosting: MVA 2×10^8 vp	EBOV; SUDV; MARV; TAFV	GMT: Priming Group 1: 295.0 (Day 28) Group 2: 204.6 (Day 28) Group 3: 555.8 (Day 28) Group 4: 1,493.6 (Day 28) Boosting: 9,279.6 (Day 28)	Pain at the injection site	[39]
rVSV	Sites 1&2: Group 1 (3×10^6 PFU) Group 2 (2×10^7 PFU) Site 3: Group 1 (3×10^5 PFU) Group 2 (3×10^6 PFU) Site 4: Group 1 (1×10^7 PFU) Group 2 (5×10^7 PFU)	EBOV	GMT: Site 1: Group 1: 1392.9 (Day 28) Group 2: 1969.8 (Day 28) Site 2: Group 1: 1492.9 (Day 28) Group 2: (-) (Day 28) Site 3: Group 1: 1055.6 (Day 28) Group 2: 2570.9 (Day 28) Site 4: Group 1: 1064.2 (Day 28) Group 2: 1780.1 (Day 28)	Pain at the injection site	[24]

rVSV	Group 1 (3×10^5 PFU)	EBOV	GMT: Group 1: 344.5 (Day 28)	Pain at the injection site	[44]
rVSV	Group 1 (3×10^6 PFU) Group 2 (2×10^7 PFU)	EBOV	GMT: Group 1: 1,300 (Day 28) Group 2: 4,079 (Day 28)	Pain at the injection site	[25]
rVSV	Group (2×10^7 PFU)	EBOV	–	Pain at the injection site	[26]
DNA	Group 1 (2.0 mg) Group 2 (4.0 mg) Group 3 (8.0 mg)	EBOV; SUDV	–	Local reactions	[15]
DNA	Priming: Group (4.0 mg) Boosting: Group (4.0 mg)	EBOV; SUDV; MARV	GMT: Group: 31.8 (Day 28)	Pain at the injection site	[45]
DNA	Group (4.0 mg)	EBOV; SUDV; MARV	GMT: Group: 31.0 (Day 28)	Pain at the injection site	[46]
VSV+Ad5	Group 1: Priming VSV 1.25×10^7 PFU Boosting Ad 1.25×10^{11} vp Group 2: Priming VSV 2.5×10^7 PFU Boosting Ad 2.5×10^{11} vp	EBOV	Group 1: 33.51 (Day 21) 343.1 (Day 28) 2,540 (Day 42) Group 2: 55.49 (Day 21) 1,230 (Day 28) 3,277 (Day 42)	Pain at the injection site	[40]

In Russia, a heterologous combined vectored EVD vaccine for prime-boost vaccination was developed in accordance with the WHO recommendations. It was based on two recombinant viral vectors expressing the Ebola virus glycoprotein: a recombinant vesicular stomatitis virus (VSV-GP) and a recombinant human adenovirus serotype 5 (Ad-GP) [40].

A series of preclinical trials in primates demonstrated that immunization with this vaccine provides 100% protection from infection to animals both 3 weeks after immunization and 5 months after immunization.

Clinical trials of safety and immunogenicity demonstrated that the vaccine provides high safety and immunogenicity levels to healthy volunteers.

No serious adverse events (AEs) occurred during the vaccine safety study. All AEs were mild or moderate, developed within the first 2 days after vaccination, and resolved within the next 3 days. The most common AEs were pain at the injection site, headache, and weakness/fatigue. These AEs are typical of most recombinant viral vectored vaccines.

The vaccine efficacy was assessed using various parameters of the humoral and cellular immune responses: The seroconversion level was 100%. The mean titer of ZEBOV-GP-specific IgGs on day 42 of the study was 1 : 3,277 in a group receiving a full dose of the vaccine. Importantly, immunization with VSV-GP alone, at the same dose, induced antibodies in a titer of 1 : 538 to day 42, which was significantly lower than the titers obtained with heterologous vaccination. On day 28, a virus neutralization assay detected virus neutralizing antibodies with a mean titer of 1 : 20 in 93.1% of volunteers receiving a full dose of the vaccine. The cellular immune response was assessed by IFN-gamma production in peripheral blood mononuclear cells after antigen challenge: a response was detected in 100% of the volunteers on day 42 of the study.

Despite the published data on the negative effect of pre-existing immunity to adenoviruses, there was no significant correlation between the level of Ad5 neutralizing antibodies and the level of a GP-specific humoral and cellular response in the case of immunization of healthy volunteers with the VSV- and Ad-based vaccine. This indicates that the use of heterologous vaccination neutralizes the negative effect of pre-existing immunity to human adenovirus serotype 5-based vaccine vectors.

Based on the findings of preclinical and clinical trials demonstrating its high vaccine efficacy and safety, the EVD vaccine developed and produced at the Gamaleya Research Center for Epidemiology and Microbiology was licensed in the Russian Federation in 2015.

CONCLUSION

EVD poses a serious threat to global security. Since 1976 when the Ebola virus was first detected, more than 20 outbreaks have been recorded. They have mainly occurred in the rural areas of East and Central

Africa. But in 2014, the outbreak that began in three countries in West Africa changed the situation. These were the first cases when the virus was detected in urban centers, and the virus could spread outside of Africa to Europe and North America.

The spread of the Ebola virus outside of Africa during the 2014–2016 EVD epidemic and the high mortality rate were a solid reason for the active development of effective preventive and therapeutic remedies. To date, various clinical trials in Africa, Europe, the U.S., and Russia have shown the good safety and immunogenicity profiles of several EVD vaccines. Eight vaccines are now under different phases of clinical trial. Two vaccines ("GamEvac" and "GamEvac-Combi") developed and produced at the Gamaleya Research Center for Epidemiology and Microbiology are currently the only licensed vaccines for Ebola fever: The "GamEvac-Combi" vaccine is a heterologous VSV- and Ad5-vectored vaccine, and the "GamEvac" vaccine is a homologous Ad5-vectored vaccine.

In conclusion, it should be noted that despite the high price already paid, mankind has learned an important lesson: It has become obvious that a timely drive against global threats to public health is possible only if the efforts of political leaders, WHO experts, and key pharmaceutical players are consolidated. The combined work of experts from different fields enabled the fast introduction of novel advanced vaccines into practical medicine.

Obviously, the gained experience will be used in the future for the timely development of vaccines for other dangerous viral infections, the preventive measures for which are absent at the moment (severe acute respiratory syndrome, Middle East respiratory syndrome caused by coronavirus, Zika virus disease, etc.).

REFERENCES

1. Fields virology. 5th ed. / Eds Knipe D.M., Howley P.M. Philadelphia: Lippincott Williams & Wilkins, 2006. P. 1409–1448.
2. Taylor D., Leach R., Bruenn J. // BMC Evolutionary Biology. 2010. V. 10. P. 193.
3. Bennett J.E., Dolin R., Blaser M.J. Mandell, Douglas, and Bennett's Principles and Practice of Infectious Diseases. 8th ed. Philadelphia: Elsevier, 2015. P. 1995–1999.
4. Hartman A.L., Towner J.S., Nichol S.T. // Clin. Lab. Med. 2010. V. 30. P. 161–177.
5. Kuhn J.H., Becker S., Ebihara H., Geisbert T.W., Johnson K.M., Kawaoka Y., Lipkin W.I., Negredo A.I., Netesov S.V., Nichol S.T., et al. // Arch. Virol. 2010. V. 155. № 12. P. 2083–2103.
6. Ebola haemorrhagic fever in Zaire, 1976. Report of an International Commission. // Bull. WHO. 1978. V. 56. № 2. P. 271–293.
7. Ebola haemorrhagic fever in Sudan, 1976. Report of an International Commission. // Bull. WHO. 1978. V. 56. № 2. P. 247–270.
8. World Health Organization. 2015. Ebola Situation Report-21.
9. Borisevich I.V., Krasnjanskij V.P., Lebedinskaja E.V., Mihajlov V.V., Timan'kova G.D., Chernikova N.K. Preparat, soderzhashhij immunoglobulin protiv lihoradki Jebola iz syvorotki krovi loshadej, zhidkij (immunoglobulin Jebola). Patent RF № 2130318. 20.05.1999.
10. Lupton H.W., Lambert R.D., Bumgardner D.L., Moe J.B., Eddy G.A. // Lancet. 1980. V. 2. P. 1294–1295.
11. Geisbert T.W., Pushko P., Anderson K., Smith J., Davis K.J., Jahrling P.B. // Emerging Infectious Diseases. 2002. V. 8. P. 503–507.
12. Volchkov V.E., Becker S., Volchkova V.A., Ternovoj V.A., Kotov A.N., Netesov S.V., Klenk H.D. // Virology. 1995. V. 214. № 2. P. 421–430.
13. Dowling W., Thompson E., Badger C., Mellquist J.L., Garrison A.R., Smith J.M., Paragas J., Hogan R.J., Schmaljohn C. // J. Virol. 2007. V. 81. № 4. P. 1821–1837.
14. Vanderzanden L., Bray M., Fuller D., Roberts T., Custer D., Spik K., Jahrling P., Huggins J., Schmaljohn A., Schmaljohn C. // Virology. 1998. V. 246. P. 134–144.
15. Martin J.E., Sullivan N.J., Enama M.E., Gordon I.J., Roederer M., Koup R.A., Bailer R.T., Chakrabarti B.K., Bailey M.A., Gomez P.L., et al. // Clin. Vaccine Immunol. 2006. V. 13. № 11. P. 1267–1277.
16. Sullivan N.J., Geisbert T.W., Geisbert J.B., Xu L., Yang Z.Y., Roederer M., Koup R.A., Jahrling P.B., Nabel G.J. // Nature. 2003. V. 424. № 6949. P. 681–684.
17. Jones S.M., Feldmann H., Ströher U., Geisbert J.B., Fernando L., Grolla A., Klenk H.D., Sullivan N.J., Volchkov V.E., Fritz E.A., et al. // Nat. Med. 2005. V. 11. № 7. P. 786–790.
18. Sridhar S. // Ther. Adv. Vaccines. 2015. V. 3. № 5–6. P. 125–138.
19. Wilson J.A., Hart M.K. // J. Virol. 2001. V. 75. № 6. P. 2660–2664.
20. Sullivan N.J., Hensley L., Asiedu C., Geisbert T.W., Stanley D., Johnson J., Honko A., Olinger G., Bailey M., Geisbert J.B., et al. // Nat. Med. 2011. V. 17. № 9. P. 1128–1131.
21. Dahlke C., Lunemann S., Kasonta R., Kreuels B., Schmiedel S., Ly M.L., Fehling S.K., Strecker T., Becker S., Altfeld M., et al. // J. Infect. Dis. 2017. V. 215. № 2. P. 287–292.
22. Geisbert T.W., Daddario-Dicaprio K.M., Lewis M.G., Geisbert J.B., Grolla A., Leung A., Paragas J., Matthias L., Smith M.A., Jones S.M., et al. // PLoS Pathog. 2008. V. 4. № 11. e1000225.
23. Geisbert T.W., Geisbert J.B., Leung A., Daddario-DiCaprio K.M., Hensley L.E., Grolla A., Feldmann H. // J. Virol. 2009. V. 83. № 14. P. 7296–7304.
24. Agnandji S.T., Huttner A., Zinser M.E., Njuguna P., Dahlke C., Fernandes J.F., Yerly S., Dayer J.A., Kraehling V., Kasonta R., et al. // N. Eng. J. Med. 2015. PMID: 25830326. http://dx.doi.org/10.1056/NEJMoa1502924.
25. Regules J.A., Beigel J.H., Paolino K.M., Voell J., Castellano A.R., Munoz P., Moon J.E., Ruck R.C., Bennett J.W., Twomey P.S., et al. // N. Eng. J. Med. 2015. PMID: 25830322. http://dx.doi.org/10.1056/NEJMoa1414216.

26. Henao-Restrepo A.M., Longini I.M., Egger M., Dean N.E., Edmunds W.J., Camacho A., Carroll M.W., Doumbia M., Draguez B., Duraffour S., et al. // Lancet. 2015. V. 386. P. 857–866.
27. Henao-Restrepo A.M., Camacho A., Longini I.M., Watson C.H., Edmunds W.J., Egger M., Carroll M.W., Dean N.E., Diatta I., Doumbia M., et al. // Lancet. 2017. V. 389. № 10068. P. 505–518.
28. Zhu F., Hou L., Li J., Wu S., Liu P., Zhang G., Hu Y., Meng F., Xu J., Tang R., et al. // Lancet. 2015. V. 385. № 9984. P. 2272–2279.
29. Li J.X., Hou L.H., Meng F.Y., Wu S.P., Hu Y.M., Liang Q., Chu K., Zhang Z., Xu J.J., Tang R., et al. // Lancet Glob Hlth. 2016. V. 5. № 3. P. e324–e334.
30. Ledgerwood J.E., Costner P., Desai N., Holman L., Enama M.E., Yamshchikov G., Mulangu S., Hu Z., Andrews C.A., Sheets R.A., et al. // Vaccine. 2010. V. 29. № 2. P. 304–313.
31. Ersching J., Hernandez M.I., Cezarotto F.S., Ferreira J.D., Martins A.B., Switzer W.M., Xiang Z., Ertl H.C., Zanetti C.R., Pinto A.R. // Virology. 2010. V. 407. № 1. P. 1–6.
32. Ledgerwood J.E., DeZure A.D., Stanley D.A., Novik L., Enama M.E., Berkowitz N.M., Hu Z., Joshi G., Ploquin A., Sitar S., et al. // N. Eng. J. Med. 2014. PMID: 25426834. http://dx.doi.org/10.1056/NEJMoa1410863.
33. Rampling T., Ewer K., Bowyer G., Wright D., Imoukhuede E.B., Payne R., Hartnell F., Gibani M., Bliss C., Minhinnick A., et al. // N. Eng. J. Med. 2015. PMID: 25629663. http://dx.doi.org/10.1056/NEJMoa1411627.
34. Moorthy V., Fast P., Greenwood B. Heterologous Prime-Boost immunisation in Ebola vaccine development, testing and licensure. Report of a WHO Consultation held on 21 November 2014, Geneva, Switzerland
35. Fausther-Bovendo H., Kobinger G. // Hum. Vaccin. Immunother. 2014. V. 10:10. P. 2875–2884.
36. VanSlyke J.K., Hruby D.E. // Curr. Top. Microbiol. Immunol. 1990. V. 163. P. 185–206.
37. National Academies of Sciences, Engineering, and Medicine. The Ebola Epidemic in West Africa: Proc. Workshop. Washington, DC: Nat. Acad. Press, 2016. P. 56–58.
38. Stanley D.A., Honko A.N., Asiedu C., Trefry J.C., Lau-Kilby A.W., Johnson J.C., Hensley L., Ammendola V., Abbate A., Grazioli F., et al. // Nat. Med. 2014. V. 20. № 10. P. 1126–1129.
39. Tapia M.D., Sow S.O., Lyke K.E., Haidara F.C., Diallo F., Doumbia M., Traore A., Coulibaly F., Kodio M., Onwuchekwa U., et al. // Lancet Infect. Diseases. 2016. V. 16. P. 31–42.
40. Dolzhikova I.V., Zubkova O.V., Tukhvatulin A.I., Dzharullaeva A.S., Tukhvatulina N.M., Shcheblyakov D.V., Shmarov M.M., Tokarskaya E.A., Simakova Y.V., Egorova D.A., et al. // Hum.Vaccin. Immunother. 2017. P. 1–8. doi: 10.1080/21645515.2016.1238535. [Epub ahead of print]
41. Milligan I.D., Gibani M.M., Sewell R., Clutterbuck E.A., Campbell D., Plested E., Nuthall E., Voysey M., Silva-Reyes L., McElrath M.J., et al. // JAMA. 2016. V. 315. P. 1610–1623.
42. Ewer K., Rampling T., Venkatraman N., Bowyer G., Wright D., Lambe T., Imoukhuede E.B., Payne R., Fehling S.K., Strecker T., et al. // N. Eng. J. Med. 2016. V. 374. P. 1635–1646.
43. De Santis O., Audran R., Pothin E., Warpelin-Decrausaz L., Vallotton L., Wuerzner G., Cochet C., Estoppey D., Steiner-Monard V., Lonchampt S., et al. // Lancet Infect. Dis. 2016. V. 16. P. 311–320.
44. Huttner A., Dayer J.A., Yerly S., Combescure C., Auderset F., Desmeules J., Eickmann M., Finckh A., Goncalves A.R., Hooper J.W., et al. // Lancet Infect. Dis. 2015. V. 15. P. 1156–1166.
45. Sarwar U.N., Costner P., Enama M.E., Berkowitz N., Hu Z., Hendel C.S., Sitar S., Plummer S., Mulangu S., Bailer R.T., et al. // J. Infect. Dis. 2015. V. 211. P. 549–557.
46. Kibuuka H., Berkowitz N.M., Millard M., Enama M.E., Tindikahwa A., Sekiziyivu A.B., Costner P., Sitar S., Glover D., Hu Z., et al. // Lancet. 2015. V. 385. P. 1545–1554.

Non-bulky Lesions in Human DNA: The Ways of Formation, Repair, and Replication

A.V. Ignatov[1,2], K.A. Bondarenko[1], A.V. Makarova[1]*
[1]Institute of Molecular Genetics of Russian Academy of Sciences, Kurchatov sq. 2, Moscow, 123182, Russia
[2]Department of Molecular Biology, Faculty of Biology, Moscow State University, Leninskie Gory 1, bldg. 12, Moscow, 119991, Russia
*E-mail: amakarova-img@yandex.ru
Received: September 10, 2016; in final form May 29, 2017

ABSTRACT **DNA damage is a major cause of replication interruption, mutations, and cell death. DNA damage is removed by several types of repair processes. The involvement of specialized DNA polymerases in replication provides an important mechanism that helps tolerate persistent DNA damage. Specialized DNA polymerases incorporate nucleotides opposite lesions with high efficiency but demonstrate low accuracy of DNA synthesis. In this review, we summarize the types and mechanisms of formation and repair of non-bulky DNA lesions, and we provide an overview of the role of specialized DNA polymerases in translesion DNA synthesis.**
KEYWORDS **DNA damage, DNA repair, DNA translesion synthesis.**
ABBREVIATIONS **AP sites – apurinic/apyrimidinic sites; BER – base excision repair; ROS – reactive oxygen species; 5'-dRP – 5'-2-deoxyribose-5-phosphate; DRR – direct reversal repair; NER – nucleotide excision repair; NIR – nucleotide incision repair; FapyA – 4,6-diamino-5-formamidopyrimidine; FapyG – 2,6-diamino-4-hydroxy-5-formamidopyrimidine; 5,6-DHU – 5,6-dihydrouracil; 5-oh-U – 5-hydroxyuracil; 8-oxo-G – 7,8-dihydro-8-oxoguanine; 5-oh-C – 5-hydroxycytosine; N1-me-A – N1-methyladenine; N3-me-A – N3-methyladenine; N5-me-C – 5-methylcytosine; N7-me-G – N7-methylguanine; O^6-me-G – O^6-methylguanine; SAM – S-adenosylmethionine; N^2-et-G – N^2-ethylguanine; TG – thymidine glycol; εA – 1,N^6-ethenoadenine; 1,2-εG – 1,N^2-ethenoguanine; 2,3-εG – N^2,3-ethenoguanine; εC – 3,N^4-ethenocytosine.**

INTRODUCTION

Numerous lesions occur daily in the DNA of living organisms, either spontaneously or caused by various chemical and physical factors, such as free radicals, ultraviolet (UV) and ionizing radiation, cell metabolites, and chemical carcinogens. In addition, DNA lesions occur during physiological cellular reactions (e.g., intermediates of DNA repair and hypermutation of immunoglobulin genes).

Chemical carcinogens, such as acrolein, cisplatin, benzo[α]pyrene, aromatic amines, nitrosamines, and UV radiation result in the preferential formation of bulky adducts, intra- and interstrand crosslinks, which substantially distort the geometry of the framework of DNA [1]. These lesions are eliminated from genomic DNA mainly by nucleotide excision repair (NER) [2, 3]. The unrepaired bulky lesions significantly inhibit the activity of the high-fidelity DNA polymerases (Pols) that are specifically involved in genomic DNA replication and are guided by the strict geometric complementarity during nucleotide incorporation [4–6]. The accumulation of these lesions in dividing cells results in replication interruption, chromosomal aberrations, and cell death.

Spontaneous DNA lesions and those formed during cell metabolism or resulting from free radical attacks are mostly non-bulky. The main groups of non-bulky DNA lesions include apurinic/apyrimidinic sites (AP sites), oxidized and some alkylated nucleotide derivatives, as well as lesions caused by deamination of DNA bases. Base excision repair (BER) is the key mechanism for the elimination of such lesions. The BER machinery has been discussed in detail in several recent reviews [7–9]. Although non-bulky lesions have a lesser effect on the DNA structure, they also alter the function of DNA replication enzymes by causing DNA copying errors and blocking replication.

In the present review, we systematize the main pathways of formation, repair, and replication of non-bulky DNA lesions and discuss the role of the specialized human Pols that ensure efficient, although often error-prone, translesion DNA synthesis.

TYPES OF DNA LESIONS AND THEIR FORMATION

Apurinic and apyrimidinic sites

Apurinic and apyrimidinic sites (AP sites), the most frequent DNA lesions, play a crucial role in mutagenesis induced by genomic DNA damage. The average number of AP sites that emerge daily in a mammalian cell is 9,000–14,000 [10, 11]. Most AP sites are a result of the spontaneous hydrolysis of the N-glycosidic bond in deoxyribonucleotides that occurs under physiological conditions at a considerably high rate [12]. The cleavage rate of purine bases (apurination) is more than 10-fold higher than that of pyrimidine bases [11]. The glycosidic bond cleavage is also catalyzed by DNA glycosylases during BER [13]. Finally, the formation of AP sites is a key stage in the hypermutation of immunoglobulin genes in mammals [14, 15].

AP sites simultaneously exhibit high mutagenic and cytotoxic properties. Since no canonical hydrogen bonds can be formed with AP sites, many Pols are paused or incorporate dAMP opposite the lesion (*Table*) [16–19]. Incorporation of dAMP opposite an AP site is energetically more favourable [20]. In the lagging DNA strand, AP sites inhibit strand displacement synthesis by Pol δ during replication, thereby disrupting Okazaki fragment maturation [21]. Unrepaired AP sites cause transcription termination and are responsible for the high frequency of mutagenesis in *Saccharomyces cerevisiae* [22]. AP sites in human DNA are predominantly recognized and cleaved by AP endonuclease 1 (APE1), yielding single-strand breaks [23, 24]. It should be noted that many other proteins have recently been found to play a role in the alternative pathways of APE1-independent repair of AP sites: subunits of the Ku protein that is a component of DNA-dependent protein kinase (DNA-PK) [25–27], tyrosyl-DNA phosphodiesterase I (TDP1) [28, 29], and poly(ADP-ribose) polymerase 1 (PARP1) [30]. The alternative pathways of AP site repair can act as auxiliary DNA repair mechanisms. The functions of Ku and TDP1 proteins in the repair of an AP site have been discussed more thoroughly in previous reviews [31, 32].

Oxidized nucleobase derivatives

DNA bases are oxidized in cells when they interact with reactive oxygen species (ROS) formed by ionizing radiation or produced under physiological conditions. The frequency of ROS-induced damage in mitochondrial DNA is much higher than that of nuclear DNA [33]. Different ROS vary in their reactivity. The superoxide radical ($O_2^{\cdot}$) and hydrogen peroxide (H_2O_2) are weakly reactive, while the hydroxyl radical ($OH^{\cdot}$) is extremely reactive and damages all four DNA bases; singlet oxygen ($^1O_2$) predominantly attacks guanine residues [34–36]. Oxidative stress is responsible for more than a hundred types of DNA lesions [34]. The most common and biologically relevant oxidized derivatives of nucleobases include 7,8-dihydro-8-oxoguanine (8-oxo-G), thymidine glycol (TG), 5-hydroxycytosine (5-oh-C), 2,6-diamino-4-hydroxy-5-formamidopyrimidine (FapyG), and 4,6-diamino-5-formamidopyrimidine (FapyA) (*Fig. 1*). Formamidopyrimidine lesions result from the opening of the imidazole ring caused by the attack of ROS [35, 37–39].

8-oxo-G and TG are among the most common DNA lesions induced by ROS. 1,000–2,000 8-oxo-G and up to 2,000 TG are formed daily in a single human cell [35]. 8-oxo-G is a highly mutagenic lesion. Most Pols incorporate opposite 8-oxo-G dAMP by forming Hoogsteen hydrogen bonds and giving rise to GC→TA transversions (*Table*) [40–42]. TG is a non-mutagenic but highly toxic lesion that suppresses the activity of replication enzymes (*Table*) [43, 44]. The mechanisms that reduce the mutagenic potential of oxidative nucleotide damage in cells are complex and include alternative variants of repair.

DNA damage caused by deamination of DNA bases

Loss of an amino group by DNA bases in the cell occurs either spontaneously [45, 46] or as a result of oxidative deamination induced by reactive nitrogen species (e.g., those formed by inflammation) [47–49] or is generated ezymatically. Deamination of cytosine residues by cytidine deaminases and the subsequent excision of uracil yielding AP sites play a crucial role in mutagenesis during the maturation of the variable regions of immunoglobulin genes in B lymphocytes in mammals [14, 15].

Single-stranded DNA (e.g., DNA being replicated or actively transcribed) undergoes deamination much more often (over 100 times) than the double-stranded DNA [50, 51]. Pyrimidine residues are more prone to spontaneous deamination than purines [51, 52]; however, purine bases undergo oxidative deamination more frequently [53]. Cytosine deamination that yields uracil is most common in the cell (*Fig. 1*). An average of 100–500 cytosine residues are deaminated daily, generating uracil in a single mammalian cell [45, 51, 54]. Uracil derivatives, 5-hydroxyuracil (5-oh-U) and 5,6-dihydrouracil (5,6-DHU), can be formed by cytosine deamination and the simultaneous attack by free radicals or ionizing radiation (*Fig. 1*) [55, 56]. Genomic DNA also contains deamination products of adenine (hypoxanthine) and guanine (xanthine and oxanine) (*Fig. 1*). The frequency of hypoxanthine and xanthine formation is 1–7 per 10^6 nucleotides [57–59]. Deaminated DNA bases do not disrupt the functioning of eukaryotic Pols but have a high mutagenic potential, generating point

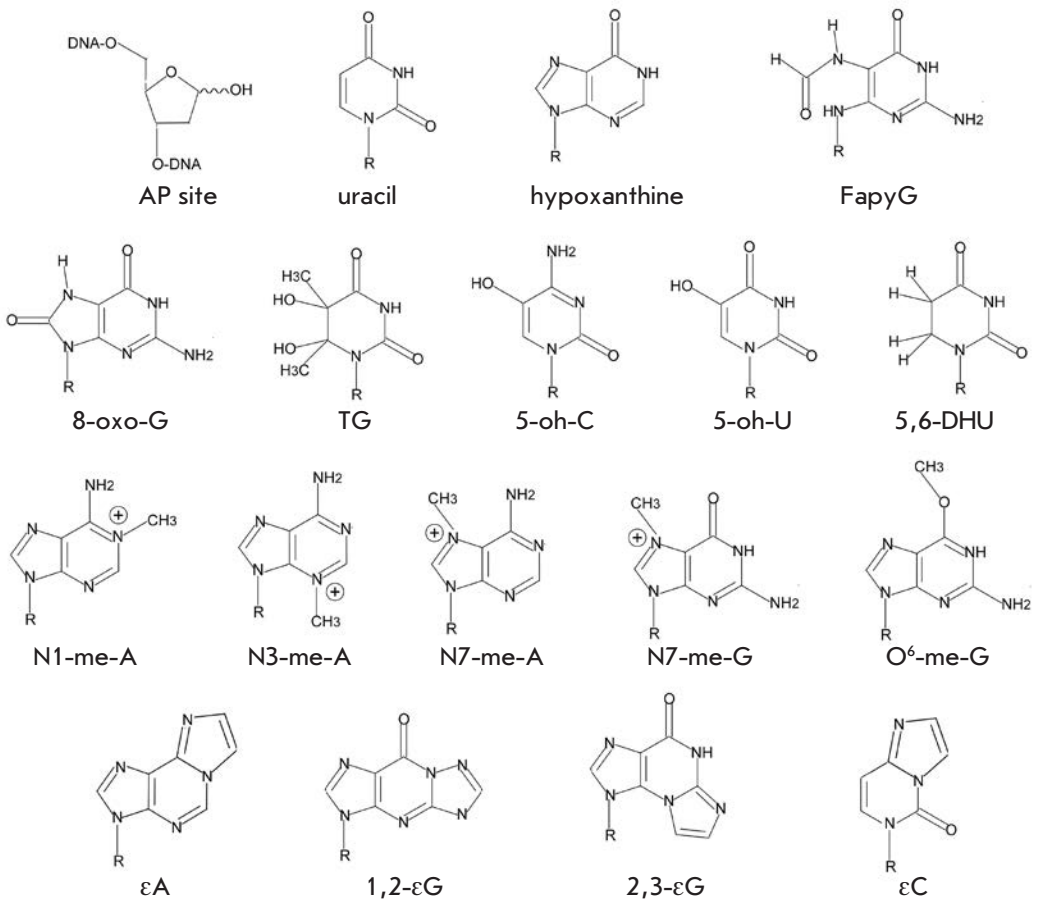

Fig. 1. Common non-bulky DNA lesions

mutations. Eukaryotic Pols incorporate dAMP opposite uracil, resulting in GC→AT transversions in the subsequent replication rounds (*Table*) [60]. Furthermore, dCMP is preferentially incorporated opposite hypoxanthine, causing the AT→GC transversion [61–63]. Xanthine and oxanine form hydrogen bonds with thymine, thereby causing GC→AT transversions during replication [64].

Deamination of 5-methylcytosine (5-me-C), which generates thymine and causes direct GC→AT transversions, also makes a significant contribution to DNA mutagenesis [45]. Although only 3% of cytosine residues in human genomic DNA is methylated, 70–80% of the GpG islands that suppress gene expression contain 5-me-C and, thus, act as mutagenesis hot spots in dividing mammalian cells [65, 66].

The lesions caused by deamination of DNA bases are predominantly repaired via the BER pathway.

Alkylated nucleobase derivatives

Exogenous alkylating agents are electrophilic compounds that exhibit an affinity for the nucleophilic centers of organic molecules and include a broad range of chemical agents which play a significant role in nucleobase alkylation. For example, exogenous alkylating agents are present in food as nitrosamines (N-nitrosodimethylamine and N-nitrosodiethylamine are formed by the interaction between amines and nitrites during smoking or intensive thermal treatment) [67, 68] and are found in the environment as haloalkanes (vinyl chloride used as a raw material in the plastics industry, agricultural fumigant bromomethane, and the coolant chloromethane) [69–71]. Some alkylating compounds, such as cyclophosphamide, melphalan, busulfan, and temozolomide, are widely used in chemotherapy [72, 73]. According to their nucleophilic substitution mechanism, alkylating agents can be subdivided into S_N1-type (monomolecular substitution with an intermediate formation: nitrogen mustard, N-nitroso-N-methylurea) and S_N2-type compounds (one-stage bimolecular substitution: methyl methanesulfonate, dimethyl sulfate, and busulfan) [74, 75].

All four DNA bases have been found to contain numerous potential sites of alkylation (N1, N3, N^6, and N7 in adenine; N1, N^2, N3, N7, and O^6 in guanine; N3, N^4, and O^2 in cytosine; and N3, O^2, and O^4 in thymine); however, all these sites differ in reactivity. The common and biologically important alkylated nucleobase

derivatives include N3-methyladenine (N3-me-A), O^6-methylguanine (O^6-me-G), 1-methyladenine (N1-me-A), N7-methylguanine (N7-me-G), and N^2-ethylguanine (N^2-et-G) (*Fig. 1*) [74–77]. The most common N-methylation products are N7-me-G and N3-me-A. N7-me-G may account for up to 70–80% of methylated DNA lesions.

Endogenous genotoxic agents also contribute to the alkylation of DNA bases. S-adenosylmethionine (SAM) is a weak alkylating agent that acts as a methyl group donor in cellular transmethylation reactions. Approximately 4,000, 600, and 10–30 residues of 7-me-G, 3-me-A and O^6-me-G, correspondingly, [78, 79] are believed to be formed daily in mammalian cells in SAM-mediated reactions.

N3-me-A accumulation is cytotoxic, because it blocks replication due to the disruption of the contacts between the polymerase active site and the N3 atom of adenine in the minor groove of DNA (*Table*) [80–82]. Studies of the effect of N7-me-G on the functions of Pols are challenging because of the high instability of the damaged base. Methylated guanine residues do not inhibit Pol I function in *Escherichia coli* [83]. However, it has been recently demonstrated using a chemically stable N7-me-G analogue that human Pol β incorporates nucleotides opposite this lesion with low efficiency and fidelity (*Table*) [84]. N7-me-G can undergo spontaneous depurination to yield cytotoxic AP sites [75]. Furthermore, N7-me-G with the opened imidazole ring (me-Fapy-G) inhibits replication [85, 86]. O^6-me-G is generated predominantly as a result of DNA exposure to S_N1-type chemical agents [78]. This lesion exhibits mutagenic and carcinogenic properties, because it forms bonds with thymine and causes GC→AT transversions during replication [87–89]. O^6-me-G can also suppress the function of certain Pols (*Table*) [90, 91]. Direct reversal repair by alkyltransferases and dioxygenases plays a crucial role in the repair of non-bulky alkylated nucelobases, along with BER [92].

Exocyclic nucleobase adducts with the etheno ring (1,N^6-ethenoadenine (εA), 1,N^2-ethenoguanine (1,2-εG), N^2,3-ethenoguanine (2,3-εG), and 3,N^4-ethenocytosine (εC)) can be classified as relatively non-bulky lesions and are also repaired by the enzymes involved in the repair of alkylated DNA bases (*Fig. 1*). The formation of these adducts is caused by aldehydes resulting from lipid peroxidation by oxygen and nitrogen free radicals [93, 94], as well as some genotoxic industrial chemicals (e.g., vinyl chloride and urethane) [95]. Exocyclic DNA lesions exhibit high mutagenic and genotoxic properties both *in vitro* and *in vivo* [96–99]. The 1,N^6-etheno group disrupts the Watson-Crick interactions and suppresses the function of most Pols, including some specialized Pols (*Table*) [17, 100, 101].

REPAIR OF NON-BULKY DNA LESIONS

Base excision repair (BER)

BER plays a key role in the elimination of non-bulky DNA lesions (*Figs. 2* and *3*). BER includes two subpathways: the short-patch and long-patch BER. The short-patch BER replaces the lesion with a single nucleotide, while the long-patch BER excises 2–8 nucleotides [102].

The classic BER pathway consists of the following key steps: 1) elimination of a damaged base: damage recognition and cleavage of the N-glycosidic bond by a specific multifunctional DNA glycosylase, yielding an AP site; 2) hydrolysis of the phosphodiester bond at the 5' end of the AP site by AP endonuclease, yielding 3'-OH and 5'-2-deoxyriboso-5-phosphate (5'-dRP); 3) excision of 5'-dRP and filling of the gap by a specialized Pol; and 4) ligation with DNA ligase (*Fig. 3*) [7–9, 102].

BER is initiated by DNA glycosylase. DNA glycosylases possessing only the glycosylase activity are known as monofunctional ones (e.g., uracil-DNA glycosylase UNG and N-methylpurine DNA glycosylase MPG, NEIL3) [103–105]. In this case, the AP site is cleaved by AP endonuclease APE1 [23, 106]. However, a number of DNA glycosylases simultaneously exhibit the DNA glycosylase and AP lyase activities: OGG1 (weak AP lyase activity), NEIL1, NEIL2, and NTH1. These DNA glycosylases are known as bifunctional: they excise a damaged base and hydrolyse DNA strands at the 3' end of the AP site to form a 3'-α,β-unsaturated aldehyde group (3'-α,β-4-hydroxypentene-2-al) (NTH1 and OGG1) or 3'-phosphate (NEIL1 and NEIL2) [103–105]. APE1 (3'-phosphodiesterase activity) and polynucleotide kinase/phosphatase (PNKP) (3'-phosphatase activity) are involved in the elimina-

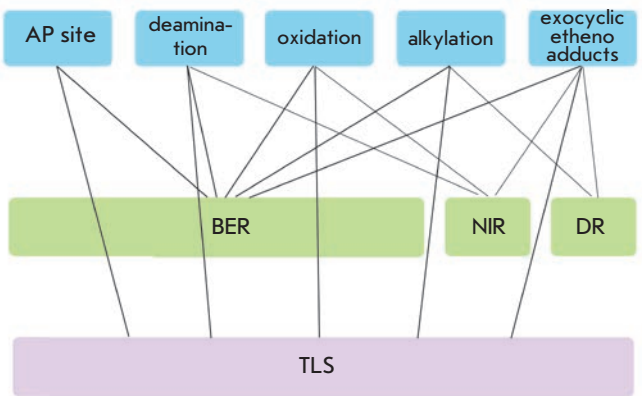

Fig. 2. Basic pathways of non-bulky DNA lesions repair in humans

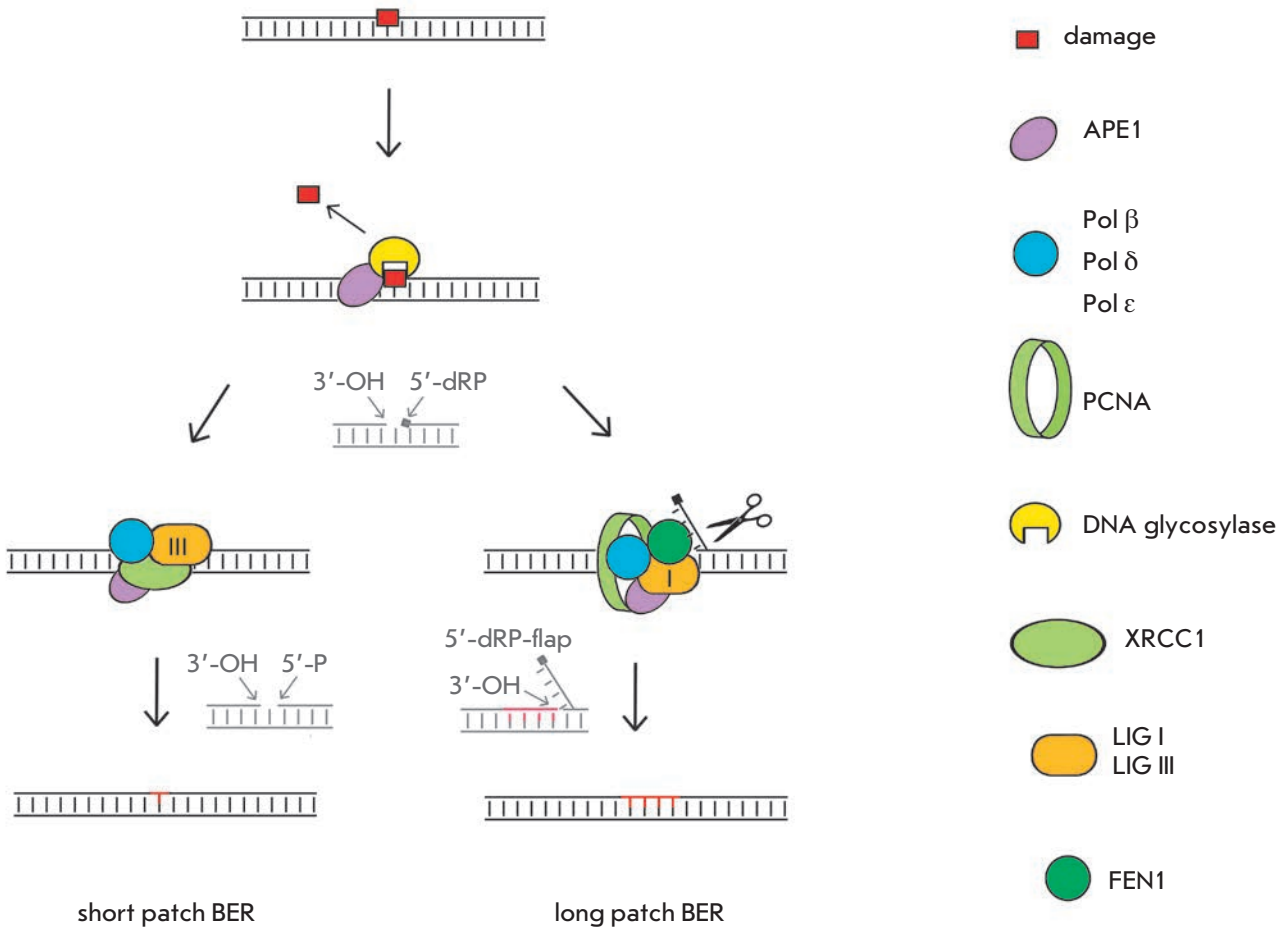

Fig. 3. The short-patch and long-patch pathways of BER in humans

tion of the 3'-aldehyde group and 3'-P, respectively [107–109].

In most cases, DNA lesions are repaired by the short-patch sub-pathway of BER. The XRCC1 protein (X-ray repair cross-complementing protein 1) plays a crucial role in the regulation of enzymatic activity during the short-patch BER and carries out structural and coordinating functions. [110, 111]. However, in some cases, BER occurs via the long-patch sub-pathway. In the latter case, the enzymatic functions are coordinated by the DNA clamp PCNA (proliferating cell nuclear antigen) and clamp loader RFC (replication factor C) [112]. The mechanisms that control the BER pathway selection have not been elucidated yet. The long-patch sub-pathway may be preferable in the S-phase in actively dividing cells [113] or when the excision of the 5'-dRP is impeded (e.g., for AP site analogues).

Pol β belongs to the X family of DNA polymerases and is a principal enzyme responsible for DNA synthesis during BER in mammals. Pol β simultaneously exhibits the 5'-dRP-lyase activity and can both efficiently fill the gap and excise the 5'-dRP formed after the AP site cleavage by APE1 [114]. Three other Pols, Pol λ, Pol ι, and Pol θ belonging to the X, Y, and A polymerase families, respectively, also retain the 5'-dRP-lyase activity and can hypothetically be involved in BER of some DNA lesions or play the role of Pol β-backup enzymes [115–118]. The high-fidelity replicative polymerases Pol δ and Pol ε can also be implicated in the long-patch BER [119]. Pol β, Pol δ, or Pol ε performs strand displacement synthesis for a DNA strand with a lesion. This produces the flap structure formed by three DNA strands; one of these strands has an overhanging single-stranded 5'-region, which is cleaved off by flap endonuclease FEN1 [120]. DNA ligase III (LIG3α) [121] and DNA ligase I (LIG1) [122] connect two DNA strands during the short- and long-patch BER sub-pathways, respectively.

There are more than 10 different human DNA glycosylases specialized in the recognition of various types

of DNA lesions [103, 104]. A single lesion can often be recognized by several DNA glycosylases.

Uracil residues are predominantly eliminated by the monofunctional uracil-DNA glycosylases that yield AP sites during BER. Five uracil-DNA glycosylases have been identified in mammals, a fact that emphasizes the special role of cytosine deamination in mutagenesis and cytotoxicity. Two uracil-DNA glycosylase variants encoded by the *UNG* gene are known in humans: UNG1 and UNG2. The isoforms are generated by alternative splicing and reading transcripts from alternative promoters. UNG2 contributes to the repair of U:A lesions in nuclear DNA, while UNG1 is involved in the repair of uracil residues in mitochondrial DNA [123–125].

SMUG1 (single-stranded selective multifunctional uracil-DNA glycosylase 1) is likely a backup uracil-DNA glycosylase that also participates in the excision of 5-hydroxymethyluracil and oxidized pyrimidines [126, 127]. UNG1 and UNG2 excise uracil residues from single- and double-stranded DNA, while SMUG1 exhibits high activity on single-stranded DNA [128]. Mismatch-specific thymine-DNA glycosylase (TDG) and methyl-CpG-binding protein 4 (MBD4) participate in the repair of U and T mispaired with G, as well as in the repair of deaminated N5-me-C in CpG islands and, therefore, are involved in DNA demethylation and the epigenetic regulation of gene expression [129–132].

Oxidized nucleobase derivatives are predominantly repaired by bifunctional DNA glycosylases. OGG1 is the key DNA glycosylase that ensures the repair of 8-oxo-G during BER [133, 134]. Several OGG1 isoforms are generated by alternative splicing. Isoform 1a is mainly encountered in the nucleus, while isoform 2a – in mitochondria [135, 136]. Another DNA glycosylase, NEIL1, is also involved in the repair of 8-oxo-G, although its activity is much less pronounced [137, 138].

The DNA glycosylases NTH1 and NEIL1 participate in the repair of various oxidized derivatives of pyrimidine nucleotides [138–143]. NEIL2 is involved in the repair of oxidized cytosine lesions (5,6-DHU, 5-oh-U, and 5-oh-C) [144]. NEIL3 can recognize and excise various oxidized base derivatives, including TG and Fapy-purine lesions; however, its functions remain insufficiently understood [145, 146]. OGG1 and NTH1 excise lesions from double-stranded DNA, while NEIL1, NEIL2, and NEIL3 function efficiently on single-stranded DNA templates and are possibly involved in the repair of oxidized nucleobases during replication and transcription [147–150].

N-methylpurine DNA glycosylase (MPG), also known as N-alkyladenine DNA glycosylase (AAG) and 3-methyladenine DNA glycosylase (MAG), is involved in the repair of alkylated purine bases during BER. MPG is characterized by a broad substrate specificity as it recognizes and excises N3-me-A, N7-me-G, N1-me-T, εA, and 1,2-εG [151–155]. In addition to repairing alkylated bases, MPG is also involved in the repair of DNA damage caused by deamination of purine bases (hypoxanthine, xanthine, and oxanine) [152, 153, 156, 157]. The structural features of the active sites of DNA glycosylases that guide the recognition of various lesions were discussed in a previous review [104].

BER of nucleotides paired with damaged DNA bases

Interesting mechanisms of DNA damage repair preventing mutagenesis involve mismatch-specific DNA glycosylases that excise undamaged bases paired with damaged nucleotides. For example, MUTYH, an adenine DNA glycosylase, recognizes adenine paired with 8-oxo-G [158, 159]. The excision and substitution of dAMP with the complementary dCMP prevents transversions in the subsequent replication rounds. The repair of the A:8-oxo-G base pair was reconstituted *in vitro* with MUTYH, APE1, Pol λ, and DNA ligase I in the presence of PCNA, RPA, and FEN1 [159]. DNA glycosylase TDG is involved in a similar mechanism of excision of thymine paired with noncomplementary cytosine and guanine bases containing the exocyclic etheno ring [160].

Nucleotide incision repair (NIR)

Nucleotide incision repair (NIR) is an alternative pathway for lesion excision that requires AP endonucleases (*Fig. 2*) [161–162]. In this process, the excision of a damaged nucleotide does not involve DNA glycosylases and does not require the formation of a potentially mutagenic intermediate product – AP site. APE1 cleaves DNA at the 5' end of the damaged nucleotide and leaves the undamaged 3' end free for Pol. The remaining damaged nucleotide can be subsequently excised by flap endonuclease FEN1. Pol β and LIG1 fill the gap and join segments of DNA *in vitro* [163]. The role of NIR was initially demonstrated for oxidized DNA nucleotides. APE1 can recognize and be involved in the excision of TG, 5,6-dihydropyrimidines and 5-hydroxypyrimidines [161, 164]. It has been recently demonstrated that NIR could also be an alternative pathway for the repair of other non-bulky lesions, such as uracil [165], εA, and εC [164].

Direct reversal repair (DRR or DR)

Several types of non-bulky lesions can be also repaired by enzymes through direct reversal (*Fig. 2*). These enzymes include the AlkB family of dioxygenases (oxidative demethylases) and alkyl transferases, which participate in the repair of alkylated DNA bases [166]. Oxidative demethylation of damaged bases catalyzed

Efficiency and fidelity of replication opposite non-bulky DNA lesions by human Pols

Damage		Pol	Replication efficiency	Preferential incorporation of nucleotides
AP site		Replicative Pols		
		Pol α	+ [18, 189]	dAMP [18] dAMP ≈ dTMP [189]
		Pol δ	+ [17]; +++ [189] (Pol δ/PCNA); inhibits strand displacement activity [21]	dAMP [189]
		Pol ε	- [16]	
		Specialized Pols		
		Pol η	+++ [189, 191] ++++ [194, 196]	dAMP [191, 192, 196] dAMP ≈ dTMP [189] dAMP ≈ dGMP [194]
		Pol ι	++ [189, 197, 199] ++++ [196] and in cooperation with ScPol ζ [197]	dTMP [189, 196] dGMP [197, 198, 199]
		Pol κ	+ [189, 196]	dCMP ≥ dAMP [189] dAMP [196]
		PrimPol	- [233, 237, 242]; + [238]; ++++ [234]	dAMP ≈ deletions [238] deletions [234]
Deamination	U	Replicative Pols		
		Pol δ	++++ [60] (ScPol δ)	dAMP [60] (ScPol δ)
		Pol ε	++++ [60] (ScPol δ)	dAMP [60] (ScPol δ)
		Specialized Pols		
		Pol ι	++++ [200] (U, 5-oh-U and 5,6-DHU)	dGMP opposite U, 5-oh-U and 5,6-DHU [200]
		PrimPol	++++ [237]	dAMP [237]
	hypoxanthine	Replicative Pols		
		Pol α	+++ [62]	dCMP [62]
		Specialized Pols		
		Pol η	++++ [62]	dCMP [62]
		Pol κ	++++ [62]	dCMP [62]
Oxidation	8-oxo-G	Replicative Pols		
		Pol α	+ [40]	dAMP [40]
		Pol δ	+ [17, 40]	dAMP [40]
		Specialized Pols		
		Pol η	++++ [195, 201] and [193] *in vivo* +++ [42]	dCMP [195] dAMP ≈ dCMP [42] dAMP [201]
		Pol ι	+ [198]; ++ [201]; ++++ [200]	dCMP [199–201]
		Pol κ	+++ [201]	dAMP [201]
		PrimPol	++++	dCMP [236, 240]
	TG	Replicative Pols		
		Pol α	- [44, 192]	dAMP [192]
		Specialized Pols		
		Pol η	+++ [192]	dAMP [192]
		Pol κ	++++ [213] ++++ in cooperation with Pol ζ *in vivo* [222]	dAMP [213, 222]
		PrimPol	- [233]	

Alkylation	N3-me-A	Replicative Pols		
		Pol α	- [82]	dAMP [82]
		Pol δ	- [82]	
		Specialized Pols		
		Pol η	++++ [82]	dTMP ≈ dAMP [82]
		Pol ι	+ [82, 202]	dTMP ≈ dAMP [82]
		Pol κ	+++ [82, 202]	dTMP [82]
	O^6-me-G	Replicative Pols		
		Pol α	+++ [90, 91]	
		Pol δ	+++ [17]; ++++ [87]	dCMP ≈ dTMP [87]
		Specialized Pols		
		Pol η	+ [90]; ++++ [87, 89]	dCMP ≈ dTMP [87, 89]
		Pol ι	++ [87, 203]	dTMP [87, 203]
		Pol κ	+++[87]	dCMP ≈ dTMP [87]
	εA	Replicative Pols		
		Pol δ	- [17, 100]	
		Specialized Pols		
		Pol η	+++ [100]	dTMP [100]
		Pol ι	++ [205, 206]; ++++ in cooperation with ScPol ζ [206]	dTMP with Mg^{2+} and dCMP with Mn^{2+} [205] dCMP ≈ dTMP [206]
		Pol κ	+ [100]	dTMP and deletions [100]

Replication efficiency:
- – inhibition;
+ – low;
++ – incorporates nucleotides opposite the lesion but extension is inefficient;
+++ – moderate;
++++ – high.

by dioxygenases proceeds through the Fe(II)-dependent mechanism of alkyl groups oxidation with molecular oxygen [167]. Eight homologues of *E. coli* AlkB (ALKBH1-8) were identified in humans. The dioxygenases ALKBH2 and ALKBH3 play a key role in the demethylation of N1-me-A, N3-me-C, εA, and alkylated thymine bases [168–170].

Human O^6-alkylguanine-DNA alkyltransferase (AGT or MGMT) is involved in the repair of O^6-me-G and O^4-me-T; it also recognizes and excises a number of relatively bulky alkyl groups in O^6-modified bases [171–173]. AGT irreversibly binds and transfers the methyl group using the thiol group of cysteine as an acceptor (the S_N2 mechanism) [174, 175].

DNA TRANSLESION SYNTHESIS

Some DNA lesions cannot be rapidly repaired. Persistent DNA damage disrupts the functions of the high-fidelity replicative Pol α, Pol δ, and Pol ε (*Table*) and interrupts replication, resulting in cell-cycle termination, chromosomal instability, or cell death. Recruitment of specialized Pols, belonging to various families and specializing in the replication of various lesions, to the stalled replication fork is the key mechanism of progression through the replication blocks (*Figs. 2* and *4* and *Table*). Y-family Pol ι, Pol η, Pol κ, and Rev1 and B-family Pol ζ play a crucial role in replication through non-bulky DNA lesions in human cells [176–179]. To function efficiently, specialized Pols form multisubunit complexes (mutasomes or translesomes) consisting of Pols and proteins that possess structural and regulatory functions and are involved in coordinating the activity of the complex (*Fig. 4*). Specialized Pols possess active sites lacking strict structural requirements to the DNA template and efficiently incorporate nucleotides opposite lesions. Due to the tolerance of the active site, non-canonical hydrogen bonds utilization during base pairing, and the absence of the 3'→5' proofreading ac-

tivity, these enzymes are characterized by low fidelity of DNA synthesis, leading to mutagenesis in the organism [180].

Role of Pol ι, Pol η, and Pol κ in DNA translesion synthesis

Y-family Pol ι, Pol η, and Pol **κ** are single-subunit enzymes characterized by very low-fidelity of synthesis (10^{-1}–10^{-4}) and low processivity [181–186]. Pol η and Pol ι incorporate only one or several nucleotides opposite a damaged site and function as inserters. The primary role of Pol η in the cell is to accurately and efficiently replicate through photoproducts (thymine–thymine cyclobutane dimers) and to protect cells against UV radiation [187, 188]. Nevertheless, Pol η efficiently incorporates nucleotides opposite some other non-bulky lesions (*Table*) [82, 89, 187, 189–196]. For example, Pol η shows high efficiency of synthesis opposite AP sites, incorporating dAMP and dTMP [189, 196], as well as opposite oxidized nucleobases preferentially incorporating correct nucleotides opposite 8-oxo-G and TG [192, 193, 195], and thereby playing a key role in the protection of cells against the most common cytotoxic and mutagenic lesions.

Pol ι efficiently incorporates nucleotides with different accuracies opposite a number of non-bulky DNA lesions, such as AP sites [189, 196–199], uracil and its derivatives [200], 8-oxo-G [201], N3-me-A [190, 202], O^6-me-G [203], 1,2-εG [204], and εA [205, 206] (*Table*). The ability of Pol ι to form non-canonical hydrogen bonds during nucleotide base pairing plays an important role in efficient translesion DNA synthesis. For example, Pol ι utilizes Hoogsteen interactions when incorporating nucleotides opposite εA with the etheno ring that blocks the formation of Watson-Crick hydrogen bonds [206]. Pol ι was also shown to use Hoogsteen interactions to incorporate dNMP opposite O^6-me-G, whose methyl group is exposed in the major groove [203].

An unusual feature of Pol ι is the preferential incorporation of dGMP opposite thymine, uracil, and uracil derivatives [184, 185, 200, 207]. This property possibly plays an important role in reducing the mutagenic potential of deaminated cytosines and 5-me-C [200]. The incorporation of dGMP opposite T in templating DNA is stabilized by the unique hydrogen bond that is formed directly between the N^2 atom of dGTP and the Gln59 residue in the active site of Pol ι [208]. Pol ι efficiently incorporates nucleotides opposite AP sites, and it is one of the few Pols that preferentially incorporate either dGMP or dTMP, rather than dAMP opposite this lesion [189, 196, 198, 199].

The main cellular function of Pol κ is DNA synthesis past guanine deoxyribonucleotide adducts with chemical groups at the N^2 position, which are formed under exposure to some carcinogens. These adducts include both bulky [209–211] and relatively non-bulky lesions (1,2-εG and 2,3-εG) (*Table*) [96, 212]. Pol κ is also involved in efficient and accurate replication past TG [213].

Pol η and Pol ι are not efficient in primer elongation after nucleotide incorporation opposite a DNA lesion. Therefore, further DNA synthesis including elongation from mispaired primer termini is carried out by the Pol-extender. Unlike Pol η and Pol ι, Pol κ efficiently extends mispaired primer termini [214, 215]. Possibly, it can act as an extender in some cases and contribute to the fixation of mutations. However, the key role in the extension step during DNA translesion synthesis is played by the B-family DNA polymerase Pol ζ [197, 216].

Role of Pol ζ and Rev1 in DNA translesion synthesis

Pol ζ consists of four subunits: the catalytic Rev3 and regulatory Rev7, p50, and p66 subunits [217–219]. The four-subunit human DNA polymerase ζ complex was isolated in 2014 [218]; however, DNA translesion synthesis of non-bulky DNA lesions involving human Pol ζ is yet to be studied. *S. cerevisiae* Pol ζ carries out efficient extension of mispaired primer termini and primers paired with lesions [215, 220].

It has also been demonstrated that yeast Pol ζ cooperates with human Pol ι or yeast Pol η for efficient replication through AP sites [215, 221], with Pol κ for accurate replication past TG [222] and Pol ι for efficient replication opposite εA [206]. Unlike Y-family Pols whose functions are interchangeable, the loss of Pol ζ catalytic activity in mammalian cells is lethal, which is indicative of its role in the replication of a large number of endogenous DNA lesions [223, 224].

Another protein belonging to the Y family, Rev1, exhibits weak DNA polymerase activity, as it preferentially incorporates dCMP opposite template G but plays key structural and regulatory roles in mutasome assembly [177]. Rev1 contains binding sites for both the Y-family Pol ι, Pol η, and Pol κ (via the RIR motif in Pol ι, Pol η, and Pol κ) [225–227] and several Pol ζ subunits [228–230]. Rev1 interacts with the nonubiquitinylated and mono-ubiquitinylated PCNA processivity factor [231, 232]. The presence of multiple binding sites for Pols and replication factors allows to coordinate the activity of replication enzymes and timely ensures DNA synthesis by switching from the high-fidelity Pols to specialized Pols, and from the Y-family Pol-inserter to the processive Pol ζ (*Fig. 4*). However, the detailed mechanism of mutasome operation within the framework of the two-polymerase replication model has not been completely elucidated.

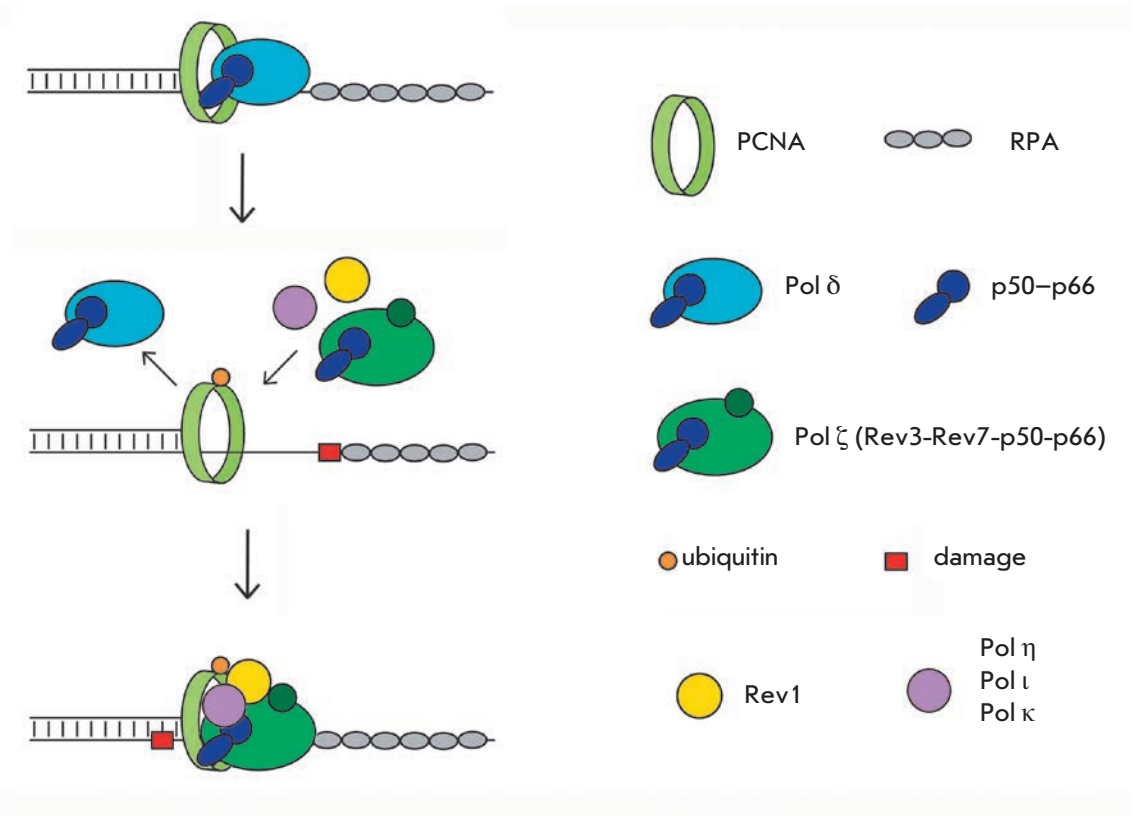

Fig. 4. DNA translesion synthesis by specialized DNA polymerases in humans

The role of PrimPol in DNA translesion synthesis

In 2013, a new type of specialized human Pol was described: primase-polymerase PrimPol. It simultaneously exhibits DNA polymerase and primase activities but differs from the Pol α-primase complex in its ability to initiate DNA synthesis using dNMP [233–235]. PrimPol does not belong to any of the families of the known eukaryotic Pols but belongs to the AEP family of primases [236]. *PRIMPOL* knockout sensitizes cells to DNA lesions [233] and slows down the replication fork progression in the absence of exogenous damaging factors [237]. PrimPol efficiently incorporates nucleotides opposite several non-bulky DNA lesions (e.g., accurate synthesis opposite 8-oxo-G) (*Table*) [234, 238]. However, re-initiation of replication downstream of DNA damage is believed to be the key function of PrimPol [239]. Unlike other human Pols, the activity of PrimPol is not stimulated by PCNA [240] but is activated by the Pol-DIP2 protein [241]. PrimPol has been detected in both the nucleus and mitochondria [234] and is activated by the mitochondrial helicase Twinkle [242].

CONCLUSIONS

In the course of evolution, living organisms have developed a machinery that efficiently protects them against the genotoxicity of DNA damage. It includes mechanisms for removing DNA damage and restoring the original DNA structure (repair), as well as mechanisms that ensure cell tolerance to DNA damage without removing them (DNA translesion synthesis). BER and DNA glycosylases with a different substrate specificity to DNA lesions play a crucial role in the repair of non-bulky DNA lesions. In recent years, alternative mechanisms for the repair of non-bulky DNA lesions have been discovered (such as NIR, direct reversal repair with dioxygenases, and APE1-independent repair of AP-sites). The cellular repair pathways have been shown to overlap and duplicate in their functions. The small number of lesions that remain in genomic DNA often block high-fidelity replicative Pols and lead to a switch to replication with specialized Pols. Recently, a new mechanism for overcoming blockages in replication caused by DNA damage has been discovered. It relies on DNA polymerase and primase PrimPol, which re-initiates replication downstream of DNA damage. The diversity of the mechanisms of DNA repair and DNA translesion synthesis provides high protection against the cytotoxic and mutagenic effects of DNA damage in cells.

Accumulation of non-bulky lesions as a result of disrupted functions of reparative/replicative enzymes leads to the development of human diseases, such as cancer. The link between the functions of reparative/replicative enzymes and human diseases has been dis-

cussed in reviews [243–246]. The search for efficient methods to regulate the activity of the enzymes involved in repair and replication is a promising strategy that could give rise to novel therapeutic approaches.

The authors are grateful to A.V. Kulbachinskiy for valuable discussions and assistance in manuscript preparation. This review was prepared with support from the Presidium of the Russian Academy of Sciences (the "Molecular and Cellular Biology. New Groups" grant), the Russian Foundation for Basic Research, the Moscow City Government (15-34-70002-mol_a_mos and 15-04-08-398-a), the Dynasty Foundation, and the Scholarship of the President of the Russian Federation.

REFERENCES

1. Geacintov N.E., Cosman M., Hingerty B.E., Amin S., Broyde S., Patel D.J. // Chem. Res. Toxicol. 1997. V. 10. № 2. P. 111–146.
2. Skosareva L.V., Lebedeva N.A., Lavrik O.I., Rechkunova N.I. // Mol. Biol. (Mosk). 2013. V. 47. № 5. P. 731–742.
3. Kamileri I., Karakasilioti I., Garinis G.A. // Trends. Genet. 2012. V. 28. № 11. P. 566– 573.
4. Hsu G.W., Huang X., Luneva N.P., Geacintov N.E., Beese L.S. // J. Biol. Chem. 2005. V. 280. № 5. P. 3764–3770.
5. O'Day C., Burgers P.M., Taylor J.S. // Nucleic Acids Res. 1992. V. 20. № 20. P. 5403–5406.
6. Wang Y. // Chem. Res. Toxicol. 2008. V. 21. № 2. P. 276–281.
7. Bauer N.C., Corbett A.H., Doetsch P.W. // Nucleic Acids Res. 2015. V. 43. № 21. P. 10083–10101.
8. Dianov G.L., Hubscher U. // Nucleic Acids Res. 2013. V. 41. № 6. P. 3483–3490.
9. Krokan H.E., Bjoras M. // Cold Spring Harb. Perspect. Biol. 2013. V. 5. № 4. a012583.
10. Nakamura J., Walker V.E., Upton P.B., Chiang S.Y., Kow Y.W., Swenberg J.A. // Cancer Res. 1998. V. 58. № 2. P. 222–225.
11. Tice R.R., Setlow R.B. Handbook of the Biology of Aging. New York: Van Nostrand Reinhold, 1985. 173 p.
12. Lindahl T., Nyberg B. // Biochemistry. 1972. V. 11. № 19. P. 3610–3618.
13. Guillet M., Boiteux S. // Mol. Cell. Biol. 2003. V. 23. № 22. P. 8386–8394.
14. Chen Z., Wang J.H. // Front. Med. 2014. V. 8. № 2. P. 201–216.
15. Petersen-Mahrt S.K., Harris R.S., Neuberger M.S. // Nature. 2002. V. 418. № 6893. P. 99–103.
16. Locatelli G.A., Pospiech H., Tanguy Le Gac N., van Loon B., Hubscher U., Parkkinen S., Syväoja J.E., Villani G. // Biochem. J. 2010. V. 429. № 3. P. 573–582.
17. Schmitt M.W., Matsumoto Y., Loeb L.A. // Biochimie. 2009. V. 91. № 9. P. 1163–1172.
18. Shibutani S., Takeshita M., Grollman A.P. // J. Biol. Chem. 1997. V. 272. № 21. P. 13916–13922.
19. Weerasooriya S., Jasti V.P., Basu A.K. // PloS One. 2014. V. 9. № 9. e107915.
20. Cuniasse P., Fazakerley G.V., Guschlbauer W., Kaplan B.E., Sowers L.C. // J. Mol. Biol. 1990. V. 213. № 2. P. 303–314.
21. Maga G., van Loon B., Crespan E., Villani G., Hubscher U. // J. Biol. Chem. 2009. V. 284. № 21. P. 14267–14275.
22. Yu S.L., Lee S.K., Johnson R.E., Prakash L., Prakash S. // Mol. Cell. Biol. 2003. V. 23. № 1. P. 382–388.
23. Demple B., Herman T., Chen D.S. // Proc. Natl. Acad. Sci. USA. 1991. V. 88. № 24. P. 11450 –11454.
24. Li M., Wilson 3rd D.M. // Antioxid. Redox Signal. 2014. V. 20. № 4. P. 678–707.
25. Choi Y.J., Li H., Son M.Y., Wang X.H., Fornsaglio J.L., Sobol R.W., Lee M., Vijg J., Imholz S., Dollé M.E., et al. // PLoS One. 2014. V. 9. № 1. e86358.
26. Ilina E.S., Lavrik O.I., Khodyreva S.N. // Biochim. Biophys. Acta. 2008. V. 1784. № 11. P. 1777–1785.
27. Roberts S.A., Strande N., Burkhalter M.D., Strom C., Havener J.M., Hasty P., Ramsden D.A. // Nature. 2010. V. 464. № 7292. P. 1214–1217.
28. Lebedeva N.A., Rechkunova N.I., Lavrik O.I. // FEBS Lett. 2011. V. 585. № 4. P. 683–686.
29. Lebedeva N.A., Rechkunova N.I., El-Khamisy S.F., Lavrik O.I. // Biochimie. 2012. V. 94. № 8. P. 1749–1753.
30. Khodyreva S.N., Prasad R., Ilina E.S., Sukhanova M.V., Kutuzov M.M., Liu Y., Hou E.W., Wilson S.H., Lavrik O.I. // Proc. Natl. Acad. Sci. USA. 2010. V. 107. № 51. P. 22090–22095.
31. Kosova A.A., Lavrik O.I., Hodyreva S.N. // Mol Biol (Mosk). 2015. V. 49. № 1. C. 67–74.
32. Rechkunova N.I., Lebedeva N.A., Lavrik O.I. // Bioorg. Khim. 2015. V. 41. № 5. P. 531–538.
33. Yakes F.M., van Houten B. // Proc. Natl Acad. Sci. USA. 1997. V. 94. № 2. P. 514–519.
34. Cadet J., Wagner J.R. // Cold. Spring Harb. Perspect. Biol. 2013. V. 5. № 2. P. a012559.
35. van Loon B., Markkanen E., Hubscher U. // DNA Repair. 2010. V. 9. № 6. P. 604–616.
36. Storr R.J., Woolston C.M., Zhang Y., Martin S.G. // Antioxid. Redox Signal. 2013. V. 18. № 18. P. 2399–2408.
37. Boiteux S., Gajewski E., Laval J., Dizdaroglu M. // Biochemistry. 1992. V. 31. № 1. P. 106–110.
38. Burgdorf L.T., Carell T. // Chemistry. 2002. V. 8. № 1. P. 293–301.
39. Dolinnaya N.G., Kubareva E.A., Romanova E.A., Trikin R.M., Oretskaya T.S. // Biochimie. 2013. V. 95. № 2. P. 134–147.
40. Shibutani S., Takeshita M., Grollman A.P. // Nature. 1991. V. 349. № 6308. P. 431–434.
41. Hsu G.W., Ober M., Carell T., Beese L.S. // Nature. 2004. V. 431. № 7005. P. 217–221.
42. McCulloch S.D., Kokoska R.J., Garg P., Burgers P.M., Kunkel T.A. // Nucleic. Acids Res. 2009. V. 37. № 9. P. 2830–2840.
43. Aller P., Rould M.A., Hogg M., Wallace S.S., Doublié S. // Proc. Natl. Acad. Sci. USA. 2007. V. 104. № 3. P. 814–818.
44. Clark J., Beardsley G.P. // Biochemistry. 1987. V. 26. № 17. P. 5398–5403.
45. Shen J.C., Rideout W.M., Jones P.A. // Nucleic Acids Res. 1994. V. 22. № 6. P. 972–976.
46. Singer B., Grunberger D. Molecular Biology of Mutagens and Carcinogens. New York: Plenum Press, 1983. 19 p.
47. Caulfield J.L., Wishnok J.S., Tannenbaum S.R. // J. Biol.

Chem. 1998. V. 273. № 21. P. 12689–12695.
48. Nguyen T., Brunson D., Crespi C.L., Penman B.W., Wishnok J.S., Tannenbaum S.R. // Proc. Natl. Acad. Sci. USA. 1992. V. 89. № 7. P. 3030–3034.
49. Ohshima H., Tatemichi M., Sawa T. // Arch. Biochem. Biophys. 2003. V. 417. № 1. P. 3–11.
50. Frederico L.A., Kunkel T.A., Shaw B. // Biochemistry. 1993. V. 32. № 26. P. 6523–6530.
51. Lindahl T., Nyberg B. // Biochemistry. 1974. V. 13. № 16. P. 3405–3410.
52. Karran P., Lindahl T. // Biochemistry. 1980. V. 19. № 26. P. 6005–6011.
53. Shapiro R., Yamaguchi H. // Biochim. Biophys. Acta. 1972. V. 281. № 4. P. 501–506.
54. Frederico L.A., Kunkel T.A., Shaw B.R. // Biochemistry. 1990. V. 29. № 10. P. 2532–2537.
55. Wagner J.R., Hu C.C., Ames B.N. // Proc. Natl. Acad. Sci. USA. 1992. V. 89. № 8. P. 3380–3384.
56. Dizdaroglu M., Laval J., Boiteux S. // Biochemistry. 1993. V. 32. № 45. P. 12105–12111.
57. Dong M., Dedon P.C. // Chem. Res. Toxicol. 2006. V. 19. № 1. P. 50–57.
58. Lim K.S., Huang S.H., Jenner A., Wang H., Tang S.Y., Halliwell B. // Free Radic. Biol. Med. 2006. V. 40. № 11. P. 1939–1948.
59. Pang B., Zhou X., Yu H., Dong M., Taghizadeh K., Wishnok J.S., Tannenbaum S.R., Dedon P.C. // Carcinogenesis. 2007. V. 28. № 8. P. 1807–1813.
60. Wardle J., Burgers P.M., Cann I.K., Darley K., Heslop P., Johansson E., Lin L.J., McGlynn P., Sanvoisin J., Stith C.M., et al. // Nucleic Acids Res. 2008. V. 36. № 3. P. 705–711.
61. Hill-Perkins M., Jones M.D., Karran P. // Mutat. Res. 1986. V. 162. № 2. P. 153–163.
62. Yasui M., Suenaga E., Koyama N., Masutani C., Hanaoka F., Gruz P., Shibutani S., Nohmi T., Hayashi M., Honma M. // J. Mol. Biol. 2008. V. 377. № 4. P. 1015–1023.
63. Hajnic M., Ruiter Ad., Polyansky A.A., Zagrovic B. // J. Am. Chem. Soc. 2016. V. 138. № 17. P. 5519–5522.
64. Nakano T., Asagoshi K., Terato H., Suzuki T., Ide H. // Mutagenesis. 2005. V. 20. № 3. P. 209–216.
65. Cooper D.N., Youssoufian H. // Hum. Genet. 1988. V. 78. № 2. P. 151–155.
66. Temiz N.A., Donohue D.E., Bacolla A., Vasquez K.M., Cooper D.N., Mudunuri U., Ivanic J., Cer R.Z., Yi M., Stephens R.M., et al. // Hum. Genet. 2015. V. 134. № 8. P. 851–864.
67. Chikan N.A., Shabir N., Shaff S., Mir M.R., Patel T.N. // Asian. Pac. J. Cancer Prev. 2012. V. 13. № 3. P. 1077–1079.
68. Sutandyo N. // Acta. Med. Indones. 2010. V. 42. № 1. P. 36–42.
69. Bolt H.M., Gansewendt B. // Crit. Rev. Toxicol. 1993. V. 23. № 3. P. 237–253.
70. Bulathsinghala A.T., Shaw I.C. // Hum. Exp. Toxicol. 2014. V. 33. № 1. P. 81–91.
71. Guengerich F.P., Min K.S., Persmark M., Kim M.S., Humphreys W.G., Cmarik J.M., Thier R. IARC Sci. Publ. 1994. № 125. P. 57–72.
72. Cheung-Ong K., Giaever G., Nislow C. // Chem. Biol. 2013. V. 20. № 5. P. 648–659.
73. Colvin M. / Holland-Frei Cancer Medicine. 6th edition. Hamilton: BC Decker, 2003. 51 chapter.
74. Beranek D.T. // Mutat. Res. 1990. V. 231. № 1. P. 11–30.
75. Fu D., Calvo J.A., Samson L.D. // Nat. Rev. Cancer. 2012. V. 12. № 2. P. 104–120.
76. Beranek D.T., Weis C.C., Swenson D.H. // Carcinogenesis. 1980. V. 1. № 7. P. 595–606.
77. Reiner B., Zamenhof S. // J. Biol. Chem. 1957. V. 228. № 1. P. 475–486.
78. Rydberg B., Lindahl T. // EMBO J. 1982. V. 1. № 2. P. 211–216.
79. Barrows L.R., Magee P.N. // Carcinogenesis. 1982. V. 3. № 3. P. 349–351.
80. Boiteux S., Huisman O., Laval J. // EMBO J. 1984. V. 3. № 11. P. 2569–2573.
81. Fronza G., Gold B. // J. Cell. Biochem. 2004. V. 91. № 2. P. 250–257.
82. Plosky B.S., Frank E.G., Berry D.A., Vennall G.P., McDonald J.P., Woodgate R. // Nucleic Acids Res. 2008. V. 36. № 7. P. 2152–2162.
83. Larson K., Sahm J., Shenkar R., Strauss B. // Mutat. Res. 1985. V. 150. № 1–2. P. 77– 84.
84. Koag M.C., Kou Y., Ouzon-Shubeita H., Lee S. // Nucleic Acids Res. 2014. V. 42. № 13. P. 8755–8766.
85. Boiteux S., Laval J. // Biochem. Biophys. Res. Commun. 1983. V. 110. № 2. P. 552–558.
86. O'Connor T.R., Boiteux S., Laval J. // Nucleic Acids Res. 1982. V. 16. № 13. P. 5879–5894.
87. Choi J.Y., Chowdhury G., Zang H., Angel K.C., Vu C.C., Peterson L.A., Guengerich F.P. // J. Biol. Chem. 2006. V. 281. № 50. P. 38244–38256.
88. Ellison K.S., Dogliotti E., Connors T.D., Basu A.K., Essigmann J.M. // Proc. Natl. Acad. Sci. USA. 1989. V. 86. № 22. P. 8620–8624.
89. Haracska L., Prakash S., Prakash L. // Mol. Cell. Biol. 2000. V. 20. № 21. P. 8001–8007.
90. Perrino F.W., Blans P., Harvey S., Gelhaus S.L., McGrath C., Akman S.A., Jenkins G.S., LaCourse W.R., Fishbein J.C. // Chem. Res. Toxicol. 2003. V. 16. № 12. P. 1616–1623.
91. Voigt J.M., Topal M.D. // Carcinogenesis. 1995. V. 16. № 8. P. 1775–1782.
92. Nay S.L., O'Connor T.R. New Research Directions in DNA Repair. InTech, 2013. 5 chapter.
93. Chung F.L., Chen H.J., Nath R.G. // Carcinogenesis. 1996. V. 17. № 10. P. 2105–2111.
94. Nair J., Barbin A., Velic I., Bartsch H. // Mutat. Res. 1999. V. 424. № 1–2. P. 59–69.
95. Barbin A. // Mutat. Res. 2000. V. 462. № 2–3. P. 55–69.
96. Chang S.C., Fedeles B.I., Wu J., Delaney J.C., Li D., Zhao L., Christov P.P., Yau E., Singh V., Jost M., et al. // Nucleic Acids Res. 2015. V. 43. № 11. P. 5489–5500.
97. Choi J.Y., Zang H., Angel K.C., Kozekov I.D., Goodenough A.K., Rizzo C.J., Guengerich F.P. // Chem. Res. Toxicol. 2006. V. 19. № 6. P. 879–886.
98. Pandya G.A., Moriya M. // Biochemistry. 1996. V. 35. № 35. P. 11487–11492.
99. Shibutani S., Suzuki N., Matsumoto Y., Grollman A.P. // Biochemistry. 1996. V. 35. № 47. P. 14992–14998.
100. Levine R.L., Miller H., Grollman A., Ohashi E., Ohmori H., Masutani C., Hanaoka F., Moriya M. // J. Biol. Chem. 2001. V. 276. № 22. P. 18717–18721.
101. Yamanaka K., Minko I.G., Takata K., Kolbanovskiy A., Kozekov I.D., Wood R.D., Rizzo C.J., Lloyd R.S. // Chem. Res. Toxicol. 2010. V. 23. № 3. P. 689–695.
102. Fortini P., Dogliotti E. // DNA Repair. 2007. V. 6. № 4. P. 398–409.
103. Zharkov D.O // Herald of the Russian Academy of Sciences. 2013. V. 83. № 2. P. 112–119.
104. Zharkov D.O. // Mol. Biol. (Mosk). 2007. V. 41. № 5. P. 772–786.
105. Brooks S.C., Adhikary S., Rubinson E.H., Eichman B.F.

// Biochim. Biophys. Acta. 2013. V. 1834. № 1. P. 247–271.
106. Demple B., Sung J.S. // DNA Repair (Amst.). 2005. V. 4. № 12. P. 1442–1449.
107. Das A., Wiederhold L., Leppard J.B., Kedar P., Prasad R., Wang H., Boldogh I., Karimi-Busheri F., Weinfeld M., Tomkinson A.E., et al. // DNA Repair. 2006. V. 5. № 12. P. 1439–1448.
108. Pascucci B., Maga G., Hübscher U., Bjoras M., Seeberg E., Hickson I.D., Villani G., Giordano C., Cellai L., Dogliotti E. // Nucleic Acids Res. 2002. V. 30. № 10. P. 2124–2130.
109. Wiederhold L., Leppard J.B., Kedar P., Karimi-Busheri F., Rasouli-Nia A., Weinfeld M., Tomkinson A.E., Izumi T., Prasad R., Wilson S.H., et al. // Mol. Cell. 2004. V. 15. № 2. P. 209–220.
110. Caldecott K.W., Tucker J.D., Stanker L.H., Thompson L.H. // Nucleic Acids Res. 1995. V. 23. № 23. P. 4836–4843.
111. Kubota Y., Nash R.A., Klungland A., Schär P., Barnes D.E., Lindahl T. // EMBO J. 1996. V. 15. № 23. P. 6662–6670.
112. Gary R., Kim K., Cornelius H.L., Park M.S., Matsumoto Y. // J. Biol. Chem. 1999. V. 274. № 7. P. 4354–4363.
113. Mjelle R., Hegre S.A., Aas P.A., Slupphaug G., Drablos F., Saetrom P., Krokan H.E. // DNA Repair. 2015. V. 30. P. 53–67.
114. Sobol R.W., Prasad R., Evenski A., Baker A., Yang X.P., Horton J.K., Wilson S.H. // Nature. 2000. V. 405. № 6788. P. 807–810.
115. Prasad R., Bebenek K., Hou E., Shock D.D., Beard W.A., Woodgate R., Kunkel T.A., Wilson S.H. // J. Biol. Chem. 2003. V. 278. № 32. P. 29649–29654.
116. Garcia-Diaz M., Bebenek K., Kunkel T.A., Blanco L. // J. Biol. Chem. 2001. V. 276. № 37. P. 34659–34663.
117. Petta T.B., Nakajima S., Zlatanou A., Despras E., Couve-Privat S., Ishchenko A., Sarasin A., Yasui A., Kannouche P. // EMBO J. 2008. V. 27. № 21. P. 2883–2895.
118. Prasad R., Longley M.J., Sharief F.S., Hou E.W., Copeland W.C., Wilson S.H. // Nucleic Acids Res. 2009. V. 37. № 6. P. 1868–1877.
119. Stucki M., Pascucci B., Parlanti E., Fortini P., Wilson S.H., Hübscher U., Dogliotti E. // Oncogene. 1998. V. 17. № 7. P. 835–843.
120. Levin D.S., Vijayakumar S., Liu X., Bermudez V.P., Hurwitz J., Tomkinson A.E. // J. Biol. Chem. 2004. V. 279. № 53. P. 55196–55201.
121. Cappelli E., Taylor R., Cevasco M., Abbondandolo A., Caldecott K., Frosina G. // J. Biol. Chem. 1997. V. 272. № 38. P. 23970–23975.
122. Levin D.S., McKenna A.E., Motycka T.A., Matsumoto Y., Tomkinson A.E. // Curr. Biol. 2000. V. 10. № 15. P. 919–922.
123. Nilsen H., Otterlei M., Haug T., Solum K., Nagelhus T.A., Skorpen F., Krokan H.E. // Nucleic Acids Res. 1997. V. 25. № 4. P. 750–755.
124. Haug T., Skorpen F., Aas P.A., Malm V., Skjelbred C., Krokan H.E. // Nucleic Acids Res. 1998. V. 26. № 6. P. 1449–1457.
125. Slupphaug G., Markussen F.H., Olsen L.C., Aasland R., Aarsaether N., Bakke O., Krokan H.E., Helland D.E. // Nucleic Acids Res. 1993. V. 21. № 11. P. 2579–2584.
126. Masaoka A., Matsubara M., Hasegawa R., Tanaka T., Kurisu S., Terato H., Ohyama Y., Karino N., Matsuda A., Ide H. // Biochemistry. 2003. V. 42. № 17. P. 5003–5012.
127. Wibley J.E., Waters T.R., Haushalter K., Verdine G.L., Pearl L.H. // Mol. Cell. 2003. V. 11. № 6. P. 1647–1659.
128. Haushalter K.A., Todd Stukenberg M.W., Kirschner M.W., Verdine G.L. // Curr. Biol. 1999. V. 9. № 4. P. 174–185.
129. Hendrich B., Hardeland U., Ng H.H., Jiricny J., Bird A. // Nature. 1999. V. 401. № 6750. P. 301–404.
130. Neddermann P., Gallinari P., Lettieri T., Schmid D., Truong O., Hsuan J.J., Wiebauer K., Jiricny J. // J. Biol. Chem. 1996. V. 271. № 22. P. 12767–12774.
131. Sjolund A., Senejani A.G., Sweasy J.B. // Mutat. Res. 2013. V. 743–744. P. 12–25.
132. Bellacosa A., Drohat A.C. // DNA Repair. 2015. V. 32. P. 33–42.
133. Boiteux S., Radicella J.P. // Arch. Biochem. Biophys. 2000. V. 377. № 1. P. 1–8.
134. Radicella J.P., Dherin C., Desmaze C., Fox M.S., Boiteux S. // Proc. Natl. Acad. Sci. USA. 1997. V. 94. № 15. P. 8010–8015.
135. Ohtsubo T., Oda H., Fujiwara T., Kang D., Sugimachi K., Nakabeppu Y., Nishioka K. // Mol. Biol. Cell. 1999. V. 10. № 5. P. 1637–1652.
136. Takao M., Aburatani H., Kobayashi K., Yasui A. // Nucleic Acids Res. 1998. V. 26. № 12. P. 2917–2922.
137. Hazra T.K., Izumi T., Boldogh I., Imhoff B., Kow Y.W., Jaruga P., Dizdaroglu M., Mitra S. // Proc. Natl. Acad. Sci. USA. 2002. V. 99. № 6. P. 3523–3538.
138. Parsons J.L., Zharkov D.O., Dianov G.L. // Nucleic Acids Res. 2005. V. 33. № 15. P. 4849–4856.
139. Aspinwall R., Rothwell D.G., Roldan-Arjona T., Anselmino C., Ward C.J., Cheadle J.P., Sampson J.R., Lindahl T., Harris P.C., Hickson I.D. // Proc. Natl. Acad. Sci. USA. 1997. V. 94. № 1. P. 109–114.
140. Bandaru V., Sunkara S., Wallace S.S., Bond J.P. // DNA Repair. 2002. V. 1. № 7. P. 517–729.
141. Dizdaroglu M., Karahalil B., Sentürker S., Buckley T.T., Roldán-Arjona T. // Biochemistry. 1999. V. 38. № 1. P. 243–246.
142. Miyabe I., Zhang Q.M., Kino K., Sugiyama H., Takao M., Yasui A., Yonei S. // Nucleic Acids Res. 2002. V. 30. № 14. P. 3443–3448.
143. Parsons J.L., Kavli B., Slupphaug G., Dianov G.L. // Biochemistry. 2007. V. 46. № 13. P. 4158–4163.
144. Hazra T.K., Kow Y.W., Hatahet Z., Imhoff B., Boldogh I., Mokkapati S.K., Mitra S., Izumi T. // J. Biol. Chem. 2002. V. 277. № 34. P. 30417–30420.
145. Liu M., Doublié S., Wallace S.S. // Mutat. Res. 2013. V. 743–744. P. 4–11.
146. Rolseth V., Krokeide S.Z., Kunke D., Neurauter C.G., Suganthan R., Sejersted Y., Hildrestrand G.A., Bjørås M., Luna L. // Biochim. Biophys. Acta. 2013. V. 1833. № 5. P. 1157–1164.
147. Dou H., Mitra S., Hazra T.K. // J. Biol. Chem. 2003. V. 278. № 50. P. 49679–49684.
148. Banerjee D., Mandal S.M., Das A., Hegde M.L., Das S., Bhakat K.K., Boldogh L., Sarkar P.S., Mitra S., Hazra T.K. // J. Biol. Chem. 2011. V. 286. № 8. P. 6006–6016.
149. Hegde M.L., Hegde P.M., Bellot L.J., Mandal S.M., Hazra T.K., Li G.M., Boldogh I., Tomkinson A.E., Mitra S. // Proc. Natl. Acad. Sci. USA. 2013. V. 110. № 33. E3090–E3099.
150. Liu M., Imamura K., Averill A.M., Wallace S.S., Doublié S. // Structure. 2013. V. 21. № 2. P. 247–256.
151. Chakravarti D., Ibeanu G.C., Tano K., Mitra S. // J. Biol. Chem. 1991. V. 266. № 24. P. 15710–15715.
152. Engelward B.P., Weeda G., Wyatt M.D., Broekhof J.L., de Wit J., Donker I., Allan J.M., Gold B., Hoeijmakers J.H., Samson L.D. // Proc. Natl. Acad. Sci. USA. 1997. V. 94. № 24. P. 13087–13092.
153. Hang B., Singer B., Margison G.P., Elder R.H. // Proc. Natl. Acad. Sci. USA. 1997. V. 94. № 24. P. 12869–12874.
154. Saparbaev M., Langouët S., Privezentzev C.V., Guenger-

ich F.P., Cai H., Elder R.H., Laval J. // J. Biol. Chem. 2002. V. 277. № 30. P. 26987–26993.
155. Wolfe A.E., O'Brien P.J. // Biochemistry. 2009. V. 48. № 48. P. 11357–11369.
156. Saparbaev M., Laval J. // Proc. Natl. Acad. Sci. USA. 1994. V. 91. № 13. P. 5873–5877.
157. Hitchcock T.M., Dong L., Connor E.E., Meira L.B., Samson L.D., Wyatt M.D., Cao W. // J. Biol. Chem. 2004. V. 279. № 37. P. 38177–38183.
158. McGoldrick J.P., Yeh Y.C., Solomon M., Essigmann J.M., Lu A.L. // Mol. Cell. Biol. 1995. V. 15. № 2. P. 989–996.
159. van Loon B., Hubscher U. // Proc. Natl. Acad. Sci. USA. 2009. V. 106. № 43. P. 18201–18206.
160. Goto M., Shinmura K., Matsushima Y., Ishino K., Yamada H., Totsuka Y., Matsuda T., Nakagama H., Sugimura H. // Free Radic. Biol. Med. 2014. V. 76. P. 136–146.
161. Gros L., Ishchenko A.A., Ide H., Elder R.H., Saparbaev M.K. // Nucleic Acids Res. 2004. V. 32. № 1. P. 73–81.
162-. Ishchenko A.A., Deprez E., Maksimenko A., Brochon J.C., Tauc P., Saparbaev M.K. // Proc. Natl. Acad. Sci. USA. 2006. V. 103. № 8. P. 2564–2569.
163. Gelin A., Redrejo-Rodríguez M., Laval J., Fedorova O.S., Saparbaev M., Ishchenko A.A. // PLoS One. 2010. V. 5. № 8. E12241.
164. Prorok P., Saint-Pierre C., Gasparutto D., Fedorova O.S., Ishchenko A.A., Leh H., Buckle M., Tudek B., Saparbaev M. // PLoS One. 2012. V. 7. № 12. E51776.
165. Prorok P., Alili D., Saint-Pierre C., Gasparutto D., Zharkov D.O., Ishchenko A.A., Tudek B., Saparbaev M.K. // Proc. Natl. Acad. Sci. USA. 2013. V. 110. № 39. E3695–E3703.
166. Yi C., He C. // Cold Spring Harb. Perspect. Biol. 2013. V. 5. № 1. a012575.
167. Yi C., Jia G., Hou G., Dai Q., Zhang W., Zheng G., Jian X., Yang C.G., Cui Q., He C. // Nature. 2010. V. 468. № 7321. P. 330–333
168. Aas P.A., Otterlei M., Falnes P.O., Vågbø C.B., Skorpen F., Akbari M., Sundheim O., Bjørås M., Slupphaug G., Seeberg E., et al. // Nature. 2003. V. 421. № 6925. P. 859–863.
169. Duncan T., Trewick S.C., Koivisto P., Bates P.A., Lindahl T., Sedgwick B. // Proc. Natl. Acad. Sci. USA. 2002. V. 99. № 26. P. 16660–16665.
170. You C., Wang P., Nay S.L., Wang J., Dai X., O'Connor T.R., Wang Y. // ACS Chem. Biol. 2016. V. 11. № 5. P. 1332–1338.
171. Lamb K.L., Liu Y., Ishiguro K., Kwon Y., Paquet N., Sartorelli A.C., Sung P., Rockwell S., Sweasy J.B. // Mol. Carcinog. 2014. V. 53. № 3. P. 201–210.
172. Pegg A.E., Boosalis M., Samson L., Moschel R.C., Byers T.L., Swenn K., Dolan M.E. // Biochemistry. 1993. V. 32. № 45. P. 11998–12006.
173. Zak P., Kleibl K., Laval F. // J. Biol. Chem. 1994. V. 269. № 1. P. 730–733.
174. Demple B., Sedgwick B., Robins P., Totty N., Waterfield M.D., Lindahl T. // Proc. Natl. Acad. Sci. USA. 1985. V. 82. № 9. P. 2688–2692.
175. Campbell C.R., Spratt T.E. // Biochemistry. 1994. V. 33. № 37. P. 11364–11371.
176. Makarova A.V., Kulbachinskiy A.V. // Biochemistry (Mosc). 2012. V. 77. № 6. 669–661.
177. Makarova A.V., Burgers P.M. // DNA Repair. 2015. V. 29. P. 47–55.
178. Yang W. // Biochemistry. 2014. V. 53. № 17. P. 2793–2803.
179. Sharma S., Helchowski C.M., Canman C.E. // Mutat. Res. 2013. V. 743–744. P. 97–110.
180. McCulloch S.D., Kunkel T.A. // Cell Res. 2008. V. 18. № 1. P. 148–161.
181. Johnson R.E., Washington M.T., Prakash S., Prakash L. // J. Biol. Chem. 2000. V. 275. № 11. P. 7447–7450.
182. Matsuda T., Bebenek K., Masutani C., Hanaoka F., Kunkel T.A. // Nature. 2000. V. 404. № 6781. P. 1011–1013.
183. Ohashi E., Bebenek K., Matsuda T., Feaver W.J., Gerlach V.L., Friedberg E.C., Ohmori H., Kunkel T.A. // J. Biol. Chem. 2000. V. 275. № 50. P. 39678–39684.
184. Tissier A., McDonald J.P., Frank E.G., Woodgate R. // Genes Dev. 2000. V. 14. № 13. P. 1642–1650.
185. Zhang Y., Yuan F., Wu X., Wang X. // Mol. Cell. Biol. 2000. V. 20. № 19. P. 7099–7108.
186. Zhang Y., Yuan F., Xin H., Wu X., Rajpal D.K., Yang D., Wang Z. // Nucleic Acids Res. 2000. V. 28. № 21. P. 4147–4156.
187. Masutani C., Kusumoto R., Iwai S., Hanaoka F. // EMBO J. 2000. V. 19. № 12. P. 3100–3109.
188. McCulloch S.D., Kokoska R.J., Masutani C., Iwai S., Hanaoka F., Kunkel T.A. // Nature. 2004. V. 428. № 6978. P. 97–100.
189. Choi J.Y., Lim S., Kim E.J., Jo A., Guengerich F.P. // J. Mol. Biol. 2010. V. 404. № 1. P. 34–44.
190. Furrer A., van Loon B. // Nucleic Acids Res. 2014. V. 42. № 1. P. 553–566.
191. Kokoska R.J., McCulloch S.D., Kunkel T.A. // J. Biol. Chem. 2003. V. 278. № 50. P. 50537–50545.
192. Kusumoto R., Masutani C., Iwai S., Hanaoka F. // Biochemistry. 2002. V. 41. № 19. P. 6090–6099.
193. Lee D.H., Pfeifer G.P. // Mutat. Res. 2008. V. 641. № 1–2. P. 19–26.
194. Patra A., Zhang Q., Lei L., Su Y., Egli M., Guengerich F.P. // J. Biol. Chem. 2015. V. 290. № 13. P. 8028–8038.
195. Patra A., Nagy L.D., Zhang Q., Su Y., Müller L., Guengerich F.P., Egli M.A. // J. Biol. Chem. 2014. V. 289. № 24. P. 16867–16882.
196. Sherrer S.M., Fiala K.A., Fowler J.D., Newmister S.A., Pryor J.M., Suo Z. // Nucleic Acids Res. 2011. V. 39. № 2. P. 609–622.
197. Johnson R.E., Washington M.T., Haracska L., Prakash S., Prakash L. // Nature. 2000. V. 406. № 6799. P. 1015–1019.
198. Nair D.T., Johnson R.E., Prakash L., Prakash S., Aggarwal A.K. // Structure. 2009. V. 17. № 4. P. 530–537.
199. Zhang Y., Yuan F., Wu X., Taylor J.S., Wang Z. // Nucleic Acids Res. 2001. V. 29. № 4. P. 928–935.
200. Vaisman A., Woodgate R. // EMBO J. 2001. V. 20. № 22. P. 6520–6529.
201. Kirouac K.N., Ling H. // Proc. Natl. Acad. Sci. USA. 2011. V. 108. № 8. P. 3210–3215.
202. Johnson R.E., Yu S.L., Prakash S., Prakash L. // Mol. Cell. Biol. 2007. V. 27. № 20. P. 7198–7205.
203. Pence M.G., Choi J.Y., Egli M, Guengerich F.P. // J. Biol. Chem. 2010. V. 285. № 52. P. 40666–40672.
204. Pence M.G., Blans P., Zink C.N., Hollis T., Fishbein J.C., Perrino F.W. // J. Biol. Chem. 2009. V. 284. № 3. P. 1732–1740.
205. Makarova A.V., Ignatov A., Miropolskaya N., Kulbachinskiy A. // DNA Repair. 2014. V. 22. C. 67–76.
206. Nair D.T., Johnson R.E., Prakash L., Prakash S., Aggarwal A.K. // Nat. Struct. Mol. Biol. 2006. V. 13. № 7. P. 619–625.
207. Makarova A.V., Grabow C., Gening L.V., Tarantul V.Z., Tahirov T.H., Bessho T., Pavlov Y.I. // PLoS One. 2011. V. 6. № 1. e16612.
208. Kirouac K.N., Ling H. // EMBO J. 2009. V. 28. № 11. P. 1644–1654.

209. Jha V., Bian C., Xing G., Ling H. // Nucleic Acids Res. 2016. V. 44. № 10. P. 4957–4967.
210. Minko I.G., Harbut M.B., Kozekov I.D., Kozekova A., Jakobs P.M., Olson S.B., Moses R.E., Harris T.M., Rizzo C.J., Lloyd R.S. // J. Biol. Chem. 2008. V. 283. № 25. P. 17075–17082.
211. Yasui M., Dong H., Bonala R.R., Suzuki N., Ohmori H., Hanaoka F., Johnson F., Grollman A.P., Shibutani S. // Biochemistry. 2004. V. 43. № 47. P. 15005–15013.
212. Zhao L., Pence M.G., Christov P.P., Wawrzak Z., Choi J.Y., Rizzo C.J., Egli M., Guengerich F.P. // J. Biol. Chem. 2012. V. 287. № 42. P. 35516–35526.
213. Fischhaber P.L., Gerlach V.L., Feaver W.J., Hatahet Z., Wallace S.S., Friedberg E.C. // J. Biol. Chem. 2002. V. 277. № 40. P. 37604–37611.
214. Lone S., Townson S.A., Uljon S.N., Johnson R.E., Brahma A., Nair D.T., Prakash S., Prakash L., Aggarwal A.K. // Mol. Cell. 2007. V. 25. № 4. P. 601–614.
215. Carlson K.D., Johnson R.E., Prakash L., Prakash S., Washington M.T. // Proc. Natl. Acad. Sci. USA. 2006. V. 103. № 43. P. 15776–15781.
216. Livneh Z., Ziv O., Shachar S. // Cell Cycle. 2010. V. 9. № 4. P. 729–735.
217. Baranovskiy A.G., Lada A.G., Siebler H.M., Zhang Y., Pavlov Y.I., Tahirov T.H. // J. Biol. Chem. 2012. V. 287. № 21. P. 17281–17287.
218. Lee Y.S., Gregory M.T., Yang W. // Proc. Natl. Acad. Sci. USA. 2014. V. 111. № 8. P. 2954–2959.
219. Makarova A.V., Stodola J.L., Burgers P.M. // Nucleic Acids Res. 2012. V. 40. № 22. P. 11618–11626.
220. Haracska L., Prakash S., Prakash L. // Mol. Cell. Biol. 2003. V. 23. № 4. P. 1453–1459.
221. Yuan F., Zhang Y., Rajpal D.K., Wu X., Guo D., Wang M., Taylor J.S., Wang Z. // J. Biol. Chem. 2000. V. 275. № 11. P. 8233–8239.
222. Yoon J.H., Bhatia G., Prakash S., Prakash L. // Proc. Natl. Acad. Sci. USA. 2012. V. 107. № 32. P. 14116–14121.
223. Esposito G., Godindagger I., Klein U., Yaspo M.L., Cumano A., Rajewsky K. // Curr. Biol. 2000. V. 10. № 19. P. 1221–1224.
224. Wittschieben J., Shivji M.K., Lalani E., Jacobs M.A., Marini F., Gearhart P.J., Rosewell I., Stamp G., Wood R.D. // Curr. Biol. 2000. V. 10. № 19. P. 1217–1220.
225. Guo C., Fischhaber P.L., Luk-Paszyc M.J., Masuda Y., Zhou J., Kamiya K., Kisker C., Friedberg E.C. // EMBO J. 2003. V. 22. № 24. P. 6621–6630.
226. Ohashi E., Hanafusa T., Kamei K., Song I., Tomida J., Hashimoto H., Vaziri C., Ohmori H. // Genes Cells. 2009. V. 14. № 2. P. 101–111.
227. Pozhidaiva A., Pustovalova Y., D'Souza S., Bezsonova I., Walker G.C., Korzhnev D.M. // Biochemistry. 2012. V. 51. № 27. P. 5506–5520.
228. Pustopalova Y., Bezsonova I., Korzhnev D.M. // FEBS Lett. 2012. V. 586. № 19. P. 3051–3056.
229. Pustovalova Y., Magalhães M.T., D'Souza S., Rizzo A.A., Korza G., Walker G.C., Korzhnev D.M. // Biochemistry. 2016. V. 55. № 13. P. 2043–2053.
230. Wojtaszek J., Lee C.J., D'Souza S., Minesinger B., Kim H., D'Andrea A.D., Walker G.C., Zhou P. // J. Biol. Chem. 2012. V. 287. № 40. P. 33836–33846.
231. Guo C., Sonoda E., Tang T.S., Parker J.L., Bielen A.B., Takeda S., Ulrich H.D., Friedberg E.C. // Mol. Cell. 2006. V. 23. № 2. P. 265–271.
232. Pustopalova Y., Maciejewski M.W., Korzhnev D.M. // J. Mol. Biol. 2013. V. 425. № 17. P. 3091–3105.
233. Bianchi J., Rudd S.G., Jozwiakowski S.K., Bailey L.J., Soura V., Taylor E., Stevanovic I., Green A.J., Stracker T.H., Lindsay H.D., et al. // Mol. Cell. 2013. V. 52. № 4. P. 566–573.
234. García-Gómez S., Reyes A., Martínez-Jiménez M.I., Chocrón E.S., Mourón S., Terrados G., Powell C., Salido E., Méndez J., Holt I.J., et al. // Mol. Cell. 2013. V. 52. № 4. P. 541–553.
235. Wan L., Lou J., Xia Y., Su B., Liu T., Cui J., Sun Y., Lou H., Huang J. // EMBO Rep. 2013. V. 14. № 12. P. 1104–1112.
236. Iyer L.M., Koonin E.V., Leipe D.D., Aravind L. // Nucleic Acids Res. 2005. V. 33. № 12. P. 3875–3896.
237. Keen B.A., Jozwiakowski S.K., Bailey L.J., Bianchi J., Doherty A.J. // Nucleic Acids Res. 2014. V. 42. № 9. P. 5830–5845.
238. Zafar M.K., Ketkar A., Lodeiro M.F., Cameron C.E., Eoff R.L. // Biochemistry. 2014. V. 53. № 41. P. 6584–6594.
239. Kobayashi K., Guilliam T.A., Tsuda M., Yamamoto J., Bailey L.J., Iwai S., Takeda S., Doherty A.J., Hirota K. // Cell Cycle. 2016. V. 15. № 15. P. 1997–2008.
240. Gulliam T.A., Jozwiakowski S.K., Ehlinger A., Barnes R.P., Rudd S.G., Bailey L.J., Skehel J.M., Eckert K.A., Chazin W.J., Doherty A.J. // Nucleic Acids Res. 2015. V. 43. № 2. P. 1056–1068.
241. Gulliam T.A., Bailey L.J., Brissett N.C., Doherty A.J. // Nucleic Acids Res. 2016. V. 44. № 7. P. 3317–3329.
242. Stojkovič G., Makarova A.V., Wanrooij P.H., Forslund J., Burgers P.M., Wanrooij S. // Sci. Rep. 2016. V. 6. 28942.
243. Köberle B., Koch B., Fischer B.M., Hartwig A. // Arch. Toxicol. 2016. V. 90. № 10. P. 2369–2388.
244. Markkanen E., Meyer U., Dianov G.L. // Int. J. Mol. Sci. 2016. V. 17. № 6. E856.
245. Lange S.S., Takata K., Wodd R.D. // Nat. Rev. Cancer. 2011. V. 11. № 2. P. 96–110.
246. Korzhnev D.M., Hadden M.K. // J. Med. Chem. 2016. V. 59. № 20. P. 9321–9336.

Antitumor Vaccines Based on Dendritic Cells: From Experiments using Animal Tumor Models to Clinical Trials

O. V. Markov*, N. L. Mironova†, V. V. Vlassov, M. A. Zenkova
Institute of Chemical Biology and Fundamental Medicine SB RAS, Lavrentieva Ave. 8, Novosibirsk, 630090, Russia
E-mail: *markov_oleg@list.ru; †mironova@niboch.nsc.ru
Received: December 01, 2016; in final form June 07, 2017

ABSTRACT **The routine methods used to treat oncological diseases have a number of drawbacks, including non-specific action and severe side effects for patients. Furthermore, tumor diseases are associated with a suppression of the immune system that often leads to the inefficiency of standard treatment methods. The development of novel immunotherapeutic approaches having specific antitumor action and that activate the immune system is of crucial importance. Vaccines based on dendritic cells (DCs) loaded with tumor antigens *ex vivo* that can activate antitumor cytotoxic T-cell responses stand out among different antitumor immunotherapeutic approaches. This review is focused on analyzing different methods of DC-based vaccine preparation and current research in antitumor DC-based vaccines using animal tumor models and in clinical trials.**
KEYWORDS **dendritic cells, antitumor vaccines, delivery of tumor antigens, murine tumor models, clinical trials.**
ABBREVIATIONS **Ag – antigen; APC – antigen-presenting cells; GM-CSF – granulocyte-macrophage colony stimulating factor; DCs – dendritic cells; IL – interleukin; IFN – interferon; NA – nucleic acid; TAAs – tumor-associated antigens; PAP – prostatic acid phosphatase; Treg – regulatory T cells; UV – ultraviolet; TNF – tumor necrosis factor; CIK – cytokine-induced killer cells; CTL – cytotoxic T lymphocytes; CP – cyclophosphamide; DTH – delayed type (IV) hypersensitivity; HLA – human leukocyte antigen; KLH – keyhole limpet hemocyanin of *F. apertura*; OVA – ovalbumin; SVV – survivin; TLR – toll-like receptor.**

INTRODUCTION

Dendritic cells (DCs) are professional antigen-presenting cells whose key function is antigen capture, processing, and presentation to naïve T cells to activate an immune response against the captured antigen. The unique ability of DCs to activate $CD4^+$ T helper cells and $CD8^+$ cytotoxic T lymphocytes (CTL) that makes them responsible for the direction of immune responses has attracted increased attention in the development of antitumor vaccines that can exhibit specific activity against certain types of tumors. The discovery of tumor-associated antigens (TAAs), i.e., proteins whose overexpression is specific only to certain tumor types, was an incentive in their application for loading DCs. The TAAs of tumor types such as melanoma (gp100, Melan-A/Mart-1, tyrosinase, MAGE-1 [1, 2]), prostate cancer (PSA [3], PSCA [4]), etc. are known.

Today, antitumor DC-based vaccines are actively studied using both murine models *in vivo* and clinical trials. In 2010, the U.S. Food and Drug Administration approved the first therapeutic vaccine, Sipuleucel-T, against castration-resistant prostate cancer based on DCs loaded with a recombinant fusion protein consisting of prostatic acid phosphatase (PAP) and a granulocyte-macrophage colony-stimulating factor (GM-CSF), which so far remains the only one worldwide [5]. Hence, there are good reasons to develop highly efficient antitumor immunotherapy approaches based on the application of modified dendritic cells in the near future.

This review focuses on strategies using DCs activated by various TAAs both in murine tumor models *in vivo* and in clinical trials.

PREPARATION OF DC-BASED ANTITUMOR VACCINES

The approaches to antitumor therapy using DCs can be classified into four main groups: (1) injections of DCs loaded with tumor-associated antigens *ex vivo*, (2) systemic administration of tumor-associated antigens to load DCs *in vivo*, (3) injections of non-modified mature DCs, and (4) injections of DC-derived exosomes. In this review, we discuss the conventional DC-based vaccines prepared by loading DCs with tumor-associated antigens *ex vivo*.

Bone marrow-derived cells (for the murine models) and peripheral monocytes (in clinical trials) are commonly used as DC precursors (pre-DCs) when preparing DC-based vaccines. The routine method for the production of DC-based vaccines involves incubation of pre-DCs in the presence of cytokines GM-CSF and IL-4 for 6–8 days, loading immature DCs with tumor-associated antigens, and subsequent activation of dendritic cell maturation using inflammatory cytokines (TNF-α, IL-1β, IL-6, IFN-γ, etc.) or xenogenous factors: LPS (bacterial lipopolysaccharide), OK-432 (low-virulence strain of *Streptococcus pyogenes*), KLH (hemocyanin from mollusk *Fissurella apertura*), etc.

The effectiveness of the antitumor immune response activated by modified DCs is strongly affected by the TAAs used to load immature DCs. Tumor lysates [6–9], synthetic tumor-specific peptides [10–13], tumor proteins [14], apoptotic tumor cells [15], nucleic acids (DNA [16], mRNA [17], total tumor RNA [18, 19]), and viral vectors [15, 20] encoding TAAs as well as immune-stimulating molecules (IL-12 [21, 22]), proliferation factors (GM-CSF [23]), and chemotactic signals (limphotactin [24]) are used as sources of TAAs.

Immature DCs can capture tumor antigens via a number of mechanisms, such as phagocytosis, macropinocytosis, receptor-mediated endocytosis, etc. Hence, tumor-associated antigens of protein nature (proteins, peptides, and lysates) or apoptotic tumor cells are delivered into DCs by passively adding TAAs to immature DCs.

The delivery of nucleic acids (NAs) encoding TAAs requires more complex approaches. NAs are hydrophilic polyanionic molecules that interact with the negatively charged plasma membrane with a poor efficiency and cannot penetrate the cells through the hydrophobic lipid bilayer of the plasma membrane. Furthermore, unprotected NAs are rapidly degraded by nucleases in body fluids. It is also known that free mRNAs can interact with Toll-like receptors (TLR3, TLR7, and TLR8), often resulting in undesired activation of the immune system [25]. Therefore, NAs are delivered into DCs using physical methods (e.g., electroporation [16, 26–28] or sonoporation [29, 30]); viral systems (adenoviruses, adeno-associated viruses, retroviruses, lentiviruses, Vaccinia virus, etc. [31–38]); and nonviral systems (polycationic polymers [31, 39–41] and cationic liposomes [28, 42–45]).

APPLICATION OF TAA-LOADED DENDRITIC CELLS IN THERAPY OF MALIGNANT NEOPLASMS

Tables 1 and *2* summarize the results of the investigations of DC-based antitumor vaccines in murine models (studies carried out in 2010–2015) and clinical trials (2005–2015). When selecting the studies to be listed, we made allowance for the variety of diseases treated with DC-based vaccines and the TAA sources for loading DCs. We would like to take notice of the great diversity of sources of TAAs for loading DCs used in studies on murine tumor models, from the conventional tumor peptides and lysates to neuraminic acid derivatives and living tumor cells. First of all, antigens of protein nature (tumor cell lysates, proteins, and peptides) were used as the main sources of TAAs for loading DCs in clinical trials. Various routes of vaccine administration (intradermal, intravenous, vaccination into the lymph nodes, etc.) were also employed [46].

IN VIVO EFFICACY OF DC-BASED VACCINES IN MURINE MODELS

Below, we discuss the results of 15 studies focused on DC-based vaccines in murine models and performed in 2010–2015. Eight of them were devoted to therapeutic DC-based vaccines, where DCs were administered to tumor-bearing mice, four studies focused on preventive DC-based vaccines with DCs administered to animals before tumor grafting, and three studies were devoted to both types of DC-based vaccines. The antitumor potential of DCs was studied in murine tumor models such as colorectal cancer [47, 48], hepatocellular carcinoma [49, 50], Dalton's lymphoma [51] and EL4 lymphoma [52], FBL3 leukemia[53], 4T1 breast carcinoma [54], B16 melanoma [30, 55–57], Lewis lung carcinoma [58, 59], and SCCVII squamous cell lung cancer models [60] (*Table 1*). In almost all the publications under analysis, DCs were prepared by incubation of bone marrow-derived pre-DCs in the presence of the cytokines GM-CSF and IL-4. Both therapeutic and preventive DC-based vaccines were administered to animals 2 or 3 times with a 7-day interval, preferentially via subcutaneous injections or, less frequently, intraperitoneal or intravenous injections.

Protein antigens (first of all, lysate and the total protein of tumor cells) were the most typically used as a source of TAAs to load DCs. The vaccines being used can be subdivided into (1) DC-based vaccines without additional stimuli (B16 melanoma [30] and Lewis lung carcinoma [59]); (2) DC-based vaccines additionally treated with siRNA against immunosuppressive enzyme indolamine 2,3-dioxygenase (4T1 breast carcinoma [54]) or with plant-based immunostimulatory polysaccharide (EL4 lymphoma [52]); and (3) DC-based vaccines combined with injections of cucurbitacin I that selectively inhibits STAT3 in tumor cells (Dalton's lymphoma [51]). In addition, AH1 tumor peptide (gp70 fragment) in combination with the non-tumor helper peptide (ovalbumin), whose key function was to increase the stability and efficiency of antigen presentation to T cells by DCs, was used as a source of TAAs

Table 1. *In vivo* efficacy of DC-based vaccines in animal tumor models

Tumor type	Antigen type	Treatment regimen*	Outcome	Reference
Colorectal cancer	AH1 peptide (gp70 fragment); helper protein ovalbumin (OVA)	SC, 5×10^5 cells/mouse; twice with a 7-day interval	decreased CT26 tumor size; increased CTL proliferation; increased animal lifespan	[47]
	Adenoviral vectors encoding CEA and SVV; CAR-TAT fusion protein	SC, 1×10^6 cells/mouse; 2–3 times with a 7-day interval	For DCs simultaneously expressing CEA and SVV: increased *in vitro* splenocyte reactivity against MC38/CEA2; reduced tumor growth being more efficient in the presence of CAR-TAT	[48]
Hepatocellular carcinoma	Adenoviral vector encoding FAT10; TNF-α	Preventive regimen: SC, 1×10^6 cells/mouse; 3 times 3 days after subcutaneous injection of Hep3G cells	increased cytotoxic CTL response against Hep3G; decreased Hep3G tumor size; increased animal lifespan	[49]
	Ca9-AbOmpA fusion protein or RENCA-Ca9 cell lysate	SC, 1×10^6 cells/mouse; 3 times with a 7-day interval	decreased tumor progression 1.5–3-fold increased *in vitro* secretion of IL-2, IFN-γ, and TNF-α by T cells; increased splenocyte reactivity against RENCA-Ca9	[50]
Dalton's lymphoma	Dalton's lymphoma cell lysate; IL-15; combination with cucurbitacin I, IL-15	IP, 1×10^6 cells/mouse; 6 times with a 4-day interval 10 IP injections (1 mg/kg) of cucurbitacin I with a 1-day interval during 19 days 5 IV injections of IL-15 (8 μg/kg) on days 25–33	The DCs/lysate/IL-15 + cucurbitacin I group: increased survival time of animals (51 days); survival time in the control group was 22 days; complete healing was not achieved. The DCs/lysate/IL-15 + cucurbitacin I + IL-15 group: increased animal survival rate, 70% of animals were alive by day 60, total tumor elimination and healing. Accumulation of $CD4^+$ and $CD8^+$ T cells in metastases	[51]
EL4 lymphoma	EL4 cell lysate; G1-4A polysaccharide from *Tinospora cordifola*	Preventive regimen: SC, 5×10^5 cells/mouse; 3 times with a 7-day interval; therapeutic regimen: SC, 5×10^5 cells/mouse; on tumor progression days 3, 7, and 10	tumor size decreased 2.2- to 3.8-fold for the preventive regimen; tumor size decreased 2.1–2.6-fold for the therapeutic regimen	[52]
FBL3 leukemia, B16F10 melanoma (modified, expressing N-phenylacetyl-*D*-neuraminic acid)	GM3NPhAc-KLH; combination with ManNPhAc	Preventive regimen: SC, 1×10^6 cells/mouse; 3 times with a 7-day interval; IP injection of ManNPhAc (50 mg/kg body weight) 7 times every day after tumor was grafted	increased CTL cytotoxicity against modified FBL3 cells; FBL3 tumor size decreased 2.5-fold; increased animal lifespan; the number of B16F10 lung metastases decreased twofold	[53]
4T1 breast carcinoma	Lysate of 4T1 cells and anti-IDO siRNA	IV, 2×10^6 cells/mouse; 3 times with a 7-day interval	tumor size decreased twofold; reduced apoptosis of $CD4^+$ and $CD8^+$ T cells; increased CTL proliferation; decreased Treg cell count	[54]
B16 melanoma	mRNA encoding β_2m-tumor peptide-TLR4 (electroporation)	Preventive regimen: IP, 2.5×10^6 cells/mouse, 3 times with a 7-day interval Therapeutic regimen: IP, 2.5×10^6 cells/mouse, 3 times with a 7-day interval	DC maturation. CTL activation. The preventive regimen ensures complete protection against tumor propagation. The therapeutic regimen ensures increased animal lifespan	[55]
	Total protein extracted from melanoma cells (sonoporation)	Preventive regimen: SC, 1×10^6 cells/mouse; 2 times with a 7-day interval	The number of lung metastases decreased fourfold	[30]
	Living B16 cells; LPS	Preventive regimen: IV, 5×10^6 cells/mouse; 2 times with a 14-day interval	Complete elimination of B16 tumor; increased CTL count	[56]
	Living or apoptotic B16 cells, $gp100_{25-33}$ and $TRP_{181-188}$ peptides, LPS, and IFN-γ	IV, 5×10^6 cells/mouse; 2 times with a 7-day interval	the number of lung metastases decreased 14.3-fold (DC-living B16 cells); the number of lung metastases decreased 2–2.7-fold (DC peptides and apoptotic B16 cells)	[57]

Lewis lung carcinoma (LLC)	Adenoviral vector encoding human livin α	Preventive regimen: SC, 5×10^5 cells/mouse; 3 times with a 7-day interval; therapeutic regimen: SC, 5×10^5 cells/mouse; 3 times with a 4-day interval	increased CTL cytotoxicity; 100% animal survival rate for the preventive regimen; tumor growth decreased twofold and the survival rate of mice increased for the therapeutic regimen	[58]
	LLC cell lysate	IP, 1×10^5 cells/mouse; 2 times with a 7-day interval	the number of lung metastases decreased 2- to 7.5-fold	[59]
SCCVII squamous cell lung cancer	Apoptotic SCCVII cells	SC, 1×10^6 cells/mouse; 2 times with a 7-day interval	the number of lung metastases decreased 3.9-fold; the survival rate of mice increased 2.4-fold; CTL cytotoxicity increased	[60]

* – Treatment according to the therapeutic regimen unless otherwise specified.

for the model of colorectal cancer [47]. In the model of hepatocellular carcinoma, a fusion protein (carboanhydrase 9 linked to the membrane protein of *Acinetobacter baumannii*) was used to load DCs [50].

Apoptotic tumor cells, another appreciably common source of TAAs for loading DCs, were used for the model of SCCVII squamous cell lung cancer [60].

DCs were also modified with genetic constructs: namely, adenoviral vectors encoding TAAs (colorectal cancer [48], hepatocellular carcinoma [49], and Lewis lung carcinoma [58]) or mRNA encoding fusion polypeptide β_2m-tumor peptide-TLR4 containing TAA linked to the components of both MHC I and the Toll-like receptor TLR4 (B16 melanoma [55]).

N-phenylacetyl-*D*-neuraminic acid, a synthetic derivative of neuraminic acid (the models of FBL3 leukemia and B16 melanoma [53]), and living tumor cells (B16 melanoma model [56, 57]) are the novel sources of TAAs used for the activation of DCs.

All the DC-based vaccines under consideration showed significant efficacy and reduced tumor size 1.5- to 3-fold with respect to the control [47–50, 52–54, 58]; injection of DC-based vaccines loaded with tumor lysate in combination with injections of cucurbitacin I resulted in complete disappearance of Dalton's lymphoma [51]. In addition, injection of preventive DC-based vaccines transfected with mRNA encoding polypeptide β_2m-tumor peptide-TLR4 [55] or prepared using living B16 melanoma cells as a source of TAA [56] fully protected animals against the development of B16 melanoma. Antitumor DC-based vaccines significantly reduced the number of metastases in mice [30, 53, 57, 59, 60], considerably increased the lifespan of tumor-bearing animals [47, 49, 51, 53, 55, 58, 60], and induced the development of a strong antitumor response from cytotoxic T lymphocytes [47–50, 53–56, 58, 60].

Hence, the highly promising results for both the therapeutic and preventive application of DC-based vaccines obtained using murine tumor models attest to their high potential and provide grounds for hoping that efficacious antitumor DC-based vaccines will be designed.

EFFICACY OF DC-BASED VACCINES IN CLINICAL TRIALS

The promising results obtained using murine models *in vivo* encouraged researchers to proceed to the clinical trials of antitumor DC-based vaccines as early as in the 1990s. The safety of antitumor DC-based immunotherapy has been documented in the clinical trials that have been carried out in the past 20 years. DC vaccination is well tolerated [61] and has minor side effects, such as local inflammation reaction at the injection site and in lymph nodes [62, 63]; manifestations similar to influenza symptoms are sometimes observed [63, 64]. Nevertheless, despite its safety and high potential, immunovaccination of cancer patients with DC-based vaccines in most cases has proved less efficacious than in experiments using murine models. There can be various reasons for this, including the fact that in most studies, DC vaccination was used for terminal patients with extremely aggressive tumors that do not respond to conventional therapy and also the fact that human tumors have a stronger immunosuppressive activity. Although there have not been that many impressive clinical results, further development of antitumor DC-based vaccines continues: our understanding of the DC function is being deepened, novel sources of tumor antigens and immunostimulatory agents for loading and activating DC are being tested, and the potential of combining DC-based vaccines with other approaches is being evaluated.

We have made an attempt to assess the variety and clinical efficacy of DC-based vaccines for tumors of different origins. With this aim in mind, we analyzed the results reported in 20 studies performed in 2005–2015; in most of them, DC-based vaccines were in phase I and II clinical trials (*Table 2*). These studies were conducted for cancers of different nosological entities. Various tumor antigens loaded into DCs, treatment regimens, and combination of DC-based vaccines with other therapeutic approaches were employed.

Table 2. DC-based antitumor immunotherapy in clinical trials

Tumor type	Phase	Number of patients	Antigen type; maturation stimulus	Treatment regimen	Outcome	Reference
Pancreatic cancer	I	10	WT-1 peptide. Combination with gemcitabine.	Days 1, 8, 1: IV injection, gemcitabine (1 g/m^2). Days 8 and 22: ID injection, 1×10^7 DCs. Three cycles	DTH$^+$ response (3/10). HLA/WT-1 tetramer-positive test (6/10). Positive IFN-γ ELISPOT (7/10). No clinical response	[65]
Pancreatic and bile duct cancer	I/II	12	MUC1 peptide; *TNF-α*, IL-1β*, IL-16**	ID – SC, 1×10^6 cells, 3 times with a 21-day interval and once 6 months after the last vaccination	perforin and granzyme expression by CD8$^+$ T cells was increased the mean survival rate increased to 26 months (8/12) and more than 7 years (4/12)	[66]
Glioblastoma	I	21	Peptides MAGE1, TRP-2, gp-100, HER-2, IL-13Rα2; *TNF-α**	ID, 1×10^7 cells, 3 times with a 14-day interval	The median survival time is 40.1 months; the mean progression-free survival time is 16.9 months; the mean overall survival time is 38.4 months; 24-month progression-free survival rate is 43.8%; the overall 36-month survival rate is 55.6%	[67]
Colorectal cancer	I	16	mRNA CEA (electroporation) (5/16) or CAP-1, peptide (11/16); *cytokine cocktail 1**	ID–IV, 5×10^6 cells, 3 times with a 7-day interval	CEA-specific T cells (8/11, peptide group; 0/5, RNA group); increased CEA blood level (7/11, peptide group; 2/5, RNA group); mean progression-free survival time is 18 months (the peptide group) and 26 months (the RNA group)	[68]
Hepatocellular carcinoma	I/II	5	Fusion protein (α-fetoprotein, glypican-3, MAGE-3, cytoplasmic transduction); *cytokine cocktail 2**	SC, 4×10^7 cells, 4 times with a 14-day interval and 2 times on weeks 12 and 14 after vaccination was started	Tumor-specific T-cell (5/5); disease stabilization (1/5)	[69]
Liver cancer (stages III and IV)	I	67	Tumor lysate of autologous and allogeneic tumor cells; TNF-α. Combination with cytokine-induced killer cells (CIKs).	DCs: injected into lymph nodes, >10^6 cells on days 10 and 12. CIKs: IV injection, >1×10^{10} cells on days 12 and 14	Complete response (0/67); partial remission (5/67); disease stabilization (29/67). DC-CIKs suppress HepG2 cell proliferation	[70]
Myeloid leukemia	I	4	Apoptotic leukemia cells; *KLH, OK432**	ID, 5 times with a 14-day interval	Antileukemia CD8$^+$ T-cell response (2/4); the leukemia cell count in bone marrow decreased 2.1-fold (1/4)	[71]
T-cell leukemia, lymphoma	I	3	Tax peptides LLFGYPVYV or SFHSLHLLY; *TNF-α*, KLH*, OK432**	SC, 5×10^6 cells, 3 times with a 14-day interval	Tax-specific CTL-response on weeks 16–20 (3/3); complete remission (1/3); partial remission (1/3); disease stabilization (1/3)	[72]
Lymphocytic leukemia	I	15	Autologous apoptotic B cells; *TNF-α**	DCs: ID (1×10^7 cells), 4 times with a 14-day interval, once 14 weeks after the first DC vaccination; GM-CSF: 4 times; after DC vaccination; CP: 2 days prior to DC injection. cohort 1: DCs cohort 2: DCs+GM-CSF cohort 3: DCs+ GM-CSF +CP	Antileukemia CD8$^+$ T-cell response 1) 2/5; 2) 3/5; 3) 5/5	[73]
Osteosarcoma	I	12	Autologous tumor lysate; *KLH; PGE_2**	ID, 10^5–10^6 cells, 3 times with a 7-day interval. After DC-based therapy, SC injections of IL-2 6 times with a 1-day interval	Antitumor CD8$^+$ T-cell response (2/12). No clinical response.	[74]
Ovarian cancer	I/II	11	hTERT 988Y, Her2/neu 369VV2V9, Her2/neu 689 and PADRE peptides; *Klebsiella pneumoniae**; *IFN-γ**	ID, 3.5×10^7 cells, 4 times with a 21-day interval; IV injection of CP	Disease relapse during vaccination (2/11); Disease relapse after vaccination (3/11); no signs of disease during > 36 months (6/11); the overall 36-month survival rate is 90%	[75]

Melanoma	I	8	Autologous melanoma cell lysate; TNF-α. Combination with tumor-infiltrating T cells. Preliminary chemotherapy.	DCs injected ID, 3 times with a 14-day interval. T cells injected IV, 1–3 times with a 7-day interval 7 days 14 days after last DC vaccination	Complete remission (1/8). Disease stabilization during 2 and 10 months (2/8). Disease progression (7/8)	[76]
	I	30	mRNA encoding fusion protein containing TAAs (MAGE-A1, - A3, -C2, tyrosinase, MelanA/MART-1 and gp100) and HLA II-targeting sequences (electroporation); *Poly (I:C)* or TriMix**. Combination with injections of IFN-α-2b	ID, 2.4×10^7 cells, 4–6 times with a 14-day interval SC injection of IFN-α-2b 3 times a week	Immune response against melanoma-associated antigens (4/10). Complete remission (10/30). Recurrence of melanoma (20/30). Mean relapse-free survival time is 22 months. The two-year survival rate is 93%. The four-year survival rate is 70%.	[77]
	I	20: 5 – III 15 – IV	Autologous melanoma cell lysate; *TNF-α**	SC, $1–5\times10^6$ cells, 4 times with a 10-day interval	Increased IFN-γ secretion (10/20); Increased CTL cytotoxicity (4/20); DTH^+ response (11/20); Time of tumor progression increased 4.1-fold (the DTH^+ response group vs the DTH^- response group); survival rate increased 2.9-fold (the DTH^+ response group vs the DTH^- response group).	[78]
	II	24	Peptides gp100, tyrosinase, MAGE-A2, MAGE-A3, MART-1, MAGE-A1; *KLH**	SC, $1–5\times10^7$ cells, 4 times with a 7-day interval, then once after 14 days and 5 times with a one-month interval.	increased count of tumor-specific $CD8^+$ T cells (18/24); activation of Th1 response (12/24); DTH^+ response to TAAs in 41% of patients; DTH^+ response to KLH in 64% of patients; patient survival rate increased 1.9-fold; partial response (1/24); disease stabilization (7/24); disease progression (16/24)	[79]
		33	Lysates of cells of allogeneic melanoma lines M44, COLO829, SK-MEL28; *IFN-γ**	Near the lymph nodes, 2.5×10^7 cells, 6 times with a 14-day interval, then twice with a 42-day interval	The count of tumor-specific $CD8^+$ T cells in blood increased (26/33). Complete remission (1/33), partial response (2/33), disease stabilization (6/33)	[80]
Non-small cell lung cancer	III	103	DCs were not loaded with TAAs. Vaccine consisted of DCs and T cells derived from pulmonary lymph nodes and incubated in the presence of IL-2 with peripheral blood T cells added	Group A: 4-month chemotherapy course, DC-based vaccine 1 week after each chemotherapy course + once a month (during 6 months) + once every 2 months (during 14 months). Group B: 4-month chemotherapy course	The overall two-year survival rate in groups A and B is 93.4 and 66.0%, respectively; the overall five-year survival rate in groups A and B is 81.4 and 48.3%, respectively; the relapse-free 2- and 5-year survival rate is 68.5 and 41.4% (group A); 56.8 and 26.2% (group B).	[81]
Prostate cancer	I/II	25	UV-treated LNCaP cells; *poly (I : C)**. Combination with chemotherapy.	1. Cyclophosphamide, 7 days 2. DCs, SC injection, 10^7 cells, 12 times within the first year (2 times with a 2-week interval) 3. Docetaxel every 3 weeks until toxicity is achieved. 4. SC injection of DCs, 10^7 cells, 10 times with a 6-week interval	PSA level decreased by ≥ 50% (8/23) PSA level decreased by 20–50% (5/23) Blood level of Tregs decreased Induction of PSA-specific CTLs. The mean survival time is 19 months.	[82]
	III	127	PAP-GM-CSF, fusion protein	IV, 3.7×10^9 cells, 3 times with a 14-day interval	Disease progression (115/127); time of disease progression increased 1.2-fold; the mean survival rate increased 1.2-fold	[83]
	III	512	PAP-GM-CSF, fusion protein	IV, 3.7×10^9 cells, 3 times with a 14-day interval	the mortality risk decreased by 22%; the mean survival rate increased 1.2-fold; the 36-month survival rate increased 1.4-fold; Activation of Th1-response.	[5]

Note: * – factors for dendritic cell maturation; SC – subcutaneous; IP – intraperitoneal; IV – intravenous; ID – intradermal; DTH response – delayed type (type IV) hypersensitivity reaction; KLH – keyhole limpet hemocyanin from *Fissurella apertura*, OK432 – a mixture of low-virulence group A *Streptococcus pyogenes*; cytokine cocktail 1 – PGE_2, TNF-α, IL-1β, IL-6; cytokine cocktail 2 – PGE_2, TNF-α, IL-1β, IL-6, IFN-γ, OK432, poly (I : C); TriMix – mRNA encoding CD40L, CD70 and the constitutively active TLR4; CP – cyclophosphamide; disease stabilization – there are no visible changes in tumor size; disease progression – there is a 20% increase in tumor size; partial response – a 30% decrease in tumor size; and complete response – tumor disappearance.

Three DC-based vaccines have passed phase III trials; one of these vaccines, Sipuleucel-T, used against castration-resistant prostate cancer was later approved by the FDA under the brand name Provenge® [5].

The antitumor potential of DC-based vaccines was evaluated in patients with a cancer of the gastrointestinal tract (liver, pancreatic, and colorectal cancer), brain (glioblastoma), blood (myeloid leukemia, lymphocytic leukemia, lymphoma), bone tissue (osteosarcoma), the reproductive system (ovarian or prostate cancer), skin (melanoma), and lungs (non-small cell cancer) both after the tumors had been surgically resected and patients had undergone conventional chemo- or radiotherapy and in treatment-naïve patients (*Table 2*). The adequacy of DC-based vaccines was evaluated using two criteria: the immunological criterion and the clinical one. The key immunological variables measured in clinical trials of DC-based vaccines were as follows: the immune response against TAAs (type IV hypersensitivity response to tumor antigens (DTH response)), the presence of HLA complexes with tumor antigens on the surface of DCs, the expression of perforin/granzyme by $CD8^+$ T cells, the activity of cytotoxic $CD8^+$ T cells against tumor cells, the level of IFN-γ synthesis by T cells, the regulatory T-cell count in blood and tumor cell count in the bone marrow, the concentration of tumor markers (PSA, CEA) in blood serum, etc. (*Table 2*). The clinical response to immunotherapy with DC-based vaccines was assessed according to the patient survival rate, disease remission/relapse (a 20% increase in tumor size was considered to be a sign of disease progression; no visible changes in tumor size were a sign of stable condition), partial response or partial remission (tumor size reduction by 30%), and complete response or complete remission (tumor disappearance) (*Table 2*).

In most of the analyzed studies, the DCs were derived from peripheral blood mononuclear cells cultured in the presence of cytokines GM-CSF and IL-4. In one case, GM-CSF and IL-13 were used to prepare the DC-based vaccine [79]. Unconventional DC-based vaccines were used as antitumor vaccines undergoing phase III clinical trials: DCs isolated from pulmonary lymph nodes were used in non-small cell lung cancer [81]; the Sipuleucel-T vaccine (a cellular agent isolated from leukapheresis-derived products that included DCs) was used in patients with prostate cancer [5, 83].

Protein antigens (peptides, synthetic proteins, and tumor cell lysates) were used most frequently (15 out of 20 publications) as a source of TAAs to load DCs. Peptide TAAs were used both as a single antigen (WT-1 or MUC1 in the case of pancreatic cancer [65, 66]) and as an antigen mixture (MAGE1, TRP-2, gp100, HER-2, IL-13Rα2 in glioblastomas [67]; gp100, tyrosinase, MAGE-A1, -A2, -A3, MART-1 in melanoma [79]; HTLV-1 Tax peptides in T-cell leukemia and lymphoma [72], and hTERT, Her2/neu, and PADRE fragments, in ovarian cancer [75]). mRNAs encoding a single antigen (CEA in the case of colorectal cancer [68]) or a combination of antigens (MAGE-A1,-A3,-C2, tyrosinase, MelanA/MART-1, and gp100 for melanoma [77]) were also used to load DCs. In the case of hepatocellular carcinoma, DCs were loaded with fusion proteins containing TAAs such as α-fetoprotein, glypican-3 and MAGE-3, each of those connected to a cytoplasmic transduction peptide [69]. Another fusion protein containing PSA coupled to GM-CSF was used for loading the Sipuleucel-T vaccine [5, 83]. Tumor cell lysates were used to prepare DC-based vaccines against osteosarcoma [74] and melanoma [76, 78, 80]; the lysate was most often prepared from autologous tumor cells. DCs were also often loaded with apoptotic tumor cells (e.g., in DC-based vaccines against myeloid [71] and lymphocytic leukemia [73] and prostate cancer [82]). In the DC-based vaccine against non-small cell lung cancer, DCs were not loaded with TAAs at all but were used together with T cells after coincubation in the presence of IL-2 [81].

It is known that injection of immature DCs into a tumor-bearing organism can cause the development of tolerance of the immune system to tumor antigens, ultimately resulting in an even greater tumor progression [84]. Therefore, much attention is paid to agents that stimulate DC maturation in almost all clinical trials of DC-based vaccines. Both single pro-inflammatory cytokines (TNF-α or IFN-γ) and cocktails containing a combination of pro-inflammatory cytokines, prostaglandin E2, and in some cases poly(I:C)oligonucleotides, low-virulence *S. pyogenes* (OK432), bacteria *Klebsiella pneumoniae* or hemocyanin from *F. apertura* (KLH) were used for this purpose (*Table 2*).

Despite the variety of protocols for tumor immunotherapy with DC-based vaccines, common features can also be listed. DCs are preferentially administered either intradermally or subcutaneously 3–4 times with a 7- to 14-day interval. The mean dose is 10^6–10^7 DCs. In some cases, DC vaccination can be combined with chemotherapy (gemcitabine for pancreatic tumor [65], cyclophosphamide for lymphocytic leukemia [73] and ovarian cancer [75], and docetaxel for prostate cancer [82]), with the application of other immune cells (e.g., cytokine-induced killer cells; i.e., T cells and natural killers activated by IL-1, IL-2, IFN-γ and anti-CD3 antibodies for hepatic tumors [70]); tumor-infiltrating lymphocytes for melanoma [76]), as well as with injections of cytokines (GM-CSF for lymphocytic leukemia [73], IL-2 for osteosarcoma [74], and IFN-α-2b for melanoma [77]).

It was demonstrated in almost all the studies under consideration that administration of DC-based vaccines activates an antitumor immune response: tumor-specific cytotoxic $CD8^+$ T cells are activated; perforin and granzyme expression and IFN-γ production are enhanced; some patients develop a hypersensitivity response to tumor antigens (the DTH response); the regulatory T-cell count decreases, etc. However, despite the substantial immune response, the clinical efficacy of antitumor DC-based therapy is less impressive. The clinical response is either rather weak or absent, which manifests itself in a large number of relapses and tumor progression. Even Sipuleucel-T, the only FDA-approved antitumor DC-based vaccine, exhibits low efficacy. Immunotherapy using this vaccine resulted in remission in none of the patients; disease progression was observed in most cases, although patient survival increased 1.2-fold compared to the placebo group [83]. Hence, a conclusion can be drawn that activation of a tumor-specific immune response after DC vaccination does not necessarily provide significant clinical outcomes. First of all, this can be attributed to the negative effect of the tumor on the immune system. Even provided that antitumor T cells are properly activated by DC-based vaccines, immunotherapy may fail, since the tumor can evade immune surveillance by suppressing the functional activity of immunocompetent cells, including T cells and DCs, via various mechanisms [85].

Tumor remission in a number of patients is indicative of the clinical significance of DC vaccination. Hence, immunotherapy with DCs loaded with a mixture of tumor-specific peptides (hTERT 988Y, Her2/neu 369VV2V9, Her2/neu 689, and PADRE) in combination with cyclophosphamide injections resulted in the absence of disease symptoms during 36 months in more than 50% of patients with ovarian cancer (6/11); the 36-month survival rate was 90% [75]. This is one of the highest indices of clinical efficacy of DC-based vaccines in the studies covered in this review.

Many remissions were observed in patients with melanoma after they had received DC-based vaccines loaded with a mixture of mRNAs encoding TAAs MAGE-A1,-A3,-C2, tyrosinase, MelanA/MART-1 and gp100 fused with HLA II-targeting sequences, in combination with IFN-α-2b injections [77]. During the mean follow-up (6.4 years), 10 out of 30 patients showed complete remission. The mean relapse-free survival time was 22 months. The mean two- and four-year survival rate was 93 and 70%, respectively. Four out of 10 patients showed an immune response against melanoma-associated antigens [77].

Either complete or partial remission of melanoma was also observed after patients had undergone immunotherapy with DC-based vaccines with lysates of autologous melanoma cells (1 out of 8 patients) [76] or the allogeneic cell lines M44, COLO829, and SK-MEL28 (complete response in one out of 33 patients; partial response, in 2 out of 33 patients) [80]. It is noteworthy that melanoma is used appreciably often in clinical studies of the antitumor activity of DCs and is relatively more susceptible to immunotherapy than other tumor types.

A high efficacy of DC-based vaccines was also observed in a pilot clinical study of DCs against T-cell leukemia and lymphoma with three patients enrolled [72]. DCs loaded with Tax peptides of human T-lymphotropic virus 1 (LLFGYPVYV and SFHSLHLLY) that matured under standard stimulus (TNF-α in combination with the xenogeneic factors KLH and OK432) have been used as DC-based vaccines. After DC vaccination, all three patients showed a significant clinical response: complete remission (1/3), partial remission (1/3), and disease stabilization (1/3). The efficacious clinical response was related to the development of a Tax-specific CTL response in all patients [72].

The survival rate of patients is also an important indicator of the efficacy of antitumor DC vaccination. Almost all clinical trials demonstrate that administration of DC-based vaccines to patients with tumors of different types increases their survival rate and life expectancy compared to patients not treated with a DC-based vaccine. Hence, the most significant increase in the survival rate in the analyzed studies was achieved in patients with pancreatic and bile tract cancers who received DCs that were loaded with MUC-1 peptide and stimulated with the cytokines TNF-α, IL-1β, and IL-16: the mean survival time was more than 7 years in 4 out of 12 patients [66].

Let us discuss three phase III clinical trials of antitumor DC-based vaccines in more detail. In the first study, a vaccine based on DCs and activated killer T cells, in combination with chemotherapy, was used in patients with non-small cell lung cancer [81] after the tumor had been surgically resected. One hundred and three patients were enrolled and divided into two groups: group A received immunochemotherapy, while group B received chemotherapy only. The vaccine was based on DCs and activated killer T cells which were isolated from the contents of lymph nodes residing at tumor sites and cultured in the presence of IL-2; peripheral blood T cells were subsequently added. The overall two-year survival rates in groups A and B were 93.4 and 66.0%, respectively; the overall five-year survival rates were 81.4 and 48.3%, respectively. The two- and five-year relapse-free survival rates were 68.5 and 41.4%; 56.8 and 26.2% in groups A and B, respectively [81].

The Sipuleucel-T DC-based vaccine, which was used for patients with castration-resistant prostate cancer, was assessed in two other trials. However, the results

of clinical trials of Sipuleucel-T were less impressive compared to those for other antitumor DC-based vaccines [83]. Sipuleucel-T is a cellular agent isolated from leukapheresis-derived products that included DCs. The cells were loaded with a fusion protein consisting of full-length PAP and full-length human GM-CSF (PAP-GM-CSF). Patients with asymptomatic metastatic hormone-refractory prostate cancer were enrolled. Administration of this vaccine caused disease progression in most patients. Nevertheless, Sipuleucel-T increased the mean survival time 1.2-fold (25.8 months vs 21.7 months in the placebo group) and resulted in the development of immune response to PAP and T-cell response [5, 83]. Soon after these results were published, Sipuleucel-T was approved by the U.S. Food and Drug Administration (FDA USA) for treating patients and commercialized under the trademark Provenge® [86].

EFFICACY OF ANTITUMOR DENDRITIC CELL-BASED VACCINES: QUESTIONS AND ANSWERS

It is clear from the studies discussed above that most of the antitumor DC-based vaccines that have successfully passed clinical trials have limited efficacy. Some researchers believe that the low efficacy of DC-based vaccines can be related to the fact that their effect on patient survival becomes noticeable only some time after treatment [5]. However, in our opinion, the key reason for the low efficacy of DC-based vaccines is the strong immunosuppressing action of the tumor that is ensured by a number of mechanisms. For example, the tumor and the surrounding tissue can reduce the penetration of T cells into the tumor site, reduce granzyme B activity, suppress death receptor CD95 expression by T cells, and induce anergy of activated T cells by enhancing the expression of the inhibitory receptors CTLA-4 and PD-1 (the so-called immune checkpoints) on the T-cell surface [87]. The immunosuppressive activity of CTLA-4 consists in the fact that it is in competition with the standard participant of the immunological synapse, CD28, for binding to the DC-derived costimulatory molecules CD80 (B7.1) and CD86 (B7.2) and the transmission of the inhibitory signal to T cells, thus attenuating the TCR/CD28 signaling pathway of T cells, reducing IL-2 production by T cells, and eventually resulting in cell cycle delay [87, 88]. The PD-1 receptor interacts with the B7-H1 molecules expressed on the tumor cell surface, which also disrupts the TCR/CD28 signaling pathway, induces the synthesis of anti-inflammatory cytokine IL-10, and eventually results in the activation of immunosuppressive Tregs and apoptosis of tumor-specific T cells [87, 89].

It is reasonable to employ additional methods aimed at reducing the inhibitory effect of the tumor to enhance the efficacy of DC-based vaccines. Thus, CTLA-4, PD-1, and B7-H1 blocking antibodies combined with antitumor DC-based vaccines will make it possible to reduce the immunosuppressive activity of the tumor, which may significantly increase the antitumor activity of DC-based vaccines. The immune checkpoint inhibitors known today are Ipilimumab [90] for CTLA-4, Nivolumab [91] and Pembrolizumab [92] for PD-1. The FDA has recently approved these monoclonal antibodies for the immunotherapy of metastatic melanoma [93, 94]. B7-H1 blocking antibodies are currently under clinical trials but have not been approved for clinical use yet [95]. Only one study reporting the use of antitumor DC-based vaccines in combination with immune checkpoint inhibitors has so far been published. In this phase II clinical trial, patients with melanoma received a combination of Ipilimumab and DC-based vaccines loaded with TriMix RNA and mRNA encoding melanoma-associated antigens. Very promising results have been obtained: after the therapy course, eight of the 39 patients showed complete remission and seven patients showed a partial response [96]. Clinical trials of antitumor DC-based vaccines in combination with immune checkpoint inhibitors will undoubtedly be forthcoming.

CONCLUSIONS

Despite the great variety of the mechanisms used by a tumor to evade the immune response, promising results have been obtained for cancer immunotherapy using modified DCs. Experiments using murine models have shown a reduced tumor growth rate, a decline in the number of metastases, an increase in the survival rate of tumor-bearing animals, and initiation of a tumor-specific CTL response [50, 54, 57, 97, 98]. The results of clinical trials of antitumor DC-based vaccines were also fairly good, although less encouraging compared to those obtained using *in vivo* murine models. A plausible reason is that clinical trials in most cases are performed on terminally ill patients when no other therapy shows any effect. Furthermore, the low efficacy of DC-based vaccines can be related to the fact that the human immune system is suppressed by the tumor to a greater extent.

The problems related to the search for the most immunogenic source of TAAs, the insufficient specificity and efficiency of TAA delivery into DCs remain to be solved. This may affect the presentation of processed TAAs bound to complexes with MHC I/II molecules on the DC surface and the weak polarization of antitumor immune responses. Therefore, further development of antitumor DC-based vaccines that would be capable of countering the negative effect of the tumor and its surroundings and initiate an efficient antitumor immune response remains a top priority.

This study was supported by the Special Purpose Program "Research and Development in a Priority Direction of Development of the Scientific and Technological Complex of Russia for 2014–2020" (Agreement No. 14.607.21.0043, project RFMEFI60714X0043)

REFERENCES

1. Slingluff C.L.Jr., Petroni G.R., Yamshchikov G.V., Hibbitts S., Grosh W.W., Chianese-Bullock K.A., Bissonette E.A., Barnd D.L., Deacon D.H., Patterson J.W., et al. // J. Clin. Oncol. 2004. V. 22. P. 4474–4485.
2. Terheyden P., Schrama D., Pedersen L.O., Andersen M.H., Kampgen E., Straten P., Becker J.C. // Scand. J. Immunol. 2003. V. 58. P. 566–571.
3. Rožková D., Tišerová H., Fučíková J., Lašťovička J., Podrazil M., Ulčová H., Budínský V., Prausová J., Linke Z., Minárik I., et al. // Clin. Immunol. 2009. V. 131. P. 1–10.
4. Koh Y.T., Gray A., Higgins S.A., Hubby B., Kast W.M. // Prostate. 2009. V. 69. P. 571–584.
5. Kantoff P.W., Higano C.S., Shore N.D., Berger E.R., Small E.J., Penson D.F., Redfern C.H., Ferrari A.C., Dreicer R., Sims R.B., et al. // N. Engl. J. Med. 2010. V. 363. P. 411–422.
6. Nestle F.O., Aligagic S., Gilliet M., Sun Y., Grabbe S., Dummer R., Burg G., Schadendorf D. // Nat. Med. 1998. V. 4. P. 328–332.
7. Fields R.C., Shimizu K., Mule J. // J. Proc. Natl. Acad. Sci. USA. 1998. V. 95. P. 9482–9487.
8. Geiger J., Hutchinson R., Hohenkirk L., McKenna E., Chang A., Mule J. // Lancet. 2000. V. 356. P. 1163–1165.
9. Geiger J.D., Hutchinson R.J., Hohenkirk L.F., McKenna E.A., Yanik G.A., Levine J.E., Chang A.E., Braun T.M., Mule J.J. // Cancer Res. 2001. V. 61. P. 8513–8519.
10 Celluzzi C.M., Mayordomo J.I., Storkus W.J., Lotze M.T., Falo L.D. // J. Exp. Med. 1996. V. 183. P. 283–287.
11. Miconnet I., Coste I., Beermann F., Haeuw J.F., Cerottini J.C., Bonnefoy J.Y., Romero P., Renno T. // J. Immunol. 2001. V. 166. P. 4612–4619.
12. Wang H.Y., Fu T., Wang G., Zeng G., Perry-Laller D.M., Yang J.C., Restifo N.P., Hwu P., Wang R.F. // J. Clin. Invest. 2002. V. 109. P. 1463–1470.
13. van Gisbergen K., Aarnoudse C., Meijer G., Geijtenbeek T., van Kooyk Y. // Cancer Res. 2005. V. 65. P. 5935–5944.
14. Curti A., Tosi P., Comoli P., Terragna C., Ferri E., Cellini C., Massaia M., D'Addio A., Giudice V., Di Bello C., et al. // Br. J. Haematol. 2007. V. 139. P. 415–424.
15. Jarnjak-Jankovic S., Pettersen R.D., Saeboe-Larssen S., Wesenberg F., Olafsen M.R., Gaudernack G. // Cancer Gene Ther. 2005. V. 12. P. 699–707.
16. van Tandeloo V., Ponsaerts P., Lardon F., Nijis G., Lenjou M., van Broeckhoven C., van Bockstaele D.R., Berneman Z.N. // Blood. 2001. V. 98. P. 49–56.
17. Suso E.M., Dueland S., Rasmussen A.M., Vetrhus T., Aamdal S., Kvalheim G., Gaudernack G. // Cancer Immunol. Immunother. 2011. V. 60. P. 809–818.
18. Boczkowski D., Nair S.K., Nam J.H., Lyerly H.K., Gilboa E. // Cancer Res. 2000. V. 60. P. 1028–1034.
19. Heiser A., Maurice M.A., Yancey D.R., Wu N.Z., Dahm P., Pruitt S.K., Boczkowski D., Nair S.K., Ballo M.S., Gilboa E., et al. // J. Immunol. 2001. V. 166. P. 2953–2960.
20. Nair S.K., Boczkowski D., Morse M., Cumming R.I., Lyerly H.K., Gilboa E. // Nat. Biotechnol. 1998. V. 16. P. 364–369.
21. Nishioka Y., Hirao M., Robbins P.D., Lotze M.T., Tahara H. // Cancer Res. 1999. V. 59. P. 4035–4041.
22. Rodriguez-Calvillo M., Duarte M., Tirapu I., Berraondo P., Mazzolini G., Qian C., Prieto J., Melero I. // Exp. Hematol. 2002. V. 30. P. 195–204.
23. Nakamura M., Iwahashi M., Nakamori M., Ueda K., Matsuura I., Noguchi K., Yamaue H. // Clin. Cancer Res. 2002. V. 8. P. 2742–2749.
24. Zhang W., He L., Yuan Z., Xie Z., Wang J., Hamada H., Cao X. // Hum. Gene Ther. 1999. V. 10. P. 1151–1161.
25. van Lint S., Renmans D., Broos K., Dewitte H., Lentacker I., Heirman C., Breckpot K., Thielemans K. // Expert Rev. Vaccines. 2015. V. 14. P. 235–251.
26. Vari F., Hart D.N. // Cytotherapy. 2004. V. 6. P. 111–121.
27. Aarntzen E.H., Schreibelt G., Bol K., Lesterhuis W.J., Croockewit A.J., de Wilt J.H., van Rossum M.M., Blokx W.A., Jacobs J.F., Duiveman-de Boer T., et al. // Clin. Cancer. Res. 2012. V. 18. P. 5460–5470.
28. Ibraheem D., Elaissari A., Fessi H. // Int. J. Pharm. 2014. V. 459. P. 70–83.
29. De Temmerman M.L., Dewitte H., Vandenbroucke R.E., Lucas B., Libert C., Demeester J., De Smedt S.C., Lentacker I., Rejman J. // Biomaterials. 2011. V. 32. P. 9128–9135.
30. Oda Y., Suzuki R., Otake S., Nishiie N., Hirata K., Koshima R., Nomura T., Utoguchi N., Kudo N., Tachibana K., et al. // J. Control. Release. 2012. V. 160. P. 362–366.
31. Chen Y.Z., Yao X.L., Tabata Y., Nakagawa S., Gao J.Q. // Clin. Dev. Immunol. 2010. V. 2010. P. 565643.
32. Yang J., Liu H., Zhang X. // Biotechnol. Adv. 2014. V. 32. P. 804–817.
33. Reeves M.E., Royal R.E., Lam J.S., Rosenberg S.A., Hwu P. // Cancer Res. 1996. V. 56. P. 5672–5677.
34. Nikitina E.Y., Clark J.I., van Beynen J., Chada S., Virmani A.K., Carbone D.P., Gabrilovich D.I. // Clin. Cancer Res. 2011. V. 7. P. 127–135.
35. Streitz J., Tormo D., Schweichel D., Tuting T. // Cancer Gene Ther. 2006. V. 13. P. 318–325.
36. Murakami T., Tokunaga N., Waku T., Gomi S., Kagawa S., Tanaka N., Fujiwara T. // Clin. Cancer Res. 2004. V. 10. P. 3771–3880.
37. Antonia S.J., Mirza N., Fricke I., Chiappori A., Thompson P., Williams N., Bepler G., Simon G., Janssen W., Lee J.H., et al. // Clin. Cancer Res. 2006. V. 12. P. 878–887.
38. Morse M.A., Clay T.M., Hobeika A.C., Osada T., Khan S., Chui S., Niedzwiecki D., Panicali D., Schlom J., Lyerly H.K. // Clin. Cancer Res. 2005. V. 11. P. 3017–3024.
39. Perche F., Benvegnu T., Berchel M., Lebegue L., Pichon C., Jaffrès P.A., Midoux P. // Nanomedicine. 2011. V. 7. P. 445–453.
40. Moffatt S., Cristiano R.J. // Int. J. Pharm. 2006. V. 321. P. 143–154.
41. Tang R., Palumbo R.N., Nagarajan L., Krogstad E., Wang C. // J. Control. Release. 2010. V. 142. P. 229–237.
42. Maslov M.A., Kabilova T.O., Petukhov I.A., Morozova N.G., Serebrennikova G.A., Vlassov V.V., Zenkova M.A. // J. Control. Release. 2012. V. 160. P. 182–193.
43. Markov O.V., Mironova N.L., Maslov M.A., Petukhov I.A., Morozova N.G., Vlassov V.V., Zenkova M.A. // J. Control. Release. 2012. V. 160. P. 200–210.
44. Markov O.V., Mironova N.L., Sennikov S.V., Vlassov V.V., Zenkova M.A. // PloS One. 2015. V. 10. P. e0136911.

45. Markov O.V., Mironova N.L., Shmendel E.V., Serikov R.N., Morozova N.G., Maslov M.A.,Vlassov V.V., Zenkova M.A. // J. Control. Release. 2015. V. 213. P. 45–56.
46. Morrison B.J., Steel J.C., Gregory M., Morris J.C., Malyguine A.M. // Dendritic Cells in Cancer / Eds Shurin M.R., Satler R.D. New York: Springer Science & Business Media, 2009. P. 347–363.
47. Zarnani A.H., Torabi-Rahvar M., Bozorgmehr M., Zareie M., Mojtabavi N. // Cancer Res. Treat. 2015. V. 47. P. 518–526.
48. Kim H.S., Kim C.H., Park M.Y., Park J.S., Park H.M., Sohn H.J., Kim H.J., Kim S.G., Oh S.T., Kim T.G. // Immunol. Lett. 2010. V. 131. P. 73–80.
49. Yang Z., Wu D., Zhou D., Jiao F., Yang W., Huan Y. // Cell. Immunol. 2015. V. 293. P. 17–21.
50. Kim B.R., Yang E.K., Kim D.Y., Kim S.H. Moon D.C., Lee J.H., Kim H.J., Lee J.C. // Clin. Exp. Immunol. 2012. V. 167. P. 73–83.
51. Hira S.K., Mondal I., Manna P.P. // Cytotherapy. 2015. V. 17. P. 647–664.
52. Pandey V.K., Shankar B.S., Sanis K.B. // Int. Immunopharmacol. 2012. V. 14. P. 641–649.
53. Qiu L., Li J., Yu S., Wang Q., Li Y., Hu Z., Wu Q., Guo Z., Zhang J. // Oncotarget. 2015. V. 6. P. 5195–5203.
54. Zheng X., Koropatnick J., Chen D., Velenosi T., Ling H., Zhang X., Jiang N., Navarro B., Ichim T.E., Urquhart B., et al. // Int. J. Cancer. 2013. V. 132. P. 967–977.
55. Cafri G., Sharbi-Yunger A., Tzehoval E., Alteber Z., Gross T., Vadai E., Margalit A., Gross G., Eisenbach L. // Mol. Ther. 2015. V. 23. P. 1391–1400.
56. Matheoud D., Perié L., Hoeffel G., Vimeux L., Parent I., Marañón C., Bourdoncle P., Renia L., Prevost-Blondel A., Lucas B., et al. // Blood. 2010. V. 115. P. 4412–4420.
57. Matheoud D., Baey C., Vimeux L., Tempez A., Valente M., Louche P., Le Bon A., Hosmalin A., Feuillet V. // PloS One. 2011. V. 6. P. e19104.
58. Xie J., Xiong L., Tao X., Li X., Su Y., Hou X., Shi H. // Lung Cancer. 2010. V. 68. P. 338–345.
59. Baek S., Lee S.J., Kim M.J., Lee H. // Immune Network. 2012. V. 12. P. 269–276.
60. Moon J.H., Chung M.K., Son Y.I. // Laryngoscope. 2012. V. 122. P. 2442–2446.
61. Van Tandeloo V.F., Ponsaerts P., Berneman Z.N. // Curr. Opin. Mol. Ther. 2007. V. 9. P. 423–431.
62. Su Z., Dannull J., Yang B.K., Dahm P., Coleman D., Yancey D., Sichi S., Niedzwiecki D., Boczkowski D., Gilboa E., et al. // J. Immunol. 2005. V. 174. P. 3798–3807.
63. Heiser A., Coleman D., Dannull J., Yancey D., Maurice M.A., Dahm P., Niedzwiecki D., Gilboa E., Vieweg J. // J. Clin. Invest. 2002. V. 109. P. 409–417.
64. Mazzolini G., Alfaro C., Sangro B., Feijoo E., Ruitz J., Benito A., Tirapu I., Arina A., Sola J, Herraiz M., et al. // J. Clin. Oncol. 2005. V. 23. P. 999–1010.
65. Mayanagi S., Kitago M., Sakurai T., Matsuda T., Fujita T., Higuchi H., Taguchi J., Takeuchi H., Itano O., Aiura K., et al. // Cancer Sci. 2015. V. 106. P. 397–406.
66. Lepisto A.J., Moser A.J., Zeh H., Lee K., Bartlett D., McKolanis J.R., Geller B.A., Schmotzer A., Potter D.P., Whiteside T., et al. // Cancer Ther. 2008. V. 6. P. 955–964.
67. Phuphanich S., Wheeler C.J., Rudnick J.D., Mazer M., Wang H., Nuño M.A., Richardson J.E., Fan X., Ji J., Chu R.M., et al. // Cancer Immunol. Immunother. 2012. V. 62. P. 125–135.
68. Lesterhuis W.J., De Vries I.J., Schreibelt G., Schuurhuis D.H., Aarntzen E.H., De Boer A., Scharenborg N.M., Van De Rakt M., Hesselink E.J., Figdor C.G., et al. // Anticancer Res. 2010. V. 30. P. 5091–5098.
69. Tada F., Abe M., Hirooka M., Ikeda Y., Hiasa Y., Lee Y., Jung N.C., Lee W.B., Lee H.S., Bae Y.S., et al. // Int. J. Oncol. 2012. V. 41. P. 1601–1609.
70. Li Q.Y., Shi Y., Huang D.H., Yang T., Wang J.H., Yan G.H., Wang H.Y., Tang X.J., Xiao C.Y., Zhang W.J., et al. // Int. J. Clin. Exp. Med. 2015. V. 8. P. 5601–5610.
71. Kitawaki T., Kadowaki N., Fukunaga K., Kasai Y., Maekawa T., Ohmori K., Itoh T., Shimizu A., Kuzushima K., Kondo T., et al. // Exp. Hematol. 2011. V. 39. P. 424–433.
72. Suehiro Y., Hasegawa A., Iino T., Sasada A., Watanabe N., Matsuoka M., Takamori A., Tanosaki R., Utsunomiya A., Choi I., et al. // Br. J. Haematol. 2015. V. 169. P. 356–367.
73. Palma M., Hansson L., Choudhury A., Näsman-Glaser B., Eriksson I., Adamson L., Rossmann E., Widén K., Horváth R., Kokhaei P., et al. // Cancer Immunol. Immunother. 2012. V. 61. P. 865–879.
74. Himoudi N., Wallace R., Parsley K.L., Gilmour K., Barrie A.U., Howe K., Dong R., Sebire N.J., Michalski A., Thrasher A.J., et al. // Clin. Transl. Oncol. 2012. V. 14. P. 271–279.
75. Chu C.S., Boyer J., Schullery D.S., Gimotty P.A., Gamerman V., Bender J., Levine B.L., Coukos G., Rubin S.C., Morgan M.A., et al. // Cancer Immunol. Immunother. 2012. V. 61. P. 629–641.
76. Poschke I., Lövgren T., Adamson L., Nyström M., Andersson E., Hansson J., Tell R., Masucci G.V., Kiessling R. // Cancer Immunol. Immunother. 2014. V. 63. P. 1061–1071.
77. Wilgenhof S., Corthals J., Van Nuffel A.M., Benteyn D., Heirman C., Bonehill A., Thielemans K., Neyns B. // Cancer Immunol. Immunother. 2015. V. 64. P. 381–388.
78. Escobar A., López M., Serrano A., Ramirez M., Pérez C., Aguirre A., González R., Alfaro J., Larrondo M., Fodor M., et al. // Clin. Exp. Immunol. 2005. V. 142. P. 555–568.
79. Oshita C., Takikawa M., Kume A., Miyata H., Ashizawa T., Iizuka A., Kiyohara Y., Yoshikawa S., Tanosaki R., Yamazaki N., et al. // Oncol. Reports. 2012. V. 28. P. 1131–1138.
80. Ribas A., Camacho L.H., Lee S.M., Hersh E.M., Brown C.K., Richards J.M., Rodriguez M.J., Prieto V.G., Glaspy J.A., Oseguera D.K., et al. // J. Transl. Med. 2010. V. 8. P. 89.
81. Kimura H., Matsui Y., Ishikawa A., Nakajima T., Yoshino M., Sakairi Y. // Cancer Immunol. Immunother. 2015. V. 64. P. 51–59.
82. Podrazil M., Horvath R., Becht E., Rozkova D., Bilkova P., Sochorova K., Hromadkova H., Kayserova J., Vavrova K., Lastovicka J., et al. // Oncotarget. 2015. V. 6. P. 18192–18205.
83. Small E., Schellhammer P.F., Higano C.S., Redfern C.H., Nemunaitis J.J., Valone F.H., Verjee S.S., Jones L.A., Hershberg R.M. // J. Clin. Oncol. 2006. V. 24. P. 3089–3094.
84. Mahnke K., Schmitt E., Bonifaz L., Enk A.H., Jonuleit H. // Immunol. Cell Biol. 2002. V. 80. P. 477–483.
85. Vinay D.S., Ryan E.P., Pawelec G., Talib W.H., Stagg J., Elkord E., Lichtor T., Decker W.K., Whelan R.L., Kumara H.M., et al. // Semin. Cancer Biol. 2015. (35. Suppl.). P. S185–S198.
86. Galluzzi L., Senovilla L., Vacchelli E., Eggermont A., Fridman W.H., Galon J., Sautès-Fridman C., Tartour E., Zitvogel L., Kroemer G. // Oncoimmunology. 2012. V. 1. P. 1111–1134.
87. Töpfer K., Kempe S., Müller N., Schmitz M., Bachmann M., Cartellieri M., Schackert G., Temme A. // J. Biomed. Biotechnol. 2011. V. 2011. P. 918471.
88. Walunas T.L., Lenschow D.J., Bakker C.Y., Linsley P.S., Freeman G.J., Green J.M., Thompson C.B., Bluestone J.A. //

Immunity. 1994. V. 1. P. 405–413.
89. Fife B.T., Pauken K.E. // Ann. N. Y. Acad. Sci. 2011. V. 1217. P. 45–59.
90. Starz H. // Expert Opin. Biol. Ther. 2012. V. 12. P. 981–982.
91. Sundar R., Cho B.C., Brahmer J.R., Soo R.A. // Ther. Adv. Med. Oncol. 2015. V. 7. P. 85–96.
92. Dang T.O., Ogunniyi A., Barbee M.S., Drilon A. // Expert Rev. Anticancer. Ther. 2015. V. 10. P. 1–8.
93. Chmielowski B. // J. Skin Cancer. 2013. V. 2013. P. 423829.
94. Ivashko I.N., Kolesar J.M. // Am. J. Hlth. Syst. Pharm. 2016. V. 73. P. 193–201.
95. Boyerinas B., Jochems C., Fantini M., Heery C.R., Gulley J.L., Tsang K.Y., Schlom J. // Cancer Immunol. Res. 2015. V. 3. P. 1148–1157.
96. Wilgenhof S., Corthals J., Heirman C., van Baren N., Lucas S., Kvistborg P., Thielemans K., Neyns B. // J. Clin. Oncol. 2016. V. 34. P. 1330–1338.
97. Koido S., Kashiwaba M., Chen D., Gendler S., Kufe D., Gong J. // J. Immunol. 2000. V. 165. P. 5713–5719.
98. Yang B.B., Jiang H., Chen J., Zhang X., Ye J.J., Cao J. // Head Neck. 2010. V. 32. P. 626–635.

Proteasomes in Protein Homeostasis of Pluripotent Stem Cells

A.V. Selenina[1,2], A.S. Tsimokha[1#], A.N. Tomilin[1,2*]
[1]Institute of Cytology, Russian Academy of Sciences, Tikhoretsky Ave. 4, Saint-Petersburg, 194064, Russia
[2]St-Petersburg State University, University Emb. 7/9, St-Petersburg, 199034, Russia
#E-mail: atsimokha@incras.ru
*E-mail: a.tomilin@incras.ru
Received: December 19, 2016; in final form September 04, 2017

ABSTRACT **Embryonic stem cells (ESCs) and induced pluripotent stem cells (iPSCs) are subjects of high interest not only in basic research, but also in various applied fields, particularly, in regenerative medicine. Despite the tremendous interest to these cells, the molecular mechanisms that control protein homeostasis in these cells remain largely unknown. The ubiquitin-proteasome system (UPS) acts via post-translational protein modifications and protein degradation and, therefore, is involved in the control of virtually all cellular processes: cell cycle, self-renewal, signal transduction, transcription, translation, oxidative stress, immune response, apoptosis, etc. Therefore, studying the biological role and action mechanisms of the UPS in pluripotent cells will help to better understand the biology of cells, as well as to develop novel approaches for regenerative medicine.**
KEYWORDS **ubiquitin-proteasome system, proteasome, immunoproteasome, embryonic stem cells, induced pluripotent stem cells.**
ABBREVIATIONS **UPS – ubiquitin-proteasome system; ESCs – embryonic stem cells; iPSCs – induced pluripotent stem cells; MEFs – mouse embryonic fibroblasts; SU – subunit; IP – immunoproteasome.**

INTRODUCTION

Embryonic stem cells (ESCs) are cultured cells derived from early epiblast (primary ectoderm) cells of mammalian preimplantation embryos. ESCs can divide in culture indefinitely, avoiding the aging process and retaining their undifferentiated state and ability to differentiate into all cell – except for two extra embryonic (trophoblast and primary endoderm) – types [1, 2]. Investigation of the molecular mechanisms that control pluripotency is one of the most important pursuits in modern biology. Exploration of gene-regulatory (transcriptional) networks is an important direction in the investigation of pluripotency and exit from this cellular state through differentiation. The expression level of transcription factors, such as Oct4, c-Myc, Nanog, Klf4, and Sox2, is a critical regulatory event in the fate of pluripotent stem cells [3–6]. Even the smallest changes in the expression level of these transcription factors through interactions with other regulatory proteins can lead to differentiation or oncogenesis [4, 7–13]. Chromatin modifiers and genome stability systems also play a key role in the functioning of ESCs [14, 15]. The ability of ESCs to avoid replicative aging and, at the same time, maintain their pluripotent state is provided by the specific cellular control systems that operate in a high-intensity mode in these cells [3]. Because these are pluripotent cells of the early epiblast (natural ESC analogs) that give rise to the whole organism, including the germ line, they must possess well-functioning processes for protecting the genome from mutations. According to some studies, ESCs exhibit increased resistance to DNA damage and a low rate of genomic mutations compared to differentiated cells [16–18]. In addition, ESCs not only produce a smaller number of active oxygen forms [14, 19], but also have mechanisms to eliminate the accumulation of genotoxic and proteotoxic factors [20]. Despite the high interest to research in the field of DNA damage, regulation, and response to oxidative stress, new data demonstrate that maintenance of protein homeostasis plays one of the central roles in the functioning of ESCs [21, 22]. Protein homeostasis is a complex network of integrated and competing pathways that maintain the cellular proteome stability [23]. This network regulates all the cellular processes involved in the life cycle of proteins, including their synthesis, folding, transport, interactions, and degradation. Disruptions in protein homeostasis lead to the accumulation of damaged proteins that, in turn, negatively affect the immortality and self-renewal ability of ESCs [20]. Therefore, ESCs should obvious-

ly have a finely regulated mechanism for maintaining protein homeostasis. For example, ESCs are known to be extremely sensitive to changes in the transcription and degradation/folding of proteins [24, 25]. Some researchers argue that the loss of protein homeostasis regulation is a distinctive feature of aging; therefore, the investigation of ESCs advances our understanding of such a phenomenon as the age-related decrease in the proteome integrity [26, 27]. Due to there is some similarity between ESCs and transformed cells, a clear understanding of the protein homeostasis of ESCs may also contribute to cancer research [27].

One of the important and open questions is the generation of induced pluripotent stem cells (iPSCs) during somatic reprogramming [28, 29]. The opportunity to derive iPSCs from mouse fibroblasts by means of forced expression of key transcription factors, such as Oct4, Sox2, Klf4, and c-Myc, has substantially contributed to our understanding of the molecular mechanisms of cellular reprogramming and has opened new approaches to alternative studies that could not be implemented using model animals for a number of reasons [28, 29]. iPSCs have a morphology, proliferative capacity, and a set of endogenous pluripotency markers similar to those of ESCs and can differentiate *in vivo* and *in vitro* [30–32]. Currently, the most efficiency in reprogramming is achieved via viral delivery of reprogramming factors [28, 33–37]. Further progress in the application of this technology in research and/or medicine will depend on the opportunity to generate iPSCs in the absence of genomic modifications. Some researchers have already achieved some progress in solving this problem; for example, reprogramming with episomal vectors such as adenoviruses, transposons, purified proteins, modified RNAs, microRNAs, etc. has been demonstrated [34]. Despite the undoubted progress achieved in the generation of iPSCs, knowledge and technology are still needed in order to improve efficiency and make the reprogramming process safer and more predictable.

THE UBIQUITIN-PROTEASOME SYSTEM

The ubiquitin-proteasome system (UPS) is a key participant in the maintenance of protein homeostasis. The UPS is a proteolytic apparatus of the eukaryotic cell which regulates the major cellular processes such as the cell cycle, signal transduction, transcription, translation, oxidative stress, immune response, and apoptosis [38, 39]. The UPS functions through post-translational modifications that occur via covalent attachment of ubiquitin, which is mediated by the ATP-dependent cascade of ubiquitin-activating enzymes (E1), ubiquitin-conjugating enzymes (E2), and ubiquitin ligases (E3) (*Fig. 1A*) [40, 41]. A single E1 enzyme can interact with a whole variety of E2 enzymes, and subsequent combinations between E2 and E3 provide substrate specificity and the regulation of downstream processes. Monoubiquitination is a label for signal transmission and endocytosis, while polyubiquitination leads to ATP-dependent protein degradation in the proteasome [42, 43]. The UPS is involved in the maintenance of protein homeostasis both during the cell life and in cell death; it plays an important role in both healthy and sick cells: e.g., in neurodegenerative diseases (Alzheimer's disease), cardiac dysfunctions (transient ischemic attack), or autoimmune diseases (Sjogren's syndrome) [44]. An important component of the UPS is a multisubunit proteolytic complex, the proteasome (*Fig. 1B*). The 20S proteasome core particle is a hollow barrel-shaped protein complex consisting of four rings, each containing seven α- or β- (7α, 7β, 7β, 7α) subunits (SUs). In eukaryotic cells, only three β-SUs have an N-terminal active-site threonine (Thr1) [45]: the SU β1/PSMB6 has a caspase-like activity; the SU β2/PSMB7 has a trypsin-like activity; the SU β5/PSMB5 has a chymotrypsin-like activity [39, 41, 46]. The 20S core particle can interact with one or two 19S regulatory particles, forming a 26S or 30S proteasome (*Fig. 2*) [39]. The 19S regulatory complex is composed of a "base" and a "lid" subcomplexes and contains at least 18 SUs, 13 of which are ATP-independent (Rpn) SUs, and the remaining six are AAA-ATPase (Rpt) SUs [47]. The main role of the 19S lid is to recognize polyubiquitinated protein substrates using SUs Rpn10/PSMD4 and Rpn13/ADRM1 and to detach the ubiquitin molecules from them. The 19S base ensures protein unfolding, opening of the gate formed by the α-ring, and protein translocation into the catalytic cavity of the 20S proteasome [39, 47, 48]. The 20S proteasome can catalyze the degradation of proteins independent of ATP; however, like the 26S proteasome, it can interact with polyubiquitinated proteins, but the mechanisms of this process have not yet been explored [49]. The 20S particle can be activated not only by 19S particles, but also by another regulator, PA200 (*Fig. 2*) [50]. This protein also binds to the 20S proteasome, but PA200 functions and regulatory mechanisms are poorly understood. This protein is known to be mainly localized in the nucleus and able to increase proteasomal production of shorter peptides and to ensure degradation of oxidant-damaged proteins during cell adaptation to oxidative stress. In addition, PA200 expression increases in response to ionizing radiation [50]. There is another regulator of the proteasome activity, PA28 (*Fig. 2*), which is a heterohexameric or heteroheptameric complex consisting of three SUs PA28α and three SUs PA28β-PA28α3β3, or PA28α3β4, or PA28α4β3 [51]. The SU PA28 C-termini by themselves bind to the α-rings of 20S proteasome in the intersubunit pocket

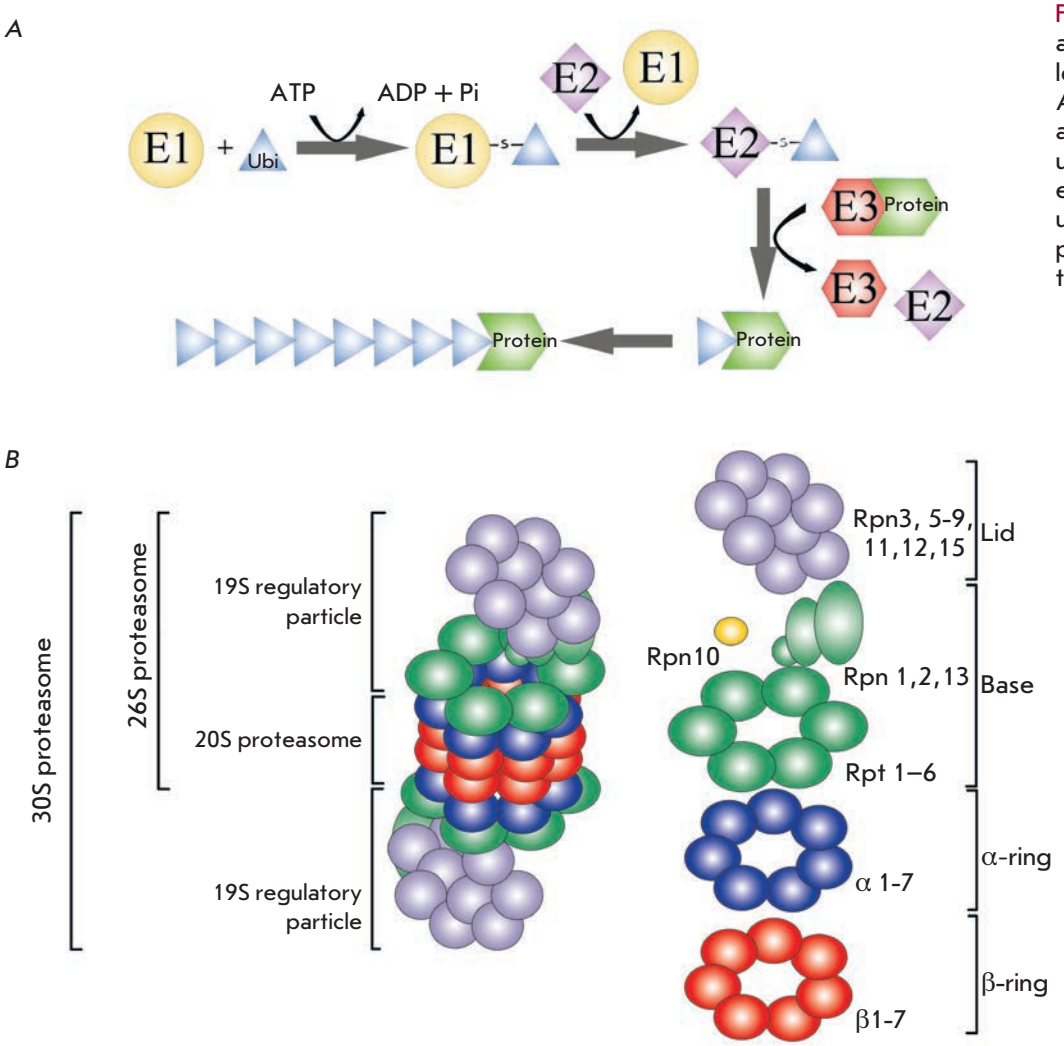

Fig. 1. The ubiquitin-proteasome system. A – covalent binding of ubiquitin to ATP-dependent ubiquitin-activation enzymes (E1), ubiquitin-conjugating enzymes (E2), and ubiquitin ligases (E3). B – the proteasome structure (see the text for details).

and, thereby, control and stabilize the open-gate conformation in the 20S proteasome, especially during the immune response [39, 52]. Under inflammatory conditions, the constitutive SUs β1/PSMB6, β2/PSMB7, and β5/PSMB5 are replaced by three inducible catalytic SUs β1i/PSMB9, β2i/PSMB10, and β5i/PSMB8. In this case, the proteasome is called an immunoproteasome (IP) (*Fig. 2*). A replacement of catalytically active SUs changes the proteasome cleavage specificity, increasing the efficiency of epitope formation for the major histocompatibility complex I (MHC I) [53–56]. Variations within the epitopes generated by IPs are caused by cleavage of proteins after basic and hydrophobic amino acid residues (trypsin- and chymotrypsin-like activities), whereas cleavage after acidic amino acid residues (caspase-like activity), according to some sources, is absent [49]. The first screening of transcriptionally active genes in human ESCs (hESCs) revealed about 900 of the most active genes, including the gene of inducible proteasomal SU β5i/PSMB8 [57]. Later, other UPS genes were found in the transcriptome hESC profile, which confirms the hypothesis on the role of UPS and protein homeostasis in maintaining ESC pluripotency [58, 59].

PROTEASOMES IN MOUSE EMBRYONIC STEM CELLS

As mentioned above, pluripotent cells are capable of generating all cell types present in the body, which suggests the existence of rigid control over self-renewal and pluripotency. This program includes transcription factors, signaling pathways, and microRNAs closely interacting with a system of regulatory proteins and other specific proteins involved in the chromatin structure formation. This interaction forms a unique state of chromatin in pluripotent cells [60]. It is noteworthy that inhibition of the proteasome proteolytic activity or knockdown of certain proteasomal SUs in mouse ESCs (mESCs) lead to the activation of normal-

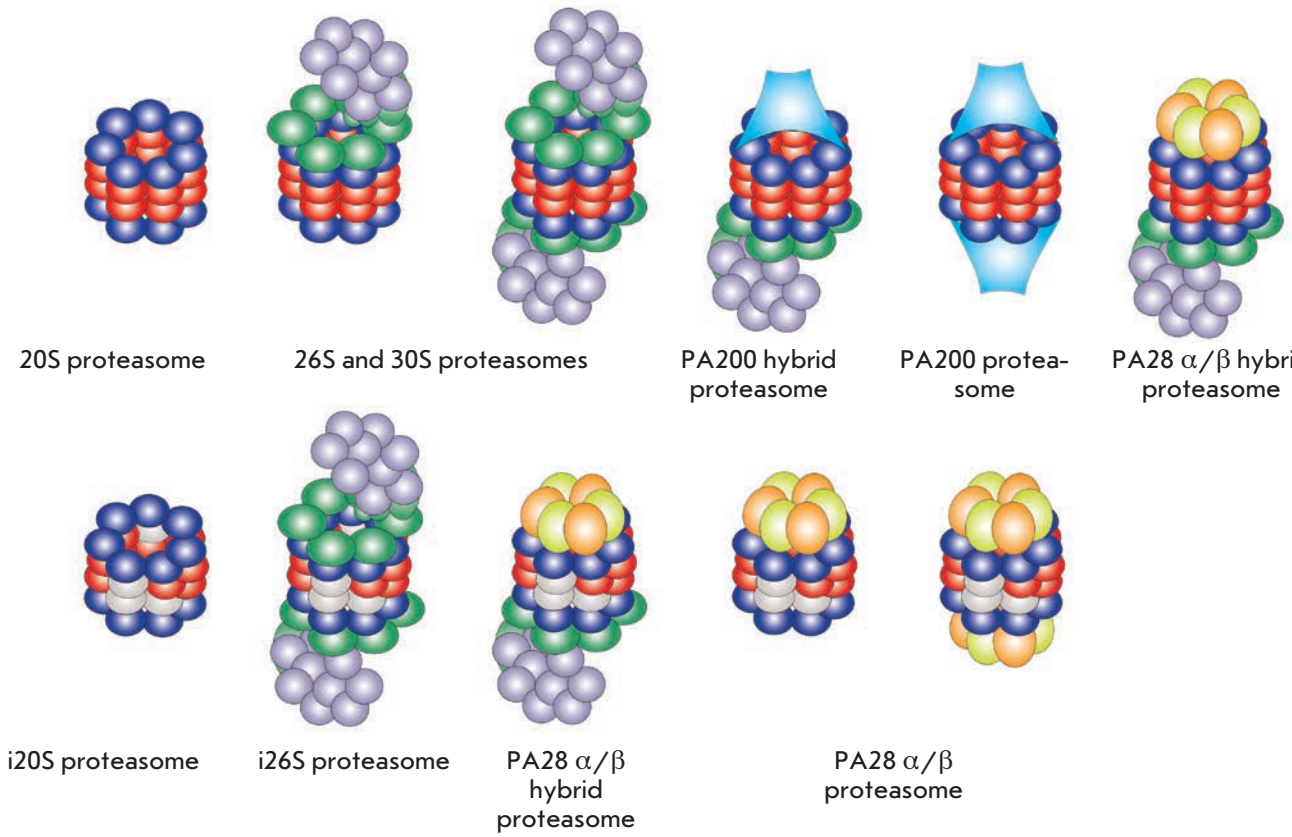

Fig. 2. Proteasome diversity in mammalian cells. A catalytically active 20S proteasome consists of four protein rings; each ring is composed of 7 α- (dark blue) or β-subunits (7α, 7β, 7β, 7α, red). Under specific conditions, the consitutive subunits β1, β2, and β5 are replaced with the inducible subunits β1i, β2i, and β5i (light grey), which leads to the formation of immunoproteasome (i20S). The 20S proteasome can interact with one or two 19S regulatory particles (purple and green), forming the 26S or 30S proteasome, respectively; the interaction with the PA200 (blue) and PA28 regulatory particles (yellow and orange) results in hybrid proteasomes. The immunoproteasome can also bind to the 19S and PA28 regulators, forming hybrid ptoteasomes with different activities and specificities.

ly inactive cryptic ("hidden") promoters [61]. The 19S complex was also shown to regulate gene expression irrespective of proteasome proteolytic activity. For example, the lid SU Rpn12/PSMD8 in mESCs controls the assembly of a transcription preinitiation complex but only in the presence of the base SU Rpt3/PSMC4 [61]. Thus, the proteasome acts as a transcriptional repressor in mESCs, preventing aberrant transcription initiation, which in turn might lead to a spontaneous exit from the pluripotency state.

The UPS actively participates in the regulation of the level and (or) functioning of various regulatory proteins in mammalian stem and germ cells, especially those proteins that are involved not only in transcription regulation, but also in the activity of signalling pathways [22]. A rapid modulation of the lifetime of these factors allows stem cells to respond to incoming signals from the environment, in response to which the cells either retain their pluripotency properties or initiate the differentiation program. The UPS is involved in the regulation of various signaling pathways: LIF/JAK/STAT3, Nodal/TGFβ/activin, Wnt/β-catenin, Notch, and BMP. The UPS is also involved in the regulation of the activity of transcription factors, such as Rel and GATA family proteins, in various stem and progenitor cells [62–66]. It is noteworthy that all these signaling cascades are involved in the regulation of cellular pluripotency.

Proteins damaged by active oxygen forms and accumulated in mESCs have been noted to be ubiquitinated and, hence, should be further subjected to proteasome degradation [67, 68]. However, the 20S proteasome turns out to reduce a number of oxidant-damaged proteins through the ATP- and ubiquitin-independent

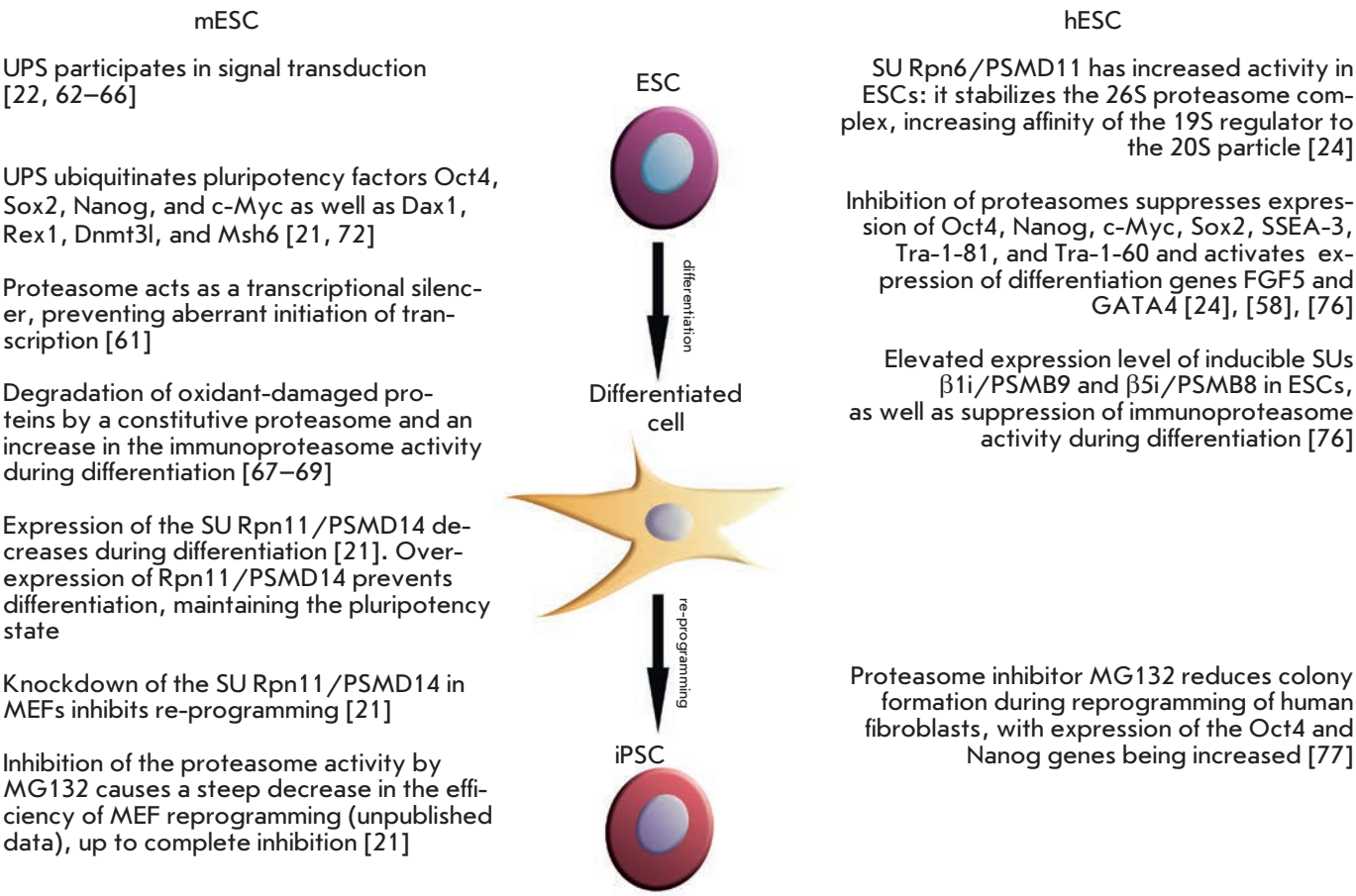

Fig. 3. The ubiquitin-proteasome system (UPS) in mouse and human pluripotent stem cells, as well as during differentiation and pluripotency induction. Summary of the most signifciant observations regarding the role of the UPS in specified cell types and processes. References are given in square brackets.

pathways [67]. Not only 20S proteasomes, but also IPs have also been found to be involved in the degradation of oxidant-damaged proteins [69], which suggests increased expression of inducible SUs and PA28 complex proteins in mESCs. However, increased levels of β5i/PSMB8 and PA28α/β proteins are observed only during the differentiation of mESCs [52]. Interestingly, in somatic mouse cells, such as skin fibroblasts, embryonic fibroblasts (MEFs), liver and brain cells, the level of oxidant-damaged proteins depends on the activity of IPs and hybrid PA28 proteasomes [69–71]. All these facts prove that IPs and the PA28 regulator play an important role in the degradation of oxidant-damaged proteins in somatic cells and in the differentiation of mESCs, but not in the pluripotent cells themselves.

The opportunity to generate iPSCs raised another important issue about the role of UPS in reprogramming and pluripotency induction. The pluripotency factors Oct4, Sox2, Nanog, and c-Myc, as well as Dax1, Rex1, Dnmt3l, and Msh6, have been shown to be ubiquitinated [21, 72]. Furthermore, inhibition of the proteasome activity by the reversible MG132 inhibitor causes a strong decrease in the efficiency of MEF reprogramming (our unpublished data), up to complete inhibition [21]. It is important to bear in mind that not only ubiquitination, but also phosphorylation play an important role in the maintenance of self-renewal and pluripotency by mESCs. For example, among the identified phosphorylated and ubiquitinated proteins (more than 280), many of them are somehow related to pluripotency [21]. The UPS is known to be involved in cell cycle regulation [73]. For example, ubiquitin ligase Fbw7/Fbxw7 can promote the degradation of important cell's regulators, such as c-Myc, c-Jun, cyclin-E, and Notch [74]. Interestingly, despite the fact that there is a similar level of this protein in mESCs and fibroblasts, expression of Fbw7 increases, and expression of c-Myc decreases during mESC differentiation.

In addition, knockdown of Fbw7 in mESCs causes increased expression of c-Myc, Oct4, Nanog, and Sox2 in the early differentiation stages, while inhibition of Fbxw7 expression during reprogramming increases the efficiency of iPSC generation [21]. Not only ubiquitin ligases E3, but also SUs of the 19S regulator are involved in pluripotency regulation. The deubiquitinating protein Rpn11/PSMD14 of this regulator is the key factor in maintaining pluripotency. For example, expression of Rpn11/PSMD14 decreases during the differentiation of mESCs, and knockdown of this SU in MEFs inhibits their reprogramming into iPSCs [21]. Interestingly, overexpression of Rpn11/PSMD14 in mESCs has prevented differentiation, maintaining the cells in the pluripotency state. According to our data, increased expression of the inducible proteasome SUs β5i/PSMB8 and β1i/PSMB9 occurs during reprogramming, and inhibition of the SU β5i/PSMB8 activity reduces the efficiency in iPSC generation (our unpublished data), which indicates the involvement of IPs in reprogramming.

PROTEASOMES IN HUMAN EMBRYONIC CELLS

A microarray analysis of the transcriptome in the case of Oct4 knockdown in H1 hESCs revealed a significant change in the expression levels of 18 genes related to the UPS [75]. Inhibition of the proteasome activity in hESCs is known to lead to various consequences. For example, the reversible proteasome inhibitor MG132 affects only pluripotent stem cells, not somatic cells [24, 58, 76]. Different periods (from 20 min to 10 h) of treating with high proteasome inhibitor concentrations (20 μM MG132 and 10 μM lactacystin) failed to alter either the viability of cells or their morphology [24, 61]. Interestingly, the presence of the MG132 proteasome inhibitor, even at low doses, completely inhibited the reprogramming of MEFs into iPSCs [21] and reduced colony formation during the reprogramming of human fibroblasts, with expression of the *Oct4* and *Nanog* genes being increased [77]. Inhibition of proteasome activity in pluripotent cells resulted in the suppression of the expression of pluripotency genes, such as Oct4, Nanog, c-Myc, Sox2, SSEA-3, Tra-1-81, and Tra-1-60, which led to the loss of self-renewal, with simultaneous activation of the expression of differentiation genes, such as FGF5 and GATA4 [24, 58, 76].

Like the mouse lid SU RPN11/PSMD14, another lid SU Rpn6/PSMD11 plays an important role in hESCs. This SU stabilizes the entire 26S proteasome complex, increasing the affinity of the 19S regulator to the 20S particle through an interaction with the SU α2/PSMA2 [24]. The Rpn6/PSMD11 expression level is high in hESCs and iPSCs, but it decreases during the differentiation of hESCs into nerve progenitor cells and mature neurons [24]. The observed decrease in the Rpn6/PSMD11 expression is accompanied by a decrease in the activity of the whole proteasome and leads to a reduced number of assembled proteasome complexes and, consequently, to the accumulation of ubiquitinated proteins in the cell. This observation, again, proves the role of the proteasome in maintaining protein homeostasis in pluripotent cells. The analysis of synthesized and functionally active proteasomes in hESCs and in comparison with nerve progenitor cells, mature neurons, fibroblasts, and hippocampal astrocytes showed the presence of a larger amount of 26S proteasomes with two 19S particles (30S proteasomes), while the amount of free 20S particles was smaller [24]. These structural rearrangements of proteasomes cause a decrease in the proteasome activity in both hESC derived cells (e.g., trophoblast) and somatic cells (e.g., fibroblasts and HEK293T cells). However, the UPS is known to play an important role in neurons, especially in the transmission of the nerve impulse [78]; so, there is still no clear explanation as to why the proteasome activity in neurons is much lower than that in hESCs.

In contrast to mESCs [52, 67], human pluripotent stem cells contain a smaller amount of oxidatively modified proteins, which is revealed when compared with human neonatal fibroblasts, as well as hESC and iPSC derivatives [79]. An increase in the number of free 20S particles during the neuronal differentiation of hESCs raises the question of whether the regulatory PA28 particle participates in this process, as it occurs in the mouse [52]. Probably, PA28 interacts with the 20S proteasome, thereby regulating its proteolytic activity. However, the emergence of the PA28 complex should be accompanied by the emergence of inducible SUs and, therefore, by the formation of IPs [69, 70]. Initially, the IP function was thought to be associated with antigen processing, protein homeostasis, and a response to oxidative stress [49, 70, 71]. Investigation of the role of IPs in maintaining hESC pluripotency demonstrated an inhibition of the proteasome chymotrypsin-like activity during the differentiation of these cells [76]. In contrast, this type of proteasome peptidase activity increases during mESC differentiation [52]. This activity is implemented by three SUs: β5/PSMB5, β1i/PSMB9, and β5i/PSMB8 [56, 80, 81]. During differentiation, the gene expression level of the constitutive proteasome SUs β1/PSMB6 and β2/PSMB7 decreases but the β5/PSMB5 protein level remains unchanged. Despite the uncovered changes in the expression of these genes, there is no change at the protein level; at the same time, the expression of the inducible SUs β1i/PSMB9 and β5i/PSMB8 decreases both at the mRNA and protein levels [76]. These data explain the observed decrease in proteasome chymotrypsin-like activity during dif-

ferentiation; however, it remains unclear if the maintenance of pluripotency is mediated by the participation of IPs. On the other hand, the use of the IP-specific inhibitors UK101 (β1i/PSMB9) and PK957 (β5i/PSMB8) activates the expression of differentiation markers and loss of hESC pluripotency [76], which indicates the role of IPs in the maintenance of pluripotency.

CONCLUSION

The UPS affects the appearance and maintenance of pluripotency, as well as the loss of this state both human and mouse cells (*Fig. 3*). Proteasomes and the PA28 regulator participate in the degradation of most oxidant-damaged proteins during differentiation [52, 67], regulate the cell cycle of ESCs via E3 ligases and deubiquitinases [21], and modulate the pluripotency state through ubiquitination of the key pluripotency transcription factors, such as Oct4, Nanog, and c-Myc [21, 52]. Inhibition of proteasome activity leads to negative regulation of pluripotency factors and activation of the factors associated with cell differentiation [24, 58, 76]. In addition, IPs are also actively involved in the maintenance of protein homeostasis, cell proliferation, and differentiation, which indicates that these proteolytic complexes play an important role beyond the immune response [52, 58, 76]. Nowadays, the role of IPs in the maintenance of pluripotency and self-renewal in ESCs and iPSCs remains unclear. Further research should clarify the role of these proteolytic complexes in the induction, maintenance, and loss of pluripotency. There are also a lot of questions about the role of UPS in processes such as reprogramming and trans-differentiation, the answers to which will enable great progress in the applied fields of medicine, including regenerative medicine, substitutive cell therapy, and drug screening [29].

The strong issue today is how to increase obtain efficiency of human naive pluripotent stem cells. Some success has been achieved in this direction [82, 83]; however, it remains unknown how regulation of the UPS changes, and whether the activities of the proteasome and IP change in this process. The significance of the UPS is related to the rapid modification of cell cycle proteins, the regulation of transcription and translation, and the control of the degradation of damaged modified proteins to maintain the proliferative potential and protein homeostasis of pluripotent cells; however, a large number of the functions of the UPS in these cells remains unexplored.

ESCs and iPSCs have the unique capability of self-renewal and are pluripotent; i.e., they are able to differentiate into all cell types of three germ layers: mesoderm, endoderm, and ectoderm [2]. Mouse ESCs and iPSCs maintain pluripotency through the gene regulatory network that is based on the LIF and Wnt signaling pathways [62], while hESCs depend on the FGF and TGFβ/Nodal/Activin signaling pathways [63]. Nowadays, the UPS is well known to be related to these signaling pathways [64–66, 84]; therefore, the discovery of new intersection nodes and mechanisms for the regulation of these pathways in the context of the UPS and pluripotent stem cells is an incredibly important and attractive prospect in biology and medicine.

This study was supported by a grant from the Russian Science Foundation (No. 14-14-00718) and a grant from the Russian Foundation for Basic Research (No. 15-04-08128).

REFERENCES

1. Evans M.J., Kaufman M.H. // Nature. 1981. V. 292. № 5819. P. 154–156.
2. Thomson J.A., Itskovitz-Eldor J., Shapiro S.S., Waknitz M.A., Swiergiel J.J., Marshall V.S., Jones J.M. // Science. 1998. V. 282. № 5391. P. 1145–1147.
3. Young R.A. // Cell. 2011. V. 144. № 6. P. 940–954.
4. Fang L., Zhang L., Wei W., Jin X., Wang P., Tong Y., Li J., Du J.X., Wong J. // Mol. Cell. 2014. V. 55. № 4. P. 537–551.
5. Sears R.C. // Cell Cycle. 2004. V. 3. № 9. P. 1131–1135.
6. Xu H., Wang W., Li C., Yu H., Yang A., Wang B., Jin Y. // Cell Research. 2009. V. 19. № 5. P. 561–573.
7. Tolkunova E., Malashicheva A., Parfenov V.N., Sustmann C., Grosschedl R., Tomilin A. // J. Molecular Biology. 2007. V. 374. № 5. P. 1200–1212.
8. Li Y., McClintick J., Zhong L., Edenberg H.J., Yoder M.C., Chan R.J. // Blood. 2005. V. 105. № 2. P. 635–637.
9. Gidekel S., Pizov G., Bergman Y., Pikarsky E. // Cancer Cell. 2003. V. 4. № 5. P. 361–370.
10. Kehler J., Tolkunova E., Koschorz B., Pesce M., Gentile L., Boiani M., Lomelí H., Nagy A., McLaughlin K.J., Schöler H.R. // EMBO Reports. 2004. V. 5. № 11. P. 1078–1083.
11. DeVeale B., Brokhman I., Mohseni P., Babak T., Yoon C., Lin A., Onishi K., Tomilin A., Pevny L., Zandstra P.W. // PLoS Genetics. 2013. V. 9. № 11. P. e1003957.
12. Wu G., Han D., Gong Y., Sebastiano V., Gentile L., Singhal N., Adachi K., Fischedick G., Ortmeier C., Sinn M. // Nature Cell Biology. 2013. V. 15. № 9. P. 1089.
13. Lengner C.J., Camargo F.D., Hochedlinger K., Welstead G.G., Zaidi S., Gokhale S., Scholer H.R., Tomilin A., Jaenisch R. // Cell Stem Cell. 2007. V. 1. № 4. P. 403–415.
14. Saretzki G., Walter T., Atkinson S., Passos J.F., Bareth B., Keith W.N., Stewart R., Hoare S., Stojkovic M., Armstrong L. // Stem Cells. 2008. V. 26. № 2. P. 455–464.
15. Watanabe A., Yamada Y., Yamanaka S. // Phil. Trans. R. Soc. B. 2013. V. 368. № 1609. P. 20120292.
16. Hong Y., Cervantes R., Tichy E., Tischfield J., Stambrook P. // Mutation Research/Fundamental and Molecular

Mechanisms of Mutagenesis. 2007. V. 614. № 1. P. 48–55.
17. Nagaria P., Robert C., Rassool F.V. // Biochimica et Biophysica Acta (BBA)-General Subjects. 2013. V. 1830. № 2. P. 2345–2353.
18. Tichy E.D., Stambrook P.J. // Exp. Cell Res. 2008. V. 314. № 9. P. 1929–1936.
19. Saretzki G., Armstrong L., Leake A., Lako M., von Zglinicki T. // Stem Cells. 2004. V. 22. № 6. P. 962–971.
20. Vilchez D., Simic M.S., Dillin A. // Trends Cell Biol. 2014. V. 24. № 3. P. 161–170.
21. Buckley S.M., Aranda-Orgilles B., Strikoudis A., Apostolou E., Loizou E., Moran-Crusio K., Farnsworth C.L., Koller A.A., Dasgupta R., Silva J.C. // Cell Stem Cell. 2012. V. 11. № 6. P. 783–798.
22. Naujokat C., Šarić T. // Stem Cells. 2007. V. 25. № 10. P. 2408–2418.
23. Powers E.T., Morimoto R.I., Dillin A., Kelly J.W., Balch W.E. // Annu Rev Biochem. 2009. V. 78. P. 959–991.
24. Vilchez D., Boyer L., Morantte I., Lutz M., Merkwirth C., Joyce D., Spencer B., Page L., Masliah E., Berggren W.T. // Nature. 2012. V. 489. № 7415. P. 304–308.
25. You K.T., Park J., Kim V.N. // Genes Dev. 2015. V. 29. № 19. P. 2004–2009.
26. López-Otín C., Blasco M.A., Partridge L., Serrano M., Kroemer G. // Cell. 2013. V. 153. № 6. P. 1194–1217.
27. Finkel T., Serrano M., Blasco M.A. // Nature. 2007. V. 448. № 7155. P. 767–774.
28. Takahashi K., Yamanaka S. // Cell. 2006. V. 126. № 4. P. 663–676.
29. Schneider T. A., Fishman V. S., Liskovykh M. A., Ponamartsev S. V., Serov O. L., Tomilin A. N., Alenina N. // Tsitologiia. 2014. V.56. №12. P.869–880.
30. Maherali N., Sridharan R., Xie W., Utikal J., Eminli S., Arnold K., Stadtfeld M., Yachechko R., Tchieu J., Jaenisch R. // Cell Stem Cell. 2007. V. 1. № 1. P. 55–70.
31. Wernig M., Meissner A., Foreman R., Brambrink T., Ku M., Hochedlinger K., Bernstein B.E., Jaenisch R. // Nature. 2007. V. 448. № 7151. P. 318–324.
32. Yu J., Vodyanik M.A., Smuga-Otto K., Antosiewicz-Bourget J., Frane J.L., Tian S., Nie J., Jonsdottir G.A., Ruotti V., Stewart R. // Science. 2007. V. 318. № 5858. P. 1917–1920.
33. Carey B.W., Markoulaki S., Hanna J., Saha K., Gao Q., Mitalipova M., Jaenisch R. // Proceedings of the National Academy of Sciences. 2009. V. 106. № 1. P. 157–162.
34. González F., Boué S., Belmonte J.C.I. // Nature Reviews Genetics. 2011. V. 12. № 4. P. 231–242.
35. Theunissen T.W., Jaenisch R. // Cell Stem Cell. 2014. V. 14. № 6. P. 720–734.
36. Liskovykh M., Chuykin I., Ranjan A., Safina D., Popova E., Tolkunova E., Mosienko V., Minina J.M., Zhdanova N.S., Mullins J.J. // PLoS One. 2011. V. 6. № 11. P. e27345.
37. Kostina A.S., Uspensky V.E., Irtyuga O.B., Ignatieva E.V., Freylikhman O., Gavriliuk N.D., Moiseeva O.M., Zhuk S., Tomilin A., Kostareva A.A. // Biochimica et Biophysica Acta (BBA)-Molecular Basis of Disease. 2016. V. 1862. № 4. P. 733–740.
38. Kloetzel P.-M., Soza A., Stohwasser R. // Biol. Chem. 1999. V. 380. № 3. P. 293–297.
39. Tanaka K. // Proceedings of the Japan Academy, Series B. 2009. V. 85. № 1. P. 12–36.
40. Glickman M.H., Ciechanover A. // Physiol. Rev. 2002. V. 82. № 2. P. 373–428.
41. Tsimokha A.// Tsitologiia. 2010. V.52. №4. P.277–300.
42. Mukhopadhyay D., Riezman H. // Science. 2007. V. 315. № 5809. P. 201–205.
43. Seifert U., Krüger E. // Biochem. Soc. Trans. 2008. V. 36. № 5. P. 879–884.
44. Dahlmann B. // BMC Biochemistry. 2007. V. 8. № 1. P. 1.
45. Fenteany G., Standaert R.F., Lane W.S., Choi S. // Science. 1995. V. 268. № 5211. P. 726.
46. Orlowski M., Wilk S. // Arch. Biochem. Biophys. 2000. V. 383. № 1. P. 1–16.
47. da Fonseca P.C., He J., Morris E.P. // Mol. Cell. 2012. V. 46. № 1. P. 54–66.
48. Smith D.M., Chang S.-C., Park S., Finley D., Cheng Y., Goldberg A.L. // Mol. Cell. 2007. V. 27. № 5. P. 731–744.
49. Ebstein F., Kloetzel P.M., Kruger E., Seifert U. // Cell Mol. Life Sci. 2012. V. 69. № 15. P. 2543–2558.
50. Pickering A.M., Davies K.J. // Arch. Biochem. Biophys. 2012. V. 523. № 2. P. 181–190.
51. Zhang Z., Krutchinsky A., Endicott S., Realini C., Rechsteiner M., Standing K.G. // Biochemistry. 1999. V. 38. № 17. P. 5651–5658.
52. Hernebring M., Fredriksson A., Liljevald M., Cvijovic M., Norrman K., Wiseman J., Semb H., Nystrom T. // Sci. Rep. 2013. V. 3. P. 1381.
53. Strehl B., Seifert U., Krüger E., Heink S., Kuckelkorn U., Kloetzel P.M. // Immunol. Rev. 2005. V. 207. № 1. P. 19–30.
54. Krüger E., Kuckelkorn U., Sijts A., Kloetzel P.-M., The components of the proteasome system and their role in MHC class I antigen processing, Reviews of physiology, biochemistry and pharmacology. Springer, 2003. P. 81–104.
55. Sijts A.J., Ruppert T., Rehermann B., Schmidt M., Koszinowski U., Kloetzel P.-M. // J. Exp. Med. 2000. V. 191. № 3. P. 503–514.
56. Boes B., Hengel H., Ruppert T., Multhaup G., Koszinowski U.H., Kloetzel P.-M. // J. Exp. Med. 1994. V. 179. № 3. P. 901–909.
57. Sato N., Sanjuan I.M., Heke M., Uchida M., Naef F., Brivanlou A.H. // Dev. Biol. 2003. V. 260. № 2. P. 404–413.
58. Assou S., Cerecedo D., Tondeur S., Pantesco V., Hovatta O., Klein B., Hamamah S., De Vos J. // BMC Genomics. 2009. V. 10. № 1. P. 1.
59. Baharvand H., Hajheidari M., Ashtiani S.K., Salekdeh G.H. // Proteomics. 2006. V. 6. № 12. P. 3544–3549.
60. Meshorer E., Misteli T. // Nat. Rev. Mol. Cell Biol. 2006. V. 7. № 7. P. 540–546.
61. Szutorisz H., Georgiou A., Tora L., Dillon N. // Cell. 2006. V. 127. № 7. P. 1375–1388.
62. Ogawa K., Nishinakamura R., Iwamatsu Y., Shimosato D., Niwa H. // Biochem. Biophys. Res. Commun. 2006. V. 343. № 1. P. 159–166.
63. James D., Levine A.J., Besser D., Hemmati-Brivanlou A. // Development. 2005. V. 132. № 6. P. 1273–1282.
64. Greber B., Lehrach H., Adjaye J. // Stem Cells and Development. 2008. V. 17. № 6. P. 1065–1078.
65. Hatakeyama S. // JAKSTAT. 2012. V. 1. № 3. P. 168–175.
66. Miyazono K., Ten Dijke P., Heldin C.-H. // Advances in Immunology. 2000. V. 75. P. 115–157.
67. Hernebring M., Brolén G., Aguilaniu H., Semb H., Nyström T. // Proceedings of the National Academy of Sciences. 2006. V. 103. № 20. P. 7700–7705.
68. Dudek E., Shang F., Valverde P., Liu Q., Hobbs M., Taylor A. // The FASEB J. 2005. V. 19. № 12. P. 1707–1709.
69. Pickering A.M., Koop A.L., Teoh C.Y., Ermak G., Grune T., Davies K.J. // Biochemical J. 2010. V. 432. № 3. P. 585–595.
70. Seifert U., Bialy L.P., Ebstein F., Bech-Otschir D., Voigt A., Schröter F., Prozorovski T., Lange N., Steffen J., Rieger M. // Cell. 2010. V. 142. № 4. P. 613–624.
71. Ebstein F., Voigt A., Lange N., Warnatsch A., Schröter F.,

Prozorovski T., Kuckelkorn U., Aktas O., Seifert U., Kloetzel P.-M. // Cell. 2013. V. 152. № 5. P. 935–937.
72. Park J.-A., Kim Y.-E., Ha Y.-H., Kwon H.-J., Lee Y.-H. // BMB Rep. 2012. V. 45. № 5. P. 299–304.
73. Konstantinova I.M., Tsimokha A.S., Mittenberg A.G. // Int. Rev. Cell Mol. Biol. 2008. V. 267. P. 59–124.
74. Tu Y., Chen C., Pan J., Xu J., Zhou Z.-G., Wang C.-Y. // Int. J. Clin. Exp. Pathol. 2012. V. 5. № 8. P. 726–738.
75. Babaie Y., Herwig R., Greber B., Brink T.C., Wruck W., Groth D., Lehrach H., Burdon T., Adjaye J. // Stem Cells. 2007. V. 25. № 2. P. 500–510.
76. Atkinson S.P., Collin J., Irina N., Anyfantis G., Kyung B.K., Lako M., Armstrong L. // Stem Cells. 2012. V. 30. № 7. P. 1373–1384.
77. Floyd Z.E., Staszkiewicz J., Power R.A., Kilroy G., Kirk-Ballard H., Barnes C.W., Strickler K.L., Rim J.S., Harkins L.L., Gao R., Kim J., Eilertsen K.J. // Cell Reprogram. 2015. V. 17. № 2. P. 95–105.
78. Cajigas I.J., Will T., Schuman E.M. // EMBO J. 2010. V. 29. № 16. P. 2746–2752.
79. Prigione A., Fauler B., Lurz R., Lehrach H., Adjaye J. // Stem Cells. 2010. V. 28. № 4. P. 721–733.
80. Kloetzel P.M. // Biochim. Biophys. Acta. 2004. V. 1695. № 1–3. P. 225–233.
81. Gaczynska M., Goldberg A.L., Tanaka K., Hendil K.B., Rock K.L. // J. Biol. Chem. 1996. V. 271. № 29. P. 17275–17280.
82. Ware C.B., Nelson A.M., Mecham B., Hesson J., Zhou W., Jonlin E.C., Jimenez-Caliani A.J., Deng X., Cavanaugh C., Cook S. // Proc. Natl. Acad. Sci. USA. 2014. V. 111. № 12. P. 4484–4489.
83. Nichols J., Smith A. // Cell Stem Cell. 2009. V. 4. № 6. P. 487–492.
84. Wang T. // Frontiers in Biosci: J. Virtual Library. 2003. V. 8. P. d1109–1127.

Predicting the Evolutionary Variability of the Influenza A Virus

T.A. Timofeeva*, M.N. Asatryan, A.D. Altstein, B.S. Narodisky, A.L. Gintsburg, N.V. Kaverin
Federal State Budgetary Institution «N.F. Gamaleya FRCEM» of the Ministry of Health of the Russian Federation, Gamaleya Str. 18, Moscow, 123098, Russia
*E-mail: timofeeva.tatyana@inbox.ru
Received: January 16, 2017; in final form August 14, 2017

ABSTRACT **The influenza A virus remains one of the most common and dangerous human health concerns due to its rapid evolutionary dynamics. Since the evolutionary changes of influenza A viruses can be traced in real time, the last decade has seen a surge in research on influenza A viruses due to an increase in experimental data (selection of escape mutants followed by examination of their phenotypic characteristics and generation of viruses with desired mutations using reverse genetics). Moreover, the advances in our understanding are also attributable to the development of new computational methods based on a phylogenetic analysis of influenza virus strains and mathematical (integro-differential equations, statistical methods, probability-theory-based methods) and simulation modeling. Continuously evolving highly pathogenic influenza A viruses are a serious health concern which necessitates a coupling of theoretical and experimental approaches to predict the evolutionary trends of the influenza A virus, with a focus on the H5 subtype.**
KEYWORDS **Influenza A virus, phylogenetic trees, escape mutants, computational tools, computational modeling, phenotypic characteristics, reverse genetics.**
ABBREVIATIONS **HA – hemagglutinin of influenza virus, NA – neuraminidase of influenza virus, WHO – World Health Organization, MHC – major histocompatibility complex, H1–H18 – subtypes of hemagglutinin of influenza A virus, N1–N11 – subtypes of neuraminidase of influenza A virus.**

A BIG PROBLEM FROM A SIMPLE THING CALLED "FLU"

The isolation of the human influenza virus was first reported by W. Smith, C.H. Andrewes, P.P. Laidlaw from the National Institute for Medical Research in England in 1933 [1, 2]. Two years before their report, in 1931 Richard E. Shope from the USA isolated a swine influenza virus [3, 4]. A considerable body of data regarding the structural and functional properties of influenza viruses, disease pathogenesis, adaptive and innate immune responses has been accumulated over the past 85 years. The human influenza virus has emerged as one of the primary public health threats due to its wide incidence and ability to cause a severe respiratory illness. Human influenza can lead to epidemics and pandemics, accompanied by high mortality rates and significant economic losses, because the influenza A virus exhibits rapid evolutionary dynamics and fast adaptation to human hosts that possess a general, non-specific immune system and vary in the levels of acquired immunity. Human influenza virus strains carry specific phenotypic characteristics that affect the disease process: i) the ability to attach to and infect the epithelium of the upper airway passages (receptor-binding activity), ii) the ability to escape the immune response, and iii) the ability to produce infectious virus progeny. The former two properties are mainly a factor of viral surface proteins, whereas input to the latter characteristic comes from the entire viral proteins. The virus undergoes phenotypic changes arising from genetic changes.

Following an infection, the virus particles are exposed to two types of immune response. The humoral immunity, mediated by neutralizing antibodies to the surface proteins hemagglutinin (HA) and neuraminidase (NA), plays an essential role in the host defense. Anti-HA antibodies bind to the virus and prevent virus infection [5]. NA-targeted antibodies show a poorer neutralizing capacity, but they can slow the spread of the disease by blocking virus release from infected cells [6]. An influenza infection is primarily countered by antibodies to surface glycoproteins; however, the conserved proteins M and NP contained in the virion also elicit antibodies, but without neutralizing activity [7]. The cellular immune response promotes the apoptosis of the infected cells through virus-specific cytotoxic T-lymphocytes. These T-cells recognize antigenic epitopes of the viral internal proteins (matrix protein (M1) and the nucleoprotein (NP)) coupled with MHC molecules [8].

The influenza virus can escape recognition by the host immunity due to antigenic drift [9], which is the gradual accumulation of point mutations, eventually resulting in a virus with new antigenic properties. This is the reason why the antibodies created against the previous virus no longer recognize the newly emerged virus. Point mutations in the antigenic epitopes of internal proteins also contribute to the evasion of the cellular immune response [8]. The other type of change is called antigenic shift – the mechanism by which segments reassort to give rise to a virus with a pandemic phenotype [10]. The genome of the influenza virus consists of several segments, each of which behaves as an independent replication unit. This feature allows different influenza virus strains to combine and undergo genetic reassortment, which results in the emergence of reassortants. If two influenza A virus strains (avian and human) infect the same cell, packaging of segments from the two parental strains into one virion can occur, leading to the production of a hybrid progeny .

The role of other mechanisms in driving viral evolution, such as the emergence of defect particles [11] and intermolecular recombination, remains unclear. Although negative-strand RNA viruses with segmented genomes, to which the influenza virus belongs, rarely recombine, there is evidence that demonstrates the presence of cellular mRNA sequences in the HA gene. This propensity of the virus permits repeated infection cycles in trypsin-free cell cultures, which correlates with high virulence [12]. It is likely that similar mechanisms are behind the fast genetic changes seen in the repertoire of influenza A virus strains.

THE VARIETY OF INFLUENZA A VIRUS STRAINS IN NATURE AND THEIR EVOLUTION

The influenza A virus strains found in animal and avian wildlife populations and recovered from humans exhibit a considerable degree of variation in their surface glycoproteins HA and NA. There are 18 known HA subtypes (H1–H18) and 11 known NA subtypes (N1–N11) [13]. Precursors to future pandemics could be viruses carrying the HA subtypes H1, H2, H3, H5, H6, H7, H9, H10, and NA subtypes N1, N2, N3, N8 that have been known to cause outbreaks or sporadic human infections. The most severe influenza pandemic ever recorded was the Spanish flu outbreak in 1918 that claimed from 50 to 100 million lives. This makes it extremely important to have models in place to predict such future disasters.

Seasonal epidemics are readily preventable with WHO recommended vaccines. But as a result of the fast evolution of a virus, the composition of such vaccines should be updated almost every year. Gaining insights into viral phylodynamics would play a crucial role in forecasting which viral subtypes are likely to affect the human population (epidemic or pandemic) and formulating a vaccine against the new strain.

Since an influenza virus evolution can be traced in real time, the field has seen an exciting flurry of methodological developments and experimental findings in the past decade.

THEORETICAL MODELS TO PREDICT THE EVOLUTIONARY DYNAMICS OF THE INFLUENZA A VIRUS

Here, we will review the approaches that, in our opinion, are very promising for predicting the evolutionary dynamics of the influenza A virus. Such approaches involve the construction of phylogenetic trees based on the alignment of viral sequences and mathematical modeling (integro-differential equations, statistics, probability tests, simulation modeling) [14, 15].

Phylogenetic trees show the evolutionary relationship among different species or distant species sharing a common ancestor. The inference of such dendrograms includes the following steps: 1) a search for a cognate nucleotide and amino acid sequences; 2) multiple alignment; 3) construction of a phylogenetic tree using an algorithm of choice (for example, maximum likelihood, bootstrap analysis, matrix method, maximum parsimony); and finally 4) viewing and editing the tree structure. Currently, there are open access software and resources available online for a phylogenetic analysis of influenza A virus sequences [16].

One of the approaches mentioned above was used to examine the positive effect of a coordinated evolution on the influenza A virus fitness [17, 18]. The phenomenon when a mutation in one gene facilitates a mutation in another gene is called epistasis. The use of NA and HA amino acid sequences (H3N2 and H1N1 subtypes) retrieved from NCBI's Influenza Virus Resource [19] to develop a statistical technique allows one to detect the potential pairs of sites involved in inter-gene epistasis. This approach uses the bootstrap algorithm. The approach is based on the identification of epistatic mutations in pairs of leading and trailing sites and the estimation of the distances between them in the tree. If the calculated distances are dramatically lower than the average distances, the mutations are considered epistatic according to the hypothesis that a mutation in one gene facilitates a mutation in another gene. However, these assumptions are not taken into account when it comes to the formulation of a vaccine, which could be very useful.

The other approach to influenza forecasting is the identification of clades (a population unit that is more than a single strain) in the phylogenic tree, which can show boom or bust dynamics of fitness in the subsequent season. A H3 subtype fitness model has been

developed to predict influenza evolution trends on an annual basis [20]. Fitness outputs inform the choice of vaccines against seasonal influenza. The concentration (frequency) of the fitness strain is defined as the ratio of hosts infected with this strain to the whole population of hosts diagnosed with influenza. Depending on the season, the clade frequency is expressed as the sum of all frequency trajectories of seasonal strains from a given clade. The fitness (evolution rate) is a parameter that could increase or decrease the frequency of strains that descend from recent common ancestors next season [14]. A phylogenetic tree is built using maximum likelihood.

A predictive fitness model for influenza A based on the above-mentioned tools requires a database which contains the most up-to-date and comprehensive collection of the nucleotide sequences of seasonal influenza viruses.

For a phylogenetic tree to reflect the true phylogenetic relationships, the input data should be thoroughly evaluated and meet the stringent inclusion criteria (availability of full genome sequences of influenza A viruses, geographical mapping and so on) that contribute to a more accurate estimation of actual evolutionary relationships.

A good strategy for validating a phylogenetic tree and the inclusion criteria is to compare escape mutants, derived from a certain parental strain, and other cognate sequence clusters, with a tree rooted in a common ancestor. Escape mutants are viral mutants with the ability to escape neutralization by a monoclonal antibody. If escape mutants are represented in a dendrogram, they should cluster along with the parental strain. If the strains fall into different clusters, that could be explained either by an error in the data set of sequences or tree inference algorithms.

EXPERIMENTAL MODELS TO PREDICT INFLUENZA A EVOLUTION

Like mathematical models, experimental models also utilize the nucleotide sequences of seasonal influenza A viruses deposited in databases. Importantly, experimental work generates new data sets containing the sequences of escape mutants. The common technique to experimentally produce HA escape mutants was reported as far back as 1980 [21]. Following the selection of escape mutants, the three-dimensional structures of a protein and the corresponding gene sequences are combined to map the epitopes (or single amino acid residues) recognized by the neutralizing antibodies. Escape mutant epitopes are spread non-randomly throughout the 3D structure (protrusions, loops, pockets).

Antigenic epitopes targeted by antibodies were first discovered in a 3D structure of the H3 hemagglutinin protein. For 20 years (from 1981 to 2001), it remained the only subtype whose 3D hemagglutinin protein structure was resolved by an X-ray analysis [22, 23]. Among the well-studied antibody interaction sites of escape mutants are such putative pandemic subtypes as H1 [24–26], H2 [26, 27], H3 [26, 28], H5 [26, 29–31] and H9 [26, 32]. There is scarce information on H7 subtypes [33], and no information on H6 and H10.

Due to fast evolutionary rates, the antibody interaction sites of the HA molecule of escape mutants are constantly evolving, generating newer viruses. This fact prompts research not only into poorly studied or completely uncharacterized subtypes (H6, H7 and H10), but also aims at further understanding the HA interaction characteristics of newly emerged viruses evolving from well-studied subtypes (H1, H2, H3, H5, H9). This thus becomes a top priority when a human pandemic caused by a new influenza subtype occurs.

The forecasting of a influenza A evolution builds upon the variation dynamics of both surface glycoproteins hemagglutinin and neuraminidase. Importantly, the coordinated evolution of the two proteins shapes the epidemiological profile of seasonal influenza strains. Our understanding of this relationship induced studies of hemagglutinin and neuraminidase proteins using escape mutants nearly at the same time.

ADDITIONAL EXPERIMENTAL MODELS AIMED AT PREDICTING INFLUENZA A EVOLUTION

The ability to predict the subtype that will cause the next influenza is not limited to the identification of interaction sites on surface proteins (such as hemagglutinin and neuraminidase), which are responsible for antibody production.

It is important to monitor the wild-type strains of the influenza A virus reported in the past to identify the emergence of a virus produced under laboratory conditions. It has been demonstrated that not all escape mutations generated in the laboratory can occur in the influenza A virus under natural conditions. This discrepancy may be explained by the phenotypic effects triggered by mutations, necessitating a laboratory examination of such phenotypic characteristics of escape mutations as virulence, the ability to bind to cellular receptors (in avian and human hosts), replicative activity, virus yield at different temperatures, and finally resistance to environmental factors (temperature, pH).

For example, studies looking into the effect of amino acid substitutions in the HA protein on phenotypic change showed that the escape mutants of such putatively pandemic subtypes as H5 and H9 exhibit different variation patterns. H9 escape mutants do not vary much in phenotypic traits [34], whereas H5 escape mutants are very sensitive to single amino acid

substitutions in the HA protein sequence [35, 36]. The RNA genome of the H9 subtype influenza virus shows lower evolutionary rates as compared to H5 subtypes in the wild. This fact is in agreement with experimental findings [34].

Overall, insights into the role of amino acid substitutions in escape mutant phenotypes will help guide our choice of experimentally produced clones with a fitness advantage and predict the epidemiological behavior of selected strains in the environmental context.

Not only mutations in surface glycoproteins, but also other capsid proteins could underlie the phenotypic variation in influenza virus A strains. Hence, to reliably confirm the association between the phenotype and a mutation in a protein (like hemagglutinin or other proteins), influenza viruses with the desired mutations should be prepared *in vitro* using reverse genetics and screened for phenotypic changes. Such an approach will thus support and narrow the diversity of predicted viruses.

Forecasting evolutionary trajectories towards pandemic H5 subtypes requires careful attention to hot spot mutations in the HA molecules that could contribute to high pathogenicity. The hot spots are:

- the receptor-binding site responsible for the attachment of the virus to the host cell surface;
- the sites involved in the binding to antibodies (antigenic epitopes);
- the glycosylation sites playing a role in the HA maturation process; and
- the proteolytic cleavage site of the hemagglutinin responsible for high pathogenicity.

This demonstrates the objective need for applying computer modeling and experimental findings to gain more in-depth knowledge of the evolutionary change in H5 influenza viruses in natural populations.

H5 subtype influenza viruses have been the focus of research since 1997, when this subtype was reported in humans [37]. The mortality rates caused by H5 subtypes of the influenza A virus hover around 53%, which is 5-fold higher than the notorious Spanish flu. There has been no report so far of human to human transmission for influenza viruses possessing H5 HA due to its high specificity to avian host cells [38]; however, upon conversion of H5 HA to an HA that could support efficient viral transmission in human populations, the pandemic would be the deadliest in human history.

The phylogenetic analysis of H5 sequences is hindered by incomplete sequence information in nucleotide databases. H5 sequences of escape mutants could enrich such databases, though it's worth bearing in mind that experimentally produced escape mutants will serve as an approximation to a true evolutionary relationship among the identified viruses.

WHAT PREVENTS AVIAN H5N1 FROM CROSSING THE SPECIES BARRIER TO INFECT HUMANS?

H5 viruses may acquire not only efficient transmission capability among humans, but also phenotypic fitness through mutations that may not take much time to occur.

Experimental studies [39, 40] have shown that a few mutations in HA of the currently circulating H5N1 are sufficient for the virus to become a pandemic human influenza virus that spreads through respiratory droplets. These mutations (*Fig. 1*) are located at the receptor binding site (N224K, Q226L are in red), in the stalk region (T318I is in green) in the HA trimer-interface (H107Y is in blue), and at the glycosylation site (N158D, T160A are in yellow). Zhang et al. predicted amino acid substitutions in the HA protein that contribute to H5N1 transmissibility in mammals [41]. The positions at residues 186, 226, and 228 are located at the receptor binding site and at residue 160 at the glycosylation site. Two of these positions were predicted by computer modeling and further confirmed in field studies. Of note, the predicted positions reside in important regions of the HA molecule: the receptor binding site and the glycosylation site. More importantly, the position at residue 186 found in a laboratory-generated escape mutant is among those predicted computationally [36]. It was recently demonstrated that the HA molecule carries new (evolutionarily successful) positions, mutations at which confer fitness advantage and are coupled to changes toward a human-type receptor specificity of highly pathogenic H5N1 [42].

Overall, a comprehensive structural and functional evaluation of the receptor binding site, antigenic epitopes, the cleavage site, and the glycosylation site of various influenza A viruses would lay the groundwork for analyzing the evolutionary trajectories of circulating subtypes and offer new possibilities for predicting the natural emergence of new clones that are selected under laboratory conditions.

ADDITIONAL PARAMETERS TO CONSIDER WHEN PREDICTING AVIAN INFLUENZA EVOLUTIONARY PATTERNS

The mammal-to-mammal transmissibility in highly pathogenic H5N1 is determined by not only HA changes, but also mutations in the PB2 polymerase subunit, in particular, the cap-dependent endonuclease responsible for the initiation of viral mRNA transcription and viral replicative ability [43]. It was recently shown that the genes of the polymerase subunit involved in the transmission to mammals contain mutations such as E192K, E627V, D701V, K702R on the PB2 subunit beside the substitution E627, (Fig. 2) and N105S on the PB1 subunit [44]. The key residues that contribute to a

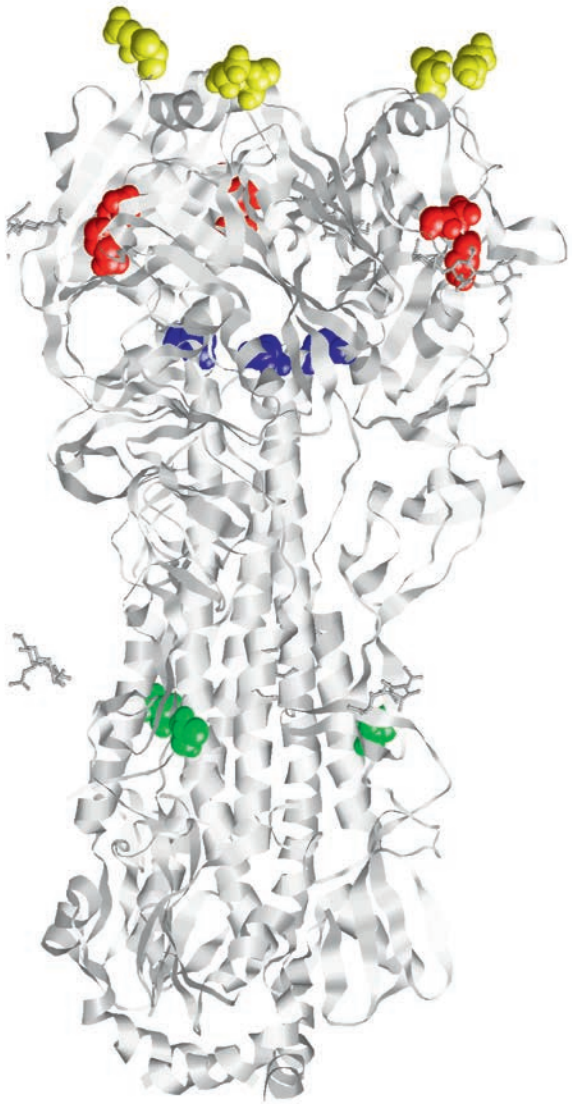

Fig. 1. Positions of amino acids in the trimer H5 hemagglutinin protein, mutations at which contribute to the transmissibility of highly pathogenic H5N1 viruses among mammals [39, 40]

pandemic potential among mammals identified based on the phylogenetic analysis of the PB2 gene [45] include the positions 590, 627, and 701. The two residues at positions 627 and 701 predicted as precursors to a pandemic were in agreement with experimental findings [41].

Until recently, it was widely held that escape mutations cluster in regions of influenza surface proteins with high mutability. Recent findings have demonstrated that escape mutations may occur in conservative regions of internal proteins like the nucleoprotein (NP). NP was initially shown to be conservative. However, using a panel of monoclonal and polyclonal antibodies, it was found that the NP gene is subject to genetic change. Selection of influenza A NP escape mutants is not possible, since the NP protein does not elicit neutralizing antibodies. In this case, site-specific mutagenesis followed by ELISA evaluation of a protein produced in a prokaryotic vector could be used. All identified antigenically important amino acids in the NP protein were shown to be mutable and spread throughout the sequence as judged by a 3D structure [45]. Reports recently appeared on the location and structure of the compact antigenic site in the head domain of the influenza A virus NP protein [46].

This fact indicates that studies of evolutionary dynamics should look into mutations in both surface and internal proteins.

CONCLUSIONS

The influenza A virus remains one of the most common and contagious human pathogens. It can cause epidemics and pandemics associated with high mortality and economic losses. These epidemiological traits are attributed to the high evolutionary rates and adaptability of A viruses to human hosts that possess a general innate immune system and varying levels of acquired immunity across individuals.

Since evolutionary dynamics can be tracked in real time, the influenza A research field has lately enjoyed a surge in experimental data (selection of escape mutants followed by phenotypic characterization, generation of viruses with the desired mutations using reverse genetics) and the development of novel techniques providing insights into the phylogenetic relationships of influenza strains, as well as mathematical (integro-differential equations, statistics, probability tests) and simulation modeling .

To ensure that the trees represent a true phylogenetic relationship among the viruses, input data should undergo quality control before being analyzed. The inclusion criteria are the availability of full genome sequences of influenza A viruses, geographical mapping and so on, which can make graphical representations more accurate. Escape mutants are a good option for validating tree-based models and, at the same time, verifying the selection criteria. In this case, all descending escape variants are compared against other viruses from different clades and the parental strain as an out group.

Relating changes in the amino acid sequences to phenotype allows one to limit the repertoire of selected escape mutants with a competitive advantage and predict their epidemiological behavior in nature. Phenotype changes result from not only mutations in the HA gene, but also other viral genes. Hence, a solid confir-

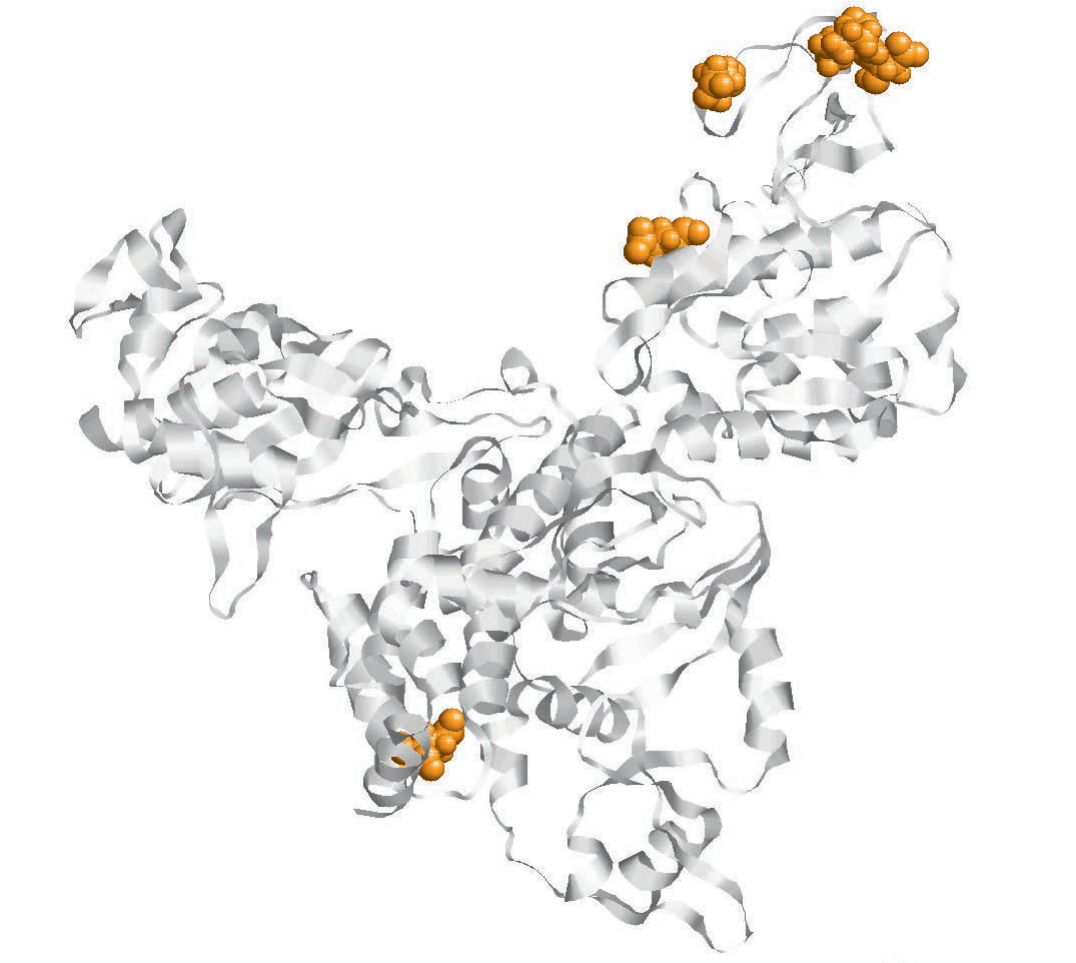

Fig. 2. Positions of amino acids in the monomer PB2 protein, mutations at which contribute to the transmissibility of highly pathogenic H5N1 viruses among mammals [44]

mation of the correlation between the HA genotype (or any other gene) and the phenotype should come from reverse genetics, whereby viruses with the desired mutations are constructed and examined for phenotypic characteristics in biological systems.

The phylogenetic analysis is impeded by incomplete data on the H5 sequences available in sequence repositories. To address this challenge, the H5 nucleotide sequences of escape mutants need to be submitted to such databases. However, it should be kept in mind that experimentally generated escape variants will be used as an approximation to a real evolutionary relationship among the viruses found in nature.

Both surface (HA and NA) and internal (NP, M1, M2, P) proteins are important when forecasting influenza A evolutionary patterns.

A combined use of state-of-the-art methods and the large body of experimental evidence should pave the way for more in-depth analyses of influenza A evolution.

REFERENCES

1. Smith W., Andrewes C.H., Laidlaw P.P. // Lancet. 1933. P. 66–68.
2. Smith W., Andrewes C.H., Laidlaw P.P. // Br. J. Exp. Pathol. 1935. V. 16. P. 291–302.
3. Shope R.E. // J. Exp. Med. 1931. V. 54. P. 373–385.
4. Shope R.E. // J. Exp. Med. 1934. V. 62. P. 49–61.
5. Donina S.A., Naydikhin A.N., Rudenko L.G. // Allergology and Immunology. 2000. № 1. P. 114.
6. Cox R.J., Brokstad K.A., Ogra P. // Scand. J. Immunol. 2004. V. 59. № 1. P. 1–15.
7. Askonas B.A., McMichael A.J., Webster R.G. // Basic and Applied Influenza Research. / Ed. Beare A.S. Boca Raton, FL: CRC Press, 1982. P. 159–188.
8. Naydikhin A.N., Losev I.V.. // Problems of Virology. 2015. V. 60. P. 11–16.
9. Both G.W., Sleigh M.J., Cox N.J., Kendal A.P. // J. Virol. 1978. V. 75. P. 4886–4890.
10. Lamb R.A., Krug R.M. // Orthomyxoviridae. Fields virology. Section 2, Specific Virus Families / Eds B.N. Fields and D.M. Knipe. Lippincott, Williams, Wilkins, 2001. P. 1091–1137.

11. Steinhauser D.A., Holland J.J. // Annu. Rev. Microbiol. 1987. V. 41. P. 409–433.
12. Khatchikian D., Orlich M., Rott R. // Virology. 1982. V. 122. P. 38–47.
13. Webster R.G., Govorkova E.A. // Ann. N.Y. Acad. Sci. 2014. V. 1323. P. 115–139.
14. Strelkowa N., Lassig M. // Genetics. 2012. V. 192. P. 671–682.
15. Shih A.C.-C., Hsiao T.-C., Ho M.-S., Li W.-H. // Proc. Natl. Acad. Sci. USA. 2007. V. 104. P. 6283–6288.
16. Neher R.A., Bedford T. // Bioinformatics. 2015. V. 31(21). P. 3546–3548.
17. Kryazhimskiy S., Dushoff J., Bazykin G.A., Plotkin J.B. // Plos Genet. 2011. V. 7. e101301.
18. Neverov A.D., Kryazhimskiy S., Plotkin J.B., Bazykin G.A. // Plos Genet. 2015. V. 11(8). e1005404.
19. https://www.ncbi.nim.nih.gov/genome/FLU.
20. Luksza M., Lassig M. // Nature. 2014. V. 507. P. 57–74.
21. Webster R.G., Laver W.G. // Virology. 1981. V. 104. P. 139–148.
22. Wilson I.A., Skehel J.J., Wiley D.C. // Nature. 1981. V. 289. P. 366–373.
23. Skehel J.J., Stevens D.J., Daniels R.S., Douglas A.R., Knossow M., Wilson I.A., Wiley C.D. // Proc. Natl. Acad. Sci. USA. 1984. V. 81. P. 1779–1783.
24. Caton A.J., Browlee G.G., Yewdell J.W., Gerhard W. // Cell. 1982. V. 31. P. 417–427.
25. Rudneva I., Ignatieva A., Timofeeva T., Shilov A., Kushch A., Masalova O., Klimova R., Bovin N., Mochalova L., Kaverin N. // Virus Res. 2012. V. 166. P. 61–67.
26. Kaverin N.V., Rudneva I.A., Timofeeva T.A., Ignatieva A.V. // Problems of Virology, App. 1. 2012. P. 148–158.
27. Tsuchiya E., Sugawara K., Hongo S., Matsuzaki Y., Muraki Y., Li Z.N., Nakamura K. // J. Gen. Virol. 2001. V. 82. P. 2475–2484.
28. Wiley D.C., Wilson I.A., Skehel J.J. // Nature. 1981. V. 289. P. 373–378.
29. Kaverin N.V., Rudneva I.A., Ilyushina N.A., Varich N.L., Lipatov A.S., Smirnov Y.A., Govorkova E.A., Gitelman A.K., Lvov D.K., Webster R.G. // J. Gen. Virol. 2002. V. 83. P. 2497–2505.
30. Kaverin N.V., Rudneva I.A., Govorkova E.A., Timofeeva T.A., Shilov A.A., Kochergin-Nikitsky K.S., Krylov P.S., Webster R.G. // J. Virol. 2007. V. 81. P. 12911–12917.
31. Rudneva I.A., Kushch A.A., Masalova O.V., Timofeeva T.A., Klimova R.R., Shilov A.A., Ignatieva A.V., Krylov P.S., Kaverin N.V. // Viral Immunol. 2010. V. 23. № 2. P. 181–187.
32. Kaverin N.V., Rudneva I.A., Ilyushina N.A., Lipatov A.S., Krauss S., Webster R.G. // J. Virol. 2004. V. 78. № 1. P. 240–249.
33. Schmeiser F., Vasudevan A., Verma S., Wang W., Alvarado E., Weiss C., Autokorale V., Maseda G., Weir J.P. // PloS One. 2015. V. 10(1). e0117108.
34. Rudneva I.A., Timofeeva T.A., Ignatieva A.V., Shilov A.A., Ilyushina N.A. // Arch. Virol. 2016. V. 161. P. 3515–3520.
35. Rudneva I.A., Timofeeva T.A., Ignatieva A.V., Shilov A.A., Krylov P.S., Ilyushina N.A., Kaverin N.V. // Virology. 2013. V. 447. P. 233–239.
36. Kaverin N.V., Rudneva I.A., Timofeeva T.A., Ignatieva A.V., Shilov A.A., Bovin N.V., Ilyushina N.A. // Virus Res. 2015. V. 210. P. 81–89.
37. Centers for Disease Control and Prevention (CDC) // MMWR Morb. Mortal Wkly Rep. 1997. V. 46(50). P. 1204–1207.
38. Matrosovich M., Zhou N., Kawaoka Y., Webster R. // J. Virol. 1999. V. 73. P. 1146–1155.
39. Imai M., Watanabe T., Hatta M., Das S.C., Ozawa M., Shinya K., Zhong G., Hanson A., Katsura H., Watanabe S., et al. // Nature. 2012. V. 486. № 7403. P. 420–428.
40. Russell C.A., Fonville J.M., Brown A.E., Burke D.E., Smith D.L., James S.L., Herfst S., van Boheemen S., Linster M., Schrauwen E.J., et al. // Science. 2012. V. 336. P. 1541–1547.
41. Zhang Z.-W., Liu T., Zeng J., Chen Y.-E., Yuan M., Zhang D.-W., Zhu F., Yuan S. // Infectious of Poverty. 2015. V. 4. № 50. P. 2–9.
42. Hanson A., Imai M., Hatta M., McBride R., Imai H., Taft A., Zhong G., Watanabe T., Suzuki Y., Neumann G., et al. // J. Virol. 2016. V. 90. № 6. P. 2981–2992.
43. Plotch S.J., Bouloy M., Krug R.M. // Proc. Natl. Acad. Sci. USA. 1979. V. 76. P. 1618–1622.
44. Taft A.S., Ozawa M., Fitch A., Depasse J.V., Halfmann P.J., Hill-Batorski L., Hatta M., Fridrich T.C., Lopes T.J.S., Maher E.A., et al. // Nat. Commun. 2015. V. 6. № 7491. P. 1–12.
45. Varich N.L., Sadykova G.K., Prilipov A.G., Kochergin-Nikitsky K.S., Kushch A.A., Masalova O.V., Klimova R.R., Gitelman A.K., Kaverin N.V. // Viral Immunol. 2011. V. 24. № 2. P. 1–7.
46. Varich N.L., Sadykova G.K., Prilipov A.G., Kochergin-Nikitsky K.S., Webster R.G., Kaverin N.V. // Arch. Virology. 2014. V. 159. P. 1493–1497.

Death Receptors: New Opportunities in Cancer Therapy

V.M. Ukrainskaya[1], A.V. Stepanov[1,2]*, I.S. Glagoleva[2], V.D. Knorre[1], A.A. Jr. Belogurov[1,2], A.G. Gabibov[1,2]

[1]M.M. Shemyakin and Yu.A. Ovchinnikov Institute of Bioorganic Chemistry, Miklukho-Maklaya Str., 16/10, Russian Academy of Sciences, Moscow, 117997, Russia

[2]Institute of Fundamental Medicine and Biology, Kremlyovskaya Str., 18, Kazan Federal University, Kazan, 420008, Russia

*E-mail: stepanov.aleksei.v@gmail.com

Received: January 12, 2017; in final form June 02, 2017

ABSTRACT This article offers a detailed review of the current approaches to anticancer therapy that target the death receptors of malignant cells. Here, we provide a comprehensive overview of the structure and function of death receptors and their ligands, describe the current and latest trends in the development of death receptor agonists, and perform their comparative analysis. In addition, we discuss the DR4 and DR5 agonistic antibodies that are being evaluated at various stages of clinical trials. Finally, we conclude by stating that death receptor agonists may be improved through increasing their stability, solubility, and elimination half-life, as well as by overcoming the resistance of tumor cells. What's more, effective application of these antibodies requires a more detailed study of their use in combination with other anticancer agents.

KEYWORDS apoptosis, death receptors, DR4, DR5, TNF, tumor cells.

ABBREVIATIONS DR4 – death receptor 4, DR5 – death receptor 5, TNF – tumor necrosis factor.

INTRODUCTION

The major current approaches to cancer therapy are based on a combination of chemotherapy and surgery. But, because of the lack of cancer specificity, they are often associated with a variety of severe side-effects and complications. For this reason, the design of highly specific drugs, such as monoclonal antibodies, for a targeted inhibition of cancer cells appears to be a very promising direction [1]. A better understanding of tumor biology and tumor immunology affords us the opportunity to use apoptosis as a target for the future development of selective anticancer agents. Apoptosis is a natural physiological process that controls the number of cells in tissues and plays a key role in the elimination of damaged, unwanted, and diseased cells. However, the malignant transformation of cells often disrupts apoptosis pathways [2]. It is noteworthy that our growing understanding of the mechanisms that regulate programmed cell death has led to the emergence of new agents capable of restarting apoptosis in malignant cells. A major proportion of current therapeutic agents capable of initiating apoptosis comprises low-molecular-weight compounds, the disadvantages of which are systemic complications [3].

A fundamentally different approach to anticancer therapy is the search for tumor necrosis factor receptor superfamily (TNFRSF) agonists. So-called death receptors containing a death domain comprise a separate group of the superfamily. These include the tumor necrosis factor receptor 1 (TNFR1), tumor necrosis factor receptor 6 (CD95, FasR, APO-1), death receptor 4 (DR4), death receptor 5 (DR5), etc. Receptors DR4 and DR5 are the most promising candidates for targeted therapy of tumor diseases, because their expression levels are significantly higher in cancer cells than in normal ones [4, 5]. Therefore, unlike chemotherapeutic agents, these receptors may potentially mediate selective killing of tumor cells.

In normal cells, the apoptotic mechanisms are regulated by anti-apoptotic proteins: for example, the cellular FLICE-like inhibitory protein (c-FLIP) suppresses caspase 8 activation, and Bcl-2 family proteins, forming part of a heterocomplex with caspases, and inhibit the apoptotic signal [6, 7].

THE STRUCTURE OF THE DEATH RECEPTORS 4 AND 5

DR4 and DR5 are type I transmembrane proteins consisting of three (extracellular, transmembrane, and intracellular) domains. The last domain comprises a homologous cytoplasmic sequence of the death domain. Furthermore, DR5 can exist as two isoforms, DR5 (L) and DR5 (S): the short form lacks 29 amino acid res-

idues between the cysteine sequences and the transmembrane region, but this does not affect the functional activity of the receptor [8].

DR4 and DR5 receptors are found in cells of various human tissues, including thymus, liver, leukocytes, activated T cells, and small intestine. They are also detected in some tumor lines, such as Jurkat [9], Ramos [10], HeLa [11], Colo205 [12], etc. Identity of the death and cysteine-rich domains of DR4 and DR5 is 64% and 66%, respectively [13].

The interaction between a receptor and a ligand (TRAIL/Apo2L) occurs first at the N-terminus of the extracellular domain, when the ligand binds to a first cysteine domain, the so-called pre-ligand assembly domain (PLAD) [14]. This sequence is not directly involved in receptor oligomerization, but it stabilizes a ligand relative to the receptor [15]. Previously, ligand trimerization was determined to occur in the presence of a Zn^{+2} ion [16] that non-covalently binds to the cysteine-rich domains of TRAIL. Stabilization of TRAIL is accompanied by a conformational change in the monomeric receptor, followed by translocation of the receptor into membrane lipid rafts and the formation of its active trimeric form [17]. Then, an adaptor protein associates with the receptor through the homotypic interaction between the adaptor's death domain and the receptor's death domain (DD-DD). Adaptor molecules include the Fas-associated DD (FADD) protein that interacts with a death domain of the Fas receptor and the TNFR1-associated DD (TRADD) protein that interacts with a death domain of the TNFR1 receptor [18]. TRADD and FADD also comprise additional protein interaction modules called death effector domains (DEDs) [19]. They can associate with procaspases 8/10 and the regulatory protein c-FLIP. The multiprotein complex formed between the death domain of the FADD receptor and caspases 8/10 is called the death-inducing signaling complex (DISC) [20] (*Fig. 1*). After the formation of DISC, the apoptotic signal is transmitted to initiator caspases.

ACTIVATION OF APOPTOSIS

Apoptosis is a complex energy-consuming process involving a cascade of molecular transformations. To date, two, mitochondrial and receptor-mediated, apoptotic pathways are known.

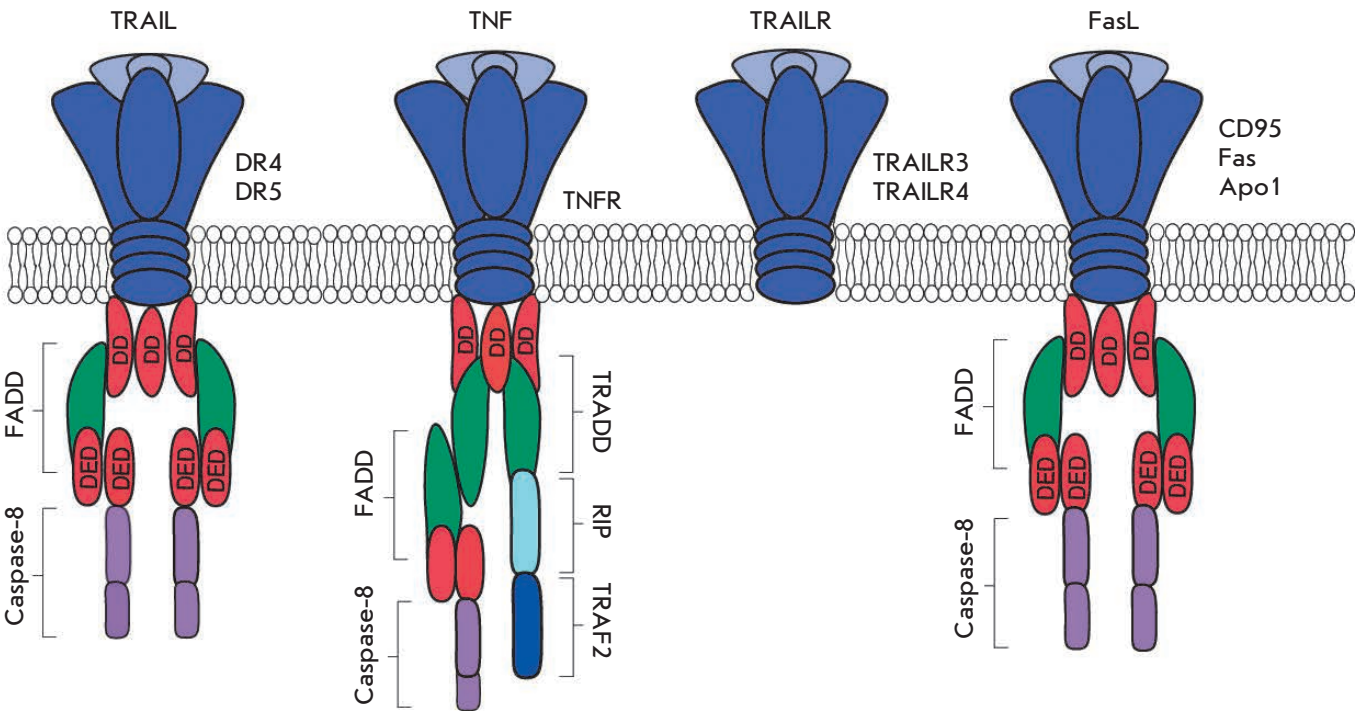

Fig. 1. Structures of death receptors. Death receptors and their ligands include: receptors DR4 (TNFRSF10A, TRAIL-R1), DR5 (TNFRSF10B, TRAIL-R2, Apo2), DcR1 (TRAILR3), and DcR2 (TRAILR4) and their ligand, TRAIL; the tumor necrosis factor receptor (TNFR) and its ligand, the tumor necrosis factor (TNF); the Fas receptor (CD95, Apo1) and its ligand, FasL. Note: TRADD – the tumor necrosis factor receptor type 1-associated death domain protein; FADD – the Fas-associated death domain protein; DD – a death domain; DED – a death effector domain; RIP – a receptor-interacting protein.

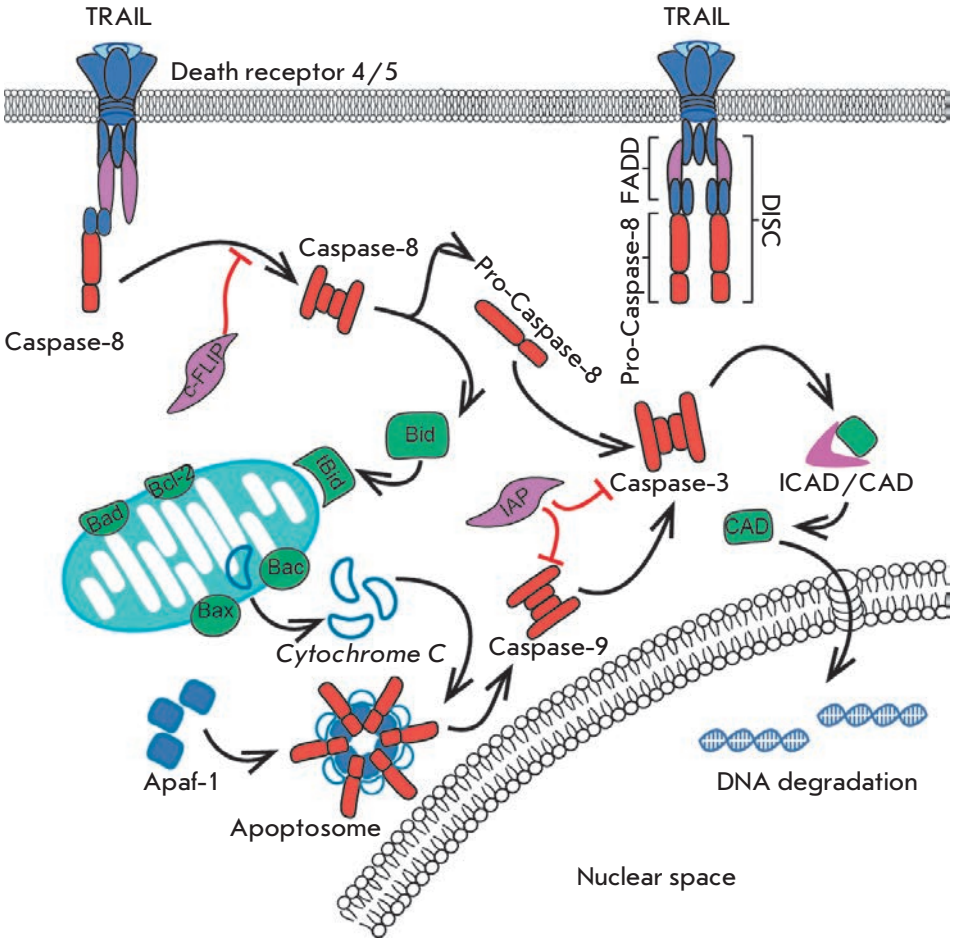

Fig. 2. Apoptosis signal transduction pathways (receptor-mediated and mitochondrial pathways): receptor-ligand interaction leads to DISC formation, which induces factors that activate apoptosis (caspase 8, caspase 3, etc.). The release of cytochrome *c* leads to apoptosome formation and activation of caspase 9. Note: DISC – the death-inducing signaling complex; Bid, Bad, Bcl-2, and Bac – Bcl2 protein family; ICAD\CAD – caspase activated DNAse; Apaf-1 – the apoptotic protease activating factor 1; IAP and c-FLIP – apoptosis inhibitory proteins.

After the DISC formation, the apoptotic signal is transmitted to initiator caspases. Caspases occur in the cell as inactive procaspases (32–56 kDa) that are monomers consisting of a N-terminal domain, large (17–21 kDa) and small (10–13 kDa) subunits, and short linking regions [21]. There are several theories of the caspase activation process. According to one of them, clustering of caspases at the DISC leads to their self-activation through autocatalytic processing. According to another theory, assembling of initiator caspases promotes their dimerization, which results in cleavage of the N-terminal pro-domain and linking regions in each monomer, with the large and small subunits forming heterodimers [22]. High local concentrations of initiator procaspases induce their binding to the FADD domain.

The substrate specificity of initiator caspases is limited by effector caspases and the pro-apoptotic Bid protein [23]. Activation of DISC-associated caspases 8/10 promotes subsequent activation of the effector caspases 3 and 7 exhibiting enzymatic activity. The effector caspase cleavage site is an Asp residue in a tetrapeptide motif [24, 25]. Activation of effector caspases triggers a variety of signaling pathways that control cell activity.

The mitochondrial apoptotic pathway is most often activated by intracellular factors in response to various signals: DNA damage, formation of reactive oxygen species, accumulation of misfolded proteins, etc. This process is regulated by the proteins of the Bcl-2 family. The family includes the Bid factor that is cleaved and activated by caspase 8 [26]. The activated form of Bid (tBid) causes permeabilization of the mitochondrial membrane, release of cytochrome *c*, and formation of the apoptosome that activates initiator caspase 9 [27]. This is a key moment in the development of intracellular apoptosis, which leads to the activation of effector caspases (*Fig. 2*).

Both the receptor-mediated and mitochondrial pathways lead to the activation of cytoplasmic DNA-degrading endonucleases and proteases that destroy intracellular proteins. Caspases 3, 6, and 7 directly cleave cytokeratin and the cell membrane, which leads to the morphological changes seen in any apoptotic cell [28].

TRAIL

Like the tumor necrosis factor (TNF), TRAIL belongs to the tumor necrosis factor superfamily (TNFSF) and par-

ticipates in the regulation of vital biological functions in vertebrates [29]. Being a ligand of DR4 and DR5, TRAIL comprises two antiparallel beta-pleated sheets that form a beta-sandwich [30]. Containing the only cysteine residue, TRAIL is capable of chelating zinc. Subunits interact with each other in a head-to-tail fashion to form a homotrimer resembling a truncated pyramid [31]. TRAIL also contains a significant number of aromatic amino acid residues, eight of which are present on the surface of the inner sheet and provide a hydrophobic platform for interaction with neighboring subunits.

TRAIL, as the basis for developing therapeutic constructs, has several advantages over other apoptosis-inducing ligands. The main feature of TRAIL is the lack of cytotoxicity to normal cells, in contrast to a Fas ligand and TNF. Presumably, this is associated with the specificity of TRAIL to decoy the receptors DcR1 and DcR2 located on the surface of normal cells [32]. They inhibit apoptosis by competing with DR4 and DR5 for binding to TRAIL. Also, the DcR2 receptor can bind to DR4 to form a ligand-independent complex [33]. However, it remains unclear what else ensures the survival of normal cells, since decoy receptors are also found on tumor cells sensitive to TRAIL.

TUMOR CELL RESISTANCE TO TRAIL

There are various causes for the resistance to TRAIL. Many molecules that regulate the apoptotic signal generation can act as its inhibitors. These molecules include the FLIP protein, inhibitors of apoptosis proteins (IAPs), the transcription factor NF-kB, etc. [34].

Overexpression of anti-apoptotic proteins belonging to the Bcl-2 family may contribute to the development of resistance to TRAIL in various tumor cells [35]. Association of cleaved c-FLIP with the DISC was found to prevent activation of caspase 8 [36]. TRAIL resistance may also be caused by various mutations in the proteins involved in the apoptosis signaling pathway: For example, mutations in the pro-apoptotic protein Bax lead to the resistance displayed by colon cancer epithelial cells [37].

For example, TRAIL-sensitive neuroectodermal tumor (PNET) cell lines express the necessary amounts of mRNA and caspase 8, while TRAIL-resistant PNET cells do not express them, which is a result of the methylation of the gene encoding caspase. It was noted that TRAIL-resistant PNET cells preserve their resistance even upon overexpression of TRAIL receptors [38, 39].

A high level of the transcription factor NF-kB in tumor cells may induce not only an increased expression of DR4 and DR5 receptors [40], but also the development of resistance to TRAIL, which is caused by increased synthesis of the anti-apoptotic proteins regulated by the factor [41].

The described variants do not encompass all the ways in which tumor cells develop resistance. Overcoming this resistance is the main thrust in the development of new agents that can activate DR4 and DR5 receptors.

TRAIL-R AGONISTS IN CANCER THERAPY

To date, a variety of strategies targeting TRAIL-R have been developed. These include various forms of recombinant soluble human TRAIL (Apo2L or AMG-951/dulanermin), DR4 and DR5 agonist antibodies, etc. [42]. These agents are safe and well tolerated by patients [43, 44].

An ideal therapeutic agent to activate TRAIL-dependent apoptosis should have activity comparable to that of the natural ligand, high antibody-like affinity to the receptor, and an elimination half-life sufficient to circulate in the bloodstream for a long time. Recombinant human TRAIL activates both death receptors, but its use is limited by its rapid hydrolysis in blood and short elimination half-life. In addition, TRAIL can bind to decoy receptors that are able to inhibit the activation of apoptosis [45]. As an alternative to TRAIL, antibodies capable of interacting only with death receptors and that do not affect decoy receptors have been developed. They are relatively safe, have improved pharmacokinetic properties compared to those of recombinant TRAIL, but they are specific only to one type of receptors. Despite the existing limitations, a variety of agents affecting death receptors, both as monotherapy and combination therapy, are now undergoing clinical trials.

The first recombinant version of TRAIL contained a TNF homologous domain with a polyhistidine tag [46] or a FLAG epitope [47] attached to the N-terminus. These fragments improve the protein purification process. Although these two modified proteins have demonstrated efficacy both in *in vitro* and *in vivo* trials, their use is hampered by their toxicity to liver hepatocytes.

To increase the stability of the TRAIL complex, several modifications have been developed. One of the approaches is to connect TRAIL with a leucine zipper motif (LZ-TRAIL) or an isoleucine zipper motif (iz-TRAIL). A similar approach is to link TRAIL with tenascin-C for the stabilization and oligomerization of the molecule. These agents have exhibited greater *in vivo* and *in vitro* activity compared to that of dulanermin, and they did not affect hepatocytes [48].

More recently, several research groups have developed a new TRAIL stabilization principle based on single-chain TRAIL (scTRAIL) [49]. In this approach, a molecule is initially expressed as a trimer in which three domains are interlinked in a head-to-tail fashion. An initially correctly assembled construct excludes the

possibility of errors during its expression and prevents non-specific interaction with other molecules. This provides advantages to scTRAIL over its analogues and demonstrates efficacy against certain drug-resistant tumor lines.

Another approach for increasing the elimination half-life of TRAIL is to link TRAIL with molecules that have better pharmacokinetic properties, e.g. human serum albumin (HSA) or polyethylene glycol (PEG). According to the results of *in vivo* studies, pegylation of iz-TRAIL increases the elimination half-life, stability, and solubility of the molecule [50].

ANTIBODIES

Antibodies to TRAIL-R1 (mapatumumab [51]) and TRAIL-R2 (conatumumab [52], lexatumumab [53], tigatuzumab [54], and drozitumab [55]) have demonstrated a degree of efficacy in preclinical trials. In clinical trials, all the antibodies exhibited safety and greater stability compared to those of TRAIL. Antibodies that had been effective in phase I clinical trials were studied in phase II clinical trials both as monotherapy and as combination chemotherapy with cisplatin, paclitaxel [56], and other anticancer agents.

The antibodies mapatumumab and conatumumab proved effective as monotherapy. In mapatumumab antibody therapy, clinical improvement was observed in 14 of 17 patients with non-Hodgkin lymphoma. Prolonged remission was observed in 29% of patients with non-small cell lung cancer and in 32% of patients with colorectal cancer [57, 58].

The combination of conatumumab with paclitaxel and carboplatin as first line treatment for patients with non-small cell lung cancer was more effective compared to a treatment with carboplatin and paclitaxel alone [59]. By contrast, mapatumumab, combined with paclitaxel and carboplatin, did not increase the efficacy of the treatment [60].

Furthermore, conatumumab was effective in combination with standard FOLFIRI chemotherapy and ganitumab as second line treatment for colorectal cancer, increasing the survival rate in patients in remission [61].

Tigatuzumab (CS-1008), combined with gentamicin, was well tolerated in the treatment of metastatic liver cancer, and the overall percentage of patients with an objective response rate amounted to 13.1% [62].

A recombinant analogue of the death receptor ligand dulanermin was tested in patients with different tumors and demonstrated activity against chondroblastoma, colorectal cancer, etc., during pre-clinical trials. Unfortunately, no similar efficacy was detected in clinical trials [63].

According to the presented data, effective treatment of cancer with death receptor agonists requires an individualized approach to each patient, because there is a risk of tumor cell resistance to such therapy. One of the principles for overcoming the resistance may be to search for the specific biomarkers of resistance, which could help characterize cells with high expression levels of death receptors, which would be sensitive to antibodies [66].

One of such approaches is the use of genetically modified T cells. T cells expressing a chimeric antigen receptor (CAR) of a TRAIL receptor single-chain antibody were capable of specific elimination of tumor cells with DR4. During interaction with tumor cells, the CAR-modified T cells were shown to trigger not only a DR4-induced apoptotic pathway, but also the mechanisms of T cell cytotoxicity [64, 65].

PEPTIDE AGONISTS OF DEATH RECEPTORS

A promising approach is the search for appropriate peptide agonists of DR4 and DR5. The advantage of peptides over TRAIL is their ability to bind only to a certain death receptor [67]. Peptide ligands are screened using a phage display technology that selects peptides with agonistic properties based on a linkage between a genotype and a phenotype. The produced peptides, in both monomeric and dimeric forms, can bind to a receptor and activate it.

By using phage display, a group of researchers selected a YCKVILTHRCY peptide that was able to bind specifically to DR5. Tyr residues were added to the ends of the peptide to increase its solubility. The peptide properties were investigated both in the monomeric and dimeric (two covalently bound monomers) forms. Both forms were demonstrated to interact with DR5 and induce apoptosis in tumor cells of the Colo205 line. The effectiveness of the monomer may be associated with the fact that the peptide contains numerous hydrophobic residues and, at high concentrations, may aggregate in an aqueous medium [68]. Another research group also used phage display to select a GRVCLTLCSRLT peptide with high affinity for DR5 (IC_{50} = 30 nM). A LTL amino acid sequence was found to play a key role in the interaction with the receptor [69].

CONCLUSION

Currently, there exist many approaches for affecting tumor cells, in particular through apoptotic pathways. Unfortunately, many of these approaches remain inappropriate due to cell resistance, as well as the inefficiency and instability of therapeutic agents. Other agents offer new opportunities for the treatment of tumor diseases. A more detailed investigation of the complex mechanism involving death receptor signaling pathways will boost the develop-

ment of new agents that could be capable of overcoming the resistance and selectively affect cancer cells. On the other hand, effective use of existing death receptor antibodies requires a more detailed investigation of their application in combination therapy.

This work was supported by a grant from the Russian Science Foundation №14-24-00106. A.V. Stepanov received personal financial support from the Russian Foundation for Basic Research and Moscow City Government in the framework of research project № 15-34-70037 mol_a_mos.

REFERENCES

1. Deyev S.M., Lebedenko E.N., Petrovskaya L.E., Dolgikh D.A., Gabibov A.G., Kirpichnikov M.P. // Russian Chemical Reviews. 2015. V. 84. № 1. P. 1–26.
2. Wong R.S. // J. Exp. Clin. Cancer Res. 2011. V. 30. P. 87.
3. Parameswaran N., Patial S. // Crit. Rev. Eukaryot. Gene Expr. 2010. V. 20. № 2. P. 87–103.
4. Strater J., Hinz U., Walczak H., Mechtersheimer G., Koretz K., Herfarth C., Moller P., Lehnert T. // Clin. Cancer Res. 2002. V. 8. № 12. P. 3734–3740.
5. Pan G., O'Rourke K., Chinnaiyan A.M., Gentz R., Ebner R., Ni J., Dixit V.M. // Science. 1997. V. 276. № 5309. P. 111–113.
6. Chinnaiyan A.M., Dixit V.M. // Semin. Immunol. 1997. V. 9. № 1. P. 69–76.
7. Reed J.C. // Semin. Hematol. 1997. V. 34. № 4. P. 9–19.
8. Wang T.T., Jeng J. // Breast Cancer Res. Treat. 2000. V. 61 № 1. P. 87–96.
9. Natoni A., MacFarlane M., Inoue S., Walewska R., Majid A., Knee D., Stover D.R., Dyer M.J., Cohen G.M. // Br. J. Haematol. 2007. V. 139. № 4. P. 568–577.
10. MacFarlane M., Kohlhaas S.L., Sutcliffe M.J., Dyer M.J., Cohen G.M. // Cancer Res. 2005. V. 65. № 24. P. 11265–11270.
11. Ren Y.G., Wagner K.W., Knee D.A., Aza-Blanc P., Nasoff M., Deveraux Q.L. // Mol. Biol. Cell. 2004. V. 15. № 11. P. 5064–5074.
12. Chiron D., Pellat-Deceunynck C., Maillasson M., Bataille R., Jego G. // J. Immunol. 2009. V. 183. № 7. P. 4371–4377.
13. Pan G., Ni J., Wei Y.F., Yu G., Gentz R., Dixit V.M. // Science. 1997. V. 277. № 5327. P. 815–818.
14. Clancy L., Mruk K., Archer K., Woelfel M., Mongkolsapaya J., Screaton G., Lenardo M.J., Chan F.K. // Proc. Natl. Acad. Sci. USA. 2005. V. 102. № 50. P. 18099–18104.
15. Sfikakis P.P., Tsokos G.C. // Clin. Immunol. 2011. V. 141. № 3. P. 231–235.
16. Ozoren N., El-Deiry W.S. // Semin. Cancer Biol. 2003. V. 13. № 2. P. 135–147.
17. Marconi M., Ascione B., Ciarlo L., Vona R., Garofalo T., Sorice M., Gianni A.M., Locatelli S.L., Carlo-Stella C., Malorni W., et al. // Cell Death Dis. 2013. V. 4. P. e863.
18. Kuang A.A., Diehl G.E., Zhang J., Winoto A. // J. Biol. Chem. 2000. V. 275. № 33. P. 25065–25068.
19. Riley J.S., Malik A., Holohan C., Longley D.B. // Cell Death Dis. 2015. V. 6. P. e1866.
20. Kischkel F.C., Lawrence D.A., Chuntharapai A., Schow P., Kim K.J., Ashkenazi A. // Immunity. 2000. V. 12. № 6. P. 611–620.
21. Earnshaw W.C. // Nature. 1999. V. 397. № 6718. P. 387, 389.
22. Riedl S.J., Shi Y. // Nat. Rev. Mol. Cell. Biol. 2004. V. 5. № 11. P. 897–907.
23. Huang K., Zhang J., O'Neill K.L., Gurumurthy C.B., Quadros R.M., Tu Y., Luo X. // J. Biol. Chem. 2016. V. 291. № 22. P. 11843–11851.
24. MacKenzie S.H., Clark A.C. // Adv. Exp. Med. Biol. 2012. V. 747. P. 55–73.
25. Thornberry N.A. // Br. Med. Bull. 1997. V. 53. № 3. P. 478–490.
26. Mukae N., Enari M., Sakahira H., Fukuda Y., Inazawa J., Toh H., Nagata S. // Proc. Natl. Acad. Sci. USA. 1998. V. 95. № 16. P. 9123–9128.
27. Finucane D.M., Bossy-Wetzel E., Waterhouse N.J., Cotter T.G., Green D.R. // J. Biol. Chem. 1999. V. 274. № 4. P. 2225–2233.
28. Slee E.A., Adrain C., Martin S.J. // J. Biol. Chem. 2001. V. 276. № 10. P. 7320–7326.
29. Banks T.A., Rickert S., Benedict C.A., Ma L., Ko M., Meier J., Ha W., Schneider K., Granger S.W., Turovskaya O., et al. // J. Immunol. 2005. V. 174. № 11. P. 7217–7225.
30. Cha S.S., Kim M.S., Choi Y.H., Sung B.J., Shin N.K., Shin H.C., Sung Y.C., Oh B.H. // Immunity. 1999. V. 11. № 2. P. 253–261.
31. Zakaria A., Picaud F., Guillaume Y.C., Gharbi T., Micheau O., Herlem G. // J. Mol. Recognit. 2016. V. 29. № 9. P. 406–414.
32. Baritaki S., Huerta-Yepez S., Sakai T., Spandidos D.A., Bonavida B. // Mol. Cancer Ther. 2007. V. 6. № 4. P. 1387–1399.
33. Marsters S.A., Sheridan J.P., Pitti R.M., Huang A., Skubatch M., Baldwin D., Yuan J., Gurney A., Goddard A.D., Godowski P., et al. // Curr. Biol. 1997. V. 7. № 12. P. 1003–1006.
34. Prasad S., Kim J.H., Gupta S.C., Aggarwal B.B. // Trends Pharmacol. Sci. 2014. V. 35. № 10. P. 520–536.
35. Sivaprasad U., Shankar E., Basu A. // Cell Death Differ. 2007. V. 14. № 4. P. 851–860.
36. Guseva N.V., Rokhlin O.W., Taghiyev A.F., Cohen M.B. // Breast Cancer Res. Treat. 2008. V. 107. № 3. P. 349–357.
37. LeBlanc H., Lawrence D., Varfolomeev E., Totpal K., Morlan J., Schow P., Fong S., Schwall R., Sinicropi D., Ashkenazi A. // Nat. Med. 2002. V. 8. № 3. P. 274–281.
38. Kim H.S., Lee J.W., Soung Y.H., Park W.S., Kim S.Y., Lee J.H., Park J.Y., Cho Y.G., Kim C.J., Jeong S.W., et al. // Gastroenterology. 2003. V. 125. № 3. P. 708–715.
39. Agolini S.F., Shah K., Jaffe J., Newcomb J., Rhodes M., Reed J.F., 3rd. // J. Trauma. 1997. V. 43. № 3. P. 395–399.
40. Ravi R., Bedi G.C., Engstrom L.W., Zeng Q., Mookerjee B., Gelinas C., Fuchs E.J., Bedi A. // Nat. Cell. Biol. 2001. V. 3. № 4. P. 409–416.
41. Kwon H.R., Lee K.W., Dong Z., Lee K.B., Oh S.M. // Biochem. Biophys. Res. Commun. 2010. V. 391. № 1. P. 830–834.
42. Lemke J., von Karstedt S., Zinngrebe J., Walczak H. // Cell Death Differ. 2014. V. 21. № 9. P. 1350–1364.
43. Joy A.M., Beaudry C.E., Tran N.L., Ponce F.A., Holz D.R., Demuth T., Berens M.E. // J. Cell Sci. 2003. V. 116. P. 4409–4417.
44. Dimberg L.Y., Anderson C.K., Camidge R., Behbakht K., Thorburn A., Ford H.L. // Oncogene. 2013. V. 32. № 11. P. 1341–1350.
45. Milutinovic S., Kashyap A.K., Yanagi T., Wimer C., Zhou S., O'Neil R., Kurtzman A.L., Faynboym A., Xu L., Hannum C.H., et al. // Mol. Cancer Ther. 2016. V. 15. № 1. P. 114–124.
46. Pitti R.M., Marsters S.A., Ruppert S., Donahue C.J., Moore A., Ashkenazi A. // J. Biol. Chem. 1996. V. 271. № 22. P. 12687–12690.

47. Wiley S.R., Schooley K., Smolak P.J., Din W.S., Huang C.P., Nicholl J.K., Sutherland G.R., Smith T.D., Rauch C., Smith C.A., et al. // Immunity. 1995. V. 3. № 6. P. 673–682.
48. Rozanov D.V., Savinov A.Y., Golubkov V.S., Rozanova O.L., Postnova T.I., Sergienko E.A., Vasile S., Aleshin A.E., Rega M.F., Pellecchia M., et al. // Mol. Cancer Ther. 2009. V. 8. № 6. P. 1515–1525.
49. Siegemund M., Pollak N., Seifert O., Wahl K., Hanak K., Vogel A., Nussler A.K., Gottsch D., Munkel S., Bantel H., et al. // Cell Death Dis. 2012. V. 3. P. e295.
50. Harris J.M., Chess R.B. // Nat. Rev. Drug Discov. 2003. V. 2. № 3. P. 214–221.
51. Greco F.A., Bonomi P., Crawford J., Kelly K., Oh Y., Halpern W., Lo L., Gallant G., Klein J. // Lung Cancer. 2008. V. 61. № 1. P. 82–90.
52. Doi T., Murakami H., Ohtsu A., Fuse N., Yoshino T., Yamamoto N., Boku N., Onozawa Y., Hsu C.P., Gorski K.S., et al. // Cancer Chemother. Pharmacol. 2011. V. 68. № 3. P. 733–741.
53. Merchant M.S., Geller J.I., Baird K., Chou A.J., Galli S., Charles A., Amaoko M., Rhee E.H., Price A., Wexler L.H., et al. // J. Clin. Oncol. 2012. V. 30. № 33. P. 4141–4147.
54. Reck M., Krzakowski M., Chmielowska E., Sebastian M., Hadler D., Fox T., Wang Q., Greenberg J., Beckman R.A., von Pawel J. // Lung Cancer. 2013. V. 82. № 3. P. 441–448.
55. Kang Z., Chen J.J., Yu Y., Li B., Sun S.Y., Zhang B., Cao L. // Clin. Cancer Res. 2011. V. 17. № 10. P. 3181–3192.
56. Sasaki Y., Nishina T., Yasui H., Goto M., Muro K., Tsuji A., Koizumi W., Toh Y., Hara T., Miyata Y. // Cancer Sci. 2014. V. 105. № 7. P. 812–817.
57. Younes A., Vose J.M., Zelenetz A.D., Smith M.R., Burris H.A., Ansell S.M., Klein J., Halpern W., Miceli R., Kumm E., et al. // Br. J. Cancer. 2010. V. 103. № 12. P. 1783–1787.
58. Trarbach T., Moehler M., Heinemann V., Kohne C.H., Przyborek M., Schulz C., Sneller V., Gallant G., Kanzler S. // Br. J. Cancer. 2010. V. 102. № 3. P. 506–512.
59. Paz-Ares L., Balint B., de Boer R.H., van Meerbeeck J.P., Wierzbicki R., De Souza P., Galimi F., Haddad V., Sabin T., Hei Y.J., et al. // J. Thorac. Oncol. 2013. V. 8. № 3. P. 329–337.
60. von Pawel J., Harvey J.H., Spigel D.R., Dediu M., Reck M., Cebotaru C.L., Humphreys R.C., Gribbin M.J., Fox N.L., Camidge D.R. // Clin. Lung Cancer. 2014. V. 15. № 3. P. 188–196.e2.
61. Cohn A.L., Tabernero J., Maurel J., Nowara E., Sastre J., Chuah B.Y., Kopp M.V., Sakaeva D.D., Mitchell E.P., Dubey S., et al. // Ann. Oncol. 2013. V. 24. № 7. P. 1777–1785.
62. Forero-Torres A., Infante J.R., Waterhouse D., Wong L., Vickers S., Arrowsmith E., He A.R., Hart L., Trent D., Wade J., et al. // Cancer Med. 2013. V. 2(6). P. 925–932.
63. Pan Y., Xu R., Peach M., Huang C.P., Branstetter D., Novotny W., Herbst R.S., Eckhardt S.G., Holland P.M. // Br. J. Cancer. 2011. V. 105. № 12. P. 1830–1838.
64. Dine J.L., O'Sullivan C.C., Voeller D., Greer Y.E., Chavez K.J., Conway C.M., Sinclair S., Stone B., Amiri-Kordestani L., Merchant A.S., et al. // Breast Cancer Res. Treat. 2016. V. 155. № 2. P. 235–251.
65. Kobayashi E., Kishi H., Ozawa T., Hamana H., Nakagawa H., Jin A., Lin Z., Muraguchi A. // Biochem. Biophys. Res. Commun. 2014. V. 453. № 4. P. 798–803.
66. Jin A., Ozawa T., Tajiri K., Lin Z., Obata T., Ishida I., Kishi H., Muraguchi A. // Eur. J. Immunol. 2010. V. 40. № 12. P. 3591– 3593.
67. Ladner R.C., Sato A.K., Gorzelany J., de Souza M. // Drug Discov. Today. 2004. V. 9. № 12. P. 525–529.
68. Vrielink J., Heins M.S., Setroikromo R., Szegezdi E., Mullally M.M., Samali A., Quax W.J. // FEBS J. 2010. V. 277. № 7. P. 1653–1665.
69. Li B., Russell S.J., Compaan D.M., Totpal K., Marsters S.A., Ashkenazi A., Cochran A.G., Hymowitz S.G., Sidhu S.S. // J. Mol. Biol. 2006. V. 361. № 3. P. 522–536.
70. Wakelee H.A., Patnaik A., Sikic B.I., Mita M., Fox N.L., Miceli R., Ullrich S.J., Fisher G.A., Tolcher A.W. // Ann. Oncol. 2010. V. 21. № 2. P. 376–381.
71. Hotte S.J., Hirte H.W., Chen E.X., Siu L.L., Le L.H., Corey A., Iacobucci A., MacLean M., Lo L., Fox N.L., et al. // Clin. Cancer Res. 2008. V. 14. № 11. P. 3450–3455.
72. Mom C.H., Verweij J., Oldenhuis C.N., Gietema J.A., Fox N.L., Miceli R., Eskens F.A., Loos W.J., de Vries E.G., Sleijfer S. // Clin. Cancer Res. 2009. V. 15. № 17. P. 5584–5590.
73. Ciuleanu T., Bazin I., Lungulescu D., Miron L., Bondarenko I., Deptala A., Rodriguez-Torres M., Giantonio B., Fox N.L., Wissel P., et al. // Ann. Oncol. 2016. V. 27. № 4. P. 680–687.
74. Herbst R.S., Kurzrock R., Hong D.S., Valdivieso M., Hsu C.P., Goyal L., Juan G., Hwang Y.C., Wong S., Hill J.S., et al. // Clin. Cancer Res. 2010. V. 16. № 23. P. 5883–5891.
75. Demetri G.D., Le Cesne A., Chawla S.P., Brodowicz T., Maki R.G., Bach B.A., Smethurst D.P., Bray S., Hei Y.J., Blay J.Y. // Eur. J. Cancer. 2012. V. 48. № 4. P. 547–563.
76. Fuchs C.S., Fakih M., Schwartzberg L., Cohn A.L., Yee L., Dreisbach L., Kozloff M.F., Hei Y.J., Galimi F., Pan Y., et al. // Cancer. 2013. V. 119. № 24. P. 4290–4298.
77. Kindler H.L., Richards D.A., Garbo L.E., Garon E.B., Stephenson J.J., Jr., Rocha-Lima C.M., Safran H., Chan D., Kocs D.M., Galimi F., et al. // Ann. Oncol. 2012. V. 23. № 11. P. 2834–2842.
78. Forero-Torres A., Shah J., Wood T., Posey J., Carlisle R., Copigneaux C., Luo F.R., Wojtowicz-Praga S., Percent I., Saleh M. // Cancer Biother. Radiopharm. 2010. V. 25. № 1. P. 13–19.
79. Forero-Torres A., Varley K.E., Abramson V.G., Li Y., Vaklavas C., Lin N.U., Liu M.C., Rugo H.S., Nanda R., Storniolo A.M., et al. // Clin. Cancer Res. 2015. V. 21. № 12. P. 2722–2729.
80. Cheng A.L., Kang Y.K., He A.R., Lim H.Y., Ryoo B.Y., Hung C.H., Sheen I.S., Izumi N., Austin T., Wang Q., et al. // J. Hepatol. 2015. V. 63. № 4. P. 896–904.
81. Ciprotti M., Tebbutt N.C., Lee F.T., Lee S.T., Gan H.K., McKee D.C., O'Keefe G.J., Gong S.J., Chong G., Hopkins W., et al. // J. Clin. Oncol. 2015. V. 33. № 24. P. 2609–2616.
82. Rocha Lima C.M., Bayraktar S., Flores A.M., MacIntyre J., Montero A., Baranda J.C., Wallmark J., Portera C., Raja R., Stern H., et al. // Cancer Invest. 2012. V. 30. № 10. P. 727–731.
83. Soria J.C., Smit E., Khayat D., Besse B., Yang X., Hsu C.P., Reese D., Wiezorek J., Blackhall F. // J. Clin. Oncol. 2010. V. 28. № 9. P. 1527–1533.
84. Soria J.C., Mark Z., Zatloukal P., Szima B., Albert I., Juhasz E., Pujol J.L., Kozielski J., Baker N., Smethurst D., et al. // J. Clin. Oncol. 2011. V. 29. № 33. P. 4442–4451.
85. Wainberg Z.A., Messersmith W.A., Peddi P.F., Kapp A.V., Ashkenazi A., Royer-Joo S., Portera C.C., Kozloff M.F. // Clin. Colorectal Cancer. 2013. V. 12. № 4. P. 248–254.
86. Cheah C.Y., Belada D., Fanale M.A., Janikova A., Czucman M.S., Flinn I.W., Kapp A.V., Ashkenazi A., Kelley S., Bray G.L., et al. // Lancet Haematol. 2015. V. 2. № 4. P. e166–174.
87. Camidge D.R., Herbst R.S., Gordon M.S., Eckhardt S.G., Kurzrock R., Durbin B., Ing J., Tohnya T.M., Sager J., Ashkenazi A., et al. // Clin. Cancer Res. 2010. V. 16. № 4. P. 1256–1263.

SUPPLEMENT Classification of the DR agonists being tested in clinical trials

Disease	Phase/Adjunct therapy	Patients	Clinical efficacy	Reference
Lexatumumab fully IgG1-kappa human monoclonal agonistic antibody directed against DR5				
Solid cancer tumors	I	24	Low	[53]
	I	32	Low	[70]
	Ib/gemcitabine, pemetrexed, doxorubicin, or FOLFIRI	41	No data	
Mapatumumab fully IgG1-kappa human monoclonal agonistic antibody directed against DR4				
Solid cancer tumors	I	49	Yes	
	I	41	No	[71]
	I/paclitaxel, carboplatin	27	No	[72]
NHL	Ib/II	40	Low	[57]
CRC	II	38	Low	[58]
Cervical cancer	Ib/II/cisplatin, gemcitabine	49	Yes	
NSCLC	II	32	Low	
	II/paclitaxel, carboplatin	100	No	[60]
HCC	II/sorafenib	101	In progress	[73]
MM	II/bortezomib (velcade)	105	No data	
Conatumumab (AMG 655) fully IgG1-kappa human monoclonal agonistic antibody directed against DR5				
Solid cancer tumors	I	37	Yes	[74]
	I/increased dose	18		[47]
	Ib/AMG 479 (IGF-IR antagonist)	108		
NSCLC	II/paclitaxel, carboplatin	150	No	[59]
Lymphoma	II/bortezomib, vorinostat	20	No	
Soft tissue sarcoma	I/doxorubicin	6		[75]
	II/doxorubicin	120	Low	
	II/FOLFOX6, bevacizumab, ganitumab		In progress	
CRC	II/FOLFIRI, ganitumab	155	Yes	[61]
	II/mFOLFOX, bevacizumab	180	No	[76]
	I, II/panitumumab	53	No	
Pancreatic cancer	II/gemcitabine	125	Low	[77]
Tigatuzumab (CS-1008) fully IgG1-kappa human monoclonal agonistic antibody directed against DR5				
Carcinoma	I	17	No	[78]
NSCLC	II/paclitaxel, carboplatin	97	No	[54]
Pancreatic cancer	II/gemcitabine	62	No	[62]
Breast cancer	II/paclitaxel	64	Low	[79]
HCC	II/sorafenib	163	No	[80]
CRC	I	19	Low	[81]
Metastatic breast cancer	II/abraxane		In progress	
Drozitumab fully IgG1-kappa human monoclonal agonistic antibody directed against DR5				
Metastatic colorectal cancer	I/mFOLFOX, bevacizumab		Low	[82]
Dulanermin (rhApo2L/TRAIL) pro-apoptotic receptor agonist				
Solid cancer tumors	I	58	Low	[63]
NSCLC	Ib/paclitaxel, carboplatin+bevacizumab	24		[83]
	II/paclitaxel, carboplatin+bevacizumab	213	No	[84]
CRC	Ib/FOLFOX6+bevacizumab	23	Yes	[85]
	II/FOLFOX6+bevacizumab		In progress	

NHL	Ib/rituximab	7	Yes	[86]
	II/rituximab	132	In progress	
PRO95780 fully IgG1-kappa human monoclonal agonistic antibody directed against DR5				
Solid cancer tumors	I	50	No	[87]
CRC	I/FOLFOX, bevacizumab	6		
NHL	I/rituximab	49	No data	
CRC	I/bevacizumab, cetuximab, FOLFIRI, irinotecan	23	No data	
Chondrosarcoma	II		In progress	
NSCLC	II/paclitaxel, carboplatin, bevacizumab	128	No data	
NSCLC – non-small cell lung cancer; NHL – non-Hodgkin lymphoma; CRC – colorectal cancer; HCC – hepatocellular carcinoma; MM – multiple myeloma				

Studying the Specific Activity of the Amide Form of HLDF-6 Peptide using the Transgenic Model of Alzheimer's Disease

A. P. Bogachouk[1]*, Z. I. Storozheva[2], G. B. Telegin[3], A. S. Chernov[3], A. T. Proshin[4], V. V. Sherstnev[4], Yu. A. Zolotarev, V. M. Lipkin[1]

[1]Shemyakin–Ovchinnikov Institute of Bioorganic Chemistry, Russian Academy of Sciences, Miklukho-Maklaya Str., 16/10, Moscow, 117997, Russia

[2]V. Serbsky Federal Medical Research Center of Psychiatry and Narcology, Ministry of Health, Kropotkinskiy Lane, 23, Moscow, 119034, Russia

[3]Branch of the Shemyakin–Ovchinnikov Institute of Bioorganic Chemistry, Russian Academy of Sciences, Nauki Ave., 6, Moscow oblast, 142290, Russia

[4]Anokhin Institute of Normal Physiology, Russian Academy of Sciences, Baltiyskaya Str., 8, Moscow, 125315, Russia

[5]Institute of Molecular Genetics, Russian Academy of Sciences, Kurchatov Sq., 2, Moscow, 123182, Russia

*E-mail:apbog@mx.idch.ru

Received: July 4, 2016; in final form, May 24, 2017

ABSTRACT **The neuroprotective and nootropic activities of the amide form (AF) of the HLDF-6 peptide (TGENHR-NH_2) were studied in transgenic mice of the B6C3-Tg(APPswe,PSEN1de9)85Dbo (Tg+) line (the animal model of familial Alzheimer's disease (AD)). The study was performed in 4 mouse groups: group 1 (study group): Tg+ mice intranasally injected with the peptide at a dose of 250 μg/kg; group 2 (active control): Tg+ mice intranasally injected with normal saline; group 3 (control 1): Tg- mice; and group 4 (control 2): C57Bl/6 mice. The cognitive functions were evaluated using three tests: the novel object recognition test, the conditioned passive avoidance task, and the Morris water maze. The results testify to the fact that the pharmaceutical substance (PhS) based on the AF of HLDF-6 peptide at a dose of 250 μg/kg administered intranasally efficiently restores the disturbed cognitive functions in transgenic mice. These results are fully consistent with the data obtained in animal models of Alzheimer's disease induced by the injection of the beta-amyloid (βA) fragment 25-35 into the giant-cell nucleus basalis of Meynert or by co-injection of the βA fragment 25-35 and ibotenic acid into the hippocampus, and the model of ischemia stroke (chronic bilateral occlusion of carotids, 2VO). According to the overall results, PhS based on AF HLDF-6 was chosen as an object for further investigation; the dose of 250 μg/kg was used as an effective therapeutic dose. Intranasal administration was the route for delivery.**

KEYWORDS **Differentiation factor HLDF, amide form of HLDF-6 peptide, neuroprotective and nootropic activities, Alzheimer's disease, transgenic mice.**

ABBREVIATIONS **HLDF – human leukemia differentiation factor; AF – amide form; NF – native form; AD – Alzheimer's disease; IS – ischemic stroke; PhS – pharmaceutical substance; βA – beta-amyloid.**

INTRODUCTION

Cerebrovascular and neurodegenerative diseases, the major cause of mortality and disability in Russia and worldwide, are among the current medical social problems ranking high on the agenda. The most common disorder, Alzheimer's disease (AD), is a neurodegenerative disorder diagnosed in almost 44 million people [1]. AD progresses slowly but inevitably results in dysfunction of the key organ, the brain, and a number of other systems of the human body. Alzheimer's disease has been recognized as one of the major four medical social issues of contemporary society.

Ischemic stroke (IS) is one of the most severe cerebrovascular diseases. More than 15 million stroke cases are reported annually [2], including over 450,000 cases in Russia. Adverse side effects, tolerance, and lack of effectiveness are the significant drawbacks of the drugs used to manage AD and IS that substantially narrow their application. All these factors call for urgent measures: elaborating and launching into clinical

practice novel effective drugs for the prevention and treatment of these diseases.

In 1994, we discovered the human leukemia differentiation factor (HLDF) and isolated it from a culture medium of HL-60 cells treated with retinoic acid [3]. The six-membered fragment TGENHR (HLDF-6 peptide), which totally reproduces the differentiation activity of the full-length factor and exhibits a broad range of nootropic and neuroprotective activities, was identified when studying HLDF. Direct evidence to the neuroprotective effect of HLDF-6 peptide was obtained for a primary culture of hippocampal and cerebellar neuronal cells, as well as immunocompetent cells. This peptide exhibits an anti-apoptotic activity and protects cells against beta-amyloid (βA) peptide, sodium azide, ceramide, ethanol, cold stress, and hypoxia. HLDF-6 peptide enhances the viability of early mouse embryos *in vitro* [4–7].

An evaluation of the effect of HLDF-6 peptide using various experimental animal models (the Morris water maze, the passive avoidance, delayed matching to position, and the recognition memory tests) demonstrated that central and systemic administration of the peptide to healthy animals enhances the formation and storage of long-term memory. The peptide was shown to eliminate the pronounced cognitive deficit in experimental models of clinical pathology (AD and IS) and to contribute to the restoration of the disturbed memory [8, 9]. The administration of HLDF-6 to animals with chronic cerebral ischemia ensures a reliable neuroprotective effect as it protects cerebral neurons against death in ischemic conditions [10].

Investigation of the pharmacokinetics of HLDF-6 peptide has demonstrated that the peptide is extremely unstable in an animal organism: its half-life in rat plasma is 2 min. HLDF-6 is hydrolyzed starting at its C-end; dicarboxypeptidases make a major contribution to it [11]. Amidation of the C-terminal carboxylic group was used to protect the peptide against dicarboxypeptidases. The half-life of the amide form (AF) of HLDF-6 peptide (TGENHR-NH_2) in rat plasma was shown to be 8 min, significantly higher than that of the native form (NF) of the peptide (TGENHR-OH) [12].

In order to choose the most effective form of HLDF-6 peptide for its investigation as a pharmacological substance (PhS), we conducted an extended comparative study of the neuroprotective and nootropic activities of FS samples based on the AF and NF of HLDF-6 peptide in animal models of AD and IS. At the first stage, we revealed the neuroprotective and nootropic activities of the PhS based on HLDF-6 peptide in models of sporadic Alzheimer's disease. The models used were as follows: a) cognitive deficit induced by injection of beta-amyloid 25–35 fragment to the giant-cell nucleus basalis of Wistar rats; b) cognitive deficit induced by co-injection of beta-amyloid 25–35 fragment and ibotenic acid to the hippocampus of Wistar rats. A comparative analysis of the data obtained using both AD models demonstrated that the neuroprotective effect of the AF of HLDF-6 peptide evaluated from the degree of restoration of the disturbed cognitive function was significantly higher than that of the NF of peptide. An almost complete function restoration was observed when using the AF of HLDF-6 peptide at a dose of 250 μg/kg (a much lower dose than those of comparator agents) [12].

We report on the results of a study of the specific activity of PhS based on the AF of HLDF-6 peptide using a transgenic model of AD. The transgenic model was used in accordance with the Guidelines for Preclinical Studies of Nootropic Drugs [13].

Alzheimer's disease is a neurodegenerative disorder characterized by cognitive impairment and dementia. The familial and sporadic forms of AD are differentiated. Familial AD has an autosomal dominant inheritance pattern. In 1991, the first gene causing familial AD was identified: the mutant gene of the amyloid precursor protein (APP) residing in chromosome 21 [14]. Mutations in other genes that increase the risk of AD were detected later. Among the products of these genes, the strongest effect was observed for presenilin-1, which is responsible for 70–80% of early-onset familial AD cases, with its gene residing in chromosome 14 [15]. The creation of transgenic animals allows one to simulate the molecular processes of AD development during the entire life of an organism. The key advantage of the transgenic model is that insertion of human genes coding for the development of familial AD (the *APP* and presenilin genes) to animals results in the development of pathogenetic processes in the animals that are similar to manifestations of AD in humans (amyloid plaque formation, oxidative stress, disruption of cholinergic transmission, and neuronal death). This provides grounds for suggesting that the processes taking place in the central nervous system of the model animals are similar to those occurring during the development of AD in humans. The so-called B6C3-Tg(APPswe,PSEN1de91)85Dbo double transgenic mice are the best choice for studying potential drugs [16]. Animals of this line express the mutant human presenilin and chimeric mouse/human amyloid protein. A typical feature of this line is early (at the age of 6 or 7 months) development of an Alzheimer-like pathology caused by accelerated βA deposition and cognitive impairment in the brain, which is evaluated using spatial learning tests [17, 18].

Our study aimed to evaluate the neuroprotective and nootropic activities of the AF of HLDF-6 peptide in

B6C3–Tg(APPswe,PSEN1de91)85Dbo transgenic mice, an animal model of familial AD.

EXPERIMENTAL

Synthesis of the AF of HLDF-6 peptide

The AF of the peptide was synthesized according to the procedure described in [12].

Experimental animals

Healthy male B6C3-Tg(APPswe,PSEN1de9)85Dbo (Tg+) mice, wild-type B6C3 (Tg-) mice, and C57Bl/6 mice were used. Eight-month-old mice weighing 28–35 g were obtained from the laboratory animal breeding nursery of the Pushchino Branch of the Institute of Bioorganic Chemistry (Russian Academy of Sciences) that has earned international AAALACi accreditation. The quality control system for the production of laboratory animals has been certified to comply with the international standard requirements ISO 9001:2008. All the experiments using animals were conducted in accordance with the Guidelines for Good Laboratory Practice of the Russian Federation (Order no. 708n of the Ministry of Healthcare and Social Development of the Russian Federation dated August 23, 2010, Moscow, "On Approval of the Guidelines for Good Laboratory Practice") and with the recommendations provided in the Guidelines for Preclinical Studies of Nootropic Drugs [13]. The mice were divided into four groups, with 10 mice per group: group 1 (experimental group) included Tg+ mice that intranasally received the PhS at a dose of 250 μg/g; group 2 (active control) consisted of Tg+ mice that intranasally received normal saline; group 3 (control 1) consisted of Tg- mice that intranasally received normal saline; and group 4 (control 2) included C57Bl/6 mice that intranasally received normal saline. The additional control group was used because several models of cognitive function were included in the experiment. An analysis of published data demonstrates that the learning and memory features in B6C3-Tg(APPswe,PSEN1de9)85Dbo mice have been evaluated mostly using spatial learning tests, while the other cognitive models have been studied insufficiently [18, 19]. The findings obtained using the spatial learning tests demonstrate that the differences between B6C3-Tg+ and B6C3-Tg- mice are most pronounced in models exposed to a high stress level (e.g., in the Morris water maze rather than in the Barnes maze test) [20]. Meanwhile, the differences between B6C3-Tg+ and B6C3-Tg- mice were detected mostly in models with positive rather than negative reinforcement [21]. The cognitive abilities of B6C3-Tg- also have not been fully characterized. In this context, we deemed it reasonable to use the group of additional control to evaluate the validity of the experimental protocols. This group consisted of C57Bl mice that had an appreciably high level of orientational and exploratory activity and stress resistance [22] and near-average cognitive abilities [23].

No comparator drug was used, since the action of clinically effective agents (memantine, donepezil, etc.) for this model is still being tested in pilot studies and has not been characterized sufficiently well [24, 25].

Protocols of PhS administration and testing of the cognitive functions

Group 1 animals intranasally received the AF of the peptide at a dose of 250 μg/kg (10 μL/kg) in each nostril every other day for 30 days (a total of 15 injections). Group 2–4 animals received normal saline according to the same scheme. The cognitive function was assessed after the injections had been completed using the following scheme: days 3–5, the novel objection recognition test; days 8–10, the passive avoidance test; and days 13–17, the Morris water maze test.

Novel object recognition test

The novel object recognition test was conducted in a 35 × 35 × 40 cm chamber made of gray plastic under room light. The test consisted of three five-minute sessions separated by a 24 h interval: 1 – without objects to allow a mouse to adapt to the apparatus; 2 – with two equal objects: metal cylinders 3 cm in diameter and 3 cm high; 3 – one of the cylinders was replaced with a plastic cube (3 cm edge length). Animal behavior was recorded using a digital video camera and analyzed using the EthoVision XT software (Noldus). The levels of orientational and exploratory activity were assessed when the mice were exploring the objects for the first time (session 2) and when exploring the "familiar" and the "novel" objects in session 3. The recognition index was calculated using the formula $(T_n - T_f / T_n + T_f) \times 100\%$, where T_n is the exploration time of the novel object, and T_f is the exploration time for the familiar object during session 3 [26–28].

Passive avoidance test

The passive avoidance test was conducted in an apparatus manufactured by Columbus Instruments (USA). The experimental chamber consisted of two identical compartments 25 × 40 × 25 cm in size with a grid-metal floor. The compartments were connected through a hole in the common wall (8 × 8 cm) equipped with guillotine doors. One of the compartments was lit, while the other one was dark. During passive avoidance training, an animal was placed into the lit compartment and the latency prior to it entering the dark compartment (emergence of the hole reflex) was recorded. Immediately after all four paws of the animal were in the dark side of the chamber, the compartments were separat-

ed by the guillotine doors. The mouse was subjected to electrocutaneous irritation through the floor grid (0.6 mA, 3 s), then it was immediately taken out of the chamber and placed into its home cage. The acquired response was tested 48 h after it had been established. The mouse was placed into the lit compartment again, and the latency prior to it entering the dark side was measured [29–31].

Morris water maze test

The Morris water maze was a circular gray pool 165 cm in diameter, with walls 60 cm high, filled with water to a level of 40 cm. A round plexiglass platform 9 cm in diameter was submerged 2 cm below the water level in the center of one of the sectors. The pool was placed in a stimulus-rich environment (posters, cabinets, etc.), without any key stimuli located above the platform. During the training session, the animals were placed in water at four different locations and the time taken to reach the platform was recorded. Once the animal had reached the platform, it was left there for 15 s and then returned back into its home cage for 2 min. Training was performed during 5 days [18].

Statistical analysis

Statistical analysis of the results was carried out using the nonparametric Mann–Whitney test. The STATISTICA 6.0 software was used for the analysis.

Parameters of orientation and exploratory activity of mice in different groups in the novel object recognition test

Animal group	Total object exploration time during the testing phase (test day 2), s			*Z* values (standardized Mann–Whitney U-test) and significance of intergroup differences
	Lower quartile	Median	Upper quartile	
1. Tg+ with PhS injected	10.2	13.4	17.4	#$Z = 0.22$, $p = 0.83$ *$Z = 1.55$, $p = 0.12$
2. Tg+ with normal saline injected	7.7	12.3	14.1	*$Z = 2.41$, $p = 0.0156$
3. Tg- with normal saline injected	15.4	16.0	17.3	&$Z = 1.06$, $p = 0.29$
4. C57Bl with normal saline injected	10.1	16.6	20.2	

– Statistical significance of the difference from group 2.
* – Statistical significance of the difference from group 3.
& – Statistical significance of the difference from group 4.

RESULTS AND DISCUSSION

Novel object recognition test

Exploration of objects during the testing session (*Table*) showed no differences in orientational and exploratory activity between the Tg- and C57Bl/6 control groups. Meanwhile, the animals in the active control group (Tg+ with normal saline injection) showed a significantly lower exploratory activity than that in the Tg- group. The study group animals differed significantly from neither the active control group nor Tg- mice. Appreciably high object recognition indices characterizing explicit long-term memory related to the function of the parahippocampal cortex (the region of the middle temporal gyrus) in C57Bl/6 mice were revealed; these indices were comparable to the published data [32]. The recognition index was significantly decreased in animals of the control group Tg- vs the C57Bl/6 group and in active control group mice vs. the Tg- control group mice. Injection of the peptide-based PhS restored the recognition index to a level higher than the values both in the active control and the Tg- groups (*Fig. 1*).

Passive avoidance model

No statistically significant intergroup difference in latency prior to entering the dark compartment was detected on training day before the mice were subjected to electrocutaneous irritation.

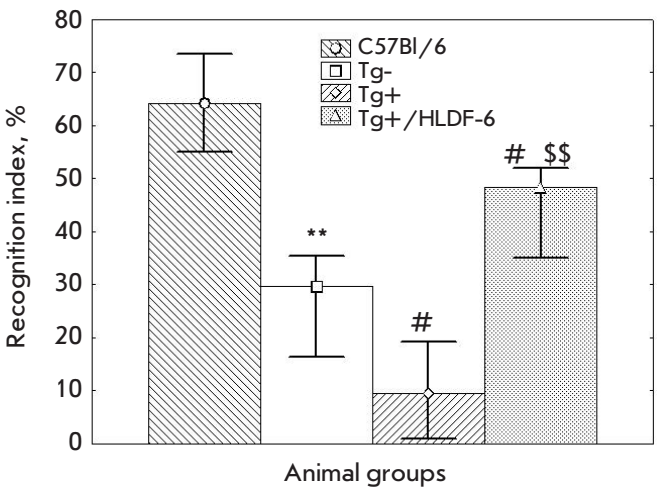

Fig. 1. Indices of long-term memory in the model of object recognition test in mice of different groups. The data are presented as the median, the upper, and lower quartiles. * – $p<0.05$, ** – $p<0.01$ compared to the C57Bl/6 group; # – $p < 0.05$ compared to the Tg- group; and $$ – $p<0.01$ compared to the Tg+ group.

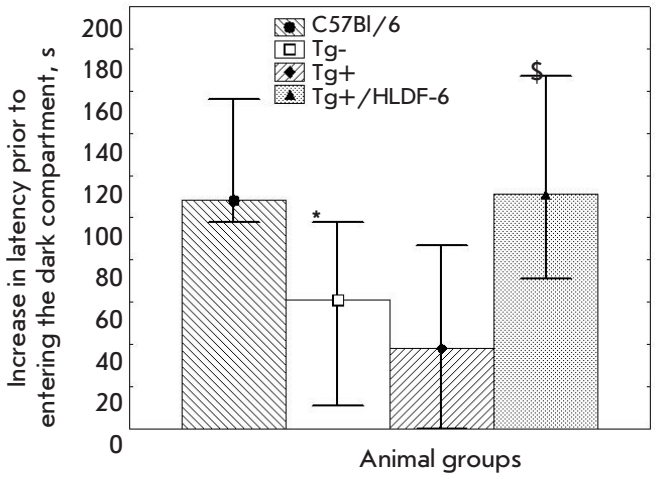

Fig. 2. Indices of learning in the passive avoidance test in mice of different groups. Y-axis – the increase in latency prior to entering the dark compartment at the training session compared to the testing one (s). The data are presented as the median, the upper, and lower quartiles. * – $p<0.05$ compared to the C57Bl/6 group and $ – $p<0.05$ compared to the Tg+ group.

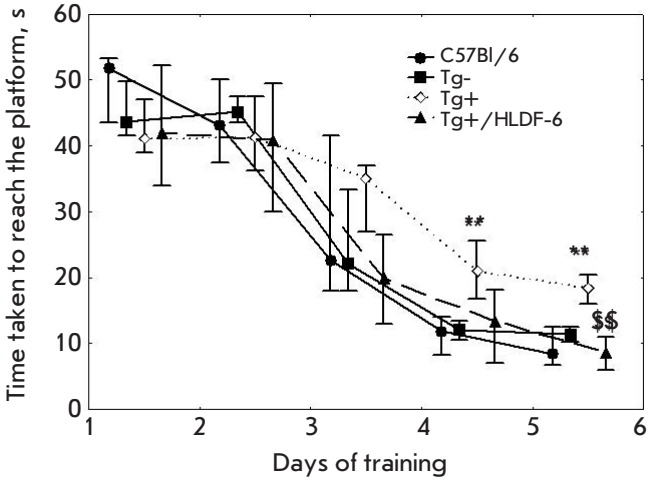

Fig. 3. The dynamics of Morris water maze training of mice. The data are presented as the median, the upper, and lower quartiles. ** – $p<0.01$ compared to the Tg- group; $$ – $p<0.01$ compared to the Tg+ group.

Meanwhile, a significant intergroup difference in the increase in latency prior to entering the dark compartment was revealed on testing day, which characterized long-term memory (*Fig. 2*).

A statistically significant difference in the increase in latency prior to entering the dark compartment on testing day characterizing long-term memory was revealed neither in the control C57Bl/6 and Tg- groups nor between the active control and the Tg- group. The animals that had received PhS were significantly superior to the active control group and showed a tendency ($p = 0.062$) to be superior to the Tg- group.

Spatial memory in the Morris water maze model

The average latency to reach the platform on training days 2–5 was an index of long-term memory in this model. The results are shown in *Fig. 3*.

A statistically significant difference between the control (C57Bl/6 and Tg-) groups was revealed by the Mann–Whitney test in none of the training days. The Tg+ animals that had been injected with normal saline showed a significant spatial memory deficit on training days 4 and 5 compared to the Tg- group. Administration of PhS partially restored spatial memory in Tg+ mice. On training day 4, the maze performance was intermediate with respect to that in Tg+ animals that had received normal saline and Tg- animals. On training day 5, the Tg+ mice that had been injected with PhS performed the task much better than the Tg+ group injected with normal saline, while showing no significant difference with respect to the control group Tg-.

CONCLUSIONS

Hence, the results demonstrate that PhS based on the AF of HLDF-6 at a dose of 250 μg/kg delivered intranasally effectively stimulated the performance of cognitive tasks by transgenic B6C3-Tg(APPswe,PSEN1de9)85Dbo mice in all the tests used. It is noteworthy that the results obtained in the additional control group of C57Bl/6 mice verify the validity of the models of cognitive functions used in our study. In the model of spatial acquisition in an enriched environment (the Morris maze), the dynamics of training of the control Tg- group did not differ from that among C57Bl/6 mice. In the active control group, the dynamics of spatial acquisition was reduced compared to that in the Tg- group, while administration of PhS had a pronounced neuroprotective effect and restored the indices of spatial acquisition to their control level.

In the novel object recognition test, the learning parameters in the Tg- group significantly decreased compared to those in the C57Bl/6 group; a less pronounced reduction was also observed in the active control group with respect to the Tg- group. Administration of PhS increased the learning index to a level exceeding that in the Tg- group.

A decrease in the learning indices in the Tg- group with respect to the C57Bl/6 group was also observed in the passive avoidance test. However, unlike in oth-

er tests, the learning ability in animals in the active control group was not worse compared to that in the Tg- group. Like in other models, administration of PhS stimulated long-term memory in transgenic mice up to a level that was even somewhat higher than that in the control groups.

A combination of the results indicates that PhS based on the AF of HLDF-6 peptide has both neuroprotective and nootropic properties; i.e., it stimulates the cognitive function regardless of whether there is a neurodegenerative process or not.

The results of our study are fully consistent with the data obtained for animal models of AD: the βA fragment (25–35) was injected into the giant-cell nucleus basalis of Meynert or the βA fragment and ibotenic acid were co-injected into the hippocampus [12]. According to the overall results, PhS based on the AF of HLDF-6 was chosen as an object for further clinical studies; the dose of 250 μg/kg was used as an effective therapeutic dose. Intranasal administration was the route for delivery.

We had previously studied the contribution of serotonin, GABA, and NMDA glutamate brain receptors to the nootropic effect of the AF form of HLDF-6 peptide by radioreceptor assay. These receptors are involved in the pathogenesis of various neurological disorders and chronic neurodegenerative diseases [33, 34]. The effect of the AF of HLDF-6 peptide on the parameters of binding between radiolabeled ligands and NMDA receptors on hippocampal membranes and between GABA-A and $5HT_{2A}$ serotonin receptors on the membranes of the prefrontal cortex in BALB/c mice was investigated. Subchronic injection of the peptide into the murine hippocampus was shown to increase the amount of the ligand (G-3H MK-801) that bound [11] only for the NMDA glutamate receptors, an indication of the density of the corresponding receptors. Hence, the AF of HLDF-6 peptide restores the amount of NMDA receptors to its normal level, thus improving cognitive behavior. Subchronic fivefold injection of the AF of HLDF-6 peptide had no effect on the densities of GABA receptors and nicotinic cholinoreceptors but was accompanied by a decrease in the density of $5\text{-}HT_2$ serotonin receptors [35]. A conclusion was drawn that the mechanism of formation of the neuroprotective activity of Thr-Gly-Glu-Asn-His-Arg-NH_2 peptide may involve an effect on the glutamate and serotoninergic systems.

HLDF-6 peptide is a fragment of the natural differentiation factor HLDF-6 that is present in blood and the central nervous system of mammals and humans. The preclinical studies of the pharmaceutical substance based on the AF of HLDF-6 peptide have demonstrated that it is satisfactorily soluble, easily metabolized, nonimmunogenic and nontoxic, characterized by a high effectiveness of specific activity, and safe at a dose tenfold higher than the therapeutic dose. The results of preclinical studies provide grounds to hope that the pharmaceutical substance will successfully pass clinical trials. In this case, one can anticipate that the agent will become widely used in the therapy of AD.

This work was supported by the Ministry of Education and Science of the Russian Federation (Government Contract no. 14N08.11.0002) and the Program of the Presidium of the Russian Academy of Sciences "Molecular and Cellular Biology."

REFERENCES

1. Prince M., Albanese E., Guerchet M., Prina M. // World Alzheimer Report. 2014. Website www.alz.co.uk/worldreport.
2. Feigin V.L., Forouzanfar M.H., Krishnamurthi R., Mensah G.A., Connor M., Bennett D.A., Moran A.E., Sacco R.L, Anderson L., Truelsen T., et al. // Lancet. 2010. V. 383. № 9913. P. 245–255.
3. Kostanyan I.A., Astapova M.V., Starovoytova E.V., Dranitsyna S.M., Lipkin V.M. // FEBS Lett. 1994. V. 356. № 2–3. P. 327–329.
4. Kostanyan I.A., Astapova M.V., Navolotskaya E.V., Lepikhova T.N., Dranitsyna S.M., Telegin G.B., Rodionov I.L., Baidakova L.K., Zolotarev Yu,F., Molotkovskkaya I.M., Lipkin V.M. // Russ. J. Bioorg. Chem. 2000. V. 26. № 7. P. 450–456.
5. Sakharova N.Yu., Kostanyan I.A., Lepikhova T.N., Lepikhov K.F., Navololtskaya T.V., Malashenko A.M., Tombran-Tink J., Lipkin V.M., Chailakhayn A.M. // Doklady Biochemistry. 2000. V. 372. № 1. P. 84–86.
6. Rzhevsky D.I., Zhokhov S.S., Babichenko I.I., Goleva A.V., Goncharenko E.N., Baizhumanov A.A., Murashev A.N., Lipkin V.M., Kostanyan I.A. // Regul. Peptides. 2005. V. 127. № 1. P. 111–121.
7. Kostanyan I.A., Zhokhov S.S., Storozheva Z.I., Proshin A.T., Surina E.A., Babichenko I.I., Sherstnev V.V, Lipkin V.M. // Russ. J. Bioorg. Chem. 2006. V. 32. № 4. P. 360–367.
8. Sewell R.D., Gruden M.A., Pache D.M., Storozheva Z.I., Kostanyan I.A., Proshin A.T., Yurashev V.V., Sherstnev V.V. // J. Psychopharmacol. 2005. V. 19. № 6. P. 602–608.
9. Storozheva Z.I., Proshin A.T., Zhokhov S.S., Sherstnev V.V., Rodionov I.L. Lipkin V.M., Kostanyan I.A.// B. Exp. Biol. Med. 2006. V. 141. № 3. P. 319–322.
10. Kostanyan I.A., Storozheva Z.I., Semenova N.A., Lipkin V.V. // Doklady Biological Sciences. 2009. V. 428. № 4. P. 418–422.
11. Zolotarev Yu.A., Kovalev G.I., Dadayan A.K. Kozik V.S., Kohlrahin E.A., Vasilieva E.V., Lipkin V.M. In: Ugrumov M.V. (ed) Neurodegenerative diseases: from genome to the whole organism. Moscow. Scientific World. 2014. V. 2. P. 763–777.

12. Bogachouk A.P., Storozheva Z.I., Solovjeva O.A., Sherstnev V.V., Zolotarev Yu.A., Azev V.N., Rodionov I.L., Surina E.A., Lipkin V.M. // J. Psychopharmacol. 2016. V. 30. № 1. P. 78–92.
13. Bunyatyan N.D., Mironov A.N., Vasilieva A.N., Verstakova O.L., Zhuravleva M.M., .Lepakhin V.K., Korobov N.V., Merkulov V.A., Orekhov S.N., Sakaeva I.V., et al. //. Guide line for preclinical study of remedies. Moscow. Grif and K. 2012. 942 p.
14. Goate A., Chartier-Harlin M.C., Mullan M., Brown J., Crawford F., Fidani L., Giuffra L., Haynes A., Irving N., James L., et al. // Nature. 1991. V. 349. № 6311. P. 704–706.
15. Selkoe D.J. // Nature. 1999. V. 399. (6738 suppl.). P. A23–A31.
16. Jankowsky J.L., Slunt H.H., Ratovitski T., Jenkins N.A., Copeland N.G., Borchelt D.R. // Biomol. Eng. 2001. V. 17. № 6. P. 157–165.
17. Su D., Zhao Y., Xu H., Wang B., Chen X., Chen J., Wang X. // PLoS One. 2012. V. 7. № 11. e50172.
18. McKenna J.T., Christie M.A., Jeffrey B.A., McCo J.G., Lee E., Connolly N.P., Ward C.P., Strecker R.E. // Arch. Ital. Biol. 2012. V. 150. № 1. P. 5–14.
19. Zhong Z., Yang L., Wu X., Huang W., Yan J., Liu S., Sun X., Liu K., Lin H., Kuang S., Tang X. // J. Mol. Neurosci. 2014. V. 53. № 3. P. 370–376.
20. Bennett L., Kersaitis C., Macaulay S.L., Münch G., Niedermayer G., Nigro J., Payne M., Sheean P., Vallotton P., Zabaras D., Bird M. // PLoS One. 2013. V. 8. № 10. e76362.
21. Semina I.I., Baichurina A.Z., Makarova E.A., Leushina A.V., Kazakevich Zh.V., Gabdrakhmanova M.R., Mukhamed'yarov M.A., Zefirov A.L. // Bull. Exp. Biol. Med. 2015. V. 158. № 5. P. 621–623.
22. Kovaljov G.I., Kondrahin E.A., Salimov R.M. // J. Neurochemical. 2013. V. 7. № 2. P. 121–127.
23. Brooks S.P., Pask T., Jones L., Dunnett S.B. // Genes Brain Behav. 2005. V. 4. № 5. P. 307–317.
24. Neumeister K.L., Riepe M.W. // J. Alzheimers Dis. 2012. V. 30. № 2. P. 245–251.
25. Nagakura A., Shitaka Y., Yarimizu J., Matsuoka N. // Eur. J. Pharmacol. 2013. V. 703. № 1–3. P. 53–61.
26. Rutten K., Reneerkens O.A., Hamers H., Sik A., McGregor I.S., Prickaerts J., Blokland A. // J. Neurosci. Meth. 2008. V. 171. № 1. P. 72–77.
27. Nimmrich V., Szabo R., Nyakas C., Granic I., Reymann K.G., Schröder U.H., Gross G., Schoemaker H., Wicke K., Möller A., Luiten P. // J. Pharmacol. Exp. Ther. 2008. V. 327. № 2. P. 343–352.
28. Zhang R., Xue G., Wang S., Zhang L., Shi C., Xie X. // J. Alzheimers Dis. 2012. V. 31. № 2. P. 801–812.
29. Harkany T., O'Mahony S., Kelly J.P., Soós K., Törõ I., Penke B., Luiten P.G., Nyakas C., Gulya K., Leonard B.E. // Behav. Brain Res. 1998. V. 90. № 2. P. 133–145.
30. Xu Z., Zheng H., Law S.L., Dong So D., Han Y., Xue H. // J. Pept. Sci. 2006. V. 12. № 1. P. 72–78.
31. Feng Z., Chang Y., Cheng Y., Zhang B.L., Qu Z.W., Qin C., Zhang J.T. // J. Pineal. Res. 2004. V. 37. № 2. P. 129–136.
32. Tucker K.R., Godbey S.J., Thiebaud N., Fadool D.A. // Physiol. Behav. 2012. V. 107. № 3. P. 3424–3432.
33. Walker DL and Davis M. 2002. Pharmacol Biochem Behav V. 71 № 3. P. 379–392.
34. Zhong Z., Yang L., Wu X., Yuang W., Yan J., Liu S., Sun X., Liu K, Lin H., Kuang S., Tang X. // J. Mol. Neurosci. 2014. V. 53. № 3. P. 370–376.
35. Zolotarev Yu.A., Kovalev G.I., Kost N.V., Voevodina M.E., Sokolov O.Y., Dadayan A.K., Kondrakhin E.A., Vasilev E.V., Bogachuk A.P., Azev V.N., et al. // J. Psychopharmacol. 2016. V. 30. № 9. P. 922–935.

Change in the Content of Immunoproteasomes and Macrophages in Rat Liver At the Induction of Donor-Specific Tolerance

Ya.D. Karpova[1]*, V.D. Ustichenko[2], N.M. Alabedal'karim[2], A.A. Stepanova[1], Yu.V. Lyupina[1], K.I. Boguslavski[2], G.A. Bozhok[2], N.P. Sharova[1]

[1]N.K. Koltsov Institute of Developmental Biology, Russian Academy of Sciences, Vavilov Str. 26, Moscow, 119334, Russia

[2]Institute of Problems in Cryobiology and Cryomedicine, National Academy of Sciences of Ukraine, Pereyaslavskaya Str. 23, Kharkov, 61016, Ukraine

*E-mail: yasiiik@gmail.com

Received: August 27, 2016; in final form June 02, 2017

ABSTRACT **Induction of donor specific tolerance (DST) by the introduction of donor cells into a recipient's portal vein is one of the approaches used to solve the problem of transplant engraftment. However, the mechanism of DST development remains unclear to this moment. In the present work, we first studied the change in the content of immunoproteasomes and macrophages of the liver at early stages of the development of allospecific portal tolerance in rats by Western blotting and flow cytofluorimetry. On the basis of the data obtained, we can conclude that the induction of DST is an active process characterized by two phases during which the level of the proteasome immune subunits LMP2 and LMP7 in liver mononuclear cells, including Kupffer cells, and the number of Kupffer cells change. The first phase lasts up to 5 days after the beginning of DST induction; the second phase – from 5 to 14 days. In both phases, the level of the subunits LMP2 and LMP7 in the total pool of mononuclear cells and Kupffer cells increases, with maximum values on days 1 and 7. In addition, the total number of Kupffer cells increases in both phases with a shift in several days. The most noticeable changes take place in the second phase. The third day is characterized by a lower content of mononuclear cells expressing immunoproteasomes compared to the control value in native animals. Presumably, at this time point a "window of opportunity" appears for subsequent filling of an empty niche with cells of different subpopulations and, depending on this fact, the development of tolerance or rejection. The results obtained raise the new tasks of finding ways to influence the cellular composition in the liver and the expression of immunoproteasomes on the third day after the beginning of DST induction to block the development of rejection.**

KEYWORDS **immunoproteasomes, donor specific tolerance, liver, Kupffer cells, rats, flow cytofluorimetry.**

ABBREVIATIONS **MHC – major histocompatibility complex; DST – donor specific tolerance; APC – antigen presenting cells; LSEC – liver sinusoid endothelial cells; Ab – antibodies; pAb – polyclonal antibodies; mAb – monoclonal antibodies.**

INTRODUCTION

The problem of transplant engraftment remains one of the concerns in transplantology. Transplantation is used in terminal organ failures, when other methods of treatment have proved ineffective. Allogenic transplantation activates the immune response, which leads to transplant rejection. Modern immunosuppressive protocols are not always able to prevent rejection. Therefore, it is necessary to search for other approaches to induce tolerance to transplants in recipients.

The critical role of the liver in the development of transplant tolerance has been known for a long time. Spontaneous liver allotransplant engraftment in recipients mismatched from donors by the major histocompatibility complex (MHC) was revealed for outbred pigs [1], inbred lineages of mice [2], and rats [3]. Combined transplantation of the liver and other organs led to better engraftment than when using single allografts [4–6].

Another key factor involved in the induction of transplant tolerance is the presence of immunocompe-

tent cells of donor origin within the liver. This is supported by studies showing that allograft tolerance is not induced after depletion of passenger leukocytes from the donor liver [7–9].

The method of inducing donor-specific tolerance (DST) is based on adherence to these two conditions. The induction is performed by transfusion of donor cells (splenocytes, lymphocytes, bone marrow cells) into the liver via the portal vein. This method leads to significant lifespan extension of allografts of the heart [10], kidneys [11], intestine [12], skin [13], pancreatic islets [14], and trachea [15] in experimental models. However, the molecular-cellular mechanisms of induction and maintenance of DST have not been elucidated, although many researchers stress the significant contribution of hepatic macrophages (Kupffer cells) [16, 17].

Multiple forms of immunoproteasomes that contain the immune subunits LMP2, LMP10, and/or LMP7 with proteolytic activities have been regarded as potential candidates for the role of messengers of immune response, which can direct the immune response either toward allograft acceptance or rejection. Immunoproteasomes participate in the formation of antigenic epitopes for the MHC molecules, the regulation of the expression of co-stimulatory molecules on antigen-presenting cells (APCs), and the differentiation of T-lymphocyte subpopulations [18–21].

We have found previously that the proportion of LMP2 and LMP7 immunoproteasome subunits changes in the liver and allografts of ovaries and thyroid after the induction of DST [22, 23]. Allograft engraftment was accompanied by a significant increase in the quantity of liver mononuclear cells expressing the immunoproteasome subunit LMP2 on the 30th day after DST induction.

Previous experimental and clinical studies have shown that induction of DST fails in some cases [24, 25]. Moreover, 7–15% of recipients develop sensitization to donor antigens [26, 27]. Since the definite mechanism of DST induction is not yet known, it is impossible to predict the vector of the immune response as either transplant acceptance or rejection. This decreases the value of this method and restricts its use in clinical transplantology.

It is evident that the immunological events occurring in the liver of a recipient immediately after the administration of donor cells and that are related to the recognition and presentation of antigen can determine the development of tolerance. Therefore, the study of the cascade of cell-mediated reactions and the change in the pool of proteasomes at early stages after the administration of a donor antigen is important for understanding the mechanism underlying DST induction.

The aim of this study was to evaluate the level of immunoproteasomes and the quantity of resident macrophages in a rat liver in the first two weeks after the beginning of DST induction.

MATERIALS AND METHODS

Reagents

DMEM medium, collagenase and DNAse I (all manufactured by Sigma, USA), percoll (Pharmacia, Sweden), saponin (Calbiochem, USA), rabbit pAb to subunit LMP7, mouse mAb to subunit LMP2 (both manufactured by Biomol International, United Kingdom), phycoerythrin-conjugated mouse mAb to macrophages (Anti-Rat Macrophage Marker, eBioscience, USA), mouse mAb to β-actin (Santa Cruz Biotechnology, USA), Alexa 488-labeled anti-rabbit IgG (Invitrogen, USA), phycoerythrin-conjugated anti-mouse IgG (eBioscience, USA) were used in this study.

Animals

The experiments were performed using 5- to 6-month-old Wistar and August female rats. The donors were Wistar rats, and the recipients were August rats. All manipulations with the animals were performed in compliance with the European Convention for the Protection of Vertebrate Animals used for Experimental and Other Scientific Purposes (Strasbourg, 1985). For the experiments, the following groups of animals were used: group 1 (n = 12) – intact control; group 2 (n = 48) – false-operated animals (an intraportal infusion of a physiological solution); and group 3 (n = 48) – animals with DST induction (an intraportal administration of splenocytes); group 4 (n = 30) – animals with DST disruption (an intraperitoneal injection of gadolinium chloride $GdCl_3$ (1 mg/100 g of body mass) and an intraportal administration of splenocytes after 24 h).

Isolation of splenocytes and induction of DST

All the procedures were performed under sterile conditions. Splenocytes were collected from the spleen of the Wistar rats according to a standard protocol [28]. Erythrocytes were removed through a three-time treatment of a cell suspension with a solution containing 154 mM of ammonium chloride, 10 mM sodium bicarbonate, and 0.082 mM ethylenediamine tetraacetic acid (EDTA). The collected cells were washed two times with a DMEM medium. The average vitality of the splenocytes, assessed with trypan blue staining, was around 90%. DST was induced by administration of 1 ml of a sterile physiological solution containing 1×10^7 splenocytes into the hepatic portal vein. The liver was studied on the 1st, 3rd, 5th, 7th, 10th, and 14th days after induction.

Isolation of liver mononuclear cells

The rat liver was perfused via the portal vein with a calcium-free buffer (5 mM EDTA per 0.1 M phosphate buffer saline, pH 7.4) for 5 min. The liver was then extracted and perfused with 0.1 M phosphate buffer saline containing 0.4 mg/ml collagenase, 3.7 M $CaCl_2$, 25 ng/ml DNAse I, and 5 mM $MgCl_2$ (pH 7.4) at 37°C for 10 min. Afterwards, the tissue was grinded with scissors and further incubated in collagenase buffer at 37°C for 30 min, disintegrated through pipetting, filtered through a nylon sieve, and centrifuged at 20 *g* at 4°C for 2 min. The supernatant was collected and centrifuged at 400 *g* for 3 min. The pellet of cells was resuspended in 30% percoll and centrifuged at 400 *g* for 30 min at 4°C. The cells were collected from the interface and washed two times with 0.1 M phosphate buffer saline at 4°C.

Phenotypical analysis of the cells using flow cytofluorimetry

In order to identify subunits of immunoproteasomes, the isolated hepatic mononuclear cells were fixated in 4% paraformaldehyde for 15 min and permeabilized for 15 min in a 1% saponin solution prepared with 0.1 M phosphate buffer saline. The cells were treated with rabbit pAb to subunit LMP7 and mouse mAb to subunit LMP2 overnight at 4°C in a sample containing 1×10^6 cells and the corresponding antibodies (dilution 1 : 600 per 0.1 M phosphate buffer saline with 1% bovine serum albumin). After washing, the cells were incubated with secondary antibodies: Alexa 488-labelled anti-rabbit IgG or phycoerythrin-conjugated antibodies to mouse IgG at a dilution of 1 : 500 for 30 min at room temperature.

For the identification of Kupffer cells, 1×10^6 cells were resuspended in 0.25 ml of phosphate buffer saline containing 10% fetal bovine serum and incubated for 30 min with phycoerythrin-conjugated anti-mouse mAb (Anti-Rat Macrophage Marker, dilution 1 : 50).

The cells were analyzed using the BD FACSCalibur flow cytometer (BD Bioscience, USA) and the CellQuestPro software.

Western blotting

The relative contents of proteasome subunits and β-actin were evaluated in clarified liver homogenates using mouse mAb to subunit LMP7, subunit LMP2, and β-actin as described previously [23].

Statistical analysis was performed using the Excel and Statistica 7.0 software packages. The data are given as a median; the difference significance between the samples was estimated using a nonparametric Manne–Whitney test with a significance level of 0.05. A Bonferroni correction was used for multiple comparisons.

RESULTS AND DISCUSSION

Content of the immunoproteasome subunits LMP2 and LMP7 in cells of the rat liver after intraportal infusion of splenocytes

A Western-blot analysis revealed an elevated level of proteasome subunits in the clarified liver homogenates of five of the six rats with induction of DST (group 3) on the 7th day after the beginning of DST induction compared to the false-operated controls (*Fig. 1*). It is evident that the mechanisms that facilitate the DST effect were impaired in one animal. In the false-operated animals there were no differences in the content of immune subunits at all studied stages after the administration of the physiological solution. No differences were also revealed in the content of immune subunits in the animals of the 4th group with gadolinium chloride infusion. Hepatic mononuclear cells were studied using flow cytofluorimetry in order to establish whether these changes in the immunoproteasome pool are associated with hepatic mononuclear cells.

Figure 2A shows histograms derived during the analysis of the rat hepatic mononuclear cells stained with antibodies to the immune subunits LMP2 and LMP7. The quantity of cells expressing the subunits LMP2 and LMP7 after the beginning of DST induction was found to change (*Fig. 2B*). It was established that as early as on the 1st day, the quantity of LMP7-positive cells increased 1.8 times in the rat livers of both groups with intraportal injection of splenocytes (groups 3 and 4) and the content of LMP2-postivie increased by 3 times compared to the false-operated controls (group 2).

Gadolinium chloride is a widely used specific inhibitor of the antigen presenting the function of Kupffer cells [29]. As shown previously, introduction of this compound to experimental animals 24 h before intraportal infusion of splenocytes abrogates the DST induction phenomenon [13, 16].

We established that the quantity of cells containing the subunits LMP2 and LMP7 in the animals treated with $GdCl_3$ (group 4) did not differ significantly on the 1st day from the quantity of cells in the animals of the 3rd group (without injection of $GdCl_3$), but it was elevated compared to the false-operated animals (group 2) (*Fig. 2B*).

Taking into account the rich composition of hepatic APCs, which, in addition to Kupffer cells and a liver sinusoidal endothelial cell (LSEC), includes dendritic and stellate cells [30], it is logic to conclude that an increase in the number of cells expressing the immune subunits LMP2 and LMP7 can also occur during an inhibition of the macrophage function. However, in this case the quantity of cells containing LMP2 and LMP7 should differ between the 3rd and 4th groups: group 4 should

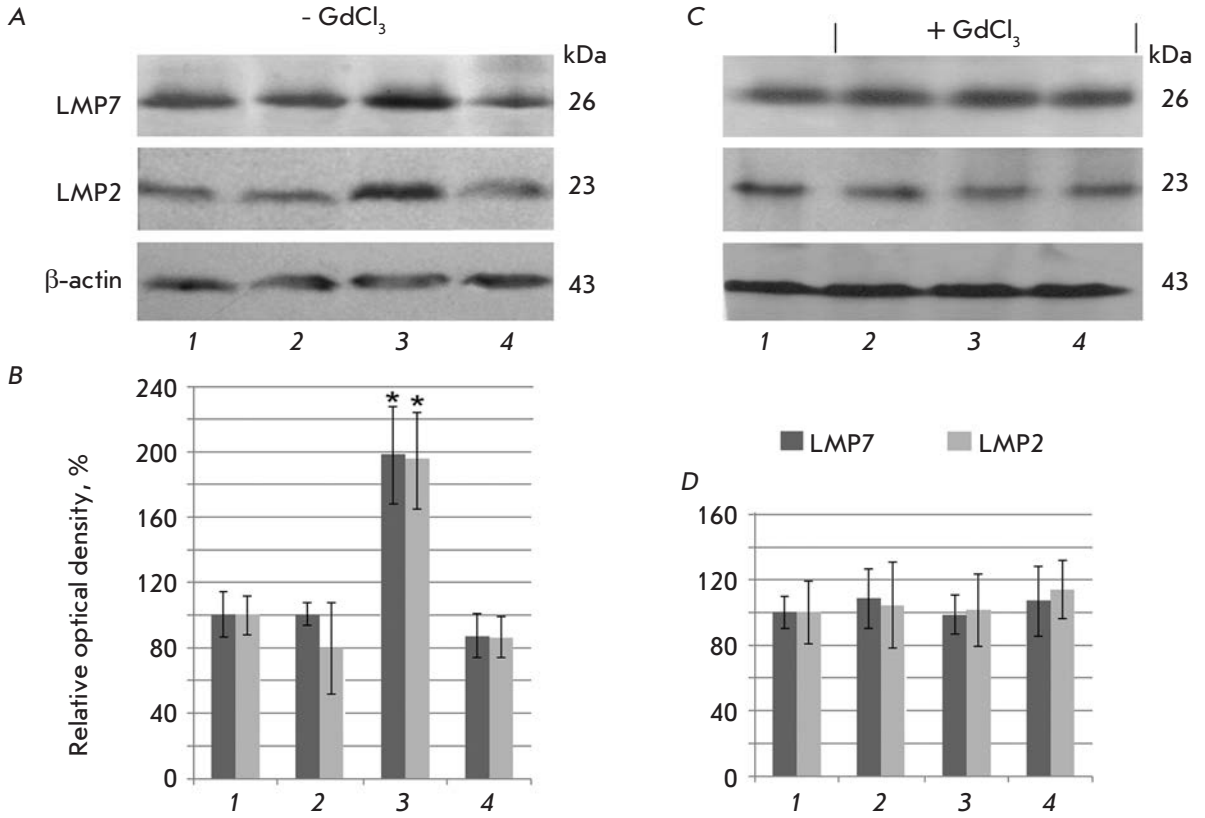

Fig. 1. Content of the proteasome subunits LMP7 and LMP2 in clarified homogenates of false-operated rat liver on the 7th day after the introduction of a physiological solution (*1*) and in rat liver on the 1st day (*2*), 7th day (*3*), and 14th day after the beginning of DST induction (*4*) with preliminary injection of $GdCl_3$ and without it. *A, C* – Western blots of subunits LMP7, LMP2 and β actin. *B, D* – Relative quantity (optical density of blots) of subunits LMP7 and LMP2 normalized to β actin content. The subunit quantity in the samples of false-operated animals was taken as 100%; means ± SEM are shown; significant difference at $p < 0.05$ and $n = 5–6$ in comparison with the false-operated control is indicated (*).

contain fewer of these cells than group 3. The absence of significant differences indicates that the increase in the quantity of cells expressing LMP2 and LMP7 on the 1st day was mostly due to a transfer of donor splenocytes containing immune proteasomes into the liver. Macrophages, even if they contribute to the total number of mononuclear cells enriched in immunoproteasomes in this period, do so in minimal fashion and the contribution does not influence the outcome.

The quantity of mononuclear cells containing immunoproteasomes in the liver of the animals of the 3rd group decreased on the 3rd day compared to the 1st day (*Fig. 3*). This could be a result of donor splenocytes leaving the liver of a recipient and migrating to regional lymph nodes [31]. It is also possible that they were eliminated as a result of the activation of recipient cytotoxic $CD8^+$ T-lymphocytes [32].

Interestingly, the quantity of mononuclear cells containing immune proteasomes decreases on the 3rd day not only compared to the 1st day of DST induction, but also relative to their basal level in the control animals of the 1st group. Taking into account the fact that immunoproteasomes are expressed mainly in APCs and immunocompetent cells, this fact indirectly points to a decrease in their quantity in the liver on the 3rd day after the beginning of induction. This can be associated with the apoptosis of activated T-lymphocytes observed in the liver during the initiation and maintenance of the tolerance status [31]. However, regardless of the mechanisms involved, the quantity of mononuclear cells enriched in immunoproteasomes in the liver is minimal at this time point, which creates a kind of "window of opportunity" for the subsequent filling of an empty niche with cells of different subpopulations and, depending on this, the development of allospecific tolerance or rejection.

On the 7th day after the infusion of splenocytes, the maximum rise in the content of mononuclear cells expressing immunoproteasomes was observed in the liver of animals of the 3rd group, which exceeded

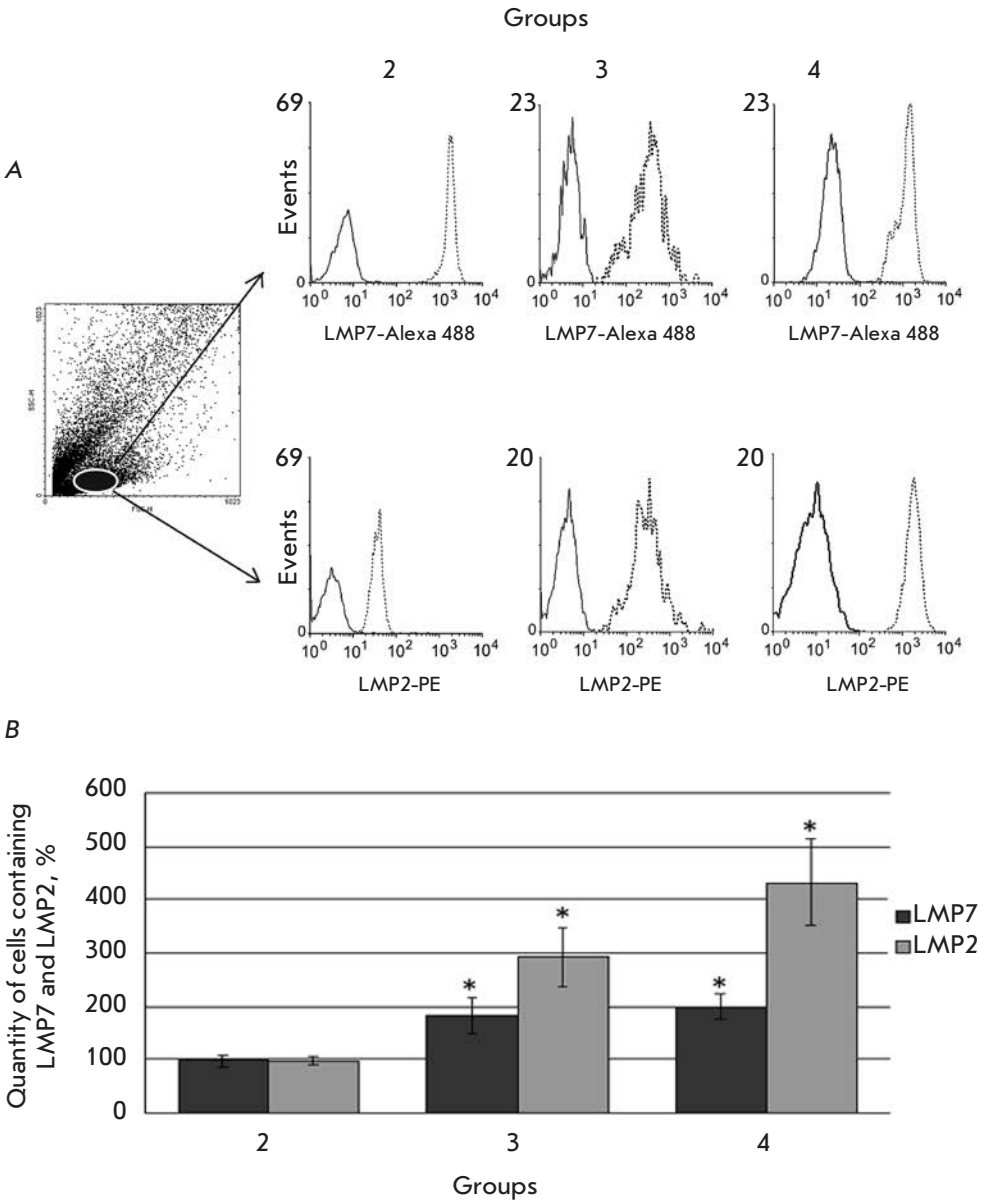

Fig. 2. Cytofluorimetric analysis of the expression of the LMP7 and LMP2 subunits in rat liver mononuclear cells. *A* – In the dotted graph of forward (FSC) and side (SSC) light scattering, the subpopulation of analyzed cells is highlighted by oval. In the right part, the histograms of LMP7 and LMP2 expression in the analyzed cell subpopulation of the liver of the 2nd, 3rd and 4th rat groups on the 1st day after the beginning of DST induction are presented. *B* – Per cent of mononuclear cells expressing the LMP2 and LMP7 subunits in the liver of the 2nd, 3rd and 4th rat groups on the 1st day. In histograms: solid line – isotypical control, dashed line – experiment. The quantity of cells containing the LMP2 and LMP7 subunits in samples of the 1st group was taken as 100%. Significant difference at $p < 0.05$ and $n = 5–6$ in comparison with the 2nd group is indicated (*).

the values for the control group almost 100 times for LMP2, and 200 times for LMP7 (*Fig. 3*). This excellent response could be rooted in both the transfer of immunocompetent cells into the liver in response to the infusion of donor splenocytes and the activation of the resident APC pool in the liver itself, which is accompanied by an increase in the content of immune subunits [33, 34]. In the subsequent days, the quantity of cells expressing immune subunits gradually decreased.

On the whole, the results of flow cytofluorimetry are consistent with Western blot findings that indicate a burst in immunoproteasome expression in the liver on the 7th day after DST induction. In addition, the discovery of this effect not in all the animals supports the hypothesis of the different possibilities of niche filling after the 3rd day that is critical for the development of tolerance or rejection.

In animals treated with $GdCl_3$, there was no similar noticeable increase in the amount of cells enriched in immunoproteasomes. The quantity of LMP7-positive cells did not differ from their quantity in false-operated animals, and the number of LMP2-positive cells on the 7th day exceeded the control values only four times. The difference between groups 3 and 4 indirectly indicates that the inhibition of Kupffer cells influences the processes dependent on the immunoproteasomes that occur in the early stages of DST induction.

Relationship between the content of Kupffer cells and the change in the expression of immunoproteasomes during DST induction

Our results led to a need for a direct assessment of the Kupffer cell content in different periods after splenocyte infusion. We used monoclonal antibodies that recognize ED2-like antigens on the membranes of rat resident macrophages, including Kupffer cells [35].

The profile of the dynamics of ED2-positive cells also had two maximums (*Fig. 4*), with the first peak occurring with a two-day shift and the second peak with a three-day shift later compared to the peaks in the content of the total mononuclear cell pool expressing immunoproteasomes (*Figs. 3* and *4*). This shift can be accounted for by the fact that, at first, APCs present a foreign alloantigen with the participation of immunoproteasomes. This process is accompanied by a release of mediators of the immune response, which serve as a signal for the proliferation of Kupffer cells [36, 37].

In animals of the 4th group, there were no bursts in the quantity of macrophages in the liver, probably because of the absence or defect stage of antigen presentation after the infusion of $GdCl_3$.

The results make it possible to state that induction of portal tolerance is an active process that affects several subpopulations of liver APCs and makes it possible for the rearrangements in the intracellular proteasome pool to be involved in the mechanisms of antigen processing and presentation. In addition, in the early stages of DST development, two waves were observed: the first (1–3 days) was associated with the transfer of donor immune system cells into the liver; the second (7–10 days) – with the activation of a response in the liver of a recipient involving Kupffer cells.

Does the expression profile of the inducible subunits LMP2 and LMP7 change in Kupffer cells after intraportal alloantigen infusion?

In order to answer this question, we studied the changes that occurred in the proteasome pool of ED2-positive cells in rat liver with DST induction (group 3) in different periods after the administration of donor splenocytes (*Fig. 5*). First, two peaks of an increase in the quantity of the subunits LMP2 and LMP7 – on the 1st and 7th days – were revealed. Second, it was revealed that the proportion of LMP2 and LMP7 subunit expression in ED2-positive cells changes with time after DST induction. During the first 5 days, the quantity of LMP2 increased more noticeably than that of LMP7; the level of both immune subunits was similarly high on the 7th day.

The time changes in the content of ED2-positive cells and immunoproteasomes were characterized by two phases. In the first phase, the quantity of LMP2 and LMP7 increased on the 1st day, similar to the one in the total pool of mononuclear cells, while the quantity of ED2-positive cells increased on the 3rd day (*Figs. 3–5*). In the second phase, all these events occurred in the same sequence: a peak in the expression of immunoproteasome subunits in ED2-positive cells was observed on the 7th day, similar to that in the total mononuclear cell

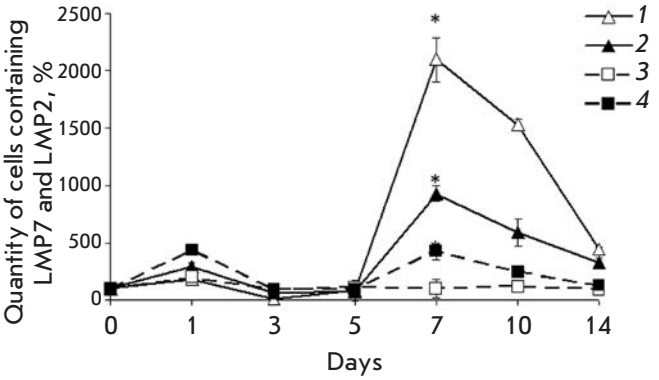

Fig. 3. Change in the quantity of mononuclear cells containing the proteasome LMP2 subunit (filled symbols) and LMP7 subunit (empty symbols) in different time intervals after the beginning of DST induction in the liver of the 3rd (lines *1* and *2*) and 4th rat groups (lines *3* and *4*). On *x* axis, days after the beginning of DST induction are shown. The quantity of cells containing the LMP2 and LMP7 subunits in samples of the 1st group was taken as 100%. Significant difference at $p < 0.05$, $n = 5$ in comparison with basal level (group 1) (*).

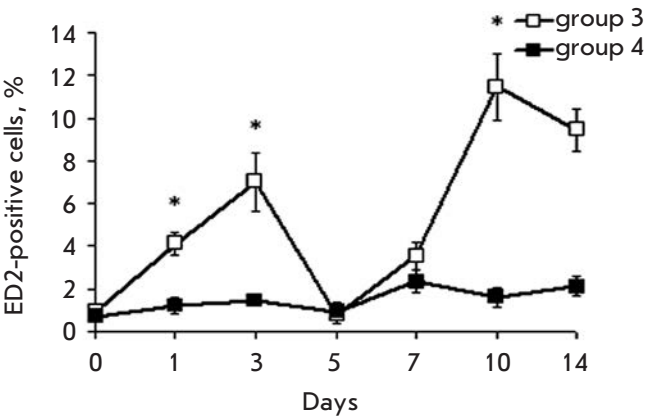

Fig. 4. Cytofluorimetric analysis of cells expressing the macrophage ED marker in the 3rd and 4th rat groups at different stages after introduction of donor splenocytes. On *x* axis, days after the beginning of DST induction are shown. The quantity of cells in samples of the 1st group was taken as 100%. Significant difference at $p < 0.05$, $n = 5$ in comparison with basal level (group 1) (*).

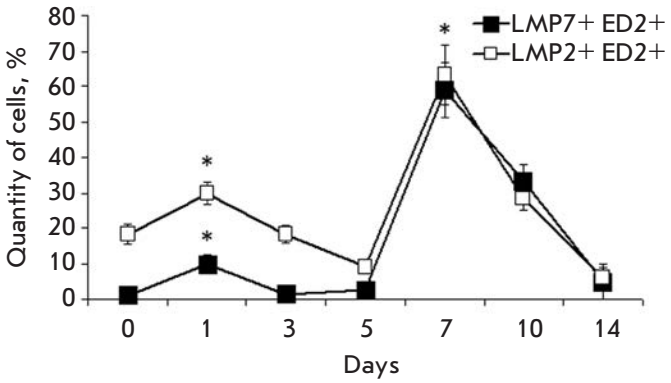

Fig. 5. Cytofluorimetric analysis of LMP7 and LMP2 subunit expression in ED2-positive cells of the liver of the 3rd rat group after the beginning of DST induction. On *x* axis, days after the beginning of DST induction are shown. The total quantity of ED2-positive cells was taken as 100%. Significant difference at $p < 0.05$, $n = 5$ in comparison with basal level (group 1) (*).

pool, followed by an increase in the quantity of ED2-positive cells on the 10th day.

It is likely that differences exist in the mechanisms underlying the increase in the expression of immunoproteasome subunits in the total mononuclear cell pool in the first and second phases. The first peak of expression of LMP2 and LMP7 subunits reflects mostly the transfer of splenocytes enriched in immunoproteasomes. At the same time, to a greater or a lesser extent the second peak can be associated with *de novo* LMP2 and LMP7 subunit synthesis in mononuclear cells of a recipient's liver, including in Kupffer cells. This synthesis is induced in the first phase, resulting from the encounter of splenocytes with hepatic APCs. LSEC are known to cross-present a foreign antigen immediately to $CD8^+$ T-lymphocytes [38], and the process requires an insignificant quantity of stimulatory biomaterial (< 1 nM). This process takes several hours [39] and is accompanied by the release of cytokines [40, 41] that send signals for expression upregulation of the inducible subunits LMP7 and LMP2 [21, 42]. The hypothesis of a *de novo* immunoproteasome synthesis in the second phase is also supported by the fact that the expression of immunoproteasome subunits in response to cytokines reaches a peak only in 5–7 days [43, 44]. The first peak of an increase in the level of proteasome subunits in Kupffer cells can reflect the initial stage of their *de novo* synthesis.

The proportion of proteasome immune subunits influences the activation of macrophages and their polarization into either an ED1- or ED2-phenotype [45]. Therefore, the change in LMP2 and LMP7 subunit levels in cell subpopulations can be associated with the activation of macrophages type 2. This in turn explains the prevalence of processes in the liver that are involved in the prevention of rejection reactions due to the fact that ED2-macrophages belong to the anti-inflammatory functional phenotype, which is characterized by the secretion of the cytokines IL-10, IL-4, and TGF-β [46].

The established dynamics of immunoproteasome expression in hepatic mononuclear cells reflects the changes in the reactivity of their subpopulations in response to the introduction of foreign antigens. Previous data showed the appearance of peaks reflecting cell activation within the liver after peptide antigen administration or adoptive transfer of lymphocytes. For example, the proliferation of donor cells occurred on the 2.5th and 6th days after adoptive transfer of CD8+ T-lymphocytes in the liver of a recipient [47]. An eight-fold expansion of the CD8+ T-lymphocyte subpopulation on the 2nd day after their intraportal infusion, followed by a gradual decline by the 4th day, was also revealed [48]. Stimulation with antigenic peptide SEFLLEKRI led to a 100-fold expansion of the mononuclear cell pool within the liver, starting from the 2nd day, followed by response extinction by the 6th day [49]. It is interesting to note that the lymphocyte proliferation peaked on the 4th day and the dynamics of the rest subpopulations was biphasic, with peaks on the 1st and 4th days.

Thus, a strong immunologic basis underlies the biphasic pattern of immune reactivity of the liver in response to intraportal infusion of a donor antigen (*Fig. 6*). In the first phase, LSEC and Kupffer cells encounter donor cells, which, due to the specific ability of the liver to retain activated CD8+ T-lymphocytes [48], remain there for a sufficient time for antigen presentation. After processing and antigen presentation with the involvement of immunoproteasomes, the proliferation of donor leukocytes and resident hepatic immunocompetent cells is triggered. Antigen presentation and activation of lymphocytes are accompanied by the release of cytokines, which play a leading role in the recruiting of the macrophages and lymphocytes of a recipient into the liver [50, 51]. This results in the appearance of the second peak in the dynamics of the hepatic immunoproteasome pool after DST induction.

The interaction of activated CD8+ T-lymphocytes with Kupffer cells leads to their apoptosis due to the absence of adequate proinflammatory stimulation [48]. In addition to the direct interaction, Kupffer cells produce some proapoptotic substances, such as TNF-α, CD95-ligand, galectin-1, and indoleamine-dioxygenase [52, 53]. A reduction in lymphocyte quantity at the end of the first phase during DST induction leads to a decline in the hepatic immunoproteasome pool. A further

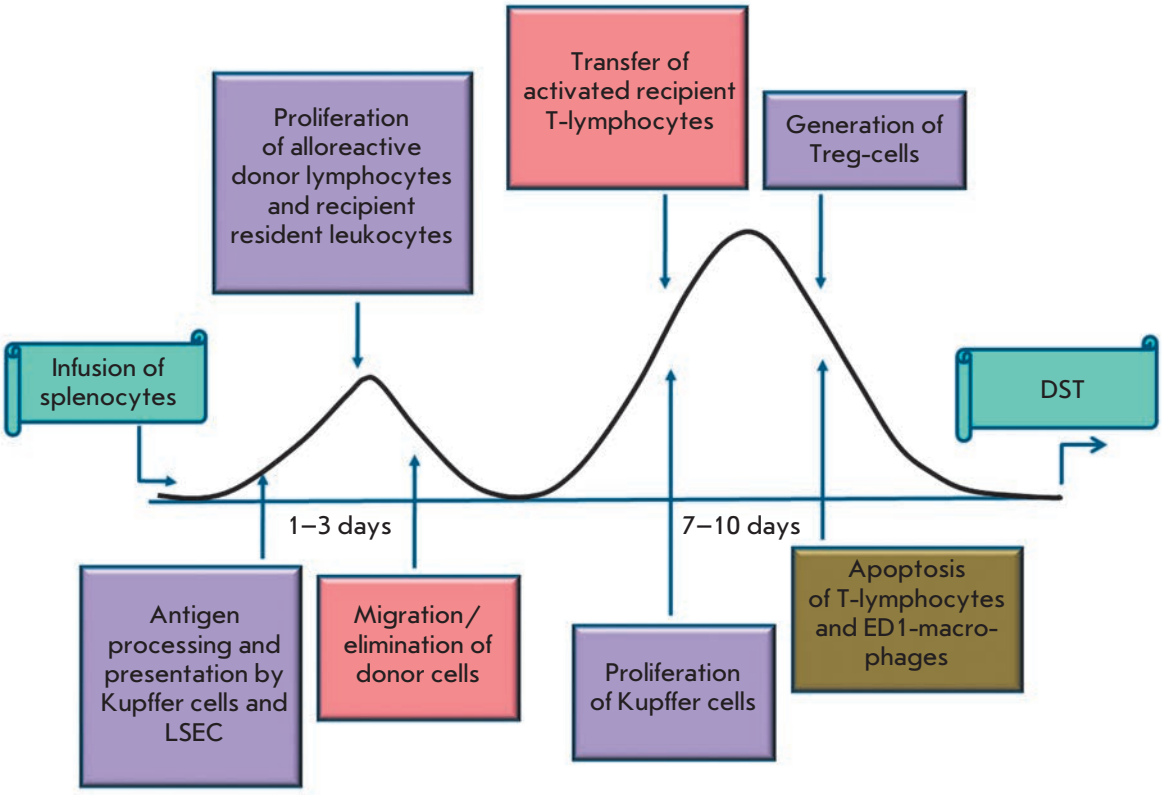

Fig. 6. Scheme of DST induction and development.

decrease in the quantity of immunoproteasomes in this period can occur due to the migration of donor cells into the blood flow of a recipient.

The ability of immunocompetent hepatic cell subpopulations of primary antigen presentation [51], which results in the deletion of alloreactive CD8+ T-lymphocytes via apoptosis, in the absence of positive costimulation [48], presents an opportunity for the prevention of the development of an immune response in the first days (1–3) after the administration of donor cells.

The second phase is associated with the clonal expansion and transfer of the activated T-lymphocytes and macrophages of a recipient into the liver. The phenotypical profile of the cells that fill the immunological niche of the liver in this phase likely contributes to either tolerance or rejection reactions. Activation of immune defense mechanisms in the liver directed towards eliminating/alleviating inflammation can shift the balance in the side of tolerance. These mechanisms include the apoptosis of the activated T-lymphocytes of a recipient [31], ED1-polarized macrophages and activated T-cells in the presence of ED2-phenotype macrophages in the liver [54, 55], and the expansion of Treg-cells [56] in response to antigen presentation in the liver.

The repertoire of immune subunits influences the hierarchy of the presented antigenic epitopes on APCs. At least four forms of immune proteasomes have been described. One form contains all three proteolytic immune subunits: LMP7, LMP2, and LMP10. Two forms contain two immune subunits and one proteolytic constitutive subunit: β5-LMP2-LMP10 and LMP7-LMP2-β2. One form contains the immune subunit LMP7 and two constitutive subunits β1 and β2 [57–60]. The combination of subunits with proteolytic activity determines the changes in the conformation of substrate-binding pockets [61], the preferable sites for protein hydrolysis and, therefore, the range of produced antigenic epitopes. Hence, the change in the balance of immune subunits in resident and transitory immune system cell subpopulations plays an important role in how a foreign antigen is presented, either as a "non-self" molecule to cause rejection or as a "self" molecule to be accepted.

CONCLUSIONS

This paper has studied for the first time the changes that occur in the immunoproteasome pool of mononuclear cells within the liver during the induction of

allospecific portal tolerance. Based on the findings, it is concluded that DST induction is an active process characterized by two phases wherein the proportion of the immunoproteasome subunits LMP2 and LMP7 and the quantity of hepatic APCs, including Kupffer cells, change. Apparently, the balance of these parameters is important for the development of tolerance to transplanted tissues. The third day after the beginning of DST induction is the key point when a kind of "window of opportunity" opens for a subsequent filling of an empty niche with cells of different subpopulations and, depending on this factor, the development of either tolerance or rejection. The results present new tasks related to the search for ways to influence the cellular composition of the liver and the expression of immunoproteasomes on the 3rd day after the beginning of DST induction for blocking rejection.

This study was partially supported by the Russian Foundation for Basic Research, grant for young scientists 16-34-60083-mol_a_dk.

REFERENCES

1. Calne R.Y., Sells R.A., Pena J.R . Davis D. R., Millard P.R., Herbertson B.M., Binns R.M., Davies D.A. // Nature. 1969. V. 2. № 223 (5205). P. 472–476.
2. Qian S., Demetris A., Murase N., Rao A.S., Fung J.J., Starzi T.E. // Hepatology 1994. V. 19. P. 916–924.
3. Zimmermann F.A., Davies H.S., Knoll P.P. // Transplantation. 1984. V. 37. P. 406–410.
4. Kamada N., Wight D.G.D. // Transplantation. 1984. V. 38. № 3. P. 217–221.
5. Cunningham E.C., Sharland A.F., Bishop G.A. // Clin. Dev. Immunol. 2013. 2013:419692. Epub 2013 Nov 6.
6. Topilsky Y., Raichlin E., Hasin T., Boilson B.A., Schriger J.A., Pereira N.L., Edwards B.C., Schriger J.A., Pereira N.L., Edwards B.S., Topilsky Y., Raichlin E., Hasin T. // Transplantation. 2013. V. 95. P. 859–865.
7. Sun J., McCaughan G.W., Gallagher N.D., Scheil A.G., Bishop G.A. // Transplantation. 1995. V. 60. P. 233–236.
8. Shimizu Y., Goto S., Lord R, Vari F., Edwards-Smith C., Chiba S., Schlect D., Buckley M., Kusano M., Kamada N. // Transpl. Int. 1996. V. 9. P. 593–595.
9. Ko S., Deiwick A., Jager M.D/., Dinkel A., Rohde F., Fisher R.T., Tsui T.Y., Rittmann K.L., Wonigeit K., Schlitt H.J. // Nat. Med. 1999. V. 5. P. 1292–1297.
10. Kenick S., Lowry R.P., Forbes R.D.S., Lisbona R. // Transplant. Proc. 1987. V. 19. P. 478–479.
11. Oko A., Idasiak-Piechocka I., Pawlaczyk K., Wruk M., Pawlaczyk E., Czekalski S. // Ann. Transplant. 2002. V. 7. № 2. P. 51–53.
12. Sheng Sun D., Iwagaki H., Ozaki M., Ogino T., Kusaka S., Fujimoto Y., Murata H., Sadamori H., Matsukawa H., Tanaka N., Yagi T. // Transpl. Immunol. 2005. V. 14. № 1. P. 17–20.
13. Diaz-Peromingo J.A., Gonzalez-Quintela A. // Eur. Surg. Res. 2005. V. 37. P. 45–49.
14. Ikebukuro K., Adachi Y., Yamada Y. Fujimoto S., Seino Y., Oyaizu H., Hioki K., Ikehara S. // Transplantation. 2002. V. 73. P. 512–518.
15. Chalermskulrat W., McKinnon K.P., Brickey.J. W., Neuringer I.P., Park R.C., Sterka D.C., Long B.R., McNeillie P., Noelle R.J., Ting J.P., Aris R.M. // Thorax. 2006. V. 61. № 1. P. 61–67.
16. Nakagawa K., Matsuno.T, Iwagaki H., Morimoto Y., Fujiwara T., Sadamori H., Inagaki M., Urushihara N., Yagi T., Tanaka N. // J. Int. Med. Res. 2001. V. 29. P. 119–130.
17. Watanabe T., Kudo M., Chiba T., Wakatsuki Y. // Hepatol. Res. 2008. V. 38. P. 441–449.
18. Gaczynska M., Rock K.L., Goldberg A.L. // Enzyme Protein. 1993. V. 47. № 4–6. P. 354–369.
19. Cong Y., Konrad A., Iqbal N., Hatton R.D., Weaver C.T., Elson C.O. // J. Immunol. 2005. V. 174. № 5. P. 2787–2795.
20. Trombetta E.S., Mellman I. // Annu. Rev. Immunol. 2005. V. 23. P. 975–1028.
21. Basler M., Kirk C.J., Groettrup M. // Curr. Opin. Immunol. 2013. V. 25. № 1. P. 74–80.
22. Karpova Ya.D., Bozhok G.A., Lyupina Yu.V., Legach E.I., Astakhova T.M., Stepanova A.A., Bondarenko T.P., Sharova N.P. // Izvestiia Rosiiskoi Akademii nauk. Seriia biologicheskaia. 2012. №. 3. P. 296–302 .
23. Stepanova A.A., Karpova Y.D., Bozhok G.A., Ustichenko V.D., Lyupina Y.V., Legach E.I., Vagida M.S., Kazansky D.B., Bondarenko T.P., Sharova N.P. // Bioorg. Khim. 2014. V. 40. № 1. P. 42–54.
24. Yunusov M.Y., Kuhr C.S., Georges G.E., Hogan W.J., Taranova A.G., Lesnikova M., Kim Y.S., Nash R.A. // Transplantation. 2006. V. 82. № 5. P. 629–637.
25. Bozhok G.A. // Problemy endokrynnoi patolohii. 2011. № 1. 2011. P. 60–66.
26. Marti H.P., Henschkowski J., Laux G., Vogt D., Seiler C., Opelz G., Frey F.J. // Transpl. Int. 2006. V. 19. P. 19–26.
27. Mackie F. // Nephrology (Carlton). 2010. Suppl 1. S101–S105.
28. Lymphocytes: A practical approach. Ed. by G.G.B. Klaus. M.: Mir. 1990. 395 p.
29. Ahmad N., Gardner C.R., Yurkow E.I., Laskin D.L. // Hepatology. 1999. V. 29. № 3. P. 728–736.
30. Crispe I. N., Giannandrea M., Klein I., John B., Sampson B., Wuensch S. // Immunol. Reviews. 2006. V. 213. P. 101–118.
31. Bishop G.A., Wang C., Sharland A.F., McCaughan G. // Immunol. Cell Biol. 2002. V. 80. № 1. P. 93–100.
32. Fast L.D. // J. Immunol. 1996. V. 157. № 11. P. 4805–4810.
33. Stevanović S. // Transpl. Immunol. 2002. V. 10. № 2–3. P. 133–136.
34. Jin Y., Fuller L., Ciancio G., Burke G.W. 3rd, Tzakis A.G., Ricordi C., Miller J., Esquenzal V. // Hum. Immunol. 2004. V. 65. № 2. P. 93–103.
35. Polfliet M.M., Fabriek B.O., Daniëls W.P., Dijkstra C.D., van den Berg T.K. // Immunobiology. 2006. V. 211. № 6–8. P. 419–425.
36. Milner J.D., Orekov T., Ward J.M., Torres-Velez F., Juntila I., Sun G., Buller M., Morris S.C., Finkelmann F.D., Paul W.E., et al. // Blood. 2010. V. 116. № 14. P. 2476–2483.
37. Jenkins S.J., Ruckerl D., Cook P.C., Jones L.H., Finkelman F.D., van Rooijen N., MacDonald A.S., Allen J.E. // Science. 2011. V. 332. № 6035. P. 1284–1288.
38. Knolle P.A., Limmer A // Swiss Med. Wkly. 2003. V. 133. № 37–38. P. 501–506.

39. Limmer A., Ohl J., Wingender G., Berg M., Jungerkes F., Schumak B., Djandji D., Scholz K., Klevenz A., Hegenbarth S., et al. // Eur. J. Immunol. 2005. V. 35. № 10. P. 2970–2981.
40. Limmer A., Ohl J., Kurts C., LjunggrensH.G., Reiss Y., Groettrup M., Momburg F., Arnold B., Knolle P.A. // Nat. Med. 2000. V. 6. № 12. P. 1348–1354.
41. Schurich A., Berg M., Stabenow D., Bottcher J., Kern M., Schild H.J., Kurts C., Schuette V., Burgdorf S., DiehlL., Limmer A., Knolle P.A. // J. Immunol. 2010. V. 184. № 8. P. 4107–4114.
42. Niewerth D., Kaspers G.J., Assaraf Y.G., van Meerloo J., Kirk C.J., Anderl J., Blank J.L., van de Ven P.M., Zweegman S., Jansen G., et al.// J. Hematol. Oncol. 2014. 7:7. doi: 10.1186/1756-8722-7-7.
43. Khan S., van den Broek M., Schwarz K., de Giuli R., Diener P.A., Groettrup M. // J. Immunol. 2001. V. 167. P. 6859–6868.
44. Heink S., Ludwig D., Kloetzel P.M., Kruger E. // Proc. Natl. Acad. Sci. USA. 2005. V. 102. P. 9241–9246.
45. Chen S., Kammerl I.E., Vosyka O., Baumann T., Yu Y., Wu Y.Irmler M., Overkleeft H.S., Beckers J., Eickelberg O., Meiners S., Stoeger T. // Cell Death Differ. 2016. Mar 18. doi: 10.1038/cdd.2016.3. [Epub ahead of print]
46. Tcke F., Zimmermann H.W. // J. Hepatol. 2014. V. 60. № 5. P. 1090–1096.
47. Bowen D.G., Zen M., Holz L., Davis T., McCaughan G.W., Bertolino P. // J. Clin. Invest. 2004. V. 114. № 5. P. 701–712.
48. Kuniyasu Y., Marfani S.M., Inayat I.B., Sheikh S.Z., Mehal W.Z. // Hepatology. 2004. V. 39. № 4. P. 1017–1027.
49. Huang L., Soldevila G., Leeker M., Flavell R., Crispe I.N. // Immunity. 1994. V. 1. № 9. P. 741–749.
50. Lalor P.F., Shields P., Grant A., Adams D.H. // Immunol. Cell Biol. 2002. V. 80. № 1. P. 52–64.
51. Robinson M.W., Harmon C., O'Farrelly C. // Cell Mol. Immunol. 2016. V. 13. № 3. P. 267–276.
52. Perillo N.L., Pace K.E., Seilhamer J.J., Baum L.G. // Nature. 1995. V. 14. № 378 (6558). P. 736–739.
53. Müschen M., Warskulat U., Peters-Regehr T., Bode J.G., Kubitz R., Häussinger D. // Gastroenterology. 1999. V. 116. № 3. P. 666–677.
54. You Q., Cheng L., Kedl R.M., Ju C. // Hepatology. 2008. V. 48. № 3. P. 978–990.
55. Wan J., Benkdane M., Teixeira-Clerc F., Bonnafous S., Louvet A., Lafdil F., Pecker F., Tran A., GualP., Mallat A., et al. // Hepatology. 2014. V. 59. № 1. P. 130–142.
56. Dangi A., Sumpter T.L., Kimura S., Stolz D.B., Murase N., Raimondi G., Vodovotz Y., Huang C., Thomson A.W., Gandhi C.R. // J. Immunol. 2012. V. 188. № 8. P. 3667–3677.
57. Groettrup M., Standera S., Stohwasser R., Kloetzel P.-M. // Proc. Natl. Acad. Sci. USA. 1997. V. 94. P. 8970–8975.
58. Griffin T.A., Nandi D., Cruz M., Fehling H.J., van Kaer L., Monaco J.J., Colbert A. // J. Exp. Med. 1998. V. 187. P. 97–104.
59. Guillaume B., Chapiro J., Stroobant V., Colau D., van Holle B., Parvizi G., Bousquet-Dubouch M.P., Théate I., Parmentier N., van den Eynde B.J. // Proc. Natl. Acad. Sci. USA. 2010. V. 107. № 43. P. 18599–18604.
60. Dahlmann B. // Arch. Biochem. Biophys. 2016. V. 591. P. 132–140.
61. Unno M., Mizushima T., Morimoto Yu., Tomisugi Y., Tanaka K., Yasuoka N., Tsukihara T. // Structure. 2002. V. 10. P. 609–618.

The Spatial Organization of the Intranuclear Structures of Human Brain Dopaminergic Neurons

D. E. Korzhevskii, V. V. Gusel'nikova*, O. V. Kirik, E. G. Sukhorukova, I. P. Grigorev
Federal State Budgetary Research Institution «Institute of Experimental Medicine», akad. Pavlov Str. 12, St. Petersburg, 197376, Russia
*E-mail: guselnicova.valeriia@yandex.ru
Received: September 15, 2016; in final form August 24, 2017

ABSTRACT **We studied the intranuclear localization of protein nucleophosmin (B23) and ubiquitin in the dopaminergic neurons of human substantia nigra (n = 6, age of 25–87 years) using immunohistochemistry and confocal laser microscopy. Intranuclear ubiquitin-immunopositive bodies that morphologically correspond to Marinesco bodies were found to be present in substantia nigra dopaminergic (tyrosine hydroxylase-immunopositive) neurons but absent in non-dopaminergic neurons. The number of bodies varied from 0 to 6 per cell nucleus. Nucleophosmin (B23) was found in the neuronal nucleolus, with the nucleolus size being constant in the nigral neurons of each individual brain. All the observed neurons had only one large nucleolus with intense nucleophosmin immunoreactivity and a lightly stained region (1–2 μm in diameter) that apparently represents the giant fibrillar center (GFC). An intensely immunostained nucleophosmin-containing granule was often observed at the GFC periphery. Double labeling demonstrated that nucleophosmin-immunoreactive nucleolus and ubiquitin-immunoreactive Marinesco bodies can occur both closely to and remotely from each other. Three-dimensional reconstruction indicates that rounded Marinesco bodies are polymorphic and often have a complex shape, with some flattening and concavities, which may be associated with contact not only with the nucleolus, but also, presumably, with other intranuclear structures free of ubiquitin or nucleophosmin. Ubiquitin-immunoreactive structures with a relatively small size (up to 1 μm in length) and various clastosome-like shapes (Lafarga et al., 2002) often occur near Marinesco bodies. There were no cases of detection of ubiquitin in the nucleoli of dopaminergic neurons and nucleophosmin/B23 in typical Marinesco bodies. The obtained information may be helpful in unraveling the molecular mechanisms of the selective vulnerability of substantia nigra dopaminergic neurons to damaging factors.**
KEYWORDS **brain, dopaminergic neurons, human, Marinesco body, nucleolus, nucleophosmin, substantia nigra, ubiquitin.**

INTRODUCTION

The eukaryotic cell nucleus is characterized by a complex internal structural and functional compartmentalization that enhances the effectiveness of intracellular processes by concentrating specific factors in certain nuclear regions. The most important nuclear compartments include nucleoli, nuclear speckles, Cajal bodies, PML bodies, etc. [1]. In this case, some intranuclear structures (e.g., nucleoli) are present in most eukaryotic cells, while others are characteristic of a specific cell type. An example of such specific intranuclear structures is the Marinesco bodies that normally occur exclusively in the neurons of substantia nigra and locus coeruleus in the brain of humans and primates [2, 3]. Despite the fact that both nucleoli and Marinesco bodies are individually well characterized structures, their shape and spatial relationship in the nuclei of nerve cells have not been explored in detail. This problem may be solved using confocal microscopy involving the use of primary antibodies to known marker proteins of various intranuclear structures. For the nucleolus, this marker is nucleophosmin (NPM, B23), a polyfunctional protein that is involved in ribosome biogenesis, centrosome duplication, and the regulation of proliferation and apoptosis [4–6]. Interestingly, B23 is expressed at a high level not only in actively proliferating cells, but also in postmitotic neurons, but its role in these neurons is actually unknown [6]. In the nucleolus of nerve cells, B23 is supposed to act as a cellular stress sensor initiating the mechanisms that promote the maintenance of neuronal viability (e.g., by stabilizing the transcription factor p53) [7]. In addition to that, a normal level of B23 in neurons is probably a condition for maintaining blockade of the cell cycle, while excessive expression of

the protein may cause the cell to return to the cell cycle and initiate neuronal death, which is observed in neurodegenerative diseases such as Alzheimer's disease, Parkinson's disease, and amyotrophic lateral sclerosis [8–10]. In this regard, an immunocytochemical study of the B23 protein distribution in substantia nigra dopaminergic neurons of the human brain is particularly important, because mass death of dopaminergic neurons is a characteristic feature of Parkinson's disease and an indispensable indicator of the adequacy of experimental models of this disease [11, 12].

In contrast to B23, whose distribution features in dopaminergic neurons have not been explored, ubiquitin, a component of the proteasome system responsible for degrading damaged proteins, has been repeatedly studied when analyzing the functional state of substantia nigra neurons in normal and pathological conditions [13, 14]. Currently, ubiquitin is considered as a specific marker of Marinesco bodies; the functional significance of the latter still remains unknown [3]. Studies of intranuclear ubiquitin-immunopositive bodies of substantia nigra neurons of the human brain using light microscopy and immunocytochemistry have demonstrated that up to 20% of substantia nigra neurons can contain ubiquitin-immunoreactive bodies whose morphological characteristics are similar to those of Marinesco bodies [15]. In the same studies, the nuclei of substantia nigra neurons were found to comprise structures that differ from Marinesco bodies in a number of characteristics but contain ubiquitin in a detectable amount [15]. In recent years, reports have appeared indicating that ubiquitin (along with ubiquitin-like proteins) plays an important role not only in intracellular protein degradation processes, but also in ribosome biogenesis [16]. This suggests the presence of this protein in the nucleolus, but the results of immunocytochemical studies, which would confirm this suggestion, are absent.

Therefore, investigation of the shape and spatial relationship of B23- and ubiquitin-immunopositive structures in dopaminergic neurons of the human brain is a topical issue of modern neuroscience and is of great interest in basic neurology. Therefore, the search for approaches to solving these issues was the purpose of the present work.

EXPERIMENTAL

We used fragments of the human midbrain (n = 6, males and females aged 25 to 87 years who died of reasons not related to brain diseases and damage). The material was received from the archive of the Department of General and Private Morphology of the Institute of Experimental Medicine. The research program was approved by the Local Ethical Committee of the Institute of Experimental Medicine.

The material was fixed in zinc-ethanol-formaldehyde [17] and immersed into paraffin. Paraffin blocks were used to prepare slices with a thickness of 5, 7, and 10 μm, which were pasted onto slides with an adhesive coating (Histobond, Polysine, SuperFrost Gold, Germany). A fraction of the samples were stained using a classical neurohistological technique – Nissl staining with toluidine blue. Before starting immunocytochemical reactions, the material was verified for suitability to analysis (a neurodegenerative process and post-mortem autolysis were excluded). To improve the immunoreactivity of detected antigens, they were thermally retrieved in modified citrate buffer, pH 6.1 (S1700, Dako, Denmark). Control immunohistochemical reactions were carried out with allowance for the recommendations of the reagent's manufacturer.

When performing immunohistochemical reactions for transmitted light microscopy, we used the following primary antibodies: rabbit polyclonal anti-ubiquitin antibodies (Dako) at a 1 : 400 dilution; mouse monoclonal anti-B23 (nucleophosmin) antibodies, clone FC82291 (Sigma-Aldrich, USA), at a 1 : 200 dilution; mouse monoclonal anti-tyrosine hydroxylase antibodies (clone 1B5) at a 1 : 50 dilution (Leica-Novocastra, UK). A MACH2-Universal HRP-Polymer reagent (Biocare Medical, USA) was used to identify the rabbit and mouse primary antibodies associated with the studied markers. The peroxidase label was detected using diaminobenzidine chromogen (DAB+; Dako). After performing immunocytochemical reactions, a fraction of the sections were stained with a 0.5% aqueous cresyl violet solution (Dr. Grubler, Germany) and a 0.1% aqueous astra blue solution (Merck, Germany).

When performing individual and combined immunohistochemical reactions for confocal laser microscopy, we used the same primary antibodies as for the immunoperoxidase reaction. In a double reaction, we used two antibody combinations antibodies to tyrosine hydroxylase/ubiquitin and antibodies to B23/ubiquitin. After thermal retrieval of antigens, they were incubated with primary antibodies at 27 ˚C for 65 h. A biotin-labeled monovalent Fab fragment of donkey immunoglobulin (Jackson ImmunoResearch, USA) was used as a secondary antibody to detect primary mouse antibodies. After treatment with secondary antibodies, the samples were incubated in a solution of streptavidin conjugated with a Cy2 fluorochrome (Jackson ImmunoResearch). Primary rabbit antibodies were detected with pig anti-rabbit immunoglobulin antibodies conjugated with tetramethylrhodamine isothiocyanate (TRITC) produced by Dako. After performing a single reaction for the B23 protein, a fraction of the samples were stained with a 7-AAD nuclear dye (Invitrogen, USA). Confocal microscopy was performed using a

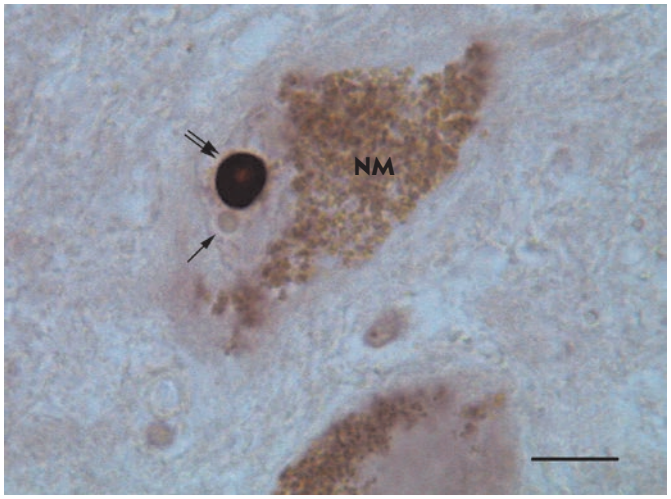

Fig. 1. A dopaminergic neuron with a B23-immunopositive nucleolus in human substantia nigra. *NM* – neuromelanin granules in the neuronal cytoplasm; *the single arrow* indicates an unstained Marinesco body; *the double arrow* indicates the immunopositive nucleolus. Protein B23 immunocytochemistry without counterstaining. Plan objective lens 100×/1.25 Oil (oil immersion). Eyepiece HC Plan s 10×/18. Scale bar=10 μm.

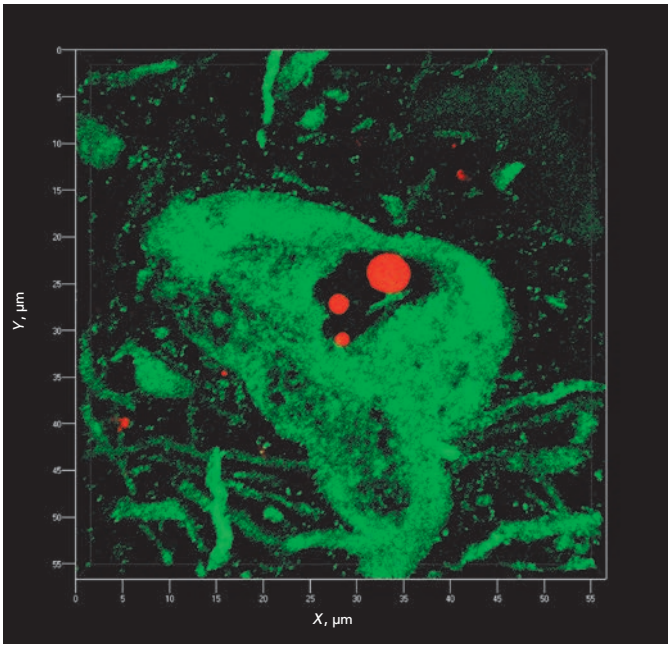

Fig. 2. Ubiquitin-immunopositive structures in human substantia nigra. An immunopositive response to ubiquitin (*red*) is provided by three rounded Marinesco bodies in the neuronal nucleus and some granules in the substantia nigra neuropil. Double immunocytochemistry for tyrosine hydroxylase is visualized with fluorochrome Cy2 (*green*), and that for ubiquitin is visualized with fluorochrome TRITC (*red*). Confocal laser microscopy. 3D reconstruction in shadow projection is carried out using a ZEN 2011 software module (Zeiss, Germany). Z-stack covers a depth of 5.6 μm and 29 optical sections. Objective lens 100×/1.40 Oil DIC M27 (oil immersion).

LSM 710 microscope (Carl Zeiss, Germany).

After performing the immunocytochemical reaction for B23, we determined the nucleolus size in substantia nigra neurons. The nucleolus diameter was measured using the LAS EZ software (Leica, Germany). We analyzed nucleoli only in neurons where neuromelanin granules were clearly visible in the cytoplasm. The measurements were performed independently by two investigators (O.V. Kirik and V.V. Gusel'nikova) on two different Leica DM750 microscopes (Leica) equipped with ICC50 and ICC50HD cameras (Leica), after additional calibration of the system using an object micrometer. Quantitative data were processed in Excel software (Microsoft, USA) and represented as the mean (X) and standard deviation (σ). The coefficient of variation (V) was calculated to evaluate population homogeneity.

RESULTS AND DISCUSSION

In all cases, neuronal nucleoli (both in Nissl staining with toluidine blue and in the B23 protein test) and ubiquitin-immunopositive bodies were found in the samples (*Fig. 1*). A double immunofluorescence reaction for tyrosine hydroxylase and ubiquitin (*Fig. 2*) showed that intranuclear ubiquitin-immunopositive bodies were actually present in substantia nigra dopaminergic neurons and were absent in the neurons not responding to a marker enzyme of catecholamine synthesis, tyrosine hydroxylase.

Visualization of nucleoli using the reaction for nucleophosmin (B23) revealed the heterogeneity of their structure, with smooth contours and a rounded shape being constant. The presence of additional nucleoli was found not to be typical of substantia nigra neurons. All observed neurons contained only one large nucleolus brightly stained in the reaction for nucleophosmin; the nucleolus often contained a slightly stained region. A similar structure, which had been previously called nucleolus vacuole, was regularly found in the nucleoli of large neurons [18]. Later, the structure was found to be a giant fibrillar center (GFC) containing, predominantly, the UBF factor [19]. Interestingly, the nucleoli of neurons from different subjects from the study sample were characterized by a degree of individuality in size and a fairly low variability in size (*Table*).

Measurements of the nucleoli of neuromelanin-containing substantia nigra neurons

Case	Mean diameter (X), μm	Standard deviation, σ	Variation coefficient (V), %
Male, 25 y.o.	5.1	0.6	11.3
Male, 51 y.o.	4.2	0.4	8.6
Male, 61 y.o.	5.9	0.5	8.9
Female, 62 y.o.	6.1	0.3	4.9
Female, 78 y.o.	5.6	0.3	5.6
Male, 87 y.o.	5.6	0.4	6.8

The investigation of the nucleolus using confocal microscopy confirmed the accuracy of the measuremets performed on the immunoperoxidase samples. In this case, a potential false increase in the size of the studied structure due to chromogen diffusion was excluded. The giant fibrillar center that was usually located at the nucleolus periphery was found to reach 1–2 μm in diameter. The GFC area was characterized by weak fluorescence in the reaction for B23, which indicates a reduced concentration (but not an absence) of the protein in this nucleolar compartment. The peripheral GFC portion often contained a brightly fluorescing granule concentrating the B23 protein (*Fig. 3*).

The double B23 protein and ubiquitin reaction clearly visualized the nucleolus and Marinesco bodies. A high fluorescence intensity during the detection of both markers enabled adequate three-dimensional reconstruction of the studied structures, both in the translucent object mode and in the object surface contour mode (*Fig. 4*). Spatial reconstruction of nucleoli and Marinesco bodies revealed that not all observed objects had a regular spherical shape. For example, ball or ellipsoid shapes were typical of the nucleoli, but single nucleoli had pear and dumbbell shapes.

Marinesco bodies were characterized by high polymorphism, but they always had clear contours (*Fig. 5*). These bodies were present in neuronal nuclei in different amounts (up to six within the nucleus of one cell) and occupied a different position relative to the nucleolus. For example, the body could be closely associated with the nucleolus and be immediately adjacent to its surface, but in most cases, the body was located at a short distance from the nucleolus or was remote from it. If one nucleus contained several Marinesco bodies, the bodies could be both remote from each other and grouped, sometimes with direct contact of the boundaries. The localization of several bodies relative to the nucleolus was also different. We observed cases where a fraction of the bodies were immediately adjacent to the nucleolus boundary, while other bodies were re-

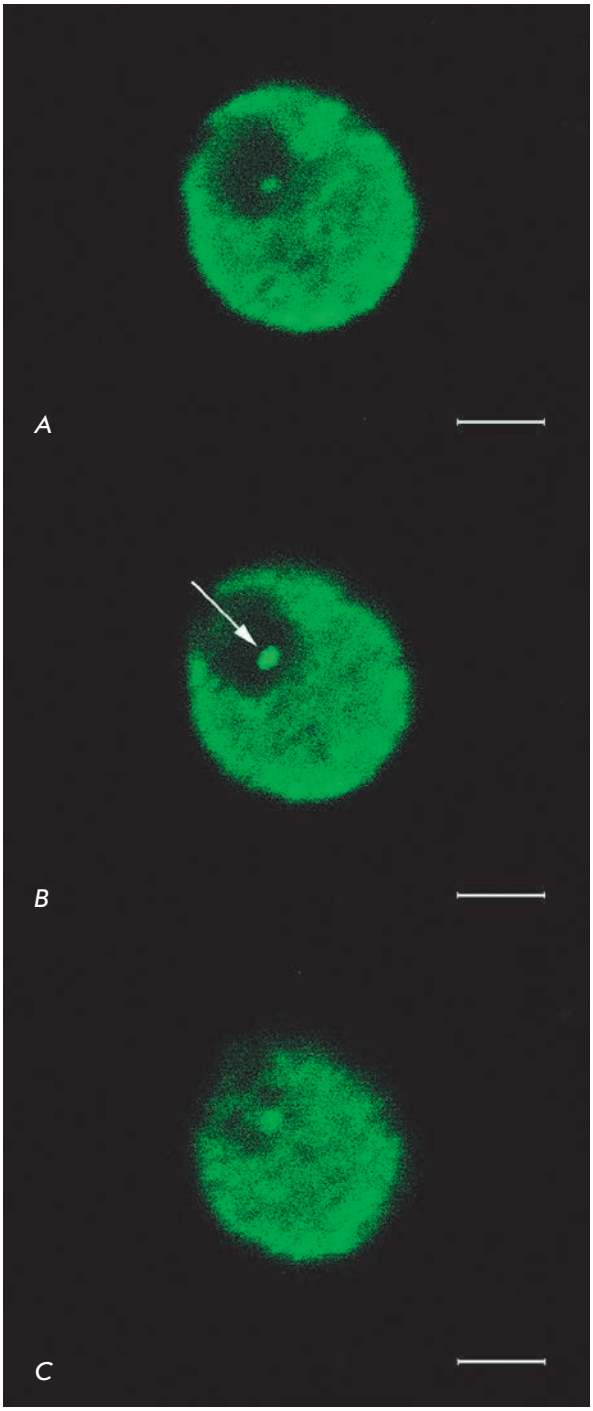

Fig. 3. The nucleolus of a human substantia nigra dopaminergic neuron. Consecutive optical sections with a 0.4 μm interval. *The arrow* indicates an immunopositive granule near a giant fibrillar center. Protein B23 immunocytochemistry is visualized with fluorochrome Cy2 (*green*). Confocal laser microscopy. Plan-Apochromat objective lens 100×/1.40 Oil DIC M27 (oil immersion). Scale bar=2 μm.

mote from it. Sometimes, bodies surrounded the nucleolus from different directions. In some cases, all bodies occurred at a considerable distance from the nucleolus. The use of 3D reconstruction enabled a visualization of all shape details of the detected Marinesco bodies (*Fig. 5*). Our findings indicate that most of the identified bodies had a regular rounded, and less often oval, shape. However, in some cases, flattened or concave regions were present on the surface of detected bodies. The formation of this complex surface pattern of the Marinesco body may be caused by the presence of another structure directly adjacent to the surface of this body. Indirectly, this is confirmed by our earlier data indicating that flattened or concave regions of ubiquitin-immunopositive bodies can form on the body surface at the contacts of the bodies with the nucleolus [15]. Furthermore, in several cases, there were ubiquitin-immunopositive bodies adjacent to the surface of a structure that we defined as an additional nucleolus; flattening or concavity was also formed on the surface of these bodies [15]. However, the double ubiquitin and B23 reaction demonstrated that, in some cases, Marinesco bodies are remote from the B23-positive nucleolus but still have a complex surface shape. This may be an indication that the nuclei of substantia nigra neurons may contain other structures that interact with Marinesco bodies. On the other hand, the irregular contour of these bodies in the absence of a bounding membrane may reflect the dynamics of macromolecules and be a result of an escape of molecules from the peripheral parts of Marinesco bodies.

Another important result obtained by confocal microscopy with layer scanning and 3D reconstruction was a detailed description of the morphology of specific ubiquitin-positive structures that, for a number of reasons, cannot be considered as Marinesco bodies but are clearly identified by an appropriate reaction for ubiquitin (*Fig. 5*). These structures are of a relatively small size (up to 1 μm in length) and of various shapes (round, oval, rod-shaped, etc.). Like Marinesco bodies, these structures are characterized by the variability of their distribution within the nucleus, with the structures being often located near typical Marinesco bodies and sometimes adjoining them. It is worth noting that when these ubiquitin-positive structures directly adjoin typical Marinesco bodies, the surface of the latter contains flattened or concave areas facing this structure, which indirectly confirms the suggestion that the complex surface of Marinesco bodies forms non-randomly. The nature of the identified ubiquitin-immunopositive structures that are not Marinesco bodies remains unknown. In this regard, of great importance are the data presented by M. Lafarga et al., who found (using confocal and electron microscopy) special structures, called

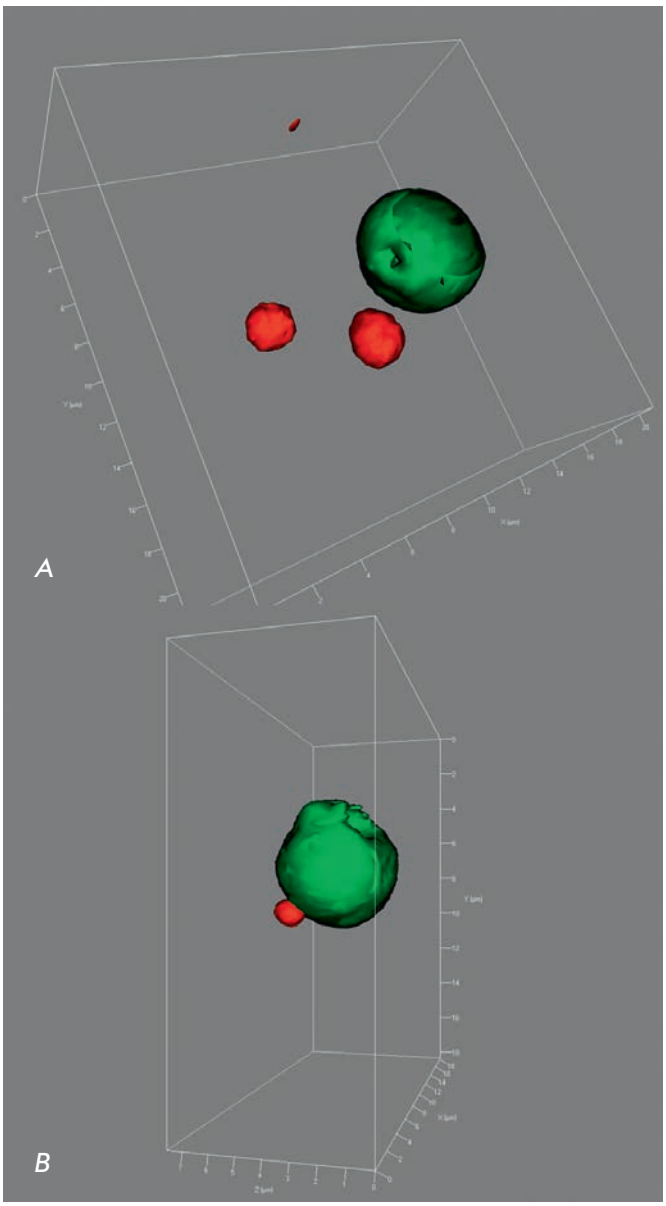

Fig. 4. 3D reconstruction of intranuclear structures of human substantia nigra dopaminergic neurons. Double immunocytochemistry for the B23 protein is visualized with fluorochrome Cy2 (*green*, stained nucleolus), and that for ubiquitin is visualized with fluorochrome TRITC (*red*). Confocal laser microscopy. 3D surface reconstruction is carried out using a ZEN 2011 software module (Zeiss, Germany). Z-stack covers a depth of 9.8 μm (*A*) and 7.6 μm (*B*); the number of optical sections is 50 (*A*) and 39 (*B*). Plan-Apochromat objective lens 100×/1.40 Oil DIC M27 (oil immersion).

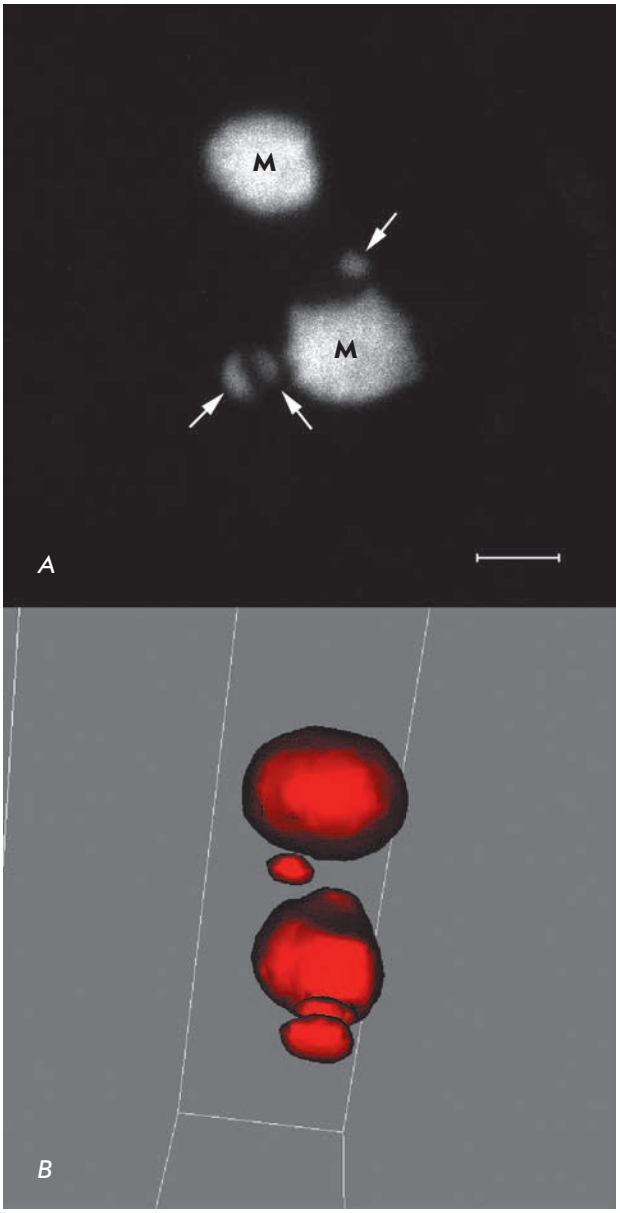

Fig. 5. Marinesco bodies in the nucleus of a dopaminergic neuron of human substantia nigra. *M* – Marinesco bodies; *arrows* – ubiquitin-immunopositive structures that are not typical Marinesco bodies. Confocal laser microscopy. *A* – the image is a superposition of 30 optical sections made with a 0.2 μm interval; *B* – 3D surface reconstruction rotated by 90° is carried out using a ZEN 2011 software module (Zeiss, Germany). Z-stack covers a depth of 5.8 μm; the number of optical sections is 30. Plan-Apochromat objective lens 100×/1.40 Oil DIC M27 (oil immersion). Scale bar = 2 μm.

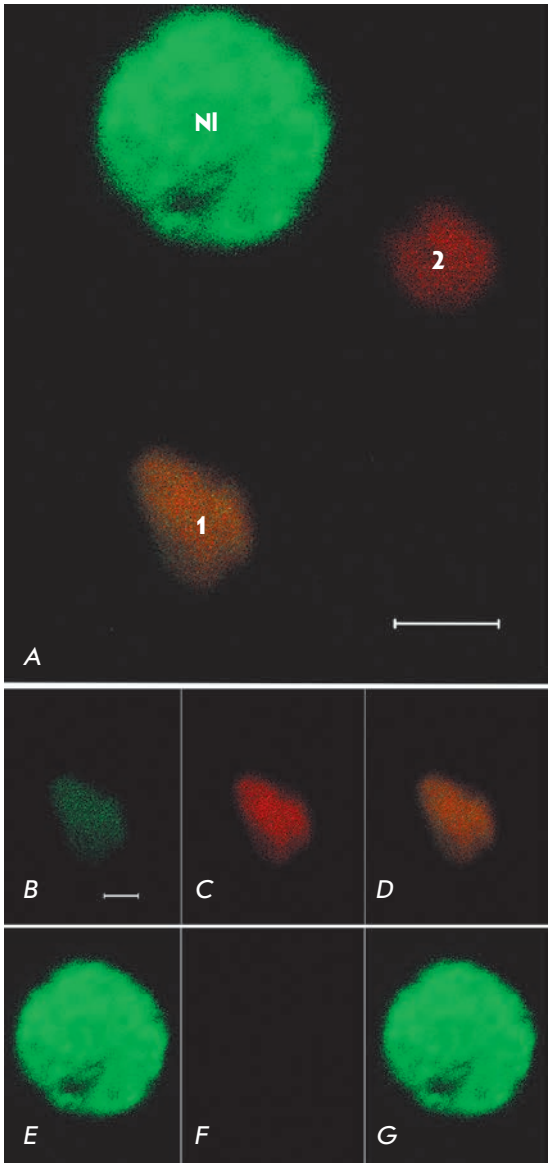

Fig.6. Colocalization of the B23 protein and ubiquitin in the nucleus of a human substantia nigra dopaminergic neuron. *A* – a general view showing the immunopositive reaction of nuclear structures; *B* – colocalization of the B23 protein and ubiquitin in a typical Marinesco body (*structure 1*). *Nl* – a B23-immunopositive neuronal nucleus (without colocalization with ubiquitin), *structure 2* – a typical Marinesco body (without colocalization of the studied proteins). *B*, *E* – a green channel (protein B23). *C*, *F* – a red channel (ubiquitin). *D*, *G* – an aligned image. Double immunocytochemistry for the B23 protein is visualized with fluorochrome Cy2 (*green*), and that for ubiquitin is visualized with fluorochrome TRITC (*red*). Confocal laser microscopy. Plan-Apochromat objective lens 100×/1.40 Oil DIC M27 (oil immersion). Scale bars = 2 μm (*A*) and 1 μm (*B*–*G*).

clastosomes, in the nuclei of several cell types [20]. According to [20], these intranuclear structures contain ubiquitin at a high concentration and are the site of destruction of various proteins. In this case, the presence of clastosomes in cell nuclei is determined by the intensity of the proteasome degradation processes in the cell: the more intense the processes, the more pronounced the clastosomes [20]. This circumstance could explain the presence of ubiquitin-positive structures only in single substantia nigra neurons, along with their absence in most cells, by the different functional states of the analyzed neurons.

An investigation of the colocalization of two proteins (ubiquitin and B23) in the nucleoli of dopaminergic neurons and Marinesco bodies demonstrated the presence of the B23 protein and the absence of ubiquitin in the nucleolus. The B23 protein never colocalizes with ubiquitin in the nucleolus. Even when ubiquitin-immunopositive bodies are in direct contact with the nucleolus (*Fig. 4B*), the area of apparent colocalization does not exceed the resolution of the used equipment (0.2 μm). In contrast to the nucleolus, the colocalization of ubiquitin and the B23 protein in Marinesco bodies is atypical but possible (*Fig. 6*). In this case, the fluorescence of B23 is much weaker than that in the area of the intensely stained nucleolar regions and is comparable to the fluorescence of the GFC region. The identification of bodies where the B23 protein is present and colocalized with ubiquitin in the neuronal nuclei raises a question as to the nature of these structures. There is evidence that ubiquitin (along with ubiquitin-like proteins) plays an important role not only in intracellular protein degradation processes, but also in ribosome biogenesis [16], which suggests the presence of this protein in the nucleolus. However, as seen from *Figure 6*, the identified B23/ubiquitin-immunopositive structure is characterized by an irregular shape, as well as by the lack of internal structuredness and a GFC region; therefore, it cannot be defined as the nucleolus, especially given the above data on the absence of additional nucleoli in substantia nigra dopaminergic neurons. The peculiarities of the shape and size of the identified bodies, as well as the high concentration of ubiquitin in them, rather indicate that these intranuclear structures are a specific type of Marinesco bodies that contain the B23 protein. However, we cannot exclude the fact that the detected B23/ubiquitin-immunopositive structures could be independent intranuclear inclusions that are not related to Marinesco bodies or clastosomes.

CONCLUSION

Our findings indicate that the nuclei of dopaminergic neurons of the human substantia nigra comprise several types of structures that contain the studied proteins and have various shapes. The clastosome-like structures are characterized by relatively small sizes (up to 2 μm in diameter), a regular shape, and location near the nucleolus. At different distances from the nucleolus, there are larger polymorphic Marinesco bodies (usually 2–4 μm in diameter) that include atypical structures containing both ubiquitin and the B23 protein. The largest and most constant structure of the nucleus is the nucleolus. We have demonstrated the monomorphism and stability of the nucleolus size in human substantia nigra neurons. The nucleolus of dopaminergic neurons was found by us to be characterized by the presence of a giant fibrillar center (GFC) that had been previously studied in detail only in the neurons of laboratory animals. We have demonstrated that human GFC, unlike rat GFC, includes a non-constant microstructure containing the B23 protein.

All of these facts provide new information on the dopaminergic neurons of the human brain. Further research in this area to investigate the spatial relationship of the nucleolus and Marinesco bodies with other intranuclear structures (Cajal bodies, PML bodies, nuclear speckles), as well as the dynamics of these structures in neurodegeneration, will elucidate how the intranuclear structures are involved in the regulation of the functional state of catecholaminergic neurons. Studying the distribution of the proteins comprised in these structures in norm and pathology may facilitate the identification of new molecular markers of the neurodegeneration process. The analysis of the intranuclear structures of neurons resistant to damaging factors will demonstrate the presence (or absence) of a relationship between the features of intranuclear inclusions and the selective sensitivity of substantia nigra dopaminergic neurons to damage.

This work was supported by the Russian Science Foundation (project No. 14-15-00014).

REFERENCES

1. Gavrilov A.A., Razin S.V. // Mol Biol (Mosk). 2015. V. 49. № 1. P. 26–45.
2. Kettner M., Willwohl D., Hubbard G.B., Rüb U., Dick E.J. Jr., Cox A.B., Trottier Y., Auburger G., Braak H., Schultz C. // Exp. Neurol. 2002. V. 176. P. 117–121.
3. Grigorev I.P., Korzhevskii D.E. // Medical Academic Journal. 2015. V. 15. № 2. P. 28–34.
4. Okuwaki M. // J. Biochem. 2008. V. 143. № 4. P. 441–448.
5. Colombo E., Alcalay M., Pelicci P.G. // Oncogene. 2011. V. 30. № 23. P. 2595–2609.
6. Pfister J.A., D'Mello S.R. // Exp. Biol. Med. (Maywood).

2015. V. 240. № 6. P. 774–786.
7. Marquez-Lona E.M., Tan Z., Schreiber S.S. // Biochem. Biophys. Res. Commun. 2012. V. 417. № 1. P. 514–520.
8. Lim A.C.B., Qi R.Z. // J. Alzheimers Dis. 2003. V. 5. P. 329–335.
9. Ranganathan S., Bowser R. // Am. J. Pathol. 2003. V. 162. P. 823–835.
10. Neve R.L., McPhie D.L. // Pharmacol. Ther. 2006. V. 111. P. 99–113.
11. Hornykiewicz O. // Pharmacol. Rev. 1966. V. 18. № 2. P. 925–964.
12. Kozina E.A., Khakimova G.R., Khaindrava V.G., Kucheryanu V.G., Vorobyeva N.E., Krasnov A.N., Georgieva S.G., Kerkerian-Le Goff L., Ugrumov M.V. // J. Neurol. Sci. 2014. V. 340. № 1–2. P. 198–207.
13. Filatova E.V., Shadrina M.I., Alieva A.K., Slominsky P.A., Kolacheva A.A., Ugrumov M.V. // Doklady Biochemistry and Biophysics. 2014. V. 456. № 1. P. 116–118.
14. Alexopoulou Z., Lang J., Perrett R.M., Elschami M., Hurry M.E., Kim H.T., Mazaraki D., Szabo A., Kessler B.M., Goldberg A.L., et al. // Proc. Natl. Acad. Sci. USA. 2016. V. 113. № 32. P. E4688–4697.
15. Grigor'ev I.P., Korzhevskii D.E., Sukhorukova E.G., Gusel'nikova V.V., Kirik O.V. // Cell Tiss. Biol. 2016. V. 10. № 1. P. 29–36.
16. Stavreva D.A., Kawasaki M., Dundr M., Koberna K., Müller W.G., Tsujimura-Takahashi T., Komatsu W., Hayano T., Isobe T., Raska I., et al. // Mol. Cell. Biol. 2006. V. 26. № 13. P. 5131–5145.
17. Korzhevskii D.E., Sukhorukova E.G., Kirik O.V., Grigorev I.P. // Eur. J. Histochem. 2015. V. 59. № 3. P. 25–30.
18. Oksova E. E. // Arch. Anat. Histol. Embryol. 1972. V.63. № 10. P. 33–36.
19. Casafont I., Bengoechea R., Navascués J., Pena E., Berciano M.T., Lafarga M. // J. Struct. Biol. 2007. V. 159. № 3. P. 451–461.
20. Lafarga M., Berciano M.T., Pena E., Mayo I., Castaño J.G., Bohmann D., Rodrigues J.P., Tavanez J.P., Carmo-Fonseca M. // Mol. Biol. Cell. 2002. V. 13. № 8. P. 2771–2782.

Induction of ICAM-1 Expression in Mouse Embryonic Fibroblasts Cultured on Fibroin-Gelatin Scaffolds

M. A. Nosenko[1,2,4], N. V. Maluchenko[1], M. S. Drutskaya[1,2], A. Y. Arkhipova [1], I. I. Agapov[3], S. A. Nedospasov[1,2,4], M. M. Moisenovich[1]*

[1]Faculty of Biology, Lomonosov Moscow State University, Leninskie Gory 1, bldg. 12, Moscow, 119234, Russia

[2]Laboratory of Molecular Mechanisms of Immunity, Engelhardt Insitute of Molecular Biology, Vavilov Str. 32, Moscow, 119991, Russia

[3]Laboratory of Bionanotechnologies, Shumakov Federal Scientific Center for Transplantology and Artificial Organs, Schukinskaya Str. 1, Moscow, 123182, Russia

[4]German Rheumatism Research Center, Chariteplatz 1, Berlin, 10117, Germany

*E-mail: mmoisenovich@mail.ru

Received: December 01, 2016; in final form May 26, 2017

ABSTRACT **Culturing of allogeneic or autologous cells in three-dimensional bioresorbable scaffolds is an important step in the engineering of constructs for regenerative medicine, as well as for experimental systems to study the mechanisms of cell differentiation and cell-to-cell interaction. Artificial substrates can modulate the phenotype and functional activity of immobilized cells. Investigating these changes is important for understanding the fundamental processes underlying cellular interactions in a 3D microenvironment and for improving tissue-engineered structures. In this study, we investigated the expression of the ICAM-1 adhesion molecule in mouse embryonic fibroblasts (MEF) when cultured on gelatin-fibroin scaffolds. Increased expression of ICAM-1 in MEF was detected only under 3D culture conditions both at the mRNA and protein levels. At the same time, the MEF cultured on various substrates did not oerexpress MAdCAM-1, indicating the selective effect of 3D culture conditions on ICAM-1 expression. One possible mechanism for ICAM-1 induction in MEF is associated with the activation of AP-1, since expression of c-Fos and Junb (but not cJun and Jund) was increased in MEF in 3D. When cultured under 2D conditions, the expression level of AP-1 components did not change.**

KEYWORDS **MEF, bioengineering, polymeric matrix, stromal cells, ICAM-1, 3D culture.**

ABBREVIATIONS **2D – two-dimensional culture conditions, 3D – three-dimensional culture conditions, MEF – mouse embryonic fibroblasts, FB – fibroblasts, ECM – extracellular matrix, FG – fibroin scaffold supplemented with 30% gelatin.**

INTRODUCTION

We have previously engineered a fibroin-gelatin sponge scaffold which provides a substrate for the adhesion and proliferation of various cell types [1]. Subcutaneous injection of 200–400 μm fragments of this scaffold facilitated the regeneration of deep skin wounds in mice, apparently because of their immunomodulating activity [2]. One possible mechanism underlying the regenerative activity of gelatin-fibroin scaffolds could be an increase in the expression of adhesion molecules, which are involved in immune responses, by fibroblasts after they come into contact with the scaffold surface. Presumably, ICAM-1 is one of such molecules. Normally, only a small amount of ICAM-1 is present on fibroblasts, but changes in the microenvironment can lead to an increase in its expression. In line with this fact, the inflammatory response results in a significant increase in ICAM-1 expression by tissue-specific fibroblasts, which in turn promotes the migration of the immune cells to the site of the inflammation [3, 4]. Moreover, ICAM-1 is important for the functioning of lymphoid organs, where this molecule facilitates contact interactions between immune, stromal, and endothelial cells [5]. Thus, reconstitution of these and other interactions mediated by the 3D environment both *in vitro* and *in vivo* is an important step in the engineering of artificial lymphoid tissue [6].

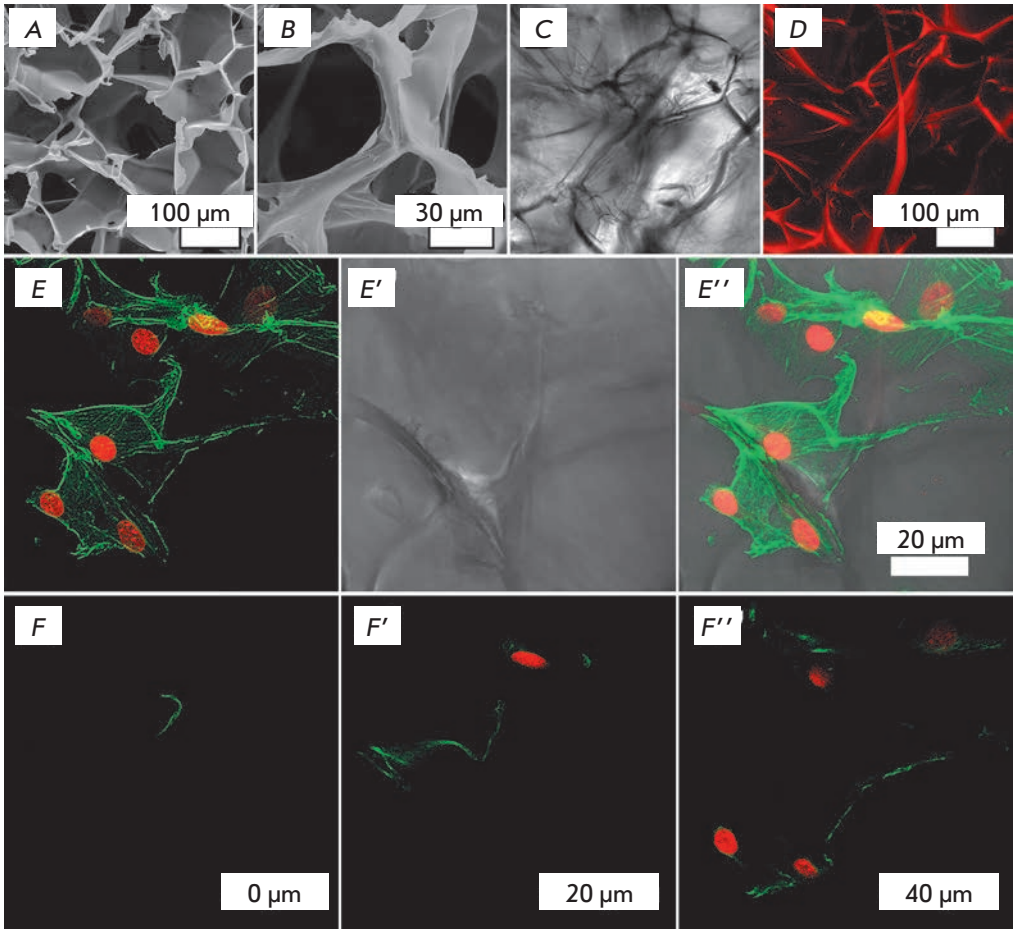

Fig. 1. Scaffold microstructure and MEF cytoskeleton under 3D culture conditions. Scaffold images obtained by scanning electron microscopy (A–B); scaffold images obtained by transmitted-light confocal scanning in an aqueous medium (DIC, C); Z-projection of 150 optical sections of the scaffold at 1.2 μm intervals, where the scaffold material was stained with TRITC and detected using a 20x/0.75 oil immersion CFI Plan Apo VC lens (D). E–E′′ – Z-projection of 242 optical sections series at 281 nm intervals (68.002 μm) of MEF cultured on a 3D scaffold. F–F′′ – Optical sections obtained 0 (F), 20 (F′) and 40 (F′′) μm apart from the initial scanning position. The cell cytoskeleton was stained with phalloidin-FITC (green), and nuclei were stained with SYTOX orange (red). CLSM images were acquired using a Apo TIRF 60x/1.49 oil DIC objective.

MATERIALS AND METHODSS

A primary culture of MEF, as well as sponge fibroin scaffolds supplemented with 30% gelatin (3D FG), was prepared as previously described [1]. For the generation of fibroin-gelatin films, the same aqueous solution as that for 3D scaffolds was used. Firboin-gelatin films or Nunc culture plastic (Thermo Fisher Scientific, USA) were used for a 2D culture.

Total RNA was isolated from MEFs and analyzed according to the standard protocol using the TRI Reagent (Sigma Aldrich, USA), reverse transcription kits (Thermo Scientific, EN0521 and K1621), and a real-time PCR kit (Synthol M-440) in compliance with the manufacturer's recommendations. The quality of the reactions was evaluated using a melting curve analysis and the electrophoresis of amplification products in 1.8% agarose gel. Photographs of the gels were prepared using the GelDoc™ XR+ System (BioRad, USA). Total RNA isolated from murine lymph nodes was used as a positive control in the analysis of *Madcam1* gene expression. A quantitative PCR analysis was performed on a 7500 RT-PCR System instrument (Applied Biosystems, USA).

Immunofluorescence staining was performed using αICAM1-Cy5 antibodies (KAT1), nuclear dye SYTOX orange, and FITC-phalloidin conjugate to visualize polymerized actin. The samples were embedded in Aqua-Poly/Mount (Polysciences,USA) and examined using an electron microscope Camscan Series II (Cambridge Instruments) in the SEI mode and a Nikon Eclipse Ti-E microscope with a confocal module A1 (Nikon Corp., Japan) and Apo TIRF 60×/1.49 Oil or CFI Plan Apo VC 20×/0.75 lens.

RESULTS AND DISCUSSION

Fibroin gelatin scaffolds have a three-dimensional porous structure characterized by complex internal and external topographies *(Fig. 1A–D)*. Importantly, when MEFs are cultured on scaffolds, the interaction of the cell surface with the substrate occurs in various directions *(Fig. 1D, 1E)*. Cell distribution on the surface of a 3D scaffold is also shown in *Fig. 2A*.

Since adhesion molecules play a key role in cell-to-cell and cell-to-extracellular matrix interactions, the expression of the ICAM-1 adhesion molecule was analyzed in 3D and 2D cultures to study the effect of

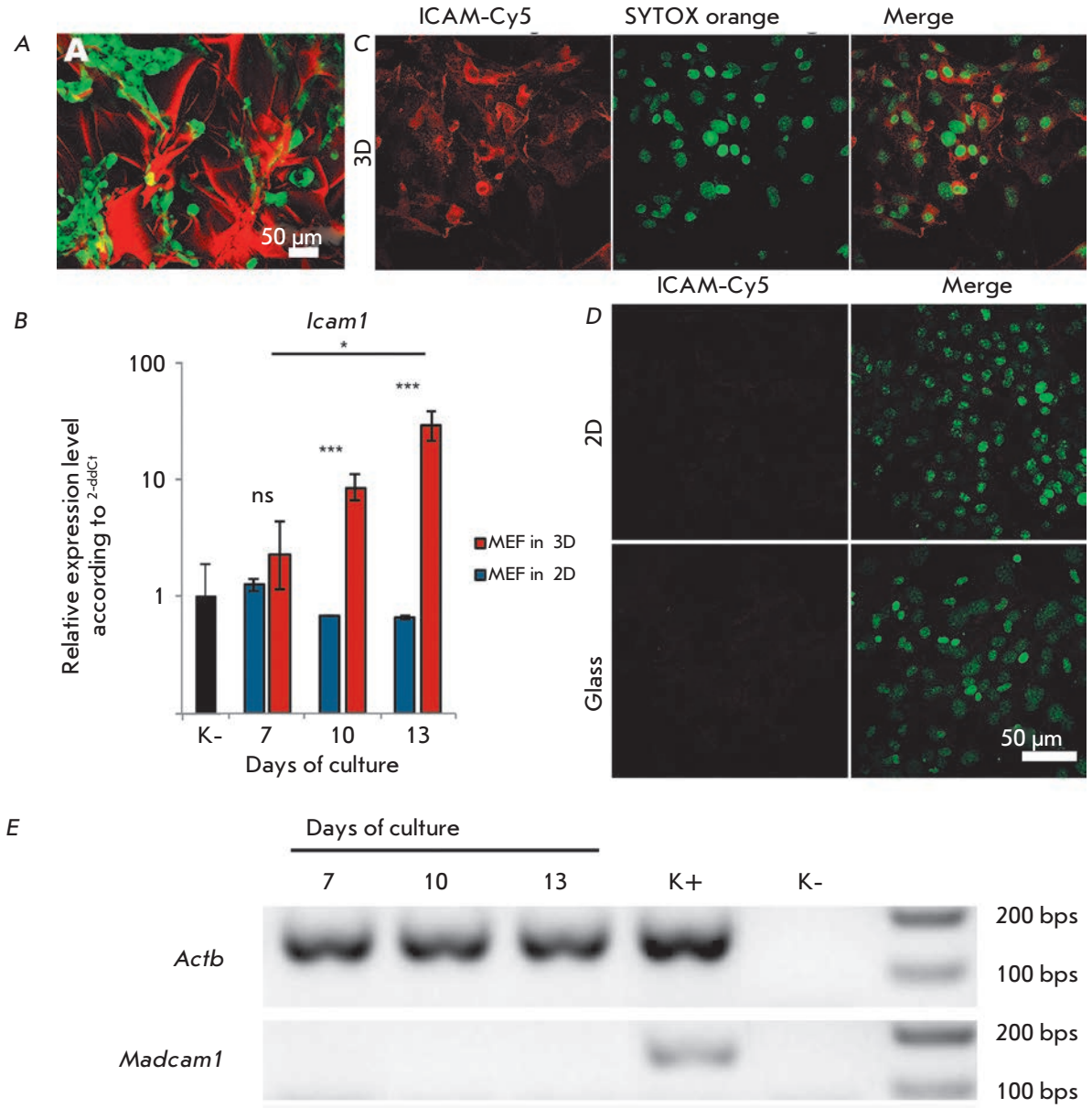

Fig. 2. ICAM-1 expression in MEF. A – Distribution of GFP+ MEF cultured on a 3D fibroin-gelatin scaffold. The scaffold was stained with TRITC. B – *Icam1* expression in MEF cultured on a 2D (plastic) and 3D fibroin-gelatin scaffold. The values were normalized on the baseline *Icam1* expression level in MEF (labeled as "K-"). The data is representative of three independent experiments. * – $p < 0.05$; *** – $p < 0.001$; ns – non-significant difference. C, D – Immunofluorescence staining of ICAM-1 in MEF cultured on a 3D scaffold (C), 2D fibroin film (D, top row), and on a culture plastic surface (D, lower row). CLSM images were acquired using CFI Plan Apo VC 20x/0,75 lens. E – Expression of the *Madcam1* gene in MEF cultured on a 3D fibroin-gelatin scaffold. Agarose gel electrophoresis of PCR products with specific primers to the specified genes is shown. Positive control (K +) – the material from murine lymph nodes; negative control (K-) – no cDNA was added to the PCR mix.

culture conditions on the MEF phenotype. It is known that the cytoplasmic domain of the ICAM-1 molecule interacts with the actin cytoskeleton [7], and ICAM-1 molecules clustering induces their association with actin-binding adapter proteins and binding to the F-actin cytoskeleton [8]. We hypothesized that the cytoskeleton reorganization caused by MEF cultured on 3D fibroin gelatin scaffolds can alter the ICAM-1 expression. Indeed, long-term MEF culture on fibroin gelatin scaffolds, but not on culture plastic, resulted is a signifi-

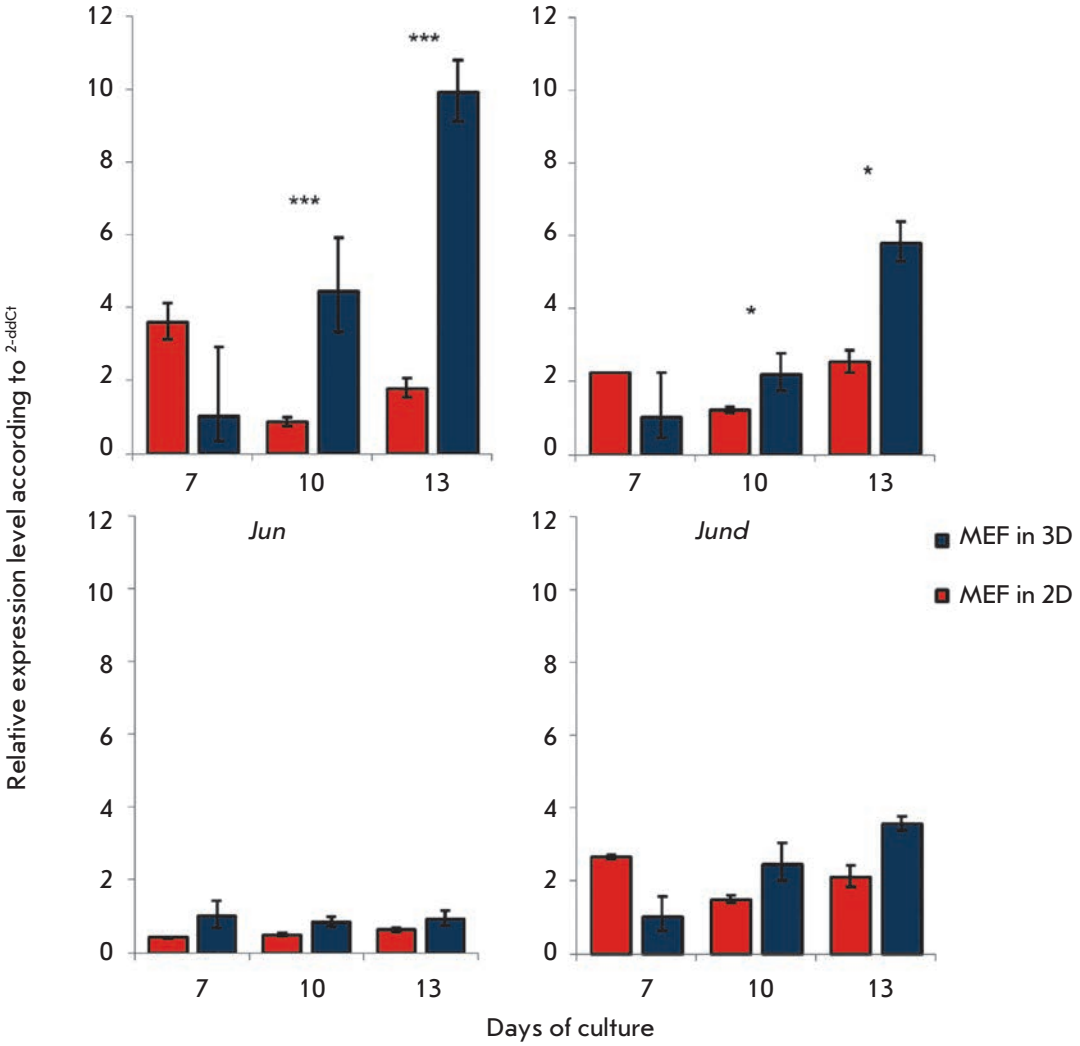

Fig. 3. Expression of AP-1 genes. Expression of AP-1 transcription factor genes in MEF cultured on plastic (2D) and fibroin-gelatin scaffolds (3D). The values were normalized on the gene expression in MEF cultured under 3D conditions on day 7. * – $p < 0.01$; *** – $p < 0.001$.

cant increase in the *Icam1* gene expression (Fig. *2B*). In full agreement with the gene expression data, bright staining of MEF with αICAM1 antibodies was observed only under 3D culture conditions *(Fig. 2B),* while in 2D cultures on FG films or on a glass surface, almost no staining was observed *(Fig. 2D)*. The presence of a very weak signal was due to baseline *Icam1* mRNA expression in 2D cultures *(Fig. 2B*).

Next, we analyzed the gene expression of another adhesion molecule, MAdCAM-1, in order to verify the specificity of the observed effect for ICAM-1 expression. Similarly to ICAM-1, MAdCAM-1 is expressed on stromal and endothelial cells and it is one of the key participants in the immune cell migration to lymphoid organs and barrier tissues, but it is characterized by a specific induction associated with cytokine signaling [9].

We did not detect *Madcam1* gene expression in MEFs cultured on scaffolds, which indicates the selectivity of the effect of 3D-culture conditions on the expression of the genes that encode adhesion molecules *(Fig. 2E*).

It is known that the promoter region of the *Icam-1* gene contains three binding sites for the AP-1 transcription factor, which is involved in its regulation [10]. Thus, one possible mechanism of ICAM-1 induction in MEF might be the altered activity of AP-1. The analysis of the expression of the genes that encode AP-1 subunits *(Fos, Jun, Jund, Junb) (Fig.* 3) demonstrated a significant increase in the level of *Fos* and *Junb* expression under 3D culture conditions as compared to 2D. At the same time, *Jun* and *Jund* expression did not depend on the culture conditions and did not change significantly.

Further investigations should explore which signaling pathways, starting from the mechanistic reception of 3D scaffolds by fibroblasts or intercellular interactions, could lead to AP-1 induction, followed by

ICAM-1 overexpression. In addition, other transcription factors could potentially be involved in the induction of ICAM-1 overexpression in MEF. For example, it is known that NF-χB can regulate ICAM-1 expression [11].

CONCLUSION

The culture of MEF in 3D fibroin-gelatin scaffolds leads to a significant increase in the ICAM-1 expression.

The increase in ICAM-1 expression is associated with the 3D structure of the scaffold rather than the influence of fibroin degradation products, since culturing on 2D fibroin films did not affect the expression of ICAM-1 in MEF.

Increased ICAM-1 expression is associated with increased expression of AP-1 genes, *Fos* and *Junb,* but not *Jun* and *Jund.*

This research was supported by The Russian Foundation for Basic Research (grant No 15-29-04903) and a President of the Russian Federation Grant for Leading Scientific Schools (10014.2016.4).

REFERENCES

1. Moisenovich M.M., Arkhipova A.Y., Orlova A.A., Drutskaya M.S., Volkova S.V., Zacharov S.E., Agapov I.I., Kirpichnikov M.P. // Acta Naturae. 2014. V. 6. № 1. P. 96–101.
2. Arkhipova A.Y., Nosenko M.A., Malyuchenko N.V., Zvartsev R.V., Moisenovich A.M., Zhdanova A.S., Vasil'eva T.V., Agapov I.I., Drutskaya M.S., Nedospasov S.A., Moisenovich M.M. // Biochemistry (Moscow). 2016. V. 81. № 11. P. 1251–1260.
3. Couture P., Paradis-Massie J., Oualha-Morin N., Thibault G. // Exp. Cell Res. 2009. V. 315. № 13. P. 2192–2206.
4. Zandvoort A., van der Geld Y.M., Jonker M.R., Noordhoek J.A., Vos J.T., Wesseling J., Kauffman H.F., Timens W., Postma D.S. // Eur. Respir. J. 2006. V. 28. № 1. P. 113–122.
5. Randall T.D., Carragher D.M., Rangel-Moreno J. // Annu. Rev. Immunol. 2008. V. 26. P. 627–650.
6. Nosenko M.A., Drutskaya M.S., Moisenovich M.M., Nedospasov S.A. // Acta Naturae. 2016. V. 8. № 2. P. 10–23.
7. Carpen O., Pallai P., Staunton D.E., Springer T.A. // J. Cell. Biol. 1992. V. 118. P. 1223–1234.
8. Schaefer A., Te Riet J., Ritz K., Hoogenboezem M., Anthony E.C., Mul F.P., de Vries C.J., Daemen M.J., Figdor C.G., van Buul J.D., Hordijk P.L. // J. Cell. Sci. 2014. V. 127. № 22. P. 4470–4482.
9. Ando T., Langley R.R., Wang Y., Jordan P.A., Minagar A., Alexander J.S., Jennings M.H. // BMC Physiol. 2007. V. 14. № 7. P. 10.
10. Voraberger G., Schafer R, Stratowa C. // J. Immunol. 1991. V. 147. № 8. P. 2777–2786.
11. Roebuck K.A., Finnegan A. // J. Leukoc. Biol. 1999. V. 66. № 6. P. 876–888.

The Minor Variant of the Single-Nucleotide Polymorphism rs3753381 Affects the Activity of a *SLAMF1* Enhancer

L.V. Putlyaeva[1]*, A.M. Schwartz[1], A.V. Klepikova[2,3], I.E. Vorontsov[4], I.V. Kulakovskiy[1,4], D.V. Kuprash[1,5]

[1]Engelhardt Institute of Molecular Biology, Russian Academy of Sciences, Vavilova Str. 32, Moscow, 119991, Russia

[2]Institute for Information Transmission Problems (Kharkevich Institute) of the Russian Academy of Sciences, Bolshoy Karetny per. 19, bldg. 1, Moscow, 127051, Russia

[3]Belozersky Institute of Physico-Chemical Biology, Lomonosov Moscow State University, Leninskie Gory 1, bldg. 40, Moscow, 119234, Russia

[4]Vavilov Institute of General Genetics, Russian Academy of Sciences, Gubkina Str. 3, Moscow, 119991, Russia

[5]Faculty of Biology, Lomonosov Moscow State University, Leninskie Gory 1, bldg. 12, Moscow, 119234, Russia.

*E-mail: lidia.mikhailova@mail.ru

Received: February 08, 2017; in final form May 31, 2017

ABSTRACT **The *SLAMF1* gene encodes CD150, a transmembrane glycoprotein expressed on the surface of T and B-lymphocytes, NK-cells, dendritic cells, and subpopulations of macrophages and basophils. We investigated the functional regulatory polymorphisms of the *SLAMF1* locus associated with autoimmune processes, using bioinformatics and a mutational analysis of the regulatory elements overlapping with polymorphic positions. In the reporter gene assay in MP-1 and Raji B-cell lines, the enhancer activity of the regulatory region of the locus containing the rs3753381 polymorphism demonstrated a twofold increase upon the introduction of the rs3753381 minor variant (G → A) associated with myasthenia gravis. An analysis of the nucleotide context in the vicinity of rs3753381 revealed that the minor version of this polymorphism improves several binding sites for the transcription factors of FOX and NFAT, and RXR nuclear receptors. All mutations that disrupt any of these sites lead to a decrease in the enhancer activity both in MP-1 and in Raji cells, and each of the two B-cell lines expresses a specific set of these factors. Thus, the minor variant of the rs3753381 polymorphism may contribute to the development of myasthenia gravis by modulating *SLAMF1* expression, presumably in pathogenic B-lymphocytes.**

KEYWORDS **autoimmunity, B cells, noncoding polymorphism, transcriptional regulation.**

ABBREVIATIONS **SLAM – signaling lymphocytic activation molecule; CD – cluster of differentiation; IFNγ – interferon gamma; TCR – T-cell receptor; IL – interleukin.**

INTRODUCTION

The SLAMF1/CD150 receptor encoded by the SLAMF1 gene is a transmembrane glycoprotein of 70 kD expressed on the surface of various hematopoietic human and murine cells: B and T cells (at various stages of differentiation), dendritic cells, and subpopulations of macrophages and basophils [1, 2]. The activation of these cells, as well as the activation of monocytes and mast cells enhances the expression of *SLAMF1* [1, 3–5]. In T-lymphocytes, SLAMF1 has a co-stimulatory effect on the antigen-specific CD28-independent proliferation and induces the synthesis of IFN-γ [6], whereas in B-lymphocytes, it induces and enhances the proliferation and synthesis of immunoglobulins [7]. SLAMF1 is also important for bi-directional T-B-cell stimulation. The SLAMF1 protein may serve as a receptor for the measles virus [2], participate in the process of recognition of Gram-negative bacteria, and the subsequent activation of macrophages to kill bacteria [8]. It was shown in murine models that disorders in the signaling pathway of this protein can lead to the development of autoimmune diseases and immunodeficiency conditions [9–11].

Table 1. Polymorphisms of the *SLAMF1* gene locus associated with autoimmune processes

SNP	rs11265455	rs3753381
SLAMF1 gene enhancer	D	E
Association with disease	Type 2 diabetes mellitus	Myasthenia gravis
Risk allele	G (minor)	A (minor)
Alternative allele	A (major)	G (major)
Frequency of risk allele	0.199	0.25
P-values	3.9×10^{-5}	9.63×10^{-6}
OR	1.32 (1.16–1.47)	1.04 (0.87–1.25)
TFBS, presumably destroyed by minor variant of SNP	BPTF	RXR, FOX

Note: *OR* – odds ratio for disease; risk allele/allele associated with the risk of disease; TFBS – transcription factor binding sites.

Today, the role of the four representatives of the SLAM/CD2 family in the development of autoimmune conditions is well-known. Changes in the nucleotide sequences of the *Ly9*, *Ly108*, *CD84*, and *CD244* genes are associated with the initiation of autoimmune processes not only in murine models, but also on a limited cohort of patients. The presence of alternative alleles of the *Ly108* gene in mice strongly affects central tolerance during the development of B- and T-cells, because the *Ly108* gene is involved in the TCR-mediated stimulation of the key proapoptotic molecules BIM and FasL [12], the regulation of immunological tolerance, and cell cycle progression [13]. Furthermore, Ly108 and CD84, along with their adapter SAP (SLAM-associated protein), are involved in a bi-directional T-B-cell stimulation which is required for the formation of germinal centers [14]. It is known that single-nucleotide polymorphisms of the genes that encode selected members of the SLAM/CD2 family are associated with the risk of developing particular autoimmune diseases. It is known that the minor variant of rs509749 in the *CD229* gene (Ly9, SLAMF3) alters the aminoacid sequence of the ITSM-motif of CD229, followed by a change in the receptor affinity to the SAP adapter, which in turn may lead to an increased risk of systemic lupus erythematosis [15, 16]. There is also evidence of an association between the heterozygous variant (GA) of the single-nucleotide polymorphism rs6427528 of the *CD84* gene with a positive response to treatment with etanercept in patients with psoriasis and rheumatoid arthritis [17] and two polymorphisms of the *CD244* (2B4) gene – rs3766379 and rs6682654 – with a progression of rheumatoid arthritis and systemic lupus erythematosus: this was established in a cohort of Japanese patients [18]. It is also known that the rs2049995 polymorphism in the *SAP* gene, encoding the basic adapter protein of SLAM family representatives, correlates with the development of systemic lupus erythematosus [19]. All this evidence is indicative of a relationship between changes in the nucleotide sequences of SLAM genes with the development of various autoimmune diseases.

Two *SLAMF1* polymorphisms associated with autoimmune processes are known *(Table 1)* [20, 21]. The results of genotyping described in these articles suggest that the minor variant of the rs11265455 polymorphism is associated with the risk of type 2 diabetes mellitus, while the minor variant of the rs3753381 polymorphism (G > A) is associated with an increased risk of myasthenia gravis.

According to data obtained in mice with induced obesity, type 2 diabetes, which has previously been known to be the only metabolic disease associated with impaired interaction between insulin and body tissue cells, also has an autoimmune nature [22, 23] and can develop concomitantly with other autoimmune diseases [24, 25]. The B cells involved in the glucose metabolism and activation of proinflammatory macrophages and T cells and the production of a unique profile of IgG autoantibodies in obese humans play an important role in the development of type 2 diabetes. It was shown in a mouse model of type 2 diabetes that anti-CD20-antibodies reduce T cell activation and improve glucose metabolism [22]: and The use of salicylates and IL-1 antagonists, which reduce the glucose level, passed clinical trials [26].

Acquired myasthenia gravis is a rare autoimmune disease which clinically manifests itself in fatigue and weakness of striated muscles [21], [27]. The trigger mechanism that activates the autoimmune response system in myasthenia gravis has not yet been established: autoantibodies against the nicotinic acetylcholine receptors located in the motor nerve termination area are produced, leading to impaired nerve impulse transmission to the muscle [28]. Injection of an immunoglobulin fraction from the serum of a patient with myasthenia gravis, comprising anti-AChR antibodies

(found in 85% of patients) and anti-MuSK antibodies (in 15% of patients), induces myasthenia symptoms in animals [9, 29, 30]. In patients with myasthenia gravis, therapy aimed at reducing the amount of B cells using monoclonal antibodies against CD20 (rituximab) is effective [31]. Change in T-cell receptor (TCR) signaling, which in turn may affect the selection system in thymus, together with the activity of T helpers and regulatory T cells, is another known risk factor of development of autoimmune diseases [32]. The development of many autoimmune diseases, such as systemic lupus erythematosus, polymyositis, dermatomyositis, rheumatoid arthritis, Sjogren's syndrome, multiple sclerosis, acquired epidermolysis bullosa, Crohn's disease, ulcerative colitis, and autoimmune hepatitis, is associated with an impaired production of NKT-cells (Natural Killer T cell)[33]. There is evidence that a twofold increase in *SLAMF1* expression in NOD.Nkrp1b.Tg (Slamf1) mice doubles thNKT-cells production in thymus by means of homotypic interactions (SLAM-SLAM) on the surface of immature NKT-cells and CD4+CD8+ thymocytes, which are required for the development of NKT-cells [9, 34]. A small increase in CD150-SLAMF1 expression also enhances the production of IL-4 and IL-17 in response to stimulation through the TCR [34]. There is evidence that *SLAMF1* is involved in the regulation of IFN-γ production by CD4+ T cells, which can also be indirectly related to the pathogenesis and immune regulation of myasthenia gravis [3]. This suggests that an increase in the production of *SLAMF1* induced by the allelic variant of a single-nucleotide polymorphism can be one of the links in the chain of autoimmune processes.

Recently, we described several regulatory regions that control the expression of the *SLAMF1* gene, including the promoter (297-0 with respect to the translation start site) and three enhancer elements of approximately 2.5 kb, two of them located in the third intron and one at a distance of 3 kbp after the coding sequence [35]. The activity of these regulatory elements was studied in Raji and MP-1 cell lines (Burkitt lymphoma and acute lymphoblastic leukemia models, respectively). It was shown that the expression of *SLAMF1* mRNA is controlled by the EBF1, SP1, STAT6, IRF4, NF-kB, ELF1, TCF3, and SPI1/PU.1 transcription factors, which bind to the promoter and enhancer regions.

This paper presents data on two additional enhancer elements of the *SLAMF1* gene locus (hereinafter enhancers E and D), where two polymorphisms, rs3753381 and rs11265455, associated with autoimmune processes, are localized. We studied the effect of each of these polymorphisms on the expression of the *SLAMF1* gene in B cells. The enhancer E comprising rs3753381 polymorphism is located in the third intron of the *SLAMF1* gene, and enhancer D is located at a distance of 1.5 kbps before the coding region of the gene.

Our study of polymorphisms in the *SLAMF1* gene locus showed that both the minor and major variants of rs11265455 have almost no effect on the activity of the *SLAMF1* promoter, while the minor variant of the rs3753381 polymorphism (located in enhancer E) increases the activity of the *SLAMF1* promoter more than twofold. We identified FOX, RXR, and NFAT as nuclear protein families whose binding depends on the allelic variant of rs3753381 and have pointed at the particular members of these families which are specifically expressed in the investigated cell lines (HNF4G, RXRB, and FOXO2 in the MP-1 and NFATC/3 and NR2C1 in Raji).

EXPERIMENTAL

Cell culture and transfection procedure

MP-1 and Raji cells were cultured in a RPMI medium (PanEco) supplemented with 10% fetal calf serum, *L*-glutamine, antibiotics, essential amino acids, HEPES, and sodium pyruvate. Transfection was performed using the Neon Transfection System (Life Technologies, USA) at the rate of 2×10^6 MP-1 cells and 7×10^6 Raji cells per transfection. Luciferase activity was assayed after 24 hours using a Dual Luciferase Assay kit (Promega, USA).

Plasmid Constructs

Genetic engineering manipulations were carried out using standard techniques; enzymes produced by Fermentas/ThermoScientific (Lithuania) were used. In order to produce the constructs pGL3-rs3753381 (G) and pGL3-rs11265455 (A), sequences of the enhancers E and D, respectively, were amplified with primers containing the restriction sites SalI and BglII (only SalI in the case of enhancer D) and then cloned into a WT SLAMF1 vector [35] cleaved at the BamHI-NcoI sites, together with a fragment of the pGL3-basic vector cleaved at the SalI-NcoI sites. Constructs with alternative variants of the respective polymorphisms, rs3753381 (A) and rs11265455 (G), were produced on the basis of the pGL3-rs3753381 (G) and pGL3-rs11265455 (A) constructs. Mutations at the binding sites of the FOX and RXR proteins were introduced via site-directed mutagenesis of the core sequences of the sites using appropriate primers. Mutagenesis was performed using two-stage PCR, and the resulting constructs were purified using the NucleoBond Xtra Midi Kit (Macherey-Nagel, Germany) and verified by

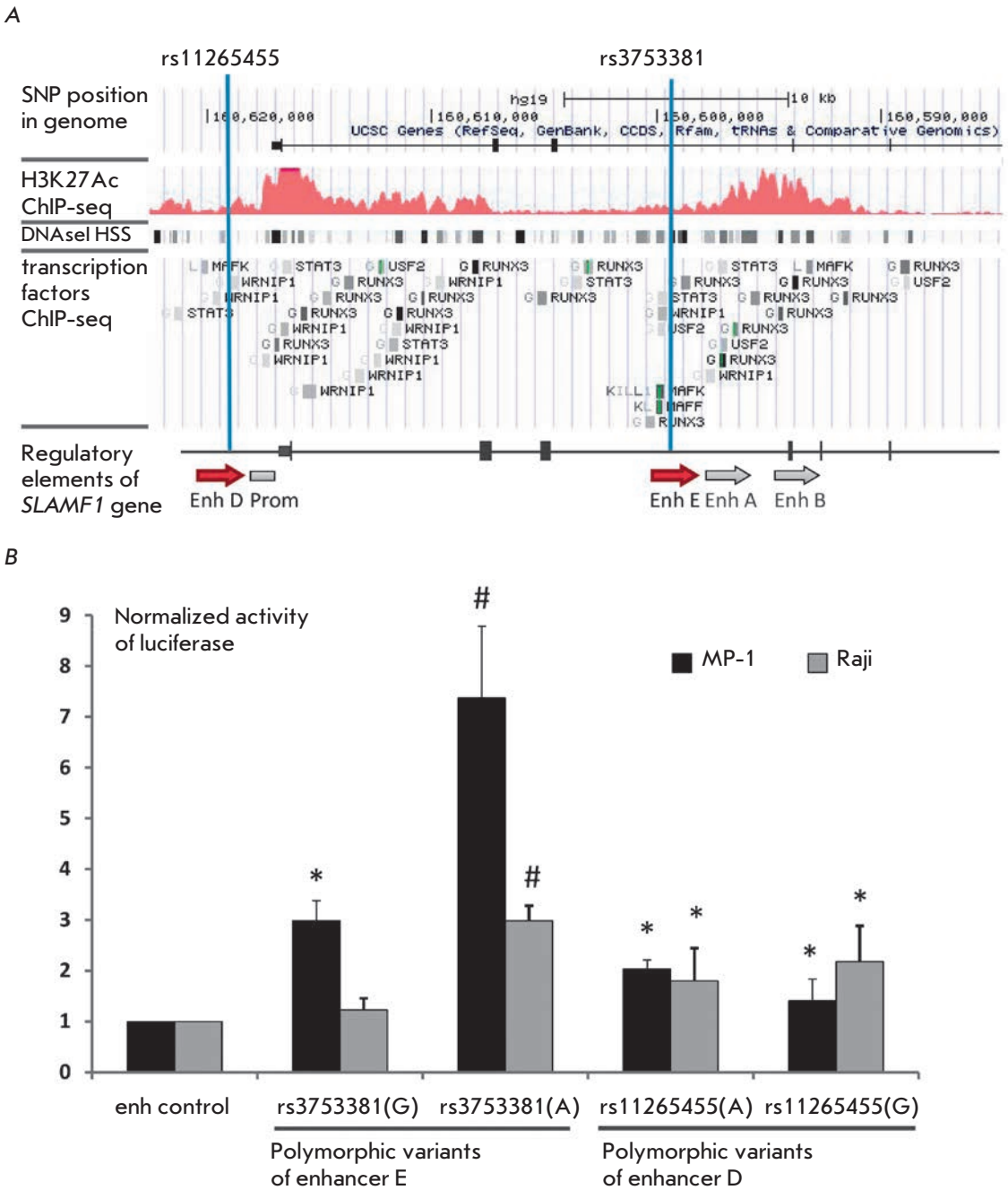

Fig. 1. Analysis of the putative enhancers of the *SLAMF1* gene locus. **A**. Schematic representation of the regulatory elements of the *SLAMF1* locus. Grey arrows indicate enhancers A and B, as described previously [32]; thick black lines indicate *SLAMF1* gene exons; thin lines indicate introns. Red histogram indicates the level of H3K27 acetylation, rectangles mark DNase I hypersensitivity clusters and transcription factor binding sites according to ENCODE ChIP-Seq data. Vertical blue lines schematically show the location of the SNPs rs3753381 and rs11265455. **B.** Effect of allelic variants of rs3753381 and rs11265455 on the activity of enhancers E and D. The bars correspond to the expression of the reporter gene in MP-1 and Raji cell lines, normalized to the activity of the construct containing the control fragment without enhancer activity [32]. All data are from three or more independent experiments. Data represent mean values ± SEM. "*" indicates a statistically significant difference between experimental and control constructs; "#" indicates a statistically significant difference between the construct containing the minor variant of the rs3753381 polymorphism and the construct containing the common variant ($P < 0.05$, Student's t-test).

Table 2. Oligonucleotide primers used in this study.

Primer	Nucleotide sequence 5'-3'	Application
E150−5Sal (for)	TTTTGTCGACCCTGTACCTTATTCT	Amplification of enhancer E and introduction of SalI and BglII restriction sites
E150−5Bgl2 (rev)	TTTAGATCTATCCTTGCCTTAAGGC	
rs3753381-F	ATTTTTACAGAGTTCACAGCTTCCAGA	rs3753381(A) design
rs3753381-R	CTGTGAACTCTGTAAAAATGTTTACTTGGA	
S1enh7F	AGAAGAATTTGGGGGCAGAGAGGACT	Amplification of enhancer D and introduction of SalI restriction site
S1enh7SalR (rev)	AAAAGTCGACCCGCCCTTTTTCATGAGTTAAAC	
for G RXRA	TACGGATTTATCAGCTTCCAGAAAA	mut RXR G design
rev G RXRA	AAGCTGATAAATCCGTAAAAATGT TTAC	
for A RXRA	TACAGATTTATCAGCTTCCAGAAAA	mut RXR A design
rev A RXRA	AGCTGATAAATCTGTAAAAATGT TTAC	
for G FOXO3	CATTACAACGGAGTTCACAGCTT	mut FOX G design
rev G FOXO3	CTCCGTTGTAATGTTTACTTGGATG	
for A FOXO3	CATTACAACAGAGTTCACAGCTT	mut FOX A design
rev A FOXO3	CTCTGTTGTAATGTTTACTTGGATG	

sequencing using the Sanger method. The nucleotide sequences of the primers are shown in *Table* 2.

Bioinformatics analysis of binding sites

The genomic segments in the vicinity of the rs3753381 and rs11265455 polymorphisms of the *SLAMF1* gene locus were analyzed using public ChIP-Seq data for the B-lymphoblastoid cell line GM12878 (which is etiologically similar to the MP-1 and Raji cell lines) available in the UCSC Genome Browser [36]. We considered the presence of the H3K27Ac histone mark, DNAse I accessibility [38] according to ENCODE DNase-Seq data for GM12878, and the presence of experimentally determined transcription factor binding sites as evidence of regulatory elements [39]. Prediction of transcription factor binding sites overlapping with polymorphic positions was carried out using the HOCOMOCO motif collection [40]. The effect of allelic variants on the the predicted binding affinity was assessed using the PERFECTOS-APE software [41] with the default settings.

The analysis of differential gene expression

The MP-1 and Raji samples analyzed in our study were obtained in [35]. The resulting sequencing reads are available in the NCBI Sequence Read Archive: project identification number is PRJNA313457.

RESULTS AND DISCUSSION

The minor variant of rs3753381 polymorphism increases the activity of the *SLAMF1* enhancer.

We have previously described the promoter and three enhancers of the *SLAMF1* gene, A, B, and C [35] (*Fig. 1A*, enhancers A and B are shown by gray arrows). In our study, we chose two additional alleged regulatory regions to analyze the possible impact of single nucleotide polymorphisms on the regulation of *SLAMF1* expression: rs3753381 polymorphism is located in the putative enhancer E (the third intron of *SLAMF1*), and rs11265455 polymorphism is located in the putative enhancer D, which is 1,500 bp upstream of the *SLAMF1* coding region *(Fig. 1A,* shown by red *arrows)*. These regulatory elements were cloned in two stages (see Experimental) into a WT SLAMF1 vector [35]. All constructs stimulated *SLAMF1* promoter activity, which confirms the function of D and E as potential transcription enhancers.

Next, single substitutions were introduced into the sequences of the enhancer elements D and E so as to replace the existing rs3753381 and rs11265455 alleles with alternative variants associated with the development of type 2 diabetes mellitus and myasthenia gravis, respectively (see *Table* 1).

Both putative enhancer elements increase *SLAMF1* promoter activity (see *Fig. 1B*) compared to the previously described [35] control sequence, whose length is equal to that of the tested enhancer elements but is not enriched in transcription factor binding sites or H3K27 acetylation marks. It is noteworthy that the activity of enhancer E was significantly higher in the MP-1 cell line than in the Raji line, and enhancer D activity was low and was about the same in both cell lines. Since these cell lines are similar in terms of maturity and etiology, the difference in the activity of alleged enhancer elements, apparently, can be explained by differences in the transcription factors expression in MP-1 and Raji.

Figure 1B shows that the presence of a minor variant of rs3753381 polymorphism increases the activity of

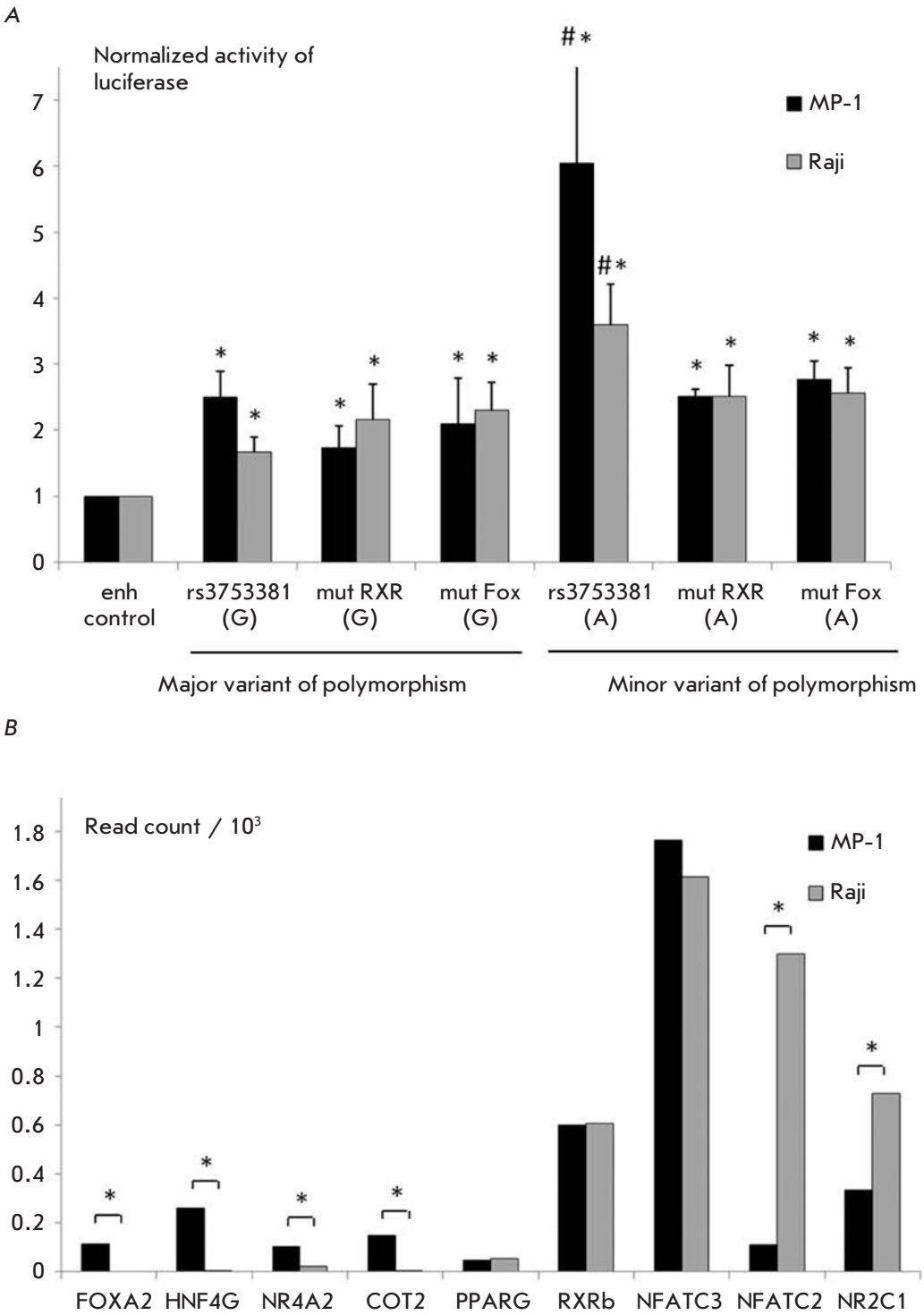

Fig. 2. The influence of allelic variants of the rs3753381 polymorphism on the binding of transcription factors. **A.** The effect of mutations in the RXR and FOX binding sites on the activity of enhancer E. See *Fig. 1B* for legend. **B.** Expression of the transcription factors whose binding could be affected by the mut RXR and mut FOX mutations. The bars correspond to the normalized number of reads obtained from a RNA-seq analysis of MP-1 and Raji cell lines. "*" indicates a statistically significant difference between the samples (FDR < 0.05).

enhancer E in both cell lines, and the minor variant of rs11265455 polymorphism has no significant effect on the activity of enhancer D in any of the examined lines. Therefore, we proceeded with studying the rs3753381 polymorphism in more detail.

Mutations at the RXR and FOX transcription factor binding sites reduce enhancer E activity in the case of minor variant of rs3753381 polymorphism. We performed a bioinformatics analysis of the transcription factor binding sites which could be affect-

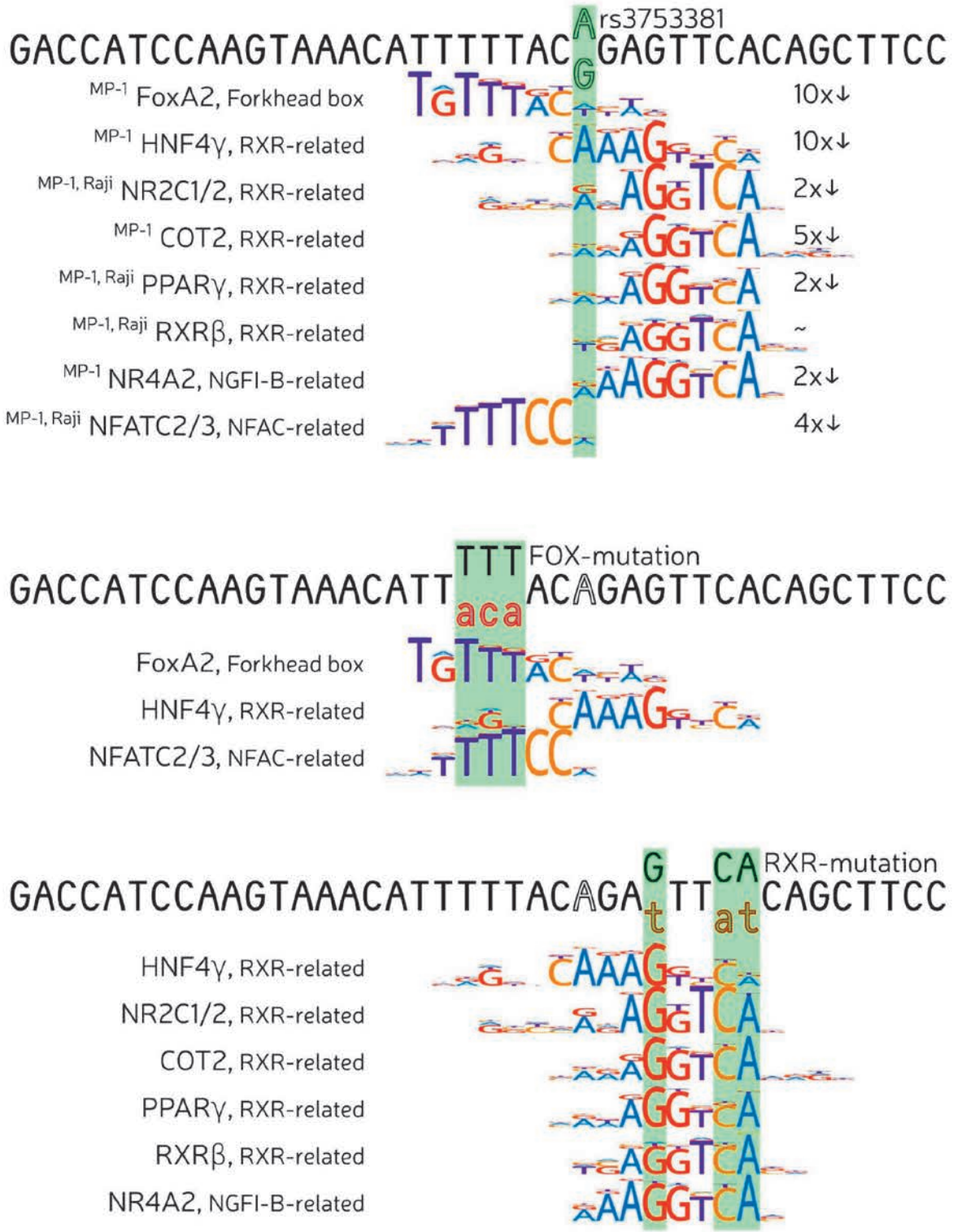

Fig. 3. Alterations of binding site motifs by rs3753381 alleles and mutations of the RXR and FOX sites. The motif logos are shown under the corresponding segments of the enhancer E sequence. The predicted affinity loss for the major allele to minor allele substitution (G > A) is also shown.

ed by the studied polymorphisms in order to explain the significant increase in enhancer E activity when a minor variant (A) of rs3753381 polymorphism was introduced. We analyzed the sites that overlapped with rs3753381 and its allelic variant using the PERFECTOS-APE software. It was found that different members of the NFAT, RXR, and FOX families could bind to the rs3753381 polymorphism region and that their binding sites were stronger in the case of the minor variant (A). The predicted sites were mutated, and the effects of the mutations were tested in a system with a reporter gene *(Fig. 2A)*.

Mutations in the RXR and FOX binding sites significantly reduce the activity of the enhancer with respect to the minor variant of rs3753381. The results were verified using a detailed bioinformatic analysis of the genomic sequence straddling the rs3753381 polymorphism. We selected the most reliable models of the binding sites from the HOCOMOCO database and conducted a joint analysis of all six sequence variants (rs3753381 (G), mut RXR (G), mut FOX (G), rs3753381 (A), mut RXR (A), mut FOX (A), using PERFECTOS-APE. We filtered only the predicted sites having a *P*-value of 0.001 or better for the wild-type sequence with the A allele. Then, we considered only those predictions where the affinity decreased or remained unchanged in all the alternative versions of the sequence (i.e., G allele or introduced mutations). Only the proteins expressed in the MP-1 and Raji cell lines were selected for further analysis *(Fig. 2B*, *Fig. 3)*.

HNF4G, NR4A2, COT2, and PPARG are actively expressed in the MP-1 cell line, which may explain the significant decrease in enhancer E activity in the case of damaged binding sites of the aforementioned factors due to the mut RXR mutation *(Fig. 2A,* mut-RXR (A) and mut RXR (G) constructs). The Raji cell line is characterized by a high expression of RXRB and NR2C1, whose binding sites can be affected by the mut RXR mutation and, therefore, a disturbed binding of each of them can contribute to a reduction in enhancer E activity. As for the FOX factors, whose sites can be affected by the respective mutation, FOXA2 is highly expressed in the MP-1 cell line. NFAC (NFATC2 and NFATC3) proteins, which potentially bind to the same site, are expressed in the Raji cell line. Further, each mut FOX (A), mut FOX (G), mut RXR (A), and mut RXR (G) can affect the HNF4G binding site, and this causes a decrease in enhancer E activity in these constructs in MP-1 cells. When summarizing data on the mut RXR and mut FOX mutations, it can be assumed that the mut RXR mutation is associated with disrupted binding of HNF4G, RXRB, NR4A2, COT2, and PPARG in MP-1, and RXRB and NR2C1 in Raji, while the mut FOX mutation can disrupt the binding of HNF4G and FOXA2 in MP-1 and NFATC2, and NFATC3 in Raji. Thus, a change from the major variant of the rs3753381 polymorphism (G) to the minor rs3753381 (A) may change the binding of the RXR, FOX, and NFAC transcription factors, which are different in the case of MP-1 and Raji cell lines. The HOCOMOCO motif database covers only 600 of more than 1,500 human transcription factors [42]: We cannot exclude the possibility that other members of the aforementioned families likewise bind to the polymorphic region of the enhancer.

CONCLUSION

Our study demonstrates the functional significance of the polymorphisms of the *SLAMF1* locus associated with autoimmune processes, indicating a possible relationship between the rs3753381 and rs11265455 polymorphisms and the regulation of *SLAMF1* gene expression. We explored the association between the minor variant of rs3753381 and the more than twofold increase in the activity of the *SLAMF1* enhancer using the experimental model of human B-lymphoblastoid cell lines. The bioinformatics analysis of the sequences of the minor and major variants of the polymorphisms predicted that transcription factors of the NFAT, FOX, and RXR families likely contribute to the increase in enhancer E activity in the case of the minor variant of the rs3753381 polymorphism. It was shown that mutations in the predicted binding sites reduce the activity of the enhancer E carrying a minor variant of the rs3753381 polymorphism. It was also found that change in the allelic variant of the rs11265455 polymorphism has no significant impact on *SLAMF1* gene expression.

This work was supported by Russian Science Foundation grant No 14-14-01140.

REFERENCES

1. Cannons J.L., Tangye S.G., Schwartzberg P.L. // Annu. Rev. Immunol. 2011. V. 29. P. 665–705.
2. Sidorenko S.P., Clark E.A. // Nat. Immunol. 2003. V. 4. № 1. P. 19–24.
3. Cocks B.G., Chang C.C., Carballido J.M., Yssel H., de Vries J.E., Aversa G. // Nature. 1995. V. 376. № 6537. P. 260–263.
4. Bleharski J.R., Niazi K.R., Sieling P.A., Cheng G., Modlin R.L. // J. Immunol. 2001. V. 167. № 6. P. 3174–3181.
5. Kiel M.J., Yilmaz O.H., Iwashita T., Yilmaz O.H., Terhorst C., Morrison S.J. // Cell. 2005. V. 121. № 7. P. 1109–1121.
6. Aversa G., Carballido J., Punnonen J., Chang C.C., Hauser T., Cocks B.G., De Vries J.E. // Immunol. Cell Biol. 1997. V. 75. № 2. P. 202–205.

7. Punnonen J., Cocks B.G., Carballido J.M., Bennett B., Peterson D., Aversa G., de Vries J.E. // J. Exp. Med. 1997. V. 185. № 6. P. 993–1004.
8. Berger S.B., Romero X., Ma C., Wang G., Faubion W.A., Liao G., Compeer E., Keszei M., Rameh L., Wang N., et al. // Nat. Immunol. 2010. V. 11. № 10. P. 920–927.
9. Berrih-Aknin S., Ragheb S., Le Panse R., Lisak R.P. // Autoimmunity Rev. 2013. V. 12. № 9. P. 885–993.
10. Keszei M., Latchman Y.E., Vanguri V.K., Brown D.R., Detre C., Morra M., Arancibia-Carcamo C.V., Paul E., Calpe S., Castro W., et al. // Internat. Immunol. 2011. V. 23. № 2. P. 149–158.
11. Huang Y.H., Tsai K., Ma C., Vallance B.A., Priatel J.J., Tan R. // J. Immunol. 2014. V. 193. № 12. P. 5841–5853.
12. Snow A.L., Marsh R.A., Krummey S.M., Roehrs P., Young L.R., Zhang K., van Hoff J., Dhar D., Nichols K.E., Filipovich A.H., et al. // J. Clin. Invest. 2009. V. 119. № 10. P. 2976–2689.
13. Kumar K.R., Li L., Yan M., Bhaskarabhatla M., Mobley A.B., Nguyen C., Mooney J.M., Schatzle J.D., Wakeland E.K., Mohan C. // Science. 2006. V. 312. № 5780. P. 1665–1669.
14. Wang A., Batteux F., Wakeland E.K. // Curr. Opin. Immunol. 2010. V. 22. № 6. P. 706–714.
15. Margraf S., Garner L.I., Wilson T.J., Brown M.H. // Immunology. 2015. V. 146. № 3. P. 392–400.
16. Cunninghame Graham D.S., Vyse T.J., Fortin P.R., Montpetit A., Cai Y.C., Lim S., McKenzie T., Farwell L., Rhodes B., Chad L., et al. // Genes Immunity. 2008. V. 9. № 2. P. 93–102.
17. van den Reek J.M., Coenen M.J., van de L'Isle Arias M., Zweegers J., Rodijk-Olthuis D., Schalkwijk J., Vermeulen S.H., Joosten I., van de Kerkhof P.C., Seyger M.M., et al. // Br. J. Dermatol. 2017. V. 176. № 5. P. 1288–1296.
18. Suzuki A., Yamada R., Kochi Y., Sawada T., Okada Y., Matsuda K., Kamatani Y., Mori M., Shimane K., Hirabayashi Y., et al. // Nat. Genet. 2008. V. 40. № 10. P. 1224–1229.
19. Furukawa H., Kawasaki A., Oka S., Shimada K., Matsui T., Ikenaka T., Hashimoto A., Okazaki Y., Takaoka H., Futami H., et al. // Lupus. 2013. V. 22. № 5. P. 497–503.
20. Tabassum R., Mahajan A., Dwivedi O.P., Chauhan G., Spurgeon C.J., Kumar M.V., Ghosh S., Madhu S.V., Mathur S.K., Chandak G.R., et al. // J. Hum. Genet. 2012. V. 57. № 3. P. 184–190.
21. Na S.J., Lee J.H., Kim S.W., Kim D.S., Shon E.H., Park H.J., Shin H.Y., Kim S.M., Choi Y.C. // Yonsei Med. J. 2014. V. 55. № 3. P. 660–668.
22. Winer D.A., Winer S., Shen L., Wadia P.P., Yantha J., Paltser G., Tsui H., Wu P., Davidson M.G., Alonso M.N., et al. // Nature Medicine. 2011. V. 17. № 5. P. 610–617.
23. Lee H.M., Kim J.J., Kim H.J., Shong M., Ku B.J., Jo E.K. // Diabetes. 2013. V. 62. № 1. P. 194–204.
24. Brooks-Worrell B., Palmer J.P. // Clin. Exp. Immunol. 2012. V. 167. № 1. P. 40-46.
25. Theodorakopoulou E., Yiu Z.Z., Bundy C., Chularojanamontri L., Gittins M., Jamieson L.A., Motta L., Warren R.B., Griffiths C.E. // Br. J. Dermatol. 2016. V. 175. № 5. P. 1038–1044.
26. Donath M.Y., Shoelson S.E. // Nat. Rev. Immunol. 2011. V. 11. № 2. P. 98–107.
27. Kaya G.A., Coskun A.N., Yilmaz V., Oflazer P., Gulsen-Parman Y., Aysal F., Disci R., Direskeneli H., Marx A., Deymeer F., et al. // PLoS One. 2014. V. 9. № 8. P. e104760.
28. Ramanujam R., Zhao Y., Pirskanen R., Hammarstrom L. // BMC Med. Genet. 2010. V. 11. P. 147.
29. Richman D.P., Gomez C.M., Berman P.W., Burres S.A., Fitch F.W., Arnason B.G. // Nature. 1980. V. 286. № 5774. P. 738–739.
30. Shigemoto K., Kubo S., Maruyama N., Hato N., Yamada H., Jie C., Kobayashi N., Mominoki K., Abe Y., Ueda N., et al. // J. Clin. Invest. 2006. V. 116. № 4. P. 1016–1024.
31. Gajra A., Vajpayee N., Grethlein S.J. // Am.J. Hematol. 2004. V. 77. № 2. P. 196–197.
32. Gregersen P.K., Kosoy R., Lee A.T., Lamb J., Sussman J., McKee D., Simpfendorfer K.R., Pirskanen-Matell R., Piehl F., Pan-Hammarstrom Q., et al. // Ann. Neurol. 2012. V. 72. № 6. P. 927–935.
33. van der Vliet H.J., von Blomberg B.M., Nishi N., Reijm M., Voskuyl A.E., van Bodegraven A.A., Polman C.H., Rustemeyer T., Lips P., van den Eertwegh A.J., et al. // Clin. Immunol. 2001. V. 100. № 2. P. 144–148.
34. Jordan M.A., Fletcher J.M., Jose R., Chowdhury S., Gerlach N., Allison J., Baxter A.G. // J. Immunol. 2011. V. 186. № 7. P. 3953–3965.
35. Schwartz A.M., Putlyaeva L.V., Covich M., Klepikova A.V., Akulich K.A., Vorontsov I.E., Korneev K.V., Dmitriev S.E., Polanovsky O.L., Sidorenko S.P., et al. // Biochim. Biophys. Acta. 2016. V. 1859. № 10. P. 1259–1268.
36. Rosenbloom K.R., Armstrong J., Barber G.P., Casper J., Clawson H., Diekhans M., Dreszer T.R., Fujita P.A., Guruvadoo L., Haeussler M., et al. // Nucl. Acids Res. 2015. V. 43. Database issue. P. D670–681.
37. Creyghton M.P., Cheng A.W., Welstead G.G., Kooistra T., Carey B.W., Steine E.J., Hanna J., Lodato M.A., Frampton G.M., Sharp P.A., et al. // Proc. Natl. Acad. Sci. USA. 2010. V. 107. № 50. P. 21931–21936.
38. Thurman R.E., Rynes E., Humbert R., Vierstra J., Maurano M.T., Haugen E., Sheffield N.C., Stergachis A.B., Wang H., Vernot B., et al. // Nature. 2012. V. 489. № 7414. P. 75–82.
39. Smith E., Shilatifard A. // Nat. Struct. Mol. Biol. 2014. V. 21. № 3. P. 210–219.
40. Kulakovskiy I.V., Vorontsov I.E., Yevshin I.S., Soboleva A.V., Kasianov A.S., Ashoor H., Ba-Alawi W., Bajic V.B., Medvedeva Y.A., Kolpakov F.A., et al. // Nucl. Acids Res. 2016. V. 44. № D1. P. D116–125.
41. Vorontsov E., Kulakovskiy I., Khimulya G., Nikolaeva D., Makeev V // BIOINFORMATICS 2015. V. 1. International Conference on Bioinformatics Models, Methods and Algorithms (BIOSTEC 2015). P. 102–108.
42. Wingender E., Schoeps T., Donitz J. // Nucl. Acids Res. 2013. V. 41. Database issue. P. D165–1670.

The Effect of the Targeted Recombinant Toxin DARPin-PE40 on the Dynamics of HER2-Positive Tumor Growth

E.A. Sokolova[1,2]*, G.M. Proshkina[1]*, O.M. Kutova[2], I.V. Balalaeva[1,2], S.M. Deyev[1,2,3]
[1]Shemyakin–Ovchinnikov Institute of Bioorganic Chemistry, Russian Academy of Sciences, Miklukho-Maklaya Str., 16/10, Moscow, 117997, Russia
[2]Lobachevsky State University of Nizhny Novgorod, Gagarin Ave., 23, Nizhny Novgorod, 603950, Russia
[3]Lomonosov Moscow State University, Faculty of Biology, Leninskie Gory, 1, build. 12, Moscow, 119234, Russia
*E-mail: malehanova@mail.ru, gmb@ibch.ru
Received June 6, 2017; in final form, September 4, 2017

ABSTRACT **The development of targeted toxins based on non-immunoglobulin targeting molecules appears to be one of the most advanced approaches in the targeted therapy of malignant tumors with a high expression of the HER2 receptor. Earlier, we showed that the targeted toxin DARPin-PE40 consisting of the HER2-specific non-immunoglobulin polypeptide (the targeting module) and a fragment of *Pseudomonas* exotoxin A (the toxic module) exhibits an antitumor effect *in vivo* against the HER2-positive adenocarcinoma xenograft. In this work, an in-depth analysis of the effect of DARPin-PE40 on the growth dynamics of experimental xenograft tumors was carried out. DARPin-PE40 was shown to inhibit tumor growth at a dose of 25 and 50 μg/animal and to cause tumor node reduction at a dose of 80 μg/animal, followed by growth resumption at the end of therapy. An evaluation of the tumor growth dynamics revealed statistically significant differences in tumor volume in mice in the experimental groups compared to the control group. The results testify to the potential of using the created targeted toxin as an agent for the targeted therapy of HER2-overexpressing tumors.**
KEYWORDS **non-immunoglobulin module DARPin, *Pseudomonas aeruginosa* exotoxin A, HER2 receptor, targeted therapy.**
ABBREVIATIONS **DARPin – designed ankyrin repeat protein; EDTA –ethylenediaminetetraacetic acid; HER 1-4 – human epidermal growth factor receptor 1-4; Ni^{2+}-NTA – nickel nitrilotriacetic acid; PE40 – fragment of *Pseudomonas aeruginosa* exotoxin A; PMSF – phenylmethylsulfonyl fluoride; a.a. – amino acid.**

INTRODUCTION

According to the statistical data provided by P.A. Herzen Moscow Oncology Research Institute in 2015, breast cancer is the most common malignant disease affecting women, accounting for 20.9% of the total number of newly diagnosed neoplasms [1]. Breast cancer also sadly holds a leading place in cancer mortality among the female population of Russia, reaching 17% in 2015. As for the global statistics, about 1.6 million women are diagnosed with breast cancer every year, and about 500,000 die of the disease.

To sum up these facts, it is obvious that the development of novel antitumor agents and new approaches to cancer therapy is a priority. Targeted therapy has been developing rapidly in recent years. The approach consists in a targeted attack on tumor cells by using specific bifunctional therapeutic agents that are capable of selectively binding to tumor cells, on the one hand, and effectively eliminating them, on the other hand [2].

The HER2 receptor, which belongs to the human epidermal growth factor receptor family, is one of the best studied therapeutic targets [3, 4]. The tyrosine kinase receptor HER2 is normally present in all types of human epithelial tissues with a density of several thousand molecules per cell. Amplification of the HER2 gene under malignant cell transformation leads to overexpression of the receptor encoded. The HER2 receptor also becomes capable of constitutive heterodimerization with other receptors of the family (HER1, HER3, HER4). Continuous signal transmission from the membrane to the nucleus leads to an increase in cell proliferation, inhibition of apoptosis and, ultimately, tumor formation and metastasis. It is known that the level of HER2 gene expression is increased in 15-20% of human breast and ovarian cancers [3, 5].

Exotoxin A of *Pseudomonas aeruginosa* is one of the most effective protein toxins used in targeted therapy [6]. *Pseudomonas* exotoxin is a three-domain protein consisting of 613 a.a. We replaced the first domain of the exotoxin (1–252 a.a.), which is responsible for toxin binding to the natural receptor, with the HER2-specific non-immunoglobulin DARPin module [7], thus turning the exotoxin into a targeted toxin. A new generation of non-immunoglobulin targeting molecules based on artificial proteins with ankyrin repeats, DARPins, are increasingly used in molecular biology as targeting modules [8–10]. DARPins contain no cysteine residues, which allows for the production of these proteins directly in the *Escherichia coli* cytoplasm. They are also characterized by a high expression level in the bacterial system, monomeric state in solution with no tendency toward aggregation, and substantial resistance to proteases [11]. Because of these features, scaffold proteins have significant advantages over immunoglobulins as alternative targeting components of multifunctional compounds for the diagnosis and therapy of various diseases.

We analyzed the dynamics of the antitumor effect of the targeted toxin based on a fragment of *Pseudomonas aeruginosa* exotoxin A and the HER2-specific scaffold protein DARPin *in vivo* on the xenograft model of human breast adenocarcinoma with high expression of the target receptor HER2.

EXPERIMENTAL

Preparation of a highly purified targeted toxin, DARPin-PE40, for in vivo studies

The DARPin-PE40 gene was expressed in *E. coli* strain BL21 (DE3) cells as described in [12]. Fresh transformants (one colony per ml) were introduced in 25 ml of the auto-induction medium TBP-5052 [13] containing 2 mM $MgSO_4$, 25 mM Na_2HPO_4, 25 mM KH_2PO_4, 50 mM NH_4Cl, 0.5% glycerol, 0.05% glucose, 0.2% lactose, 0.5% yeast extract, 1% tryptone, and 0.1 g/l ampicillin and grown in a 250 ml flask for 24 h at 25 ˚C until the culture density reached OD_{600} of 20-25. The cells were harvested by centrifugation on a cooled centrifuge at 6,000 *g* for 10 min. The pellet was re-suspended in 10 ml of lysis buffer (200 mM Tris-HCl, 500 mM sucrose, 1 mM EDTA, pH 8.0, 60 μg/ml lysozyme). The suspension was diluted with sterile water and incubated for 30 min at room temperature. The cells were then lysed on ice using a Vibra Cell sound disruptor (Sonics, USA) in a cycle mode of 10 s sonication, followed by 10 s cooling, for a total of 30 cycles. Cell debris was removed by centrifugation at 15,000 *g* for 20 min on a cooled centrifuge. The PMSF protease inhibitor (1 mM) and NaCl (100 mM) were added to the cleared supernatant. In order to remove the nucleic acids, polyethylenimine was added to the supernatant dropwise under constant stirring to a final concentration of 0.03%. The lysate was stirred for an additional 15 min at 4 ˚C and centrifuged at 15,000 *g* for 20 min. The resulting lysate was filtered through a 0.22 μm filter. Imidazole (30 mM final concentration) and NaCl (500 mM final concentration) were then added, and the solution was loaded to a Ni^{2+}-NTA column (GE Healthcare, USA) equilibrated with buffer: 20 mM Na-Pi, pH 7.5, 500 mM NaCl, 30 mM imidazole). The DARPin-PE40 protein was eluted using a linear gradient of imidazole (30-500 mM). The fraction eluted at ~ 150 mM imidazole was used for purification using ion exchange chromatography. The buffer was exchanged with one containing 20 mM Tris-HCl, pH 8.0, 150 mM NaCl using a PD10 column (GE Healthcare, USA). The protein solution was diluted three times with 20 mM Tris-HCl, pH 8.0, and applied on a MonoQ5/50 GL column (GE Healthcare, USA) equilibrated with 20 mM Tris-HCl, pH 8.0. A linear gradient of NaCl (0-1 M) was used to elute the protein. DARPin-PE40 was eluted at a NaCl concentration of about 500 mM. The yield of the target protein was 140 mg per liter of culture.

Evaluation of the antitumor efficacy of DARPin-PE40 *in vivo*

The antitumor activity was determined using a human tumor xenograft. Six- to eight-week-old athymic BALB/c nude mice were subcutaneously inoculated with 10^7 cells of human breast adenocarcinoma SK-BR-3 in 200 μl of phosphate-buffered saline. HER2 overexpression in tumor tissue was confirmed *ex vivo* by immunohistochemical analysis using the HercepTest kit (DAKO, USA). Tumor growth was monitored by the standard method for determining tumor size by measuring two diameters using a caliper. The tumor volume was calculated using the equation: $V = a \times b^2 / 2$, where a represents a larger diameter; and b, a smaller diameter [14]. Starting on day 9 after tumor cell inoculation, when the average tumor volume was ~ 100 mm^3, the animals were randomly divided into the experimental and control groups (five animals per group). Animals in the experimental groups received 200 μl intravenous injections of DARPin-PE40 in phosphate buffered saline daily at a total dose of 25 μg/animal (five injections of 5 μg on days 9, 11, 13, 15, and 17), 50 μg/animal (five injections of 10 μg on days 9, 11, 13, 15, and 17) or 80 μg/animal (four injections of 20 μg DARPin-PE40 on days 9, 11, 13, and 15). The animals in the control group received 200 μl of phosphate-buffered saline on days 9, 11, 13, 15, and 17 after tumor cell inoculation. When the tumor node reached a volume of ~ 2500 mm^3, the animals were euthanized. To plot tu-

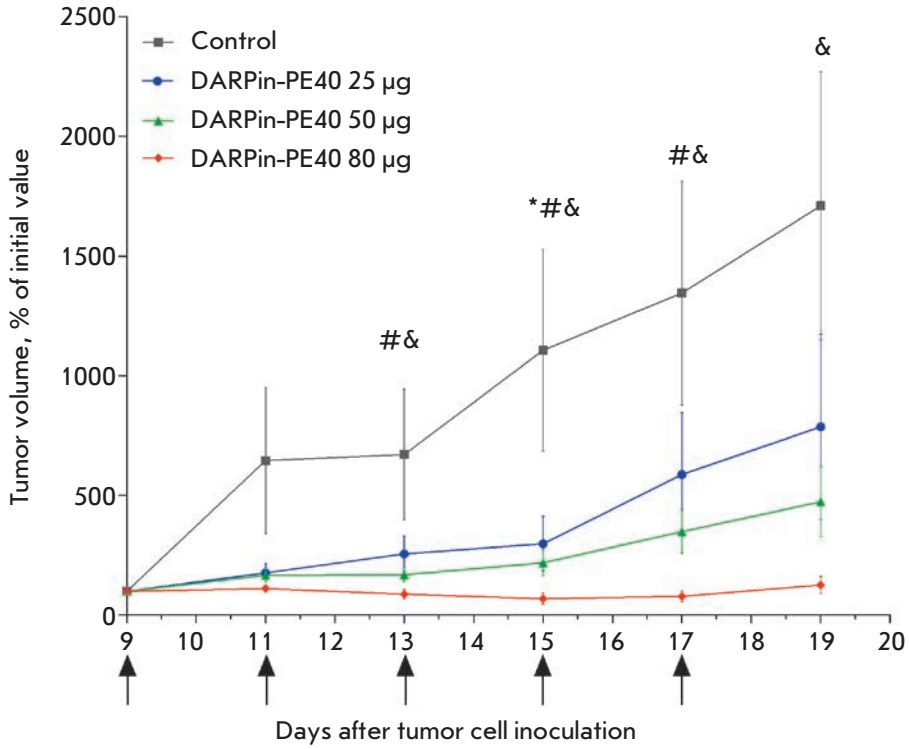

Fig. 1. The curves of SK-BR-3 xenograft tumor growth in different groups of animals. The day of subcutaneous inoculation of SK-BR-3 cells to animals was set as day 0. The days of DARPin-PE40 injection are indicated with arrows. *, #, & – the statistically significant difference between the control and experimental groups: 25 μg, 50 μg and 80 μg DARPin-PE40, respectively ($p < 0.05$, Dunnett's test, $n = 5$).

mor growth curves, the calculated tumor volume values were used, expressed as a percentage of the values at the initial time point (on the therapy start day). The data were represented as the mean ± standard error of the mean at each time point.

To quantify the antitumor effect, the initial stage of the tumor growth curve in the animals of each group was fitted by the equation $V = V_0 \times e^{kt}$, where V_0 represents the tumor node volume at the initial time corresponding to therapy start, and k is the tumor growth rate coefficient.

The k values were determined by linearization of the exponential phase of tumor growth (i.e. taking the logarithm of the tumor volume), followed by linear approximation. The tumor doubling time was calculated using the equation $\ln 2/k$. The data were represented using the box-and-whiskers diagram reflecting the median, the 25th and 75th percentiles, and the spread of values in each animal group.

RESULTS AND DISCUSSION

We have previously created the recombinant targeted toxin DARPin-PE40 and studied its properties *in vitro* as a targeted agent for the highly effective targeted therapy of HER2-positive tumors. This agent possesses an antitumor effect that comes to inhibiting the growth of xenograft tumors *in vivo* [15]. The targeting module in this construct consists of a molecule of non-immunoglobulin nature based on an artificial ankyrin repeat protein, DARPin, capable of recognizing the HER2 receptor with high affinity (K_D = 3.8 nM) [7]. The PE40 fragment of *Pseudomonas* exotoxin A (M = 40 kDa), which lacks a natural receptor-binding domain, is used as a cytotoxic module [16]. The genetic construct encoding this fusion protein was expressed in *E.coli* BL21(DE3) cells. The DARPin-PE40 fusion protein was purified by metal-chelate affinity and anion exchange chromatography.

An in-depth analysis of the effect of DARPin-PE40 on the dynamics of experimental tumor growth *in vivo* was carried out. Athymic BALB/c nude mice (6-8 weeks old) with subcutaneously established human breast adenocarcinoma SK-BR-3 (see the Experimental section) were repeatedly injected intravenously with DARPin-PE40 at a total dose of 25, 50 or 80 μg per animal (1.25, 2.5 or 4 mg/kg, respectively).

The tumor growth dynamics showed a pronounced antitumor effect of the recombinant targeted toxin DARPin-PE40: statistically significant differences in the tumor volume in mice of the experimental groups were found in comparison with the control animals ($p < 0.05$) (*Fig. 1*). The tumors in control animals, as well as in the animals treated with 25 and 50 μg DARPin-PE40, exhibited an exponential growth at the initial stage (*Fig. 2A*). Meanwhile, the tumors grew significantly slower after DARPin-PE40 treatment: a statistically significant decrease in the tumor growth rate coefficient (*Fig. 2B*) and, correspondingly, an increase

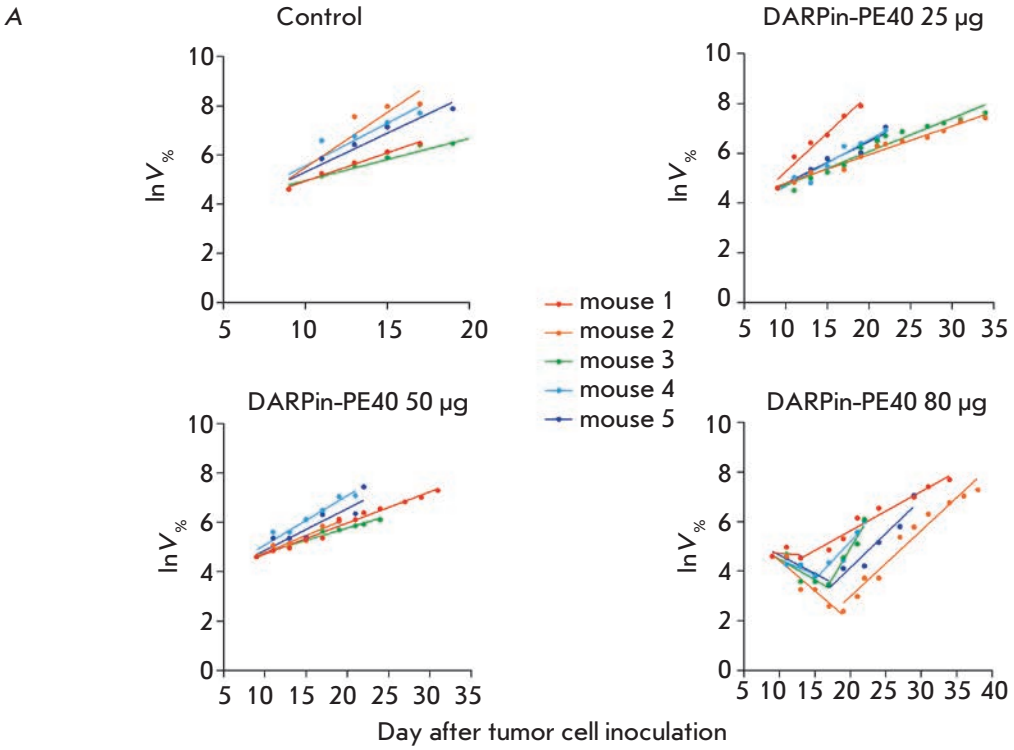

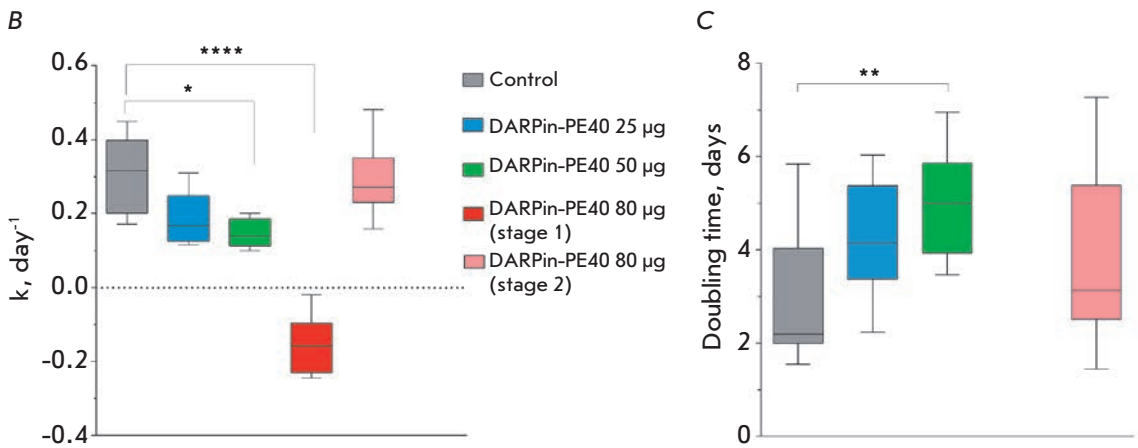

Fig. 2. Analysis of SK-BR-3 xenograft tumor growth in different groups of animals. A – Linearization of the exponential phase of tumor growth ($V_{\%}$ represents tumor volume as a percentage of that at the therapy start time). Data are shown for individual animals in each group. B – The box-and-whisker plot of the tumor growth rate coefficient (k). C – The box-and-whisker plot of the tumor doubling time (* – $p < 0.05$, ** – $p < 0.01$, **** – $p < 0.0001$).

in the tumor doubling time (*Fig. 2C*) in the experimental groups compared with the control group were observed. This effect can be explained by a reduction in the pool of proliferating cancer cells in the growing tumor node as a result of the cytotoxic effect of the targeted toxin. Experimental tumors treated with a maximum dose of DARPin-PE40 (80 μg/animal) showed two distinct stages of growth. At stage 1, during the DARPin-PE40 injections, an exponential decrease in tumor volume on average by 60% relative to the volume registered at the beginning of the therapy was observed. At stage 2, after the DARPin-PE40 treatment was completed, the tumors resumed exponential growth (*Fig. 2*).

Taking into account tumor heterogeneity and the high genetic instability of tumor cells [17], the insufficient effectiveness of DARPin-PE40 may be caused by the presence or emergence of a resistant tumor cell population that leads to further tumor progression after the therapy is ended. In addition, since the experimental conditions simulated the situation of a therapeutic effect on an already formed tumor node, the limitations in the efficacy of the targeted toxin can also be related to its insufficient penetration into the tumor tissue. This, in turn, is due to a number of structural features of the tumor *in vivo*, including numerous cell-cell contacts, interstitial fluid pressure, and the presence of the extracellular matrix. Thus, along with an

increase in dosage and/or therapy duration, the antitumor effect of the recombinant targeted toxin DARPin-PE40 could be enhanced by combining its action with a targeted increase in its permeability and accumulation in the tumor. This problem has been variously addressed; in particular, via the control of the formation of the extracellular matrix components and/or their degradation [18–20], as well as temporary disruption of cell-cell contacts in the tumor [21]. The latter approach proved effective with the use of HER2-specific full-length therapeutic antibodies [22] and, apparently, is one of the promising ways to develop targeted antitumor therapy.

CONCLUSION

The use of non-immunoglobulin scaffold proteins, in particular DARPins, as targeting molecules is relevant for the development of new agents for targeted antitumor therapy. The dynamics of the antitumor activity of the targeted toxin DARPin-PE40, in which HER2-specific DARPin is fused with a toxic fragment of *Pseudomonas* exotoxin A into a single polypeptide chain, was studied. The effectiveness and reliability of the DARPin-PE40 antitumor effect demonstrate that it is a promising candidate for further study as an agent for the targeted therapy of tumors with high expression of the HER2 receptor.

Recombinant targeted toxin purification was supported by the Russian Science Foundation (project No. 14-24-00106P); animal studies were supported by the Ministry of Education and Science of the Russian Federation (project No. 6.7109.2017/9.10).

REFERENCES

1. Kaprin A.D., Starinsky V.V., Petrova G.V. Malignant neoplasms in Russia in 2015 (morbidity and mortality). Moscow: P.Herzen Moscow oncology research institute – branch of FSBI NMRRC of the Ministry of Health of the Russian Federation, 2017. 250 p.
2. Madhumathi J., Verma R.S. // Curr Opin Microbiol. 2012. V. 15. P. 300–309.
3. Polanovski O.L., Lebedenko E.N., Deyev S.M. // Biochemistry (Mosc). 2012. V. 77. Issue 3. P. 227–245.
4. Deyev S.M., Lebedenko E.N. // Bioessays. 2008. V. 30. P. 904–918.
5. Slamon D.J., Clark G.M., Wong S.G., Levin W.J., Ullrich A., McGuire W.L. // Science. 1987. V. 235. P. 177–182.
6. Kreitman R.J. // Aaps J. 2006. V. 8. P. E532–E551.
7. Steiner D., Forrer P., Plückthun A. // J. Mol. Biol. 2008. V. 382. P. 1211–1227.
8. Deyev S.M., Lebedenko E.N., Petrovskaya L.E., Dolgikh D.A., Gabibov A.G., Kirpichnikov M.P. // Russian chemical reviews. 2015. V. 84. №1. P. 1–26.
9. Proshkina G.M., Shilova O.N., Ryabova A.V., Stremovskiy O.A., Deyev S.M. // Biochimie. 2015. V. 118. P. 116–122.
10. Verdurmen W.P., Luginbühl M., Honegger A., Plückthun A. // J. Control Release. 2015. V. 200. P. 13–22.
11. Plückthun A. // Annu. Rev. Pharmacol. Toxicol. 2015. V. 55. P. 489–511.
12. Sokolova E.A., Schulga A.A., Stremovskiy O.A., Balalaeva I.V., Proshkina G.M., Deyev S.S. // Biochemistry (Moscow) Supplement. Series A: Membrane and Cell Biology. 2016. V. 33. № 6. P. 429–434.
13. Studier F.W. // Protein Expr. Purif. 2005. V. 41. P. 207–234.
14. Geran R.I., Greenberg N.H., Macdonald M.M., Schumacher A.M., Abbott B.J. // Cancer Chemother. Rep. 1972. V. 3. P. 1–104.
15. Sokolova E., Proshkina G., Kutova O., Shilova O., Ryabova A., Schulga A., Stremovskiy O., Zdobnova T., Balalaeva I., Deyev S. // J Control Release. 2016. V. 233. P. 48–56.
16. Sokolova E.A., Zdobnova T.A., Stremovskiy O.A., Balalaeva I.V., Deyev S.M. // Biochemistry (Mosc). 2014. V. 79. Issue 12. P. 1376–1381.
17. Pribluda A., de la Cruz C.C., Jackson E.L. // Clin Cancer Res. 2015. V. 21. P. 2916–2923.
18. Eikenes L., Tufto I., Schnell E.A., Bjorkoy A., De Lange Davies C. // Anticancer Res. 2010. V. 30. P. 359–368.
19. Cheng J., Sauthoff H., Huang Y., Kutler D.I., Bajwa S., Rom W.N., Hay J.G. // Mol Ther. 2007. V. 15. P. 1982–1990.
20. Zeisberger S.M., Odermatt B., Marty C., Zehnder-Fjällman A.H., Ballmer-Hofer K., Schwendener R.A. // Br J Cancer. 2006. V. 95. P. 272–281.
21. Beyer I., Cao H., Persson J., Song H., Richter M., Feng Q., Yumul R., van Rensburg R., Li Z., Berenson R., et al. // Clin Cancer Res. 2012. V. 18. P. 3340–3351.
22. Beyer I., van Rensburg R., Strauss R., Li Z., Wang H., Persson J., Yumul R., Feng Q., Song H., Bartek J., et al. // Cancer Res. 2011. V. 71. P. 7080–7090.

Expression Levels of the Uridine-Cytidine Kinase Like-1 Protein As a Novel Prognostic Factor for Hepatitis C Virus-Associated Hepatocellular Carcinomas

A. Buivydiene[1]*, V. Liakina[2,3], J. Valantinas[1], J. Norkuniene[4,5], E. Mockiene[6,7], S. Jokubauskiene[8,9], R. Smaliukiene[9], L. Jancoriene[10], L. Kovalevska[11], E. Kashuba[11,12]*

[1]Vilnius University, Clinic of Gastroenterology, Nephrourology and Surgery, Centre of Hepatology, Gastroenterology and Dietetics, Vilnius, Lithuania

[2]Vilnius University, Center of Hepatology, Gastroenterology and Dietetics, Vilnius, Lithuania

[3]Vilnius Gediminas Technical University, Department of Biomechanics, Vilnius, Lithuania

[4]Vilnius Gediminas Technical University, Department of Mathematical Statistics, Vilnius, Lithuania

[5]Vilnius College of Higher Education, Vilnius, Lithuania

[6]Centre of Radiology and Nuclear Medicine, Vilnius, Lithuania

[7]Vilnius University, Faculty of Medicine, Vilnius, Lithuania

[8]Vilnius University, Department of Pathology, Forensic Medicine and Pharmacology, Vilnius, Lithuania

[9]National Center of Pathology, Vilnius, Lithuania

[10]Vilnius University, Clinic of Infectious, Chest Diseases, Dermatovenerology and Allergy, Center of Infectious Diseases, Vilnius, Lithuania

[11]R.E. Kavetsky Institute of Experimental Pathology, Oncology and Radiobiology, Kyiv, Ukraine

[12]Department of Microbiology, Tumor and Cell Biology, Karolinska Institutet, Stockholm, Sweden

*E-mail: arida.buivydiene@santa.lt, Elena.Kashuba@ki.se

Received: September 10, 2016; in final form May 31, 2017

ABSTRACT **The expression levels of the two novel oncoproteins uridine-cytidine kinase like-1 (UCKL-1) and mitochondrial ribosomal protein S18-2 (MRPS18-2) were assessed in samples of hepatitis C virus (HCV)-associated hepatocellular carcinoma (HCC) using immunohistochemistry. Tissue microarray (TMA) paraffin blocks were prepared from 42 HCC tumor samples with the corresponding peri-tumor tissues and from 11 tissues of a liver with HCV-induced cirrhosis. We found that the UCKL-1 signal in the liver tissues of the peri-tumor zone in the HCC samples was stronger than that in cirrhosis (50 ± 49.44 vs. 24.27 ± 14.53; $p = 0.014$). The MRPS18-2 expression was weak, and there was no differences between the groups ($p = 0.26$). Noteworthy, the UCKL-1 protein was expressed at higher levels in peri-tumor tissues in the cases of HCC recurrence; this was confirmed for 27 older patients (63.78 ± 9.22 vs. 53.53 ± 4.07 years, $p < 0.001$), in parallel with enhanced UCKL-1 staining in former HCC nodules (62.69 ± 50.4 vs. 26.0 ± 30.19, $p = 0.006$) and microvascular invasion ($p = 0.02$). A multivariate analysis of prognostic factors for HCC recurrence showed that the best predictive factors for these conditions were UCKL-1 expression in tumor, vascular invasion, and HCC treatment modality, other than liver transplantation (odds ratios: 1.029, 18.143 and 11.984, $R^2 = 0.633$, $p = 0.002$). In conclusion, the high UCKL-1 expression might be a prognostic factor for HCC relapse, in combination with age and microvascular invasion. MRPS18-2 protein expression has no prognostic significance in the cases of HCV-associated HCC.**

KEYWORDS **hepatitis C virus (HCV), hepatocellular carcinoma (HCC), recurrence of hepatocellular carcinoma, UCKL-1, MRPS18-2, prognostic factors.**

INTRODUCTION

Liver cancer (predominantly HCC) is the second-most deadly cancer for men worldwide [1]. HCC incidence in Nordic countries, including Lithuania, reaches up to 10/100,000 inhabitants [2]. In developed countries, one factor that is responsible for the increased HCC incidence is HCV [3]. In Lithuania, anti-HCV prevalence in adults stands at about 2.78% [4]. HCV-induced HCC development is a multi-step process that may last 20–40 years and involves chronic hepatic inflamma-

tion, progressive liver fibrosis, initiation of neoplastic clones, and tumor progression in a carcinogenic tissue microenvironment [5]. Noteworthy, eradication of HCV reduces, but does not eliminate, the risk of HCC development, especially when advanced hepatic fibrosis has already originated [6, 7]. It becomes difficult then and hardly manageable to follow patients at early-stage asymptomatic HCV-induced cirrhosis. Thus, it was discovered in a population-based study that less than 20% of patients with cirrhosis who had developed HCC were subject to regular monitoring [8]. Therefore, prognostic markers are now being actively developed to stratify HCV patients into clearly defined risk groups. Successful employ of these predictors in clinical practise could improve the clinical management of these patients [9]. Additionally, even with a successful HCC treatment by liver transplantation, liver resection, or radiofrequency-induced thermotherapy (RFITT), high risk of HCC recurrence persists [7, 8]. The recurrence rate of HCC is estimated at 70% after 5 years of liver resection [10]. The validated prediction markers of recurrence are the tumor size, multifocality, macroscopic and microscopic vascular invasion, as well as poor differentiation [11].

It is widely accepted that malignant transformation of liver cells is stimulated by various factors. However, studies on the mechanisms of HCV-induced cell transformation are inhibited by the lack of animal and cell models. Obviously, better understanding of molecular mechanisms would help us identify new diagnostic and/or prognostic markers, most importantly, for the early detection of HCC [11]. This would allow us to develop better approaches to clinical treatment.

Usually, the molecular mechanisms that are responsible for virus-induced cell transformation include the inactivation of the two tumor suppressor protein pathways: i.e., the p53 (TP53) and retinoblastoma (RB) pathways [12, 13]. There is little doubt that other proteins can play an important role in cell transformation: for example, the putative human enzyme UCKL-1 that is involved in cellular nucleotide metabolism [14, 15] and the new oncoprotein MRPS18-2 that can bind RB [13, 16, 17]. There are no data on the expression of both of these proteins in HCC, and we asked ourselves the question of whether the UCKL-1 and MRPS18-2 expressions in HCC tissues could be used as prognostic markers for the course of the disease in HCV-bearing patients.

EXPERIMENTAL

Patient samples

The retrospective cohort study was conducted at Vilnius University Hospital Santariskiu Klinikos, Vilnius, Lithuania, according to the guidelines of the Helsinki Declaration. The study was approved by the Vilnius Regional Biomedical Research Ethics Committee (158200-13-698-224, from 2013-11-12). The HCC tumor and the corresponding peri-tumor (normal) liver tissue samples were collected from 53 patients who had undergone liver transplantation, liver resection, or RFITT for a complicated chronic HCV infection. Tissue sections from 42 HCV positive cirrhotic patients with HCC and 11 samples from transplanted HCV cirrhotic patients without HCC, as a control group, were analyzed. All the specimens are preserved at the National Lithuanian Center of Pathology. A histological activity index (HAI) was scored, according to K. Ishak et al., and liver fibrosis was assessed, according to METAVIR [18–20]. In HCC cases, tumor differentiation and microvascular invasion were evaluated.

Analysis of UCKL-1 and MRPS18-2 expression in HCC and liver tissue specimens

Tissue samples after surgery, hepatic resection, and/or liver transplantation were fixed in a buffered 10% formalin solution. Expression of the UCKL-1 and MRPS18-2 proteins was performed by immunohistochemistry (IHC) on tissue microarrays (TMAs) constructed of paraffin-embedded tissues, selected by the pathologist. Cores one millimeter in diameter were punched from the selected areas. Paraffin sections of the TMAs were cut (2 μm thick), dewaxed, deparaffinized, and rehydrated. Epitopes were heat-activated in a EnVision FLEX target retrieval solution for 20 min, while the pH of the buffer was low for UCKL-1 and high for MRPS18-2. The samples were cooled at room temperature for 15 min. A two-step IHC procedure was performed with the EnVision FLEX detection system (DAKO), using an automatic staining Link instrument (DAKO). The primary anti-UCKL-1 (diluted 1 : 200) and anti-MRPS18-2 (diluted 1 : 150) antibodies (Sigma-Aldrich) were applied for 60 and 30 min, respectively. The secondary antibody FLEX/HRP (DAKO) was applied for 20 min. The peroxidase enzyme was then visualized with 3,3'-diaminobenzidine, tetrahydrochloride, and hydrogen peroxide. Hematoxylin was used as a counterstain for 10 min. Visual evaluation of the UCKL-1 and MRPS18-2 signals was performed by an experienced pathologist. Each spot was graded individually. The UCKL-1 and MRPS18-2 cytoplasmic reactions were considered as negative if no positive cells were observed. If a MRS18-2 signal was detected mainly in the perinuclear cytoplasm, this was noted in the table of results, as well. The results of IHC reactions were evaluated semiquantitatively, by counting the number of positively stained cells in 1,000 analysed cells as a specified percentage – a label index (LI%). LI values lower than the median expression of the marker

Table 1. Demographic, clinical, and laboratory characteristics of patient groups

Characteristics	HCC (n = 42)	Non-HCC (n = 11)	p-value
Follow up, mean ± SD*, years	2.82±1.76	5.27 ± 2.49	<0.005
Age, mean ± SD, years	60.1 ± 9.29	49.42 ± 9.29	0.001
Gender, count (rate, %): Women/ Men	16 (38.1%)/ 26 (61.9%)	4 (36.4%)/ 7 (63.6%)	0.917
BMI, mean ± SD, kg/m^2	26.32 ± 4.61	26.75 ± 4.18	0.774
HCV genotype (GT*): GT-1, count (rate, %) GT-2, count (rate, %) GT-3, count (rate, %)	27 (64.3) 3 (7.1) 12 (28.6)	9 (81.8) 0 (0) 2 (18.2)	0.314

*SD – standard deviation.

Table 2. Histological and immunohistochemical differences in liver tissue samples in groups

Characteristics	HCC (n = 42)	Non-HCC (n = 11)	p-value
HAI, mean ± SD	6.71 ± 1.49	6.64 ± 2.34	0.892
UCKL-1, mean ± SD, LI (%)	50 ± 49.44	24.27 ± 14.53	0.014
MRPS18-2, mean ± SD, LI (%)	8.68 ± 16.61	15.00 ± 15.17	0.260

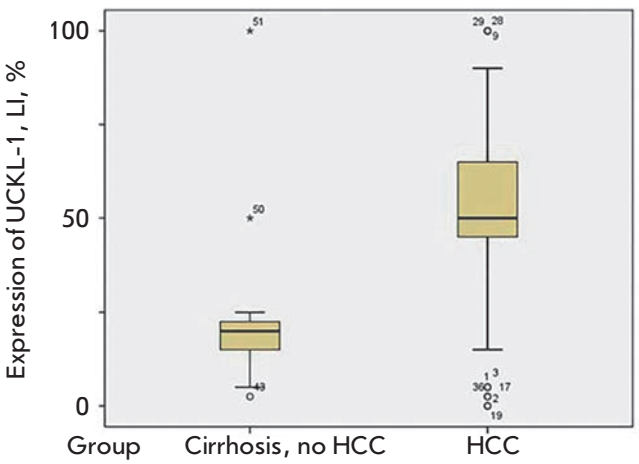

Fig. 1. The UCKL-1 expression in the liver tissue. Notice the significant increase in the UCKL-1 staining in samples with HCC in comparison with patients with cirrhosis without HCC

were considered as low, and if a LI value overran the median expression it was considered as high.

In addition, demographic information (age, body mass index (BMI), gender), laboratory data on the HCV infection (HCV genotype (GT)), the cumulative size of HCC assessed radiologically, the HCC treatment modality (liver transplantation, liver resection or RFITT), and the time period of follow-up were evaluated for each patient.

Statistics

A statistical analysis was performed using the IBM SPSS 19.0 statistical program. The Kolmogorov–Smirnov test was used to assess data normality. Group differences were determined using the Student t test when data distribution was normal: in other cases, the Mann Whitney and the Kruskal–Wallis criteria were used. χ^2 tests were conducted for the categorical variables. To establish a connection between categorical variables, the Spearman correlation coefficient was calculated. A logistic regression model was constructed in order to investigate the association between the intensity of the UCKL-1 and MRPS18-2 signals in the HCC and microvascular invasion, the HCC treatment modality, and HCC recurrence after treatment. All hypotheses were verified with a selected significance level of $p < 0.05$.

RESULTS AND DISCUSSION

Characterization of patients

Forty-two out of the 53 patients had developed the HCV-associated HCC and received treatment; 11 patients were diagnosed only with HCV-induced cirrhosis. All participants were followed up for at least 1 year at the Santariškiu Klinikos of Vilnius University Hospital; the HCC patients were observed for about 2.82 ± 1.76 years; and the patients with HCV-induced cirrhosis – for 5.27 ± 2.49 years. Noteworthy, the HCC patients were significantly older than the individuals with cirrhosis (p = 0.001): the mean age of the HCC patients was 60.1 ± 9.29 years, while the persons in the cirrhosis group were about 49.42 ± 9.29 years old. No differences in gender distribution (male/female ratio) in HCC and non-HCC (cirrhosis) groups were detected (p = 0.917). The BMI value was also similar in these groups (p = 0.774) (see *Table 1*).

All participants had histologically confirmed advanced fibrosis, and HAI did not differ between the HCC and non-HCC groups (p = 0.892) (*Table 2*).

The expression of UCKL-1 was high in the liver tissues of patients with HCC. We found that the UCKL-1 signal was stronger in the peri-tumoral liver tissue in HCC cases, compared with non-HCC (cirrhosis) cases (50 ± 49.44 vs. 24.27 ± 14.53, p = 0.014), as is presented in *Table 2* and *Figs. 1* and *2*.

On the contrary, the MRPS18-2 signal was observed rarely in the liver tissue and this low expression did not differ between the groups ($p = 0.26$) (see *Table 2*).

A description of the cohort of patients with HCC relapse

HCC recurrence in patients with HCV-induced cirrhosis after curative treatment (liver transplantation, liver resection or RFITT) was confirmed radiologically in 27 of 42 patients. All patients were observed for at least 1 year before the diagnosis of HCC relapse (the mean observation time was 2.93 ± 2.43) (see *Table 3*). HCC relapse appeared usually after 2.76 ± 1.3 years. The recurrence rate (62%) in the studied cohort and the time of relapse were similar to those reported earlier by other authors [10]. Moreover, the mortality rate in the relapsers was significantly higher than that in non-relapsers (59.3 and 6.7%, respectively, $p = 0.001$) (see *Table 3*).

Importantly, the age of the patients in both groups differed significantly: 63.78 ± 9.22 years in those that showed a relapse and 53.53 ± 4.07 years in non-relapsers ($p < 0.001$)(see *Table 3*).

Noteworthy, women were diagnosed with HCC relapse more often than men: 87.5% (14 out of 16) and 50% (13 out of 26), respectively ($p = 0.015$) (see *Table 3*). However, an absolutely larger number of men were diagnosed with HCC (26 men versus 16 women). It had also been reported earlier that older age and male gender are associated with an increased risk of HCC development in HCV cirrhotic patients [21, 22].

In our studied cohort of patients, no differences in BMI values, HAI, and HCC differentiation were detected between the groups of relapsers and non-relapsers (*Table 3*). We have to mention that, in the studied cohort, there were only two cases of poorly differentiated HCC (grade G3) in the group of relapsers and no G3 cases in the non-relapsers. Probably, this is one reason why in our case the histological differentiation grade was not associated with HCC recurrence, contrary to published data [23].

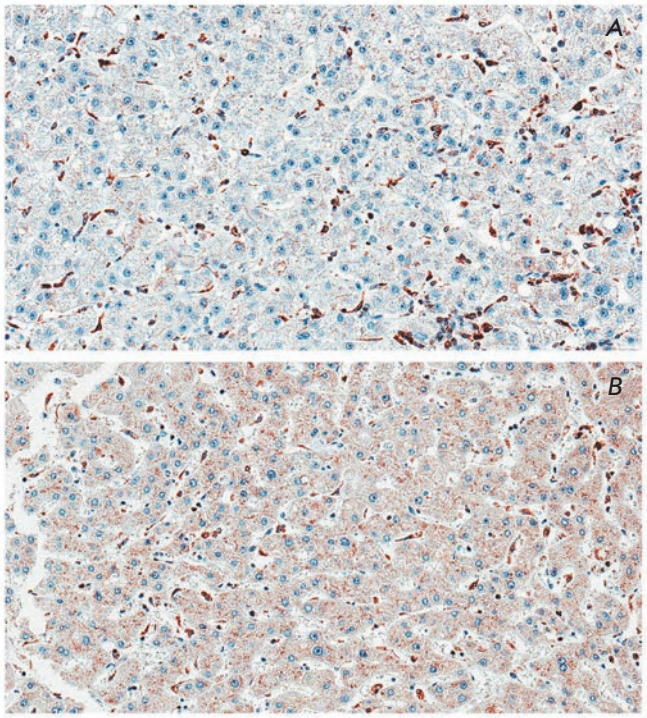

Fig. 2. The UCKL-1 cytoplasmic expression in liver tissue. Notice that the UCKL-1 cytoplasmic signal was significantly lower in the hepatocytes (expression was observed in 40% of the cells) of a cirrhosis patient (*A*) in comparison with the UCKL-1 signal in 100% of the peri-tumor hepatocytes of a HCC patient (*B*). Objective ×40

When microvascular invasion was observed, HCC recurrence was diagnosed significantly more often ($p = 0.02$, *Table 4*). As a rule, tumors were larger in HCC

Table 3. Characteristics of patient groups with and without HCC recurrence

Characteristics	HCC recurrence ($n = 27$)	no HCC recurrence ($n = 15$)	p-value
Follow up, mean ± SD, years	2.76 ± 1.3	2.93 ± 2.43	0.8
Lethality, count (rate, %)	16 (59.3)	1 (6.7)	0.001
Age, mean ± SD, years	63.78 ± 9.22	53.53 ± 4.07	<0.001
Gender, count (rate, %): -women/men	14 (51.9%)/13 (48.1%)	2 (13.3%)/13 (86.7%)	0.015
BMI average ± SD, kg/m^2	27.05 ± 4.88	25.3 ± 4.01	0.245
HCC treatment method: -resection, count (rate, %) -RFITT, count (rate, %) -transplantation, count (rate, %)	 20 (74.1) 6 (22.2) 1 (3.7)	 6 (40) 1 (6.7) 8 (53.3)	0.001

Table 4. Histological differences in liver tissue samples in HCC recurrence and non-HCC recurrence groups

Characteristics	HCC recurrence ($n = 27$)	no HCC recurrence ($n = 15$)	p-value
HAI, mean ± SD, count	6.89 ± 1.19	6.4 ± 1.92	0.381
HCC size, mean ± SD, mm	50.44 ± 17.831	41.47 ± 20.757	0.558
HCC grade of differentiation -G1, count (rate, %) -G2, count (rate, %) -G3, count (rate, %)	 6 (23.07) 18 (69.23) 2 (7.69)	 1 (6.67) 14 (93.33) 0 (0)	0.64
Vascular invasion, count (rate, %)	13 (50)	2 (13.33)	0.02

relapsers (50.44 ± 17.83 mm vs. 41.47 ± 20.76 mm), but these differences were not statistically significant (*Table 4*). Thus, in our study the microvascular invasion, proven histologically, was an independent predictive factor of a lower disease-free survival rate. Actually, tumor size and vascular invasion are well-known predictive factors of HCC recurrence [24, 25]. The studied cohort in the present paper was rather small, and that could be the reason why the size of the HCC nodules did not differ significantly between relapsers and non-relapsers, even when such a trend was observed.

The high expression of UCKL-1 and MRPS18-2 in HCC tissues

Comparing the expression of UCKL-1 and MRPS18-2 proteins in HCC nodules, a significantly stronger UCKL-1 signal was observed in HCC relapsers compared with non-relapsers: 62.69 ± 50.4 and 26.0 ± 30.19, respectively ($p = 0.006$). We have to emphasize that, at the same time, in the peri-tumor liver tissue no dramatic differences in UCKL-1 staining were detected when relapsers and non-relapsers were compared (*Fig. 3* and *Table 5*). Hence, the UCKL-1 expression levels

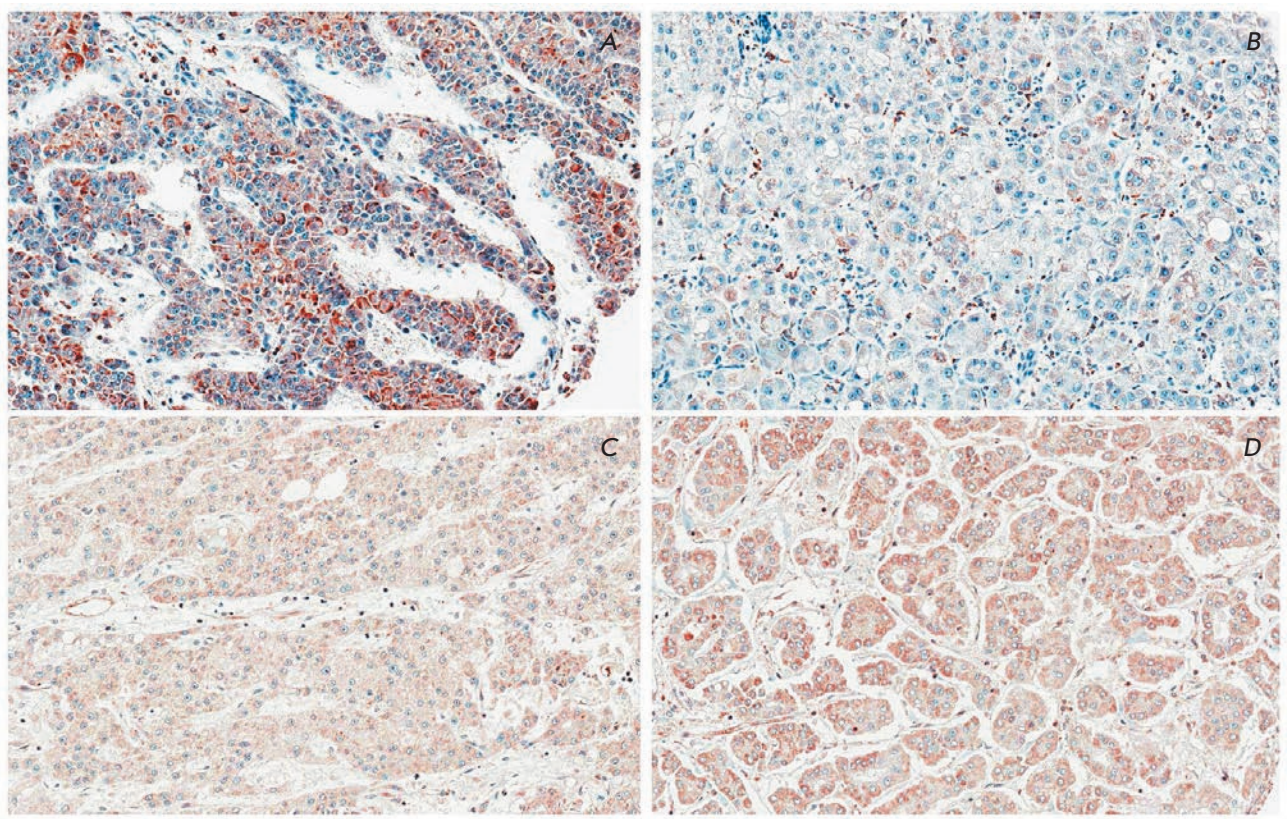

Fig. 3. The UCKL-1 and MRPS18-2 expression pattern in cancer tissues. Notice that the UCKL-1 cytoplasmic signal was significantly higher in the HCC samples of relapsers (*A*) in comparison with the UCKL-1 signal in non-relapsing HCC (*B*). The MRPS18-2 signal was strong in cancer tissues, regardless relapsing (*C*) or non-relapsing (*D*) HCC. Objective ×40

Table 5. Immunohistochemical differences in liver tissue samples in groups of patients with and without HCC recurrence

Characteristics	HCC recurrence (n =27)	no HCC recurrence (n=15)	p-value
UCKL-1, mean ± SD, LI (%)	49 ± 32.44	50.27 ± 14.53	0.510
MRPS18-2 in liver tissue, mean ± SD, LI (%)	9.42 ± 18.239	7.40 ± 13.835	0.583
UCKL-1 in HCC nodule, mean ± SD, LI (%)	62.69 ± 50.4	26 ± 30.19	0.006
MRPS18-2 in HCC nodule, mean ± SD, LI (%)	78.08 ± 54.54	61.67 ± 60.52	0.378

Table 6. Logistic regression

Characteristics	B	SE	Wald	DV	p-value	Exp(B)
UCKL-1 in HCC	0.029	0.013	5.022	1	0.025	1.029
Vascular microinvasion	2.898	1.176	6.072	1	0.014	18.143
HCC treatment modality (transplantation->resection->RFITT)	2.484	0.933	7.084	1	0.008	11.984
Constant	-6.316	2.178	8.413	1	0.004	0.002

Note. B – regression coefficient, SE – standard error, Wald – Wald statistics value, DV – the dependent variable (1 – for HCC recurrence), Exp (B) – odds ratio.

might have a prognostic value in terms of HCC occurrence and recurrence.

At the same time, the MRPS18-2 expression was several folds greater in the HCC nodules than in the unaffected liver, but no differences were observed between HCC relapsers and non-relapsers (*Table 5*). Therefore, the levels of MRPS18-2 could be considered as lacking prognostic significance for patients with HCV cirrhosis.

The high expression of UCKL-1 in HCC nodules can be a prognostic factor of HCC relapse

As was expected based on the data published earlier [26], the method of HCC treatment on its own had a significant predictive value of HCC recurrence: in the case of liver transplantation, the HCC recurrence rate was significantly lower than that after liver resection or RFITT – the were the only cases of HCC recurrence after liver transplantation (*Table 3*).The high rate of tumor recurrence after surgical resection and RFITT corresponded to the data in the literature [27].

After a multivariate analysis of prognostic factors for HCC recurrence was performed, we could conclude that the most significant variables were the levels of UCKL-1 expression in tumor nodes, vascular invasion, and the modality of the primary HCC treatment (other than liver transplantation) with odds ratios of 1.029, 18.143, and 11.984, respectively (R^2 = 0.633, p = 0.002) (*Table 6*). As has already been mentioned, the expression levels of MRS18-2 and the differentiation of HCC could not be predictive factors for HCC relapse.

Thus, the addition of the expression levels of UCKL-1 as a predictive factor for the risk of HCC relapse resulted in a better prognosis of the course of the disease. A higher UCKL-1 expression in HCC nodules can be indicative of a higher risk of HCC relapse after curative treatment, especially if the treatment was not liver transplantation.

MRS18-2 was expressed at significantly higher levels in HCC nodules, compared with normal liver tissues, but it was not predictive of HCC recurrence.

These promising results regarding the prognostic value of UCKL-1 in terms of HCC occurrence and recurrence should be confirmed in a larger prospective-retrospective clinical study.

CONCLUSIONS

A high level of UCKL-1 expression in HCC nodules, in combination with microvascular invasion and HCC treatment modality (other, than liver transplantation), is a predictor of a higher risk of HCC recurrence.

This work was supported by the Swedish Cancer Society, matching grants from the Concern Foundation (Los Angeles) and the Cancer Research Institute (New York), the Ministry of Education and Science of Ukraine (No.0116U005456), and the Research Council of Lithuania (No.TAP-LU-15-003).

REFERENCES

1. Torre L.A., Bray F., Siegel R.L., Ferlay J., Lortet-Tieulent J., Jemal A. // CA: Cancer JClinicians. 2015. V. 65. № 2. P. 87–108.
2. McGlynn K.A., London W.T. // Clinics Liver Disease. 2011. V. 15. № 2. P. 223–243, vii-x.
3. El-Serag H.B. // N. Eng. J. Med. 2011. V. 365. № 12. P. 1118–1127.
4. Liakina V., Valantinas J. // Med. Sci. Monitor: Internat. Med. J. Exp. Clin. Res. 2012. V. 18. № 3. P. PH28–PH35.
5. Goossens N., Hoshida Y. // Clin. Mol. Hepatol. 2015. V. 21. № 2. P. 105–114.
6. van der Meer A.J., Veldt B.J., Feld J.J., Wedemeyer H., Dufour J.F., Lammert F., Duarte-Rojo A., Heathcote E.J., Manns M.P., Kuske L, et al.// JAMA. 2012. V. 308. № 24. P. 2584–2593.
7. Bruno S., Crosignani A., Roffi L., De Lisi S., Rossi S., Boccaccio V., Zermiani P., Mondelli V., Maisonneuve P.// J. Hepatol. 2014. V. 60. № 1. P. S224.
8. Davila J.A., Morgan R.O., Richardson P.A., Du X.L., McGlynn K.A., El-Serag H.B. // Hepatology. 2010. V. 52. № 1. P. 132–141.
9. Hoshida Y., Fuchs B.C., Bardeesy N., Baumert T.F., Chung R.T. // J. Hepatol. 2014. V. 61. (1 Suppl.). P. S79–S90.
10. Waghray A., Murali A.R., Menon K.V.N. // W.J. Hepatol. 2015. V. 7. № 8. P. 1020–1029.
11. Colecchia A., Schiumerini R., Cucchetti A., Cescon M., Taddia M., Marasco G., Festi G.// World J. Gastroenterol. 2014. V. 20. № 20. P. 5935–5950.
12. Smirnova I.S., Aksenov N.D., Kashuba E.V., Payakurel P., Grabovetsky V.V., Zaberezhny A.D., Vonsky M.S., Buchinska L., Biberfeld P., Hinkula J., et al. // Cell. Oncol.: Official J. Internat. Soc. Cell. Oncol. 2006. V. 28. № 4. P. 177–190.
13. Darekar S.D., Mushtaq M., Gurrapu S., Kovalevska L., Drummond C., Petruchek M., Tirinato L., Di Fabrizio E., Carbone E., Kashuba E.// Oncotarget. 2015. V. 6. № 25. P. 21016–21028.
14. Ambrose E.C., Kornbluth J. // Apoptosis: Internat. J. Programmed Cell Death. 2009. V. 14. № 10. P. 1227–1236.
15. Kashuba E., Kashuba V., Sandalova T., Klein G., Szekely L. // BMC Cell Biol. 2002. V. 3. № 1. P. 1–12.
16. Kashuba E., Pavan Yenamandra S., Darekar S.D., Yurchenko M., Kashuba V., Klein G., Szekely L. // Proc. Natl. Acad. Sci. USA. 2009. V. 106. № 47. P. 19866–19871.
17. Shevchuk Z., Yurchenko M.Y., Darekar S.D., Holodnuka-Kholodnyuk I., Kashuba V.I., Kashuba E.V. // Acta Naturae. 2013. V. 5. № 1. P. 85–89.
18. Ishak K., Baptista A., Bianchi L., Callea F., De Groote J., Gudat F., Denk H., Desmet V., Korb G., MacSween R.N.M., et al.// J. Hepatol. 1995. V. 22. № 6. P. 696–699.
19. Bedossa P., Poynard T. // Hepatology. 1996. V. 24. № 2. P. 289–293.
20. Goodman Z.D. // J. Hepatol. 2007. V. 47. № 4. P. 598–607.
21. Llovet J.M., Burroughs A., Bruix J. // Lancet. 2003. V. 362. № 9399. P. 1907–1917.
22. El-Serag H.B., Rudolph K.L. // Gastroenterology. 2007. V. 132. № 7. P. 2557–2576.
23. Lauwers G.Y., Terris B., Balis U.J., Batts K.P., Regimbeau J.M., Chang Y., Graeme-Cook F., Yamabe H., Ikai I., Cleary K.R., et al. // Am. J. Surgical Pathol. 2002. V. 26. № 1. P. 25–34.
24. Wahab M.A., Shehta A., Hamed H., El Nakeeb A., Salah T. // Eurasian J. Med. 2014. V. 46. № 1. P. 36–41.
25. Llovet J.M., Schwartz M., Mazzaferro V. //Semin. Liver Dis. 2005. V. 25. № 2. P. 181–200.
26. Welker M.-W., Bechstein W.-O., Zeuzem S., Trojan J. // Transplant Internat. 2013. V. 26. № 2. P. 109–118.
27. Lim K.C., Chow P.K., Allen J.C., Siddiqui F.J., Chan E.S., Tan S.B. // Br. J. Surgery. 2012. V. 99. № 12. P. 1622–1629.

GENERAL RULES

Acta Naturae publishes experimental articles and reviews, as well as articles on topical issues, short reviews, and reports on the subjects of basic and applied life sciences and biotechnology.

The journal is published by the Park Media publishing house in both Russian and English.

The journal *Acta Naturae* is on the list of the leading periodicals of the Higher Attestation Commission of the Russian Ministry of Education and Science. The journal Acta Naturae is indexed in PubMed, Web of Science, Scopus and RCSI databases.

The editors of *Acta Naturae* ask of the authors that they follow certain guidelines listed below. Articles which fail to conform to these guidelines will be rejected without review. The editors will not consider articles whose results have already been published or are being considered by other publications.

The maximum length of a review, together with tables and references, cannot exceed 60,000 characters with spaces (approximately 30 pages, A4 format, 1.5 spacing, Times New Roman font, size 12) and cannot contain more than 16 figures.

Experimental articles should not exceed 30,000 symbols (approximately 15 pages in A4 format, including tables and references). They should contain no more than ten figures.

A short report must include the study's rationale, experimental material, and conclusions. A short report should not exceed 12,000 symbols (8 pages in A4 format including no more than 12 references). It should contain no more than four figures.

The manuscript and the accompanying documents should be sent to the Editorial Board in electronic form:
1) text in Word 2003 for Windows format;
2) the figures in TIFF format;
3) the text of the article and figures in one pdf file;
4) the article's title, the names and initials of the authors, the full name of the organizations, the abstract, keywords, abbreviations, figure captions, and Russian references should be translated to English;
5) the cover letter stating that the submitted manuscript has not been published elsewhere and is not under consideration for publication;
6) the license agreement (the agreement form can be downloaded from the website www.actanaturae.ru).

MANUSCRIPT FORMATTING

The manuscript should be formatted in the following manner:

- Article title. Bold font. The title should not be too long or too short and must be informative. The title should not exceed 100 characters. It should reflect the major result, the essence, and uniqueness of the work, names and initials of the authors.
- The corresponding author, who will also be working with the proofs, should be marked with a footnote *.
- Full name of the scientific organization and its departmental affiliation. If there are two or more scientific organizations involved, they should be linked by digital superscripts with the authors' names. Abstract. The structure of the abstract should be very clear and must reflect the following: it should introduce the reader to the main issue and describe the experimental approach, the possibility of practical use, and the possibility of further research in the field. The average length of an abstract is 20 lines (1,500 characters).
- Keywords (3 – 6). These should include the field of research, methods, experimental subject, and the specifics of the work. List of abbreviations.
- INTRODUCTION
- EXPERIMENTAL PROCEDURES
- RESULTS AND DISCUSSION
- CONCLUSION

  The organizations that funded the work should be listed at the end of this section with grant numbers in parenthesis.
- REFERENCES

  The in-text references should be in brackets, such as [1].

RECOMMENDATIONS ON THE TYPING AND FORMATTING OF THE TEXT

- We recommend the use of Microsoft Word 2003 for Windows text editing software.
- The Times New Roman font should be used. Standard font size is 12.
- The space between the lines is 1.5.
- Using more than one whole space between words is not recommended.
- We do not accept articles with automatic referencing; automatic word hyphenation; or automatic prohibition of hyphenation, listing, automatic indentation, etc.
- We recommend that tables be created using Word software options (Table → Insert Table) or MS Excel. Tables that were created manually (using lots of spaces without boxes) cannot be accepted.
- Initials and last names should always be separated by a whole space; for example, A. A. Ivanov.
- Throughout the text, all dates should appear in the "day.month.year" format, for example 02.05.1991, 26.12.1874, etc.
- There should be no periods after the title of the article, the authors' names, headings and subheadings, figure captions, units (s – second, g – gram, min – minute, h – hour, d – day, deg – degree).
- Periods should be used after footnotes (including those in tables), table comments, abstracts, and abbreviations (mon. – months, y. – years, m. temp. – melting temperature); however, they should not be used in subscripted indexes (T_m – melting temperature; $T_{p.t}$ – temperature of phase transition). One exception is mln – million, which should be used without a period.
- Decimal numbers should always contain a period and not a comma (0.25 and not 0,25).
- The hyphen ("-") is surrounded by two whole spaces, while the "minus," "interval," or "chemical bond" symbols do not require a space.
- The only symbol used for multiplication is "×"; the "×" symbol can only be used if it has a number to its

right. The "·" symbol is used for denoting complex compounds in chemical formulas and also noncovalent complexes (such as DNA·RNA, etc.).
- Formulas must use the letter of the Latin and Greek alphabets.
- Latin genera and species' names should be in italics, while the taxa of higher orders should be in regular font.
- Gene names (except for yeast genes) should be italicized, while names of proteins should be in regular font.
- Names of nucleotides (A, T, G, C, U), amino acids (Arg, Ile, Val, etc.), and phosphonucleotides (ATP, AMP, etc.) should be written with Latin letters in regular font.
- Numeration of bases in nucleic acids and amino acid residues should not be hyphenated (T34, Ala89).
- When choosing units of measurement, SI units are to be used.
- Molecular mass should be in Daltons (Da, KDa, MDa).
- The number of nucleotide pairs should be abbreviated (bp, kbp).
- The number of amino acids should be abbreviated to aa.
- Biochemical terms, such as the names of enzymes, should conform to IUPAC standards.
- The number of term and name abbreviations in the text should be kept to a minimum.
- Repeating the same data in the text, tables, and graphs is not allowed.

GUIDENESS FOR ILLUSTRATIONS

- Figures should be supplied in separate files. Only TIFF is accepted.
- Figures should have a resolution of no less than 300 dpi for color and half-tone images and no less than 500 dpi.
- Files should not have any additional layers.

REVIEW AND PREPARATION OF THE MANUSCRIPT FOR PRINT AND PUBLICATION

Articles are published on a first-come, first-served basis. The members of the editorial board have the right to recommend the expedited publishing of articles which are deemed to be a priority and have received good reviews.

Articles which have been received by the editorial board are assessed by the board members and then sent for external review, if needed. The choice of reviewers is up to the editorial board. The manuscript is sent on to reviewers who are experts in this field of research, and the editorial board makes its decisions based on the reviews of these experts. The article may be accepted as is, sent back for improvements, or rejected.

The editorial board can decide to reject an article if it does not conform to the guidelines set above.

The return of an article to the authors for improvement does not mean that the article has been accepted for publication. After the revised text has been received, a decision is made by the editorial board. The author must return the improved text, together with the responses to all comments. The date of acceptance is the day on which the final version of the article was received by the publisher.

A revised manuscript must be sent back to the publisher a week after the authors have received the comments; if not, the article is considered a resubmission.

E-mail is used at all the stages of communication between the author, editors, publishers, and reviewers, so it is of vital importance that the authors monitor the address that they list in the article and inform the publisher of any changes in due time.

After the layout for the relevant issue of the journal is ready, the publisher sends out PDF files to the authors for a final review.

Changes other than simple corrections in the text, figures, or tables are not allowed at the final review stage. If this is necessary, the issue is resolved by the editorial board.

FORMAT OF REFERENCES

The journal uses a numeric reference system, which means that references are denoted as numbers in the text (in brackets) which refer to the number in the reference list.

For books: the last name and initials of the author, full title of the book, location of publisher, publisher, year in which the work was published, and the volume or issue and the number of pages in the book.

For periodicals: the last name and initials of the author, title of the journal, year in which the work was published, volume, issue, first and last page of the article. Must specify the name of the first 10 authors. Ross M.T., Grafham D.V., Coffey A.J., Scherer S., McLay K., Muzny D., Platzer M., Howell G.R., Burrows C., Bird C.P., et al. // Nature. 2005. V. 434. № 7031. P. 325–337.

References to books which have Russian translations should be accompanied with references to the original material listing the required data.

References to doctoral thesis abstracts must include the last name and initials of the author, the title of the thesis, the location in which the work was performed, and the year of completion.

References to patents must include the last names and initials of the authors, the type of the patent document (the author's rights or patent), the patent number, the name of the country that issued the document, the international invention classification index, and the year of patent issue.

The list of references should be on a separate page. The tables should be on a separate page, and figure captions should also be on a separate page.

The following e-mail addresses can be used to contact the editorial staff: vera.knorre@gmail.com, actanaturae@gmail.com, tel.: (495) 727-38-60, (495) 930-87-07